MATERIALES COMPUESTOS DE UNA POLIAMIDA DE ORIGEN RENOVABLE Y FIBRAS NATURALES DE ALTO RENDIMIENTO: UNA SÓLIDA ALTERNATIVA A LOS MATERIALES COMPUESTOS DE POLIPROPILENO REFORZADOS CON FIBRA DE VIDRIO

Helena Oliver Ortega

Universitat de Girona

TESIS DOCTORAL

Materiales compuestos de una poliamida de origen renovable y fibras naturales de alto rendimiento: una sólida alternativa a los materiales compuestos de polipropileno reforzados con fibra de vidrio

Helena Oliver Ortega

2018

Universitat de Girona

TESIS DOCTORAL

Materiales compuestos de una poliamida de origen renovable y fibras naturales de alto rendimiento: una sólida alternativa a los materiales compuestos de polipropileno reforzados con fibra de vidrio

Helena Oliver Ortega

2018

PROGRAMA DE DOCTORADO EN TECNOLOGÍA

Dirigida por: Dr. Pere Mutjé, Dra. Mònica Ardanuy y Dr. Joaquim Agustí Tarrés

Tutor: Dr. Pere Mutjé

MEMORIA PRESENTADA PARA OBTAR AL TÍTULO DE DOCTORA POR LA UNIVERSITAT DE GIRONA

El Dr. Pere Mutjé Pujol, catedrático del departamento de Ingeniería Química, Agraria y Tecnología Alimentaria de la Universitat de Girona, la Dra. Mònica Ardanuy Raso, profesora del departamento de Ciencias de los Materiales e Ingeniería Metalúrgica de la Universitat Politècnica de Catalunya, y el Dr. Joaquim Agustí Tarrés Farrés, profesor asociado del Departamento de Ingeniería Química, Agraria y Tecnología Alimentaria de la Universitat de Girona,

DECLARAN:

Que el trabajo titulado "*Materiales compuestos de una poliamida de origen renovable y fibras naturales de alto rendimiento: una sólida alternativa a los materiales compuestos de polipropileno reforzados con fibra de vidrio*", que presenta la Srta. Helena Oliver Ortega para la obtención del título de doctora ha sido realizado bajo nuestra dirección.

Y para que así conste y a los efectos oportunos, firmamos el presente documento:

Dr. Pere Mutjé Pujol ***Dra. Mònica Ardanuy Raso*** ***Dr. Joaquim Agustí Tarrés Farrés***

Girona, 8 de mayo de 2018

Sofismes els sofismes per als qui només veuen amb els ulls del cervell

Joan Salvat-Papasseit. *Poemes en ondes hertzianes*. Columna Vertebral.

AGRADECIMIENTOS

Me gustaría empezar agradeciendo a todos los que explícita o implícitamente han contribuido a la realización de esta tesis.

En primer lugar, me gustaría agradecer al Dr. Pere Mutjé, tutor y director de esta tesis, la oportunidad que me brindo, las enseñanzas recibidas y su guía durante el desarrollo de esta tesis. A la Dra. Mònica Ardanuy, por su contribución, ayuda y consejo desde que se unió a este proyecto y al Dr. Joaquim Tarrés que se incorporó a la dirección en la segunda parte de esta tesis pero que sin él no hubiese sido posible su culminación.

Al grupo LEPAMAP-PA y a todos sus integrantes que me han acogido durante este proyecto. En especial a la Dra. Farners Corrales y el Sr. Albert Serra que han hecho de los días de mayor cansancio algo más soportables; al Dr. José Alberto Méndez, por sus sabios consejos y por tener siempre una puerta abierta para mí; y a los Dres. Francesc Xavier Espinach y Fernando Julián, de los cuales puedo afirmar que no he salido ninguna vez de su despacho sin haber aprendido alguna cosa nueva. También, y aunque no forme parte actualmente del grupo, al Dr. Luis Angel Granda, por su ayuda, sobre todo en los primeros pasos de esta tesis, consejo y apoyo, incluso cuando ya no formaba parte del grupo.

Tampoco puedo olvidarme de agradecer, a todas esas personas que me han apoyado y han estado a mi lado durante todo este proyecto, de una forma quizás más personal. A todos mis amigos y en especial a: mis chicas del máster Anna y Núria; mis químicos favoritos Adrià, Anna, Antoni, Georgina, Jordi, Judit y Vanessa; "les meves nenes" Cristina, Laia, Raquel y Mireia que es como una "nena" más; y a Laura, mi futura psicóloga. Gracias, por tener tiempo para estar ahí y por todo el apoyo durante esta aventura que ha sido la tesis.

Finalmente, aunque no por ello menos importantes, a toda mi familia. Principalmente a mi hermana Ariadna y a mis padres Dolors y Jose Luis, que me han apoyado siempre, en cada paso y decisión que he tomado. Vosotros, que habéis creído en mí hasta cuando yo dejaba de hacerlo. Me faltan palabras para agradecer todo lo que habéis y continuáis haciendo por mí.

LISTADO DE PUBLICACIONES

Esta tesis está formada por el siguiente compendio de publicaciones:

1. Oliver-Ortega H., Granda L.A., Espinach F.X., Méndez J.A., Julian F., Mutjé P. Tensile properties and micromechanical analysis of stone groundwood from softwood reinforced bio-based polyamide11 composites. Composite Science and Technology. 2016, 132, 123–30. doi: 10.1016/j.compscitech.2016.07.004

   Factor de impacto 2016: 4,873. Posición 1 de 25 en Materials Science, Composites. Primer cuartil.

2. Oliver-Ortega H., Granda L.A., Espinach F.X., Delgado-Aguilar M., Duran J., Mutjé P. Stiffness of bio-based polyamide 11 reinforced with softwood stone ground-wood fibres as an alternative to polypropylene-glass fibre composites. European Polymer Journal. 2016 , 84, 481–9. doi:10.1016/j.eurpolymj.2016.09.062

   Factor de impacto 2016: 3,531. Posición 13 de 86 en Polymer Science. Primer cuartil.

3. Oliver-Ortega H., Méndez J.A., Mutjé P., Tarrés Q., Espinach F.X., Ardanuy M. Evaluation of Thermal and Thermomechanical Behaviour of Bio-Based Polyamide 11 Based Composites Reinforced with Lignocellulosic Fibres. Polymers. 2017, 9, 522. doi:10.3390/polym9100522

   Factor de impacto 2016: 3,364. Posición 16 de 86 en Polymer Science. Primer cuartil.

4. Oliver-Ortega H., Méndez J.A., Reixach R., Espinach F.X., Ardanuy M., Mutjé P. Towards More Sustainable Material Formulations: A Comparative Assessment of PA11-SGW Flexural Performance versus Oil-Based Composites. Polymers. 2018, 10, 440. Available from: doi:10.3390/polym10040440

Factor de impacto 2016: 3,364. Posición 16 de 86 en Polymer Science. Primer cuartil.

Y por tres artículos en estado de revisión:

5. Oliver-Ortega H., Llop M.F., Méndez J.A., Tarrés Q., Ardanuy M., Mutjé P. Study of the flexural modulus of lignocellulosic fibres reinforced bio-based polyamide11 green composites. Enviado al Composites Part B: Engineering.

   Factor de impacto 2016: 4,727. Posición 2 de 25 en Materials Science, Composites. Primer cuartil.

6. Oliver-Ortega H., Méndez J.A., Espinach F.X., Tarrés Q., Ardanuy M., Mutjé P. Fully bio-based composites from PA11-SGW: Notable impact strength and water uptake. Enviado al International Journal of Biological Macromolecules.

   Factor de impacto 2016: 3,671. Posición 12 de 86 en Polymer Science. Primer cuartil.

7. Oliver-Ortega H., Julián F., Espinach F.X, Tarrés Q., Ardanuy M., Mutjé P. Research on the use of bio-polyamide 11 reinforced with lignocellulosic fibers composites in automotive parts. The case of a car doors handle. Enviado al Journal of Cleaner Production.

   Factor de impacto 2016: 5,715. Posición 5 de 31 en Green and Sustainable Science and Technology. Primer cuartil.

CONTRIBUCIÓN DE LA AUTORA

La autora de esta tesis contribuyó a los artículos incluidos en el compendio de la siguiente forma:

Artículo 1

Preparó y obtuvo mediante inyección los especímenes de los materiales compuestos para los ensayos de tracción. Diseñó los experimentos y realizó la caracterización mecánica y los ensayos micromecánicos. Además, efectuó las extracciones de las fibras y los análisis morfológicos. Interpretó los resultados obtenidos en la espectroscopia electrónica de rayos X. Evaluó los resultados obtenidos y participó en la redacción de la publicación.

Artículo 2

Elaboró las mezclas de los materiales compuestos y obtuvo las probetas para el ensayo del módulo. Realizó la caracterización, aplicó los modelos micromecánicos y analizó los resultados. Los comparó con los resultados obtenidos con compuestos comerciales. Contribuyó en la redacción y corrección del artículo.

Artículo 3

Planificó y concibió los experimentos incluyendo el proceso de *annealing*. Realizó todos los ensayos de caracterización térmica, termomecánica y los espectros de infrarrojo. Analizó los difractogramas de rayos X y diferenció las fases. Evaluó los resultados y redactó el primer esbozo del artículo. Participó en la redacción final y corrección del trabajo conjuntamente con el resto de autores.

Artículo 4

Produjo los materiales compuestos y los especímenes necesarios para los ensayos de flexión. Obtuvo la caracterización mecánica, realizó los cálculos derivados de los modelos micromecánicos y evaluó los resultados. Efectuó la búsqueda bibliográfica y comparó los resultados con los productos comerciales. Participó en la redacción de la publicación.

Artículo 5

Fabricó los materiales compuestos y produjo las probetas necesarias para el ensayo de módulo a flexión. Diseño y realizó los experimentos y cálculos. Comparó los resultados con los obtenidos anteriormente en la literatura y redactó conjuntamente al resto de autores el artículo.

Artículo 6

Preparó las probetas de los materiales compuestos para los ensayos de impacto y absorción de agua. Diseño y realizó la caracterización mecánica y los perfiles de absorción de agua. Midió el ángulo de contacto de las muestras y realizó los cálculos. Modelizó los resultados y los evaluó. Redactó junto a los demás autores el documento.

Artículo 7

Planificó el artículo y participó en el diseño de la pieza. Realizó la caracterización mecánica de los compuestos y elaboró el análisis de elementos finitos y realizó el LCA. Evaluó los resultados y contribuyó en la redacción del documento.

ABREVIATURAS

α :	Ángulo medio de orientación de las fibras (º)
β :	Factor de transferencia del esfuerzo fibra-matriz
χ_1 :	Factor de orientación
χ_1^f :	Factor de orientación a flexión
χ_2 :	Factor de longitud e interfase
χ_2^f :	Factor de longitud e interfase a flexión
ε_f^C :	Deformación del material compuesto a flexión (%)
ε_t^C :	Deformación del material compuesto a tracción (%)
γ :	Tensión superficial del agua ($mJ \cdot m^{-2}$)
λ :	Longitud de onda (nm)
η_e :	Factor de eficacia del módulo en la RoM
η_L :	Factor longitudinal de Tsai-Pagano
η_l :	Factor de longitud del módulo en la RoM
η_T :	Factor transversal de Tsai-Pagano
η_0 :	Factor de orientación del módulo en la RoM
ρ_{water} :	Densidad del agua ($g \cdot cm^{-3}$)
ρ^C :	Densidad del material compuesto ($g \cdot cm^{-3}$)
ρ^F :	Densidad de la fibra ($g \cdot cm^{-3}$)
ρ^m:	Densidad de la matriz ($g \cdot cm^{-3}$)
σ_f^C :	Resistencia a flexión de los materiales compuestos (MPa)
σ_f^F :	Resistencia intrínseca de la fibra a flexión (MPa)
σ_f^{m*} :	Resistencia a flexión de la matriz en el punto de resistencia máxima del material compuesto (MPa)
σ_t^C :	Resistencia a tracción de los materiales compuestos (MPa)
σ_t^F :	Resistencia intrínseca de la fibra a tracción (MPa)
σ_t^{m*} :	Resistencia a tracción de la matriz en el punto de resistencia máxima del material compuesto (MPa)
τ :	Tensión interfacial de cizalla (MPa)
θ :	Ángulo de contacto del agua (º)

υ :	Coeficiente de Poisson
BioPA :	Bio-poliamidas
C :	Carbono
CNF :	Nanofibras de celulosa
CO_2 :	Dióxido de carbono
D :	Deflexión (mm)
D_F :	Coeficiente de difusión de Fick ($m^2 \cdot s^{-1}$)
D_0 :	Índex de permeabilidad
d :	Grosor del espécimen (mm)
d^F :	Diámetro aritmético medio de la fibra (µm)
DSC :	Calorimetría diferencial de rastreo
DMTA :	Análisis dinámico termomecánico
EU :	Unión Europea
E_d :	Energía necesaria para iniciar el proceso de difusión ($kJ \cdot mol^{-1}$)
E_f^C :	Módulo elástico a flexión de los materiales compuestos (GPa)
E_f^F :	Módulo elástico a flexión de la fibra (GPa)
E_t^C :	Módulo de Young de los materiales compuestos (GPa)
E_t^F :	Módulo de Young intrínseco de la fibra (GPa)
E_t^m :	Módulo de Young de la matriz (GPa)
E_w :	Energía de humectabilidad
E^{11} :	Módulo elástico longitudinal
E^{22} :	Módulo elástico transversal
E' :	Módulo de almacenamiento
E" :	Módulo de perdidas
f_c :	Factor de acoplamiento
f_c^f :	Factor de compatibilidad a flexión
f_c^t :	Factor de compatibilidad a tracción
FFSF :	Factor de resistencia a flexión de las fibras
FTMF :	Factor de módulo a tracción de las fibras
FTSF :	Factor de resistencia a tracción de las fibras

FT-IR :	Espectroscopia de Infrarrojo con la Transformación de Fourier
GF :	Fibra de Vidrio
$\widehat{Hm}$ ***:***	Entalpia teórica de la matriz a la temperatura de fusión ($J \cdot g^{-1}$)
IFSS :	Fuerza interfacial de cizalla (MPa)
K :	Constante cinética de Fick relacionada con el sistema
L :	Distancia entre los soportes del ensayo a flexión (mm)
LCA :	Análisis de ciclo de vida
LEPAMAP :	Laboratori d'Enginyeria Paperera i Materials Polímerics
L^C ***:***	Longitud crítica (µm)
l^F ***:***	Longitud aritmética media de la fibra (µm)
l^{WF} ***:***	Longitud ponderada en longitud de la fibra (µm)
MAPP :	Polipropileno con injertos de ácido maleico
MFI :	Índice de fluidez ($cc \cdot min^{-1}$)
M_t ***:***	Absorción de agua
M_∞ ***:***	Absorción de agua en el punto de saturación (%)
n :	Constante cinética de Fick relacionada con el tiempo de saturación
PA :	Poliamida
PA6 :	Poliamida 6
PA6.6 :	Poliamida 6.6
PA6.10 :	Poliamida 6.10
PA10.10 :	Poliamida 10.10
PA11 :	Poliamida 11
PBS :	Polibutileno succinato
PLA :	Ácido poliláctico
PE :	Polietileno
PP :	Polipropileno
PVC :	Policloruro de vinilo
R :	Constante de los gases ideales ($J \cdot mol^{-1} \cdot K^{-1}$)
RH :	Humedad relativa
RoM :	Regla de las mezclas

SEM :	Microscopio electrónico de barrido
SGW :	Fibras obtenidas a través de un proceso mecánico de muela de piedra
T :	Temperatura (ºC)
TGA :	Análisis termogravimétrico
T_c **:**	Temperatura de cristalización (ºC)
T_g **:**	Temperatura de transición vítrea (ºC)
T_m **:**	Temperatura de fusión (ºC)
T_{max} **:**	Temperatura donde la cinética de degradación es máxima
$T_{5\%}$ **:**	Temperatura en la que el material ha perdido el 5% de su peso inicial
$T_{10\%}$ **:**	Temperatura en la que el material ha perdido el 10% de su peso inicial
$T_{95\%}$ **:**	Temperatura en la que el material ha perdido el 95% de su peso inicial
USA :	Estados Unidos de América
U_R **:**	Resiliencia del material ($kJ \cdot m^3$)
U_T **:**	Tenacidad del material ($kJ \cdot m^3$)
V_{total} **:**	Volumen total
V^F **:**	Volumen de fibra
v/v :	Relación entre el volumen de la fase respecto volumen total
w :	Trabajo total disipado
w_f **:**	Trabajo disipado por las fibras
w_{fm} **:**	Trabajo disipado en la interfase fibra-matriz
w_i **:**	Trabajo disipado al iniciar una fractura
w_m **:**	Trabajo disipado por la matriz
w/w :	Relación entre el peso de la fase y el peso total (%)
XRD :	Difracción de Rayos X
XPS :	Espectroscopia fotoelectrónica de rayos X

ÍNDICE DE FIGURAS

ÍNDICE DE TABLAS

ÍNDICE DE CONTENIDOS

RESUMEN

El creciente uso de recursos no renovables hace reflexionar sobre la necesidad de que la sociedad debe encaminarse hacia el desarrollo de productos y procesos más sostenibles de forma que nuestro desarrollo y bienestar no comprometa el de generaciones futuras. Uno de los requisitos más importantes en el desarrollo de materiales sostenibles, es el uso de materias primas de origen renovable. Si estos materiales tienen un carácter biodegradable, el impacto ambiental disminuye aún más. Estos requisitos están establecidos por los principios de la química verde y de la ingeniería verde.

En el caso de los materiales compuestos de matriz polimérica su sostenibilidad es más que cuestionable. Más del 90% de estos materiales se producen a partir de matrices derivadas del petróleo y utilizando fibra de vidrio (GF) como refuerzo. En ambos casos, tanto la matriz como el refuerzo difícilmente pueden clasificarse como sostenibles. Aunque a nivel industrial el desarrollo de materiales más sostenibles es muy reducido, a nivel de investigación sí que se han realizado grandes avances. Inicialmente, se sustituyeron refuerzos minerales como las GF por refuerzos de origen natural como las fibras celulósicas y lignocelulósicas. A pesar de las propiedades inferiores de las fibras celulósicas y lignocelulósicas en comparación con las GF, el incremento del porcentaje de refuerzo en el material compuesto compensaba parcialmente las carencias mecánicas de las fibras vegetales. Además, se aumentaba el contenido de material de origen renovable en el compuesto. No obstante, la gran mayoría de matrices empleadas en materiales compuestos provienen del petróleo, por lo que su reemplazo es necesario para el desarrollo de materiales compuestos totalmente sostenibles.

Esta tesis propone la fabricación de materiales compuestos de poliamida 11 (PA11) y fibras mecánicas de alto rendimiento de pino (98% respecto a la materia prima) procedentes de un proceso de muela de piedra (SGW). La PA11 es una poliamida de origen totalmente renovable por lo que estos compuestos tienen un origen totalmente renovable. Además, estos materiales se han fabricado sin la necesidad de aplicar ningún tratamiento a la fibra o a la matriz, reduciendo el impacto ambiental derivado de estos procesos. Los materiales de PA11-SGW se han evaluado de forma mecánica y se ha estudiado su comportamiento térmico, termomecánico y de absorción de agua. Los resultados obtenidos se han comparado con materiales compuestos de polipropileno (PP) reforzado con GF, uno de los *commodities* más empleados en la industria. La idoneidad de los compuestos de PA11-SGW para remplazar los compuestos de PP-GF

se ha constatado mediante la modelización de un producto. Los resultados obtenidos muestran la capacidad de los materiales compuestos de PA11 de ser una sólida alternativa a los materiales compuestos de PP-GF. La producción de estos materiales representa un avance significativo en el desarrollo de productos y procesos sostenibles.

RESUM

El creixent ús de materials d'origen no renovable fa reflexionar sobre el camí que la societat necessita recórrer cap al desenvolupament de productes i processos més sostenibles, de forma que el nostre desenvolupament i benestar actual no comprometi el de les pròximes generacions. Un dels requisits més importants en el desenvolupament de materials sostenibles es l'ús de matèries primeres d'origen renovable. Si aquests materials son biodegradables també, l'impacte ambiental decreix encara més. Aquests requisits estan establerts pels principis de la química verda i l'enginyeria verda.

En el cas dels materials compostos de matriu polimèrica, la seva sostenibilitat es qüestionable. Més del 90% d'aquets materials es produeixen mitjançant matrius derivades del petroli i utilitzant fibra de vidre (GF) com a reforç. En ambdós casos, tant la matriu com el reforç difícilment poden ser considerats materials sostenibles. Tot i que a nivell industrial el desenvolupament de materials més sostenibles es escàs, a nivell d'investigació si que si han realitzat grans avenços. Inicialment, es van substituir els reforços minerals com les GF per reforços d'origen natural com ho son les fibres cel·lulòsiques i lignocel·lulòsiques. Tot i les propietats inferiors de les fibres cel·lulòsiques i lignocel·lulòsiques en comparació amb les GF, l'increment del seu percentatge de reforç en el material compost compensava les mancances mecàniques de les fibres vegetals. A més a més, s'augmentava el contingut de material d'origen renovable en el material compost. Tot i això, les matrius més emprades en materials compostos provenen majoritàriament del petroli, i per tant, la seva substitució es necessària pel desenvolupament de materials compostos totalment sostenibles.

En aquesta tesi es proposa la fabricació de materials compostos de poliamida 11 (PA11) i fibres mecàniques de pi d'alt rendiment (98% respecte la matèria primera) procedents d'un procés de mola de pedra (SGW). La PA11 és una poliamida d'origen totalment renovable i per tant aquest compostos ho seran també totalment. A més a més, aquests materials s'han fabricat sense la necessitat d'aplicar un tractament a la fibra o a la matriu, reduint d'aquesta forma l'impacte ambiental que es deriva d'aquests processos. Els materials de PA11-SGW s'han avaluat mecànicament i s'ha estudiat el seu comportament tèrmic, termomecànic i d'absorció d'aigua. Els resultats obtinguts s'han comparat amb els materials compostos de polipropilè (PP) reforçat amb GF, un dels *commodities* més utilitzats a la industria. La idoneïtat dels materials compostos de PA11-SGW per substituir els compostos de PP-GF es va constatar mitjançant la

modelització d’un producte. Els resultats obtinguts mostren la capacitat dels materials compostos de PA11 de ser una sòlida alternativa als materials compostos de PP-GF. La producció d’aquests materials representa un avanç significatiu en el desenvolupament de productes i processos sostenibles.

ABSTRACT

The society has to make an effort in the development of more sustainable products and processes. The actual development and well-being cannot compromise the well-being of the future generations. One of the most important requirements in the development of sustainable materials is the use of renewable raw materials. Moreover, the use of biodegradable renewable raw materials also reduces significantly the environmental impact. The requirements are stablished by the green chemistry and engineering principles.

In the case of composites materials using polymeric matrixes, their sustainability is questionable. More of the 90% of these composites are produced using oil-based matrices and glass fibres (GF) as reinforcement. Both components cannot be classified as sustainable materials. Although in an industrial scale the development of sustainable materials is scarce, in the development and innovation field there is an important progress. Initially, mineral reinforcements such as GF were replaced by renewable reinforcements like cellulosic and lignocellulosic fibres. Despite the lower mechanical properties of cellulosic and lignocellulosic fibres in comparison with GF, an increment of the fibre content in the material led to similar mechanical performance. Moreover, the renewable material in the composite was increased by the presence of higher fibre contents. Nonetheless, composites materials are usually produced using oil-based matrices. It is necessary to replace these matrices for renewable ones in the development of sustainable composite materials.

In this thesis the manufacture of composites materials of polyamide 11 (PA11) and high yield pine fibres (98% of yield process) from a stoneground wood process is proposed. PA11 is a polyamide totally bio-based. Thus, make its composites with SGW fibres totally bio-based also. In addition, these material were prepares without any modification of the fibres or the matrix, reducing the environmental impact of these process. The PA11-SGW composites were mechanically evaluated and its thermal, thermomechanical and water uptake behaviour was studied. The results were compared with GF reinforced polypropylene (PP). PP-GF is one of the most used commodities in the industry. The suitability of PA11-SGW composites to replace PP-GF composites was checked in the modelling of a product. The obtained results showed the capacity of PA11-based composites to become a solid alternative to PP-GF. The production of these

materials represents a significant progress in the development of sustainable products and process.

CAPÍTULO 1: *INTRODUCCIÓN, OBJETIVOS Y JUSTIFICACIÓN DE LA TESIS*

1.1 Introducción general

Desde prácticamente la última década del siglo XX, la concepción, diseño y aplicación de materiales en la fabricación de materiales compuestos ha experimentado, por lo menos a nivel de investigación, desarrollo e innovación, un auge notable hacia una mayor sostenibilidad. Bajo el concepto de sostenibilidad se engloban materiales y procesos en los que la materia prima es de origen renovable; procesos en el que el producto final y los residuos generados pueden ser reciclados y/o biodegradado; procesos donde la cantidad de residuos generados, sólidos, líquidos y gaseosos, es la mínima posible; el consumo energético y de materia están optimizados, obteniendo procesos eficientes; o la disminución la toxicidad del proceso y substitución compuestos tóxicos por otros con menor impacto en la salud y en el medio ambiente.

Mayoritariamente, los criterios de sostenibilidad están vinculados a problemáticas ambientales. Los efectos de la actual problemática ambiental (emisiones descontroladas de CO_2, acumulación de residuos, contaminación de suelos, etc.) y las grandes catástrofes que se produjeron en la industria química (Seveso 1974 y Bophal 1984) a consecuencia de fugas y las reacciones espontaneas derivadas sin control, ayudaron a una mayor concienciación de la sociedad.

Cronológicamente, los primeros pasos hacia la sostenibilidad se iniciaron en 1984, cuando se creó en Canadá la marca *Responsable Care*®, pionera en establecer unos principios que promueven la seguridad, la reducción del impacto ambiental, el reciclaje, etc. [1]. En 1987, el informe Brundtland de la Comisión Mundial del Medio Ambiente y Desarrollo introdujo por primera vez el concepto de desarrollo sostenible [2]. El objetivo a partir de entonces fue satisfacer las necesidades de la sociedad sin comprometer las capacidades de las futuras generaciones. En este sentido, la declaración Brundtland constituyó un cambio político relevante para todos los países que la suscribieron. Tres años más tarde, en 1990, en Estados Unidos (USA) se presentó el Acta de Prevención de la Contaminación (*Pollution Prevention Act*) que establecía la reducción de residuos como prioridad para resolver los problemas medioambientales. A partir de esta Acta, se produjo otro cambio trascendental en la mediación ambiental: se propuso un modelo basado en la prevención, con prioridad sobre la gestión de los residuos. Durante el año 1991, se estableció el primer programa de Química Verde (*Green Chemistry Program*) por parte de la Agencia de Protección del Medioambiente

de USA. Este programa de Química Verde, se centró fundamentalmente en la investigación sobre metodologías de síntesis alternativas y al diseño y rediseño de los procesos químicos. A partir del 1996, se crearon distintas entidades relacionadas con la química verde alrededor del mundo, destacando entre ellas el Instituto de Química Verde (*Green Chemistry Institute*) del *School of Forestry and Environmental Studies* de la University of Yale, New Haven en USA o la plataforma Europea *SusChem* (European Technology Platform for Sustainable Chemistry) [3], la *Green Chemistry Network* en el Reino Unido, el INCA (*Consorzio Interuniversitario Nazionale "La Chimica per l'Ambiente")* en Italia, el *Center for Green Chemistry* en Austràlia y el *Green an a Sustainable Network* en Japon. A partir de este momento se fomentaron las actividades de difusión científica en congresos y revistas científicas tales como *Green Chemistry,* de la Royal Society of Chemistry o *Green Chemistry Letters and Reviews* de la editorial Taylor&Francis.

En 1998, Anastas P. T. y Warner J.C. [4] de la University of Yale formularon por primera vez los doce principios de la química verde. Posteriormente el año 2003, Anastas P. T. y Zimmerman J., desarrollaron también los doce principios de la ingeniería química verde [5]. Buena parte de estos principios, tanto los referentes a química verde como a la ingeniería química verde, pueden servir para la mejora de la sostenibilidad de los procesos de síntesis, producción y transformación de plásticos y materiales compuestos.

La sostenibilidad de la industria del plástico, incluyendo los materiales compuestos de matriz polimérica, hace tiempo que se encuentra en entredicho. El crecimiento exponencial de la producción y consumo de materiales plásticos desde los años 50 produjo a su vez un incremento muy importante de residuos generados. De las 60 millones de toneladas de materiales plásticos que aproximadamente se produjeron en 2017 en Europa, el 27.1% se dispuso en vertederos controlados [6]. Por otra parte, algunos países de la Unión Europea (UE) han prohibido este tipo de abocamientos, ofreciendo o propugnando dos alternativas principales, el reciclado o la incineración. De esta forma, cuando los materiales plásticos no son reciclados, se incineran con el objetivo de producir energía. No obstante, la incineración de estos compuestos incrementa las emisiones de CO_2, favoreciendo el efecto invernadero y el calentamiento global del planeta. Recientemente la Unión Europea ha publicado el informe *A European Strategy for Plastics in a Circular Economy* [7], con el que se pretende impulsar un modelo de economía circular, similar al de la industria papelera sobre reciclado y reutilización de los materiales plásticos. En dicho informe, se mencionan escasamente los

plásticos biodegradables y se obvian los plásticos termoestables. No cabe duda que ello puede representar un valor añadido importante al sector de reciclado de plásticos. Actualmente, solamente un 30% de los materiales plásticos consumidos son reciclados y reutilizados.

En el campo de los materiales compuestos con matrices termoplásticas, la situación queda reflejada esquemáticamente en el gráfico de la figura 1. El principal objetivo en la producción de materiales compuestos es la obtención de materiales que combinen las propiedades de los materiales utilizados. La inmiscibilidad de los distintos componentes de los materiales compuestos da lugar a la formación de dos fases perfectamente diferenciadas: una fase continua, la matriz, y una fase discontinua, el refuerzo [8]. Uno de los principales objetivos que se persigue en la producción de un material compuesto es el incremento notable en sus propiedades mecánicas. El incremento de éstas se encuentra estrechamente relacionado con las propiedades de las dos fases, la morfología del refuerzo, su orientación y la dispersión de este en el interior de la matriz y la calidad de la interfase que se produce entre la matriz y el refuerzo [8]. No obstante, la poca miscibilidad de las dos fases dificulta la dispersión del refuerzo en la matriz y la creación de unas interacciones adecuadas en la interfase, que permitan la transferencia de los esfuerzos. En muchos casos, el uso de un agente de acoplamiento es necesario para garantizar una correcta dispersión e interfase en el material compuesto.

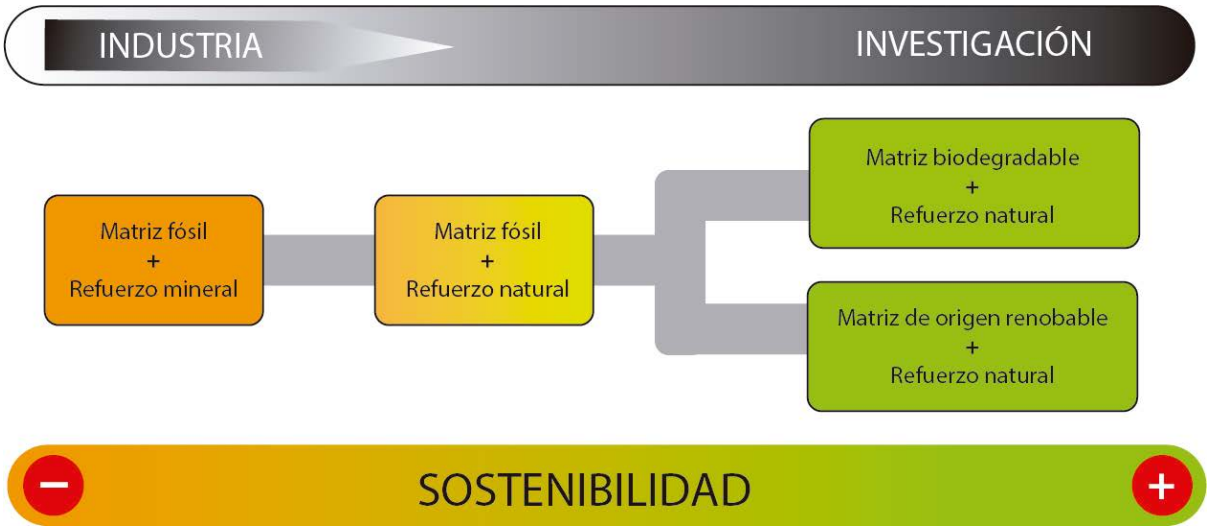

Figura 1. Evolución esquemática de la evolución de los materiales compuestos.

Los primeros materiales compuestos de matriz polimérica se diseñaron en los años 50 con la intención de disminuir el peso y coste de materiales convencionales, mientras se mantenían o incrementaban las propiedades mecánicas [9–12]. Debido a la gran disponibilidad de matrices poliméricas derivadas del petróleo y de refuerzos minerales (fibras sintéticas y partículas minerales), y a la poca concienciación y escasa legislación ambiental en esa época, los primeros materiales compuestos cumplían pocos requisitos para ser sostenibles. El principal exponente de estos materiales compuestos son las poliolefinas reforzadas con fibras de vidrio (GF). En la actualidad, de las aproximadamente 4 millones de toneladas de materiales compuestos de matriz polimérica que se producen, más del 90% de estos están reforzados con GF [13,14].

Las GF son fibras muy frágiles, pero tienen una gran estabilidad térmica y unas elevadas propiedades mecánicas. Si consideramos la resistencia a tracción (σ_t^C), el módulo de Young (E_t^C) y la deformación (ε_t^C) como referentes de las propiedades mecánicas, en el caso de las GF, éstas son muy superiores cuando son comparadas con las matrices poliolefínicas: una σ_t^C entre 2400-2900MPa frente a 10-30MPa y un E_t^C de alrededor de 70 GPa respecto a los 1-2 GPa de las poliolefinas [15]. Por otra parte, la elevada rigidez de las fibras conlleva una ε_t^C baja. Estas propiedades suponen que cuando una poliolefina como el polipropileno (PP) se refuerce con solamente un 20% w/w (relación peso de la fase respecto al peso total) de GF y un 6% w/w de agente de acoplamiento, su σ_t^C aumente de 28MPa a 68MPa y su E_t^C de 1,5 GPa a 4,1 GPa. Aunque existen otras fibras con propiedades aún más elevadas como las fibras de carbono [16], el coste, disponibilidad y la relativamente facilidad para obtener las longitudes y diámetros deseados en las GF, hacen que sean el refuerzo más empleado actualmente. A pesar de ello, las GF presentan grandes inconvenientes e incumplen muchos de los principios anteriormente mencionados: aunque su coste sea bajo, su coste energético es muy elevado; su elevada fragilidad dificulta su reciclaje, y por ende el de sus materiales compuestos [17]; su elevada abrasividad produce un gran desgaste en los equipos de transformación [18]; y la manipulación de éstas puede causar enfermedades tópicas y respiratorias [19,20].

Su reemplazo por fibras naturales como lo son las fibras celulósicas representa un avance tanto a nivel ambiental, como en su manipulación y procesado y supone una disminución del coste y del peso (la densidad de las GF es de alrededor de 2,5g·cm^{-3} mientras que en el caso de las fibras naturales es de 1,4 g·cm^{-3}) [21]. Aunque la σ_t^C , de alrededor de 700MPa, y su

E_t^C de 20 MPa son muy inferiores a las de las GF, su ε_t^C es mayor debido a la menor rigidez, lo que permite aumentar los contenidos de refuerzo y facilita el reciclaje mecánico de éstos materiales [22,23]. En el caso del PP, el refuerzo de éste con un 50% w/w de fibras lignocelulósicas de alto rendimiento y en presencia de un agente de acoplamiento reportó una σ_t^C de 56 MPa y de 60 MPa para un compuesto mezclado mediante dos equipamientos diferentes, en un plastógrafo y en un mezclador cinético, respectivamente [22]. La aplicación de tratamientos superficiales sobre la fibra celulósica condujo a una σ_t^C de 68 MPa, igual a la obtenida por PP+20%GF con agente de acoplamiento (GF *coupled*). De esta forma, mediante la utilización de mayores contenidos de fibras naturales dentro del material es posible la sustitución de los materiales compuestos de GF. Además, ello conlleva una importante reducción de la cantidad de material de origen fósil (matriz), a la vez que se aumenta el de origen renovable (refuerzo).

En la utilización de fibras celulósicas, la capacidad de refuerzo principalmente debida a la celulosa. No obstante, la presencia de celulosa en la superficie de las fibras suele ser reducida, ya que los extractivos, lignina y hemicelulosas están situados en las capas más externas de las fibras. En este sentido, la utilización de tratamientos superficiales que conduzcan a la reducción o eliminación de estos compuestos, permite incrementar la presencia de celulosa superficialmente, aumentando la interacción de la celulosa con el polímero y por ende la consecución de mayores incrementos en las propiedades mecánicas [24,25].

Por otra parte, se han desarrollado investigaciones centradas en el aprovechamiento de residuos agrícolas como refuerzo [26–28] o residuos de fibras con un valor en la industria textil como el algodón, el lino o incluso el bambú [29–31], en vez del uso de fibras madereras [22,32]. Como es ampliamente conocido, las propiedades mecánicas de las fibras celulósicas varían en función del tipo de planta, el crecimiento o el recurso aprovechado (hojas, madera, etc.). Fibras filamentosas como el lino, jute, esparto o algodón, tienen mejores propiedades que las madereras y considerablemente superiores a las extraídas de residuos agrícolas [29]. No obstante, estas fibras tienen un elevado coste debido a su interés en la industria textil, mientras que el aprovechamiento de residuos agrícolas representa la revalorización de un producto producido en grandes cantidades. El conjunto de estas propiedades mencionadas han hecho que en algunos sectores como el del automovilismo empiecen a emplear materiales compuestos reforzados con fibras celulósicas [33].

Tal y como se muestra en la figura 1, el avance hacia la sostenibilidad en el campo de los materiales compuestos debe pasar por el uso de matrices de origen renovable o biodegradable. Mayoritariamente, las matrices empleadas en la producción de materiales compuestos actualmente derivan del petróleo. En el caso de materiales termoplásticos, las matrices utilizadas suelen ser poliolefinas [34,35]. En la actualidad únicamente la producción de polipropileno (PP) y polietileno (PE) supera el 50% en peso de la producción total de plásticos (tabla 1) [6,36]. La gran versatilidad de ambas matrices, su fácil aditivación, transformación y reciclaje, así como su baja densidad y su gran resistencia química han favorecido su presencia en el mercado [36]. Sin embargo, la previsible extinción de las reservas de petróleo del planeta, como consecuencia del elevado consumo de estas frente a la capacidad de la naturaleza para su producción, han generado la necesidad de reemplazar estas matrices fósiles por matrices de origen renovable [37].

Tabla 1. Demanda europea de plásticos en porcentaje. En otros se incluyen polimetilmetacrilato, policarbonato, tereftalato de polibutileno y otros polímeros de menor producción.

Polímeros	Demanda Europea de Polímeros (%)
Polipropileno	19,3
Polietileno de baja densidad	17,5
Polietileno de alta densidad	12,3
Policloruro de vinilo	10,0
Poliuretanos	7,5
Tereftalato de polietileno	7,4
Poliestireno	6,7
Poliamidas	2,0
Otros	17,3

En este sentido, existen una gran variedad de rutas sintéticas y materias primas para la producción de polímeros de origen renovable. Halley P.J. y Dorgan J.R. [38] propusieron una breve clasificación en función de la cantidad de etapas necesarias para su producción. De esta forma, se clasifican en 3 tipos: 1 etapa, 2 etapas y 3 etapas (figura 2).

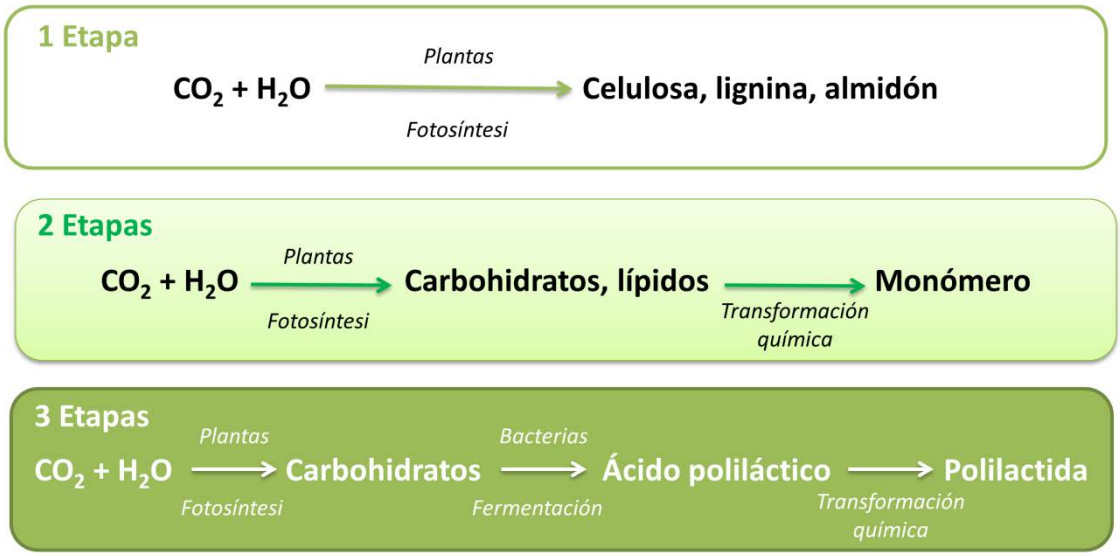

Figura 2. Clasificación por etapas propuesta por P.J. Halley y J.R. Dorgan [38].

En la clasificación desarrollada por Halley P.J. y Dorgan J.R., se consideraron como materiales poliméricos producidos por una única etapa a aquellos polímeros que son producidos por los organismos vegetales o bacterianos a través de la fotosíntesis (celulosa, lignina o almidón). La utilización de estos polímeros en otros sectores tales como, la celulosa y el almidón en la producción de papel o en el sector alimentario es ampliamente conocida. Sin embargo, polímeros obtenidos mediante la fotosíntesis de las plantas como el almidón y la lignina pueden también ser plastificados de forma simple, obteniendo un material capaz de ser procesado mediante las técnicas de transformación habituales en materiales plásticos. Aunque la producción de estos materiales termoplásticos basados en polímeros obtenidos mediante la fotosíntesis presentan un bajo coste de producción, sus propiedades mecánicas (una σ_t^C de alrededor 10 MPa y un E_t^C inferior a 1 GPa) son también sustancialmente inferiores a las de los polímeros de origen fósil [38–41]. Además, son muy susceptibles a la

humedad [38]. A pesar de ello, a día de hoy ya se pueden encontrar algunos ejemplos a nivel industrial de su comercialización, como por ejemplo, bolsas de almidón de patata con el objetivo de reducir el material plástico desechado.

Por otra parte, en el caso de las rutas sintéticas de 2 y 3 etapas, mostradas en la figura 2, el monómero del polímero se produce a través de varias etapas de síntesis química o biotecnológica a partir de fuentes ricas en carbohidratos y lípidos, como pueden ser los residuos agrícolas y forestales. Por otra parte, la producción de materiales plásticos a partir de estos residuos permite dotar-los de valor añadido. De esta forma, la producción de polilactidas como el ácido poliláctico (PLA) se produce en 3 etapas. Inicialmente, los carbohidratos de la celulosa y hemicelulosa son hidrolizados para la obtención del azúcar simple, que posteriormente será fermentado para obtener ácido láctico. A partir de éste, se produce la lactida, que es polimerizada obteniendo el polímero final [42]. En el caso del PLA, sus elevadas propiedades mecánicas, origen renovable y biodegradabilidad lo han situado como el polímero de origen renovable más prometedor del sector. Actualmente, el PLA se encuentra bien instalado en el mercado y con una enorme previsión de crecimiento para los próximos años. Las previsiones actuales para el 2019 sitúan la producción anual de PLA alrededor de los 6 millones de toneladas [42].

Aunque tal y como se ha mencionado anteriormente las poliolefinas se obtienen usualmente del petróleo, existen hoy en día poliolefinas producidas a partir de materiales de origen renovable. Uno de estos casos, es el PE comercializado por Braskem bajo la marca I'm green™ PE [43]. El PE de origen renovable es producido a partir de un proceso de 2 etapas, durante el cual, los carbohidratos obtenidos generalmente de residuos derivados de la actividad agrícola son fermentados mediante la acción de bacterias o enzimas hasta la obtención de etanol [44]. Seguidamente, el etanol es deshidratado obteniendo el monómero de etileno [45]. La única diferencia entre el PE de recursos fósiles y el PE de recursos renovables se encuentra en el proceso de obtención del monómero, ya que el proceso de polimerización es el mismo y en el caso de Braskem, se produce en la misma planta. A pesar de ser una alternativa con un mayor grado de sostenibilidad que el PE de recursos fósiles, este producto se encuentra limitado por la capacidad y precio de la producción de etanol. A día de hoy, la planta de Braskem es capaz de producir solamente 200000 toneladas de PE de origen renovable por año, un valor muy reducido en comparación con la demanda europea de PE que actualmente ronda los 17 millones de toneladas.

Por otro lado, tal y como se ha mencionado, las rutas sintéticas de polímeros clasificados por Halley P.J. y Dorgan J.R. como polímeros de 2 etapas (figura 2), la materia prima para obtener el monómero puede provenir de lípidos. Estos lípidos, abundan en los aceites extraídos de las semillas de las plantas. En este sentido, uno de los aceites más utilizados para la producción de compuestos químicos y polímeros es el aceite de ricino [46,47]. A partir de estos lípidos, que generalmente son cadenas de carbono (C) considerablemente largas (entre 18 y 22 C), se pueden producir monómeros de entre 4 y 12C mediante un craqueo químico o un ataque enzimático. Algunos ejemplos de este tipo de polímeros producidos a partir de lípidos son poliésteres como el polisuccinato de butileno (PBS) o las poliamidas (PA) parcial o totalmente de origen renovable (bioPA) como la poliamida 6.10 (PA6.10) que contiene un 62% de C de origen renovable [48] o la poliamida 11 (PA11) que es 100% renovable. Las PA son polímeros de altas prestaciones con elevadas propiedades mecánicas y estabilidad térmica: con una σ_t^C que puede variar entre los 35-60MPa y en general unas T_m superiores a los 200ºC. Sin embargo, estas elevadas de T_m dificultan la producción de materiales compuestos sin la degradación de las fibras celulósica.

Finalmente, tal y como se muestra en la figura 1, aunque los estudios en este campo son bastante recientes, la evolución hacia materiales plásticos compuestos sostenibles tiende a la producción de materiales compuestos con polímeros de origen renovable y fibras celulósicas. Generalmente, las investigaciones se han centrado en el refuerzo de matrices de PLA y otros poliésteres [49–52] debido a la biodegradabilidad de estas matrices, dando lugar a materiales compuestos totalmente de origen renovable y biodegradables. Aunque las propiedades mecánicas de estos materiales plásticos se ven incrementadas mediante la incorporación de fibras naturales, y pueden llegar a alcanzar valores similares a los de los compuestos de PP-GF con un agente de acoplamiento en la formulación, la capacidad de refuerzo de estas es menor que el observado cuando son incorporadas en matrices como poliolefinas [34,53]. Este hecho, se encuentra probablemente relacionado con una calidad inferior de la interfase, debido a que los poliésteres interactúan con las fibras a través de enlaces intermoleculares débiles como las fuerzas de Van der Waals [54]. Algunos autores, han propuesto el uso de tratamientos superficiales en la fibra o agentes de acoplamiento para los compuestos de PLA [55,56].

Por otra parte, las bioPA y el PE de origen renovables no son biodegradables, por lo que los materiales compuestos que se podrían obtener deberían ser destinados a la fabricación de

productos con una vida útil superior y se debería evaluar su reciclabilidad. Sin embargo, en el caso de las PA, actualmente se han llevado a cabo pocas investigaciones, principalmente por la elevada temperatura de fusión (T_m) de las PA, superior en algunos casos a la degradación de las fibras. No obstante, algunas PA de larga cadena tienen puntos de fusión relativamente bajos que pueden permitir su refuerzo con fibras celulósicas. Además, debido a la capacidad de las PA de establecer enlaces de hidrogeno, la interfase producida en estos compuestos es significativamente mejor que la obtenida en poliésteres, descartando la necesidad de un agente de acoplamiento con esta matriz [57].

1.2 Objetivos

El objetivo principal de la presente tesis es la producción y caracterización de materiales compuestos sostenibles a partir de PA11 y reforzados con fibras mecánicas de alto rendimiento (SGW). Se pretende que estos compuestos puedan ser una alternativa de origen totalmente renovable a los materiales compuestos de PP reforzado con fibra de vidrio (GF).

De acuerdo con el objetivo general de la tesis, se plantean los siguientes objetivos específicos:

- La obtención de materiales compuestos de PA11 reforzados con SGW. Como continuación de este objetivo específico, se pretende alcanzar una buena interfase fibra-matriz sin la necesidad de modificar la fibra o la matriz. Además, estos materiales compuestos se extrudirán en un mezclador multicinético evitando el uso de extrusoras co-rotativas. Finalmente, su transformación tendrá lugar mediante un proceso de inyección.
- Se establecerá el límite de refuerzo en el material compuesto (w/w, relación peso de la fase respecto el peso total).
- Para cada compuesto, se determinarán las propiedades mecánicas a nivel macroscópico mediante el uso de los ensayos a tracción, flexión e impacto. Se analizará la resistencia, los módulos elásticos y la deformación a tracción y flexión. En el caso del ensayo a impacto, se determinará la resistencia a impacto en muestras entalladas y sin entallar.
- La modelización del comportamiento de la resistencia a tracción, para la obtención de la tensión interfacial de cizalla (τ), la resistencia intrínseca media de las fibras (σ_t^F) y el factor de acoplamiento (f_c).

- Se modelizará el comportamiento del E_t^C y el módulo elástico a flexión (E_f^C), lo cual permitirá la obtención de los factores de eficacia (η_e), orientación (η_0) y longitud (η_l) de la regla de las mezclas, así como el módulo intrínseco de la fibra a tracción (E_t^F) y a flexión (E_f^F).
- Se determinará la resistencia intrínseca a flexión, "teórica", de las fibras de SGW (σ_f^F), lo cual debe permitir los factores de acoplamiento de los materiales compuestos a flexión (f_c^f).
- Se caracterizará la composición química superficial de las fibras. Esta caracterización permitirá dirimir el tipo de interacción entre fibra y matriz en la interfase.
- El estudio de la estabilidad térmica y el comportamiento termomecánico de los materiales compuestos obtenidos y el efecto de las fibras en las principales transiciones térmicas de la matriz de PA11. El estudio se lleva a cabo mediante el análisis termogavimétrico (TGA), la calorimetría diferencia de rastreo (DSC) y el ensayo dinámico termomecánico (DMTA).
- Se determinará la microestructura de los compuestos de PA11-SGW y la influencia de las fibras en ésta. Para ello se empleará el DSC, la difracción de rayos X (XRD) y la espectroscopia de infrarrojo con la transformación de Fourier (FT-IR).
- El análisis del comportamiento térmico y termomecánico y el efecto en la microestructura de los compuestos tras un proceso térmico (*annealing*) según las técnicas descritas en los objetivos anteriores.
- Se estudiará la cinética de absorción de agua en función del contenido de fibra y de la temperatura, teniendo en cuenta la polaridad de la matriz PA11 y de las fibras SGW. Para ello se modelizarán las curvas de absorción de agua mediante el model de Fick.
- Se determinará la idoneidad de los compuestos de PA11-SGW a través de la modelización teórica de una pieza de coche obtenida con los materiales desarrollados y comparándolos con los compuestos de PP-GF. Además, un análisis de ciclo de vida (LCA) se realizará para la pieza estudiada.

1.3 Justificación de la tesis doctoral

El grupo de investigación LEPAMAP (Laboratori d'Enginyeria Paperera i Materials Polímerics), dónde se ha llevado a cabo esta tesis doctoral, ha estado trabajando en la producción y caracterización de materiales compuestos des del año 2003. Tras una larga

experiencia en materiales compuestos de poliolefinas y fibras celulósicas [22,58–61], la investigación en materiales compuestos en los últimos años en el grupo se ha dirigido hacia la obtención de materiales compuestos totalmente de origen renovable. Por un lado, se ha indagado en el uso de matrices de orígenes renovables y biodegradables, como es el caso del PLA.

Por otra parte, el carácter biodegradable de los compuestos de fibras de celulosa con PLA representa un inconveniente en aplicaciones de larga duración. Es por este motivo, que en el estudio de materiales compuestos para estas aplicaciones las matrices de origen renovable pero no biodegradable son una alternativa más deseable. Con el objetivo de substituir el PP-GF, una de las alternativas a considerar como matriz son las bioPA. Las PA son una familia de polímeros con enlaces amida como grupo funcional y están formadas por uno o dos monómeros. Además, están consideradas como polímeros de elevadas prestaciones, tal y como se ha mencionado anteriormente, debido a las buenas propiedades mecánicas, resistencia química y estabilidad térmica que estas presentan. Por otra parte, a pesar de no ser biodegradables [62], las PA si son reciclables [63]. Estas elevadas propiedades mecánicas son principalmente como consecuencia de la capacidad de establecer enlaces de hidrógeno del grupo amida, que permite que estos se establezcan entre las cadenas de PA. Sin embargo, a su vez la presencia de estos enlaces son también una de las causas de las elevadas $T_{m,}$ de las PA. Además, esta capacidad de establecer enlaces de hidrogeno incrementa la higroscopicidad de estos materiales [63].

No obstante, existen PA con Tm inferiores a 200ºC y que se encuentran desde hace años disponibles en el mercado (tabla 2). Las propiedades mecánicas y térmicas de las PA disminuyen al incrementar el número de grupos metilo en la cadena alifática, ya que se reduce la densidad de los enlaces de hidrogeno generados [63]. Por ello, es necesario el uso de PA con monómeros de larga cadena si se quieren obtener compuestos de PA reforzados con fibras celulósicas.

Tabla 2. Poliamidas de mayor consumo. Se indica su contenido de C de origen renovable y su T_m.

Poliamida	Porcentaje de origen renovable (%)	T_m (ºC)
Poliamida 6	0	218
Poliamida 6.6	0	258
Poliamida 6.10	62	206
Poliamida 10.10	> 99	191
Poliamida 11	100	183
Poliamida 12	0	176

De entre las PA con temperaturas de fusión aptas para la producción de compuestos reforzados con fibras celulósicas, se encuentra la PA11, que es totalmente de origen renovable. Al igual que las otras poliamidas, es un polímero de elevadas prestaciones y aunque tiene una menor σ_t^C (38 MPa) que las PA6 o PA6.6, tiene una mayor tenacidad (U_T). La producción de materiales compuestos a partir de PA11 y fibras naturales representa la obtención de unos materiales totalmente sostenibles, pues ambas fases provienen de recursos naturales renovables y sus materiales compuestos podrían ser reciclados. Además, debido a la capacidad de las PA de producir enlaces de hidrógeno y su carácter ligeramente más polar que otras matrices, no es necesario el uso de agentes de acoplamiento para obtener una buena interfase.

La PA11 se fabricó por primera vez en 1947 y hace más de 75 años que se produce industrialmente y que se encuentra disponible en el mercado [48,64]. Esta tipología de PA es comercializada principalmente por Arkema S.A. bajo la marca Rilsan®, siendo este su producto más destacado hoy en día. Su producción anual se sitúa en aproximadamente las 21.000 toneladas [65]. Comúnmente, se ha utilizado para aplicaciones en tuberías de gas y petróleo, piezas del sector de la automoción y en medicina, debido a la biocompatibilidad con el cuerpo humano.

Por otra parte, es remarcable la no utilización de cultivos alimentarios para la producción de esta PA. El monómero de la PA11, el ácido aminoundecanoico (figura 3), se produce a partir del aceite de ricino. El ricino es una planta de poco interés para el consumo humano o animal (su semilla es tóxica para el consumo humano y animal y solamente pequeñas dosis del aceite son aceptables para el cuerpo humano [46]). Cada semilla contiene alrededor del 50% de aceite del cual su componente mayoritario es el ácido ricinoleico (alrededor del 85-90%) [47,64].

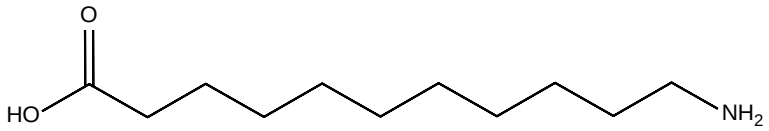

Figura 3. Ácido aminoundecanoico, el monómero de la PA11.

La utilización de fibras celulósicas SGW como refuerzo para esta PA, se desprende de los buenos resultados obtenidos previamente en PP. Estos resultados fueron muy similares e incluso superiores a los alcanzados con otras fibras celulósicas tratadas cuando fueron utilizadas como refuerzo en PP [15,22,59,60]. Estas fibras SGW de alto rendimiento sometidas solamente a un proceso mecánico de muela de piedra, mantienen casi intacta su composición química inicial. Su morfología es bastante irregular, observándose fibras con una superficie bastante irregular y una abundante cantidad de finos (figura 4).

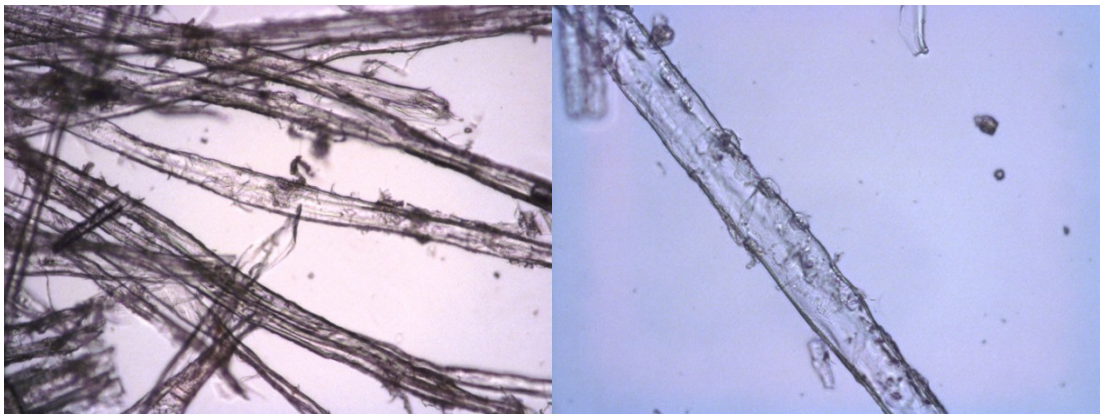

Figura 4. Microfotografías ópticas de fibras SGW a 100 aumentos (izquierda) y a 200 aumentos (derecha).

A pesar de que el alto contenido en lignina de estas fibras mecánicas (tabla 3) puede inhibir las interacciones entre la celulosa y la matriz [22], dando como resultado peores propiedades mecánicas de las deseadas, se ha observado que el mayor carácter apolar de las fibras lignocelulósicas favorece la dispersión del material en el interior de la matriz [34]. En el caso de la PA11, pruebas previas mostraron una dificultad de dispersión de fibras celulósicas blanqueadas, observándose aglomeraciones de las fibras detectables a simple vista en el material.

Tabla 3. Composición química en superficie y global de una fibra maderera conífera [66].

Componente	Composición en superficie (%)	Composición global (%)
Celulosa	40,8	41-46
Hemicelulosa	27,6	25-32
Lignina	27,6	26-31
Extractivos	0,69	10-15

Además, estas fibras celulósicas de alto rendimiento son normalmente utilizadas en el sector papelero y, aunque no representan una valorización de un residuo, su producción está asegurada a nivel industrial con un coste muy bajo además de provenir de una producción sostenible y tener un rendimiento superior al 95%. También, hay que tener en cuenta que, aunque es posible que el uso de unas fibras con menor contenido en lignina derivara en mejores resultados, puede que esta mejoría no fuese suficiente teniendo en cuenta la generación de residuos durante el tratamiento y el incremento en el coste de las fibras, y en resultado del material compuesto.

1.4 Estado del arte

El manifiesto éxito en la utilización de materiales compuestos inicialmente poliolefinas reforzadas con GF y posteriormente con fibras celulósicas, atrajeron el interés hacia otras matrices poliméricas como las PA [67]. En este sentido, a pesar de sus elevadas propiedades

mecánicas, las PA son incapaces de reemplazar sin un refuerzo los materiales metálicos [63]. El refuerzo de las poliamidas 6 y 6.6 (PA6 y PA6.6), las más estudiadas y de mayor consumo [68], con GF fue logrado rápidamente de forma exitosa. No obstante, al igual que en el caso de las poliolefinas, atendiendo a los principios de sostenibilidad, el siguiente paso fue el uso de refuerzos más sostenibles como las fibras celulósicas. Los primeros estudios en este sentido se iniciaron en 1984 [69]. Desafortunadamente, las elevadas temperaturas de fusión (T_m) de la PA6 y la PA6.6 impidieron su refuerzo con fibras celulósicas sin que estas sufrieran una elevada degradación durante el proceso [69,70]. Aunque finalmente se consiguió la producción de materiales compuestos de PA6 y PA6.6 con fibras naturales, en muchos casos fue necesario el uso de fibras modificadas o celulosa pura para incrementar la temperatura de degradación de las fibras; el uso de varios aditivos que disminuyeran la T_m o procesados con varias etapas [67,70–72]. En cualquier caso, todas las alternativas incrementaron considerablemente el coste de los materiales compuestos respecto a los conseguidos con plásticos "*commodity*". Además, hay que tener en cuenta que el precio de los polímeros de alto rendimiento son superiores a los precios de dichos "*commodity*" [70,73]. La obtención de materiales compuestos de PA reforzados con fibras naturales sin incrementar el coste y el tiempo de procesado es imposible actualmente si no se emplean PA con T_m inferiores a los 200ºC.

No obstante, los estudios sobre estas poliamidas de baja Tm reforzadas con fibras celulósicas son más bien escasos. Los primeros estudios fueron llevados a cabo con poliamida 12 (PA12) en 1985 [74] y no fue hasta el año 2006 que volvieron a recuperar interés a nivel científico con estudios sobre materiales compuestos producidos mediante PA12 y materiales celulósicos [75]. Estas investigaciones se centraron en el refuerzo de la PA12 con fibras de viscosa, empleando un agente de acoplamiento para favorecer la dispersión y la interfase del material. Años más tarde, se probó su refuerzo con nanofibras de celulosa (CNF) sin y con tratamientos superficialmente con un reactivo catiónico. Aunque se logró aumentar ligeramente las propiedades mecánicas, los mejores resultados fueron obtenidos cuando se utilizaron nanoarcillas y CNF modificadas conjuntamente [76].

Este poco interés en la producción de materiales compuestos de PA12 reforzados con fibras naturales, por parte de la comunidad científico-tecnológica, puede estar relacionado con el origen fósil. En este sentido, en el caso de las bioPA, existen más investigaciones, aunque en general estas fueron realizadas a partir del 2013. Ese año, Panaitescu D.M et al. [77]

reforzaron la PA11 con CNF mezclándolas directamente en un plastógrafo sin el uso de agente de acoplamiento. Los materiales obtenidos fueron transformados posteriormente mediante un proceso de moldeado por compresión. En este estudio se observó un ligero incremento en la σ_t^C y en el E_t^C (de 4 MPa y 0,5 GPa aproximadamente) como consecuencia de la presencia de CNF. En un siguiente trabajo consiguieron aumentar las propiedades de los materiales compuestos mediante un *annealing* [78]. A pesar de ello, las propiedades no fueron lo suficientemente competitivas comparadas con las que se obtienen con fibras de tamaño microscópico en otros materiales compuestos. Feldmann M. et al. [79] reforzaron PA10.10 y PA6.10 con viscosa empleando un compuesto superficial en las fibras, observando incrementos significativos en las propiedades mecánicas de los materiales compuestos, a pesar de que la adhesión en las fibras fue relativamente pobre incluso con el tratamiento superficial en las fibras. Tal y como se puede observar en las imágenes de microscópio electrónico de barrido (SEM) donde se muestran los agujeros creados por el deslizamiento de fibras. Feldmann M. continuó la investigación en PA10.10 cambiando el sistema de mezclado (pasó a utilizar una extrusora de doble fuso) y mediante su optimización, logró obtener materiales compuestos sin el uso de un agente de acoplamiento [80]. Estos materiales alcanzaron σ_t^C superiores a los 90 MPa con un 30% w/w de viscosa, partiendo de una matriz con una σ_t^C de 50 MPa. Aunque la σ_t^C de la PA10.10 reforzada con un 30% w/w de GF presenta valores de 135 MPa, la ε_t^C se reduce a un 2%. En cambio, en los materiales compuestos reforzados con viscosa, la ε_t^C es de un 6%.

En 2015, Zierdt P. et al. [81] produjeron por primera vez de forma exitosa materiales compuestos de PA11 y fibras de haya de tamaño micrométrico utilizando una mezcladora interna y posteriormente transformando los materiales con inyección. En este estudio se utilizaron fibras de haya y fibras de haya modificadas mediante un tratamiento químico. En los resultados obtenidos se observaron incrementos considerables de la σ_t^C y del E_t^C al aumentar el contenido de fibra en el compuesto (hasta 65 MPa y 5 GPa respectivamente con un 50% w/w de refuerzo). Además, estos incrementos se produjeron sin el uso de un agente de acoplamiento en la formulación. Estos resultados demostraron la viabilidad de producir materiales compuestos totalmente sostenibles empleando PA11 como matriz. Es importante mencionar que en el análisis térmico no observaron tampoco ninguna degradación de las fibras a las temperaturas de procesado. Cherizol R. et al. [82] el mismo año evaluaron los parámetros de procesado y el efecto de la morfología de la fibra en el procesado de materiales

compuestos de PA11 y fibras celulósicas de alto rendimiento empleando una extrusora de doble husillo. Los compuestos de PA11 presentaron valores de viscosidad aceptables en todos los casos que indicaban la facilidad de procesado a pesar de la morfología de la fibra. Al año siguiente, Le Duigou A. et al. [83] evaluaron la interacción entre la PA11 y una malla fabricada con fibras de lino y, posteriormente en otro trabajo, su reciclado en comparación con compuestos de PP reforzados con la misma malla de lino [84]. El valor de resistencia interfacial fue elevado indicando la capacidad de interacción entre las fibras y la matriz. Los resultados de E_t^C y viscosidad fueron similares a los alcanzados con los compuestos de PP manteniendo los ciclos de reciclado. Estos resultados evidenciaron la capacidad de reciclaje de estos compuestos. Por otro lado, los resultados de σ_t^C fueron muy superiores a los obtenidos anteriormente por Zierdt P. et al. [81], casi 4 veces, debido a la orientación de las fibras de la malla. Finalmente, Armioun S. et al. [85,86] produjeron también materiales compuestos de PA11 y fibras madereras, y compuestos híbridos con fibras de carbono, pero sus resultados en los materiales de PA11 y fibras madereras fueron inferiores a los alcanzados anteriormente debido a un gran volumen hueco en los materiales compuestos (con un 30% w/w de refuerzo tienen una σ_t^C de 46 MPa mientras que anteriormente se habían observado σ_t^C entre 53 y 57 MPa).

1.5 Estructura de la investigación

La presente tesis se encuentra enfocada en la formulación de compuestos de PA11 reforzada con fibras SGW de pino. Estas formulaciones no tienen en cuenta el uso de un agente de acoplamiento debido a la capacidad de la PA11 de establecer enlaces de hidrogeno con las fibras que puede ser suficiente para producir una interfase adecuada. En la figura 5, se presenta de forma esquematizada la estructura de la investigación.

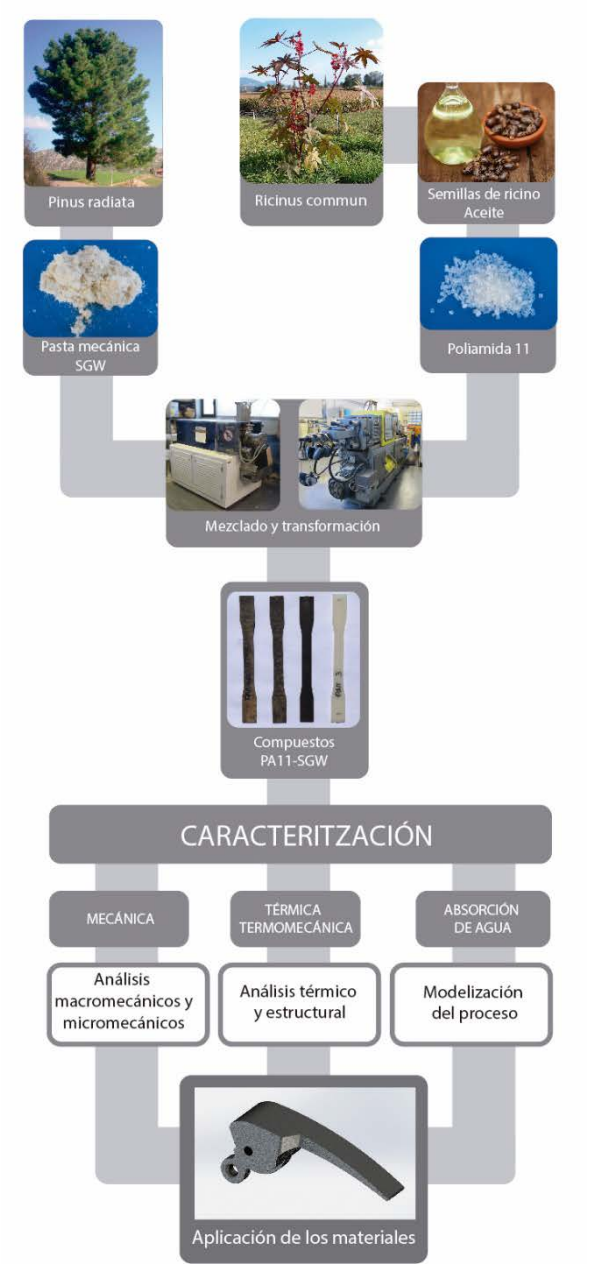

Figura 5. Esquema de la estructura de la tesis doctoral.

Para la realización de esta tesis, se formularon diferentes materiales compuestos con contenidos de fibra variando del 20 al 60% w/w y se caracterizaron sus propiedades mecánicas y termomecánicas y se estudió la absorción de agua de estos materiales. El objetivo de su caracterización fue, además de conocer el comportamiento mecánico, térmico y el de absorción de agua de los materiales, estudiar el efecto de las fibras sobre estos.

Tras la producción de los materiales compuestos y su transformación, se midió su σ_t^C, ε_t^C y U_T. Al tratarse de fibras leñosas en las que la composición química no se ha visto modificada, el alto contenido en lignina, compuesto que recubre superficialmente las fibras celulósicas [87], podía inhibir la interacción entre la celulosa y la PA11, no obteniendo cambios en la resistencia de los materiales respecto a la matriz y disminuyendo su U_T. Tras el resultado positivo obtenido, debido a un aumento lineal de la resistencia que se debía a una buena interacción entre las dos fases del compuesto, se realizó el estudio micromecánico mediante el modelo de Kelly-Tyson [88], basado en la regla de las mezclas modificada (RoM) y se resolvió mediante el método propuesto por Bowyer y Bader [89]. Este modelo permitió el cálculo de la tensión interfacial de cizalla (τ), indicativo de la calidad de las interacciones entre la matriz y el refuerzo, la σ_t^F, y el factor de compatibilidad (f_c), todas incógnitas en la RoM. Paralelamente, se estudió la composición química superficial de la fibra mediante espectroscopia fotoelectrónica de rayos X (XPS) con el objetivo de comprender la química de la interfase. Además, se estudió y evaluó el efecto de incluir o excluir las fibras de menor longitud llamadas finos en la modelización y la aportación de éstos finos en la resistencia del material compuesto, teniendo su inclusión un cambio significativo en los resultados. Tras ello, se analizó la predicción obtenida mediante los modelos con los resultados experimentales obtenidos. De todos estos resultados, se desprende la primera publicación de esta tesis doctoral: "*Tensile properties and micromechanical analysis of stone groundwood from softwood reinforced bio-based polyamide11 composites*" [90].

Tras los resultados obtenidos de la resistencia a tracción, se valoró el incremento de rigidez mediante el módulo de Young (E_t^C) en los materiales compuestos en función del contenido de fibra, así como la disminución de la deformación. Seguidamente, se estudió el efecto de las fibras en el módulo del compuesto a través del FTMF (Fiber Tensile Modulus Factor) y se compararon los resultados con los de los *commodities* de PP reforzado con GF. Además, se calculó el módulo a tracción intrínseco de la fibra SGW (E_t^F), difícil de determinar experimentalmente, mediante los modelos de Hirsch y Tsai Pagano [91,92], para observar el efecto en el cálculo de incluir o excluir la morfología de las fibras. En el segundo artículo titulado "*Stiffness of bio-based polyamide 11 reinforced with softwood stone ground-wood fibres as an alternative to polypropylene-glass fibre composites*" [93] se publicaron los resultados obtenidos que indicaban una factibilidad por parte de los compuestos de PA11

reforzada con fibras naturales como una posible alternativa más sostenible y respetuosa con el medio ambiente que el polipropileno reforzado con fibra de vidrio.

En el tercer artículo, *"Evaluation of thermal and thermomechanical behaviour of bio-based polyamide 11 based composites reinforced with lignocellulosic fibres"* [94], se publicaron los resultados de las propiedades térmicas y termomecánicas de los compuestos. La PA11 tiene una T_m de 189ºC, una temperatura relativamente baja comparada a otras poliamidas. Aunque esta T_m es inferior, es muy cercana a la de inicio de degradación de las fibras lignocelulósicas (200ºC) [95], por lo que durante el procesado de los materiales podría producirse una degradación del refuerzo que afectaría a las propiedades de los compuestos. Además, las propiedades del refuerzo y su interacción con la matriz polimérica han demostrado en la literatura que pueden influenciar las principales temperaturas de transición de la matriz, su cristalinidad, estabilidad térmica e incluso estructura [70,73,96–98]. La estabilidad térmica de los compuestos se midió mediante el TGA de la PA11 y se comparó con los compuestos reforzados con un 20 y un 50% w/w de contenido en fibra. Para los ensayos de DSC y DMTA se fabricó el compuesto con un 10% w/w de fibra para observar el efecto de muy bajos contenidos de estas en el material compuesto. La estructura de las regiones cristalinas de la PA11 varían en función de la orientación del enlace de hidrogeno [99], por lo que la interacción de las fibras podía tener un efecto sobre la estructura. La estructura de la PA11 y sus compuestos se analizó mediante XRD y se complementó con el FT-IR. Posteriormente, se aplicó un *annealing*, y se repitieron los ensayos de DSC, DMA y XRD para las muestras tratadas.

Tras el estudio de las propiedades a tracción y termomecánicas, era importante conocer el efecto de las fibras en las propiedades a flexión e impacto, propiedades de gran relevancia para el diseño y desarrollo de productos [28]. El análisis de la resistencia a flexión σ_f^C y su comparativa con productos comerciales se presentó en el artículo: "*Towards more sustainable material formulations: A comparative assessment of PA11-SGW flexural performance versus Oil-based composites"* [100]. La σ_f^C, la deformación (ε_f^C) y densidad (ρ^C) de la PA11 y de sus compuestos se analizó respecto el contenido de fibra. Debido a que solo las muestras con un contenido mayor al 30% w/w de fibra colapsaban durante el ensayo, se analizó la resiliencia (U_R) en vez de la U_T. Seguidamente se comparó con productos de ámbito comercial como lo son el PP reforzado con GF y fibras naturales como el SGW. Se observó la necesidad de incrementar el contenido de fibra en los compuestos de PA11-SGW

para conseguir resultados similares. Este hecho llevó al estudio de la contribución de la fibra en la resistencia del material compuesto mediante el FFSF (Fibre Flexural Strength Factor). A partir de él se calculó la σ_f^F y el factor de acoplamiento (f_c^f) y se compararon con los hallados previamente en la literatura para fibras de SGW y GF [101,102].

El E_f^C se evaluó en el artículo: "Study of the flexural modulus of lignocellulosic fibres reinforced bio-based polyamide11 green composites". Al igual que en el caso de la σ_f^C, el E_f^C es más relevante que su análogo a tracción para el diseño y desarrollo de productos [28]. Se analizó el E_f^C de los materiales compuestos respecto al contenido de fibra. Estos resultados se compararon con los obtenidos en compuestos de PP-GF y PP-SGW. Al igual que en el caso de la σ_f^C se observó la necesidad de incrementar el contenido de fibra en el material para alcanzar valores similares. No obstante, se observó una menor contribución de la fibra SGW en los materiales de PA11 que en los de PP. Este fenómeno se corroboró de nuevo mediante el FFMF (Fibre Flexural Modulus Factor). El modelo de Hirsch permitió obtener el E_f^F y los η_e, η_l y η_0. El resultado de E_f^F podía verse afectado por la presencia de volumen vació en el material por lo que se realizó una estimación de éste en los materiales compuestos.

Las propiedades a impacto fueron evaluadas en un posterior artículo, conjuntamente con la absorción de agua de los compuestos de PA11 y SGW y sus resultados fueron descritos en el artículo: "*Fully bio-based composites from PA11-SGW: Notable impact strength and water uptake"*. La energía absorbida por la matriz de PA11 y los materiales compuestos se estudió mediante el test Charpy, con entalla y sin entalla. Ambos ensayos permitieron calcular la energía necesaria para iniciar una fractura en el material. Por otro lado, está más que aceptado que el agua actúa como plastificante en materiales plásticos disminuyendo generalmente sus propiedades mecánicas [103], por lo que es de importancia el estudio de su absorción. Para ello se realizaron los ensayos a 23ºC y 40ºC, temperatura cercana a la T_g de la PA11, y se estudiaron sus cinéticas y curvas de absorción. Previamente, también se valoró mediante ángulo de contacto el comportamiento hidrófilo de la PA11 y sus compuestos a 20,50 y 60% w/w de contenido en fibra de SGW. Finalmente, con los resultados obtenidos de la modelización de los ensayos de absorción de agua, se pudo establecer la energía necesaria para iniciar el proceso de difusión de la PA11 y los compuestos de PA11-SGW.

Finalmente, la capacidad de los materiales de PA11-SGW a reemplazar compuestos comerciales se comprobó mediante la simulación de un producto. En el artículo "*Research on*

the use of bio-polyamide 11 reinforced with lignocellulosic fibers composites in automotive parts. The case of a car doors handle" se describen los resultados de esta simulación con una maneta interior de coche, utilizando los compuestos de PA11-SGW. Para establecer los requerimientos de la pieza, se comparó con los resultados obtenidos con la misma pieza por compuestos de PP-GF. El diseño del producto se hizo en similitud con otras manetas actuales. Una vez se obtuvo el diseño técnico en papel, se realizó la simulación en tres dimensiones mediante el uso del software SolidWorks®. En el mismo software se realizó la simulación de análisis de elementos finitos a dos fuerzas diferentes 20 N y 70 N. Los 70 N corresponden a un valor superior al máximo que puede realizar una persona adulta con los dedos de la forma que abrimos la maneta [104], mientras que los 20 N corresponden a una fuerza superior a la que se realiza habitualmente. Posteriormente, mediante la base de datos del software y el análisis de ciclo de vida realizados por Arkema S.A. [64] sobre la PA11 permitió estimar la sostenibilidad de los materiales ensayados suponiendo su producción en Europa y compararla con los producidos con PP-GF.

1.6 Bibliografía

1. American Chemistry Council Responsable Care. Guiding principles. Available online: https://responsiblecare.americanchemistry.com/Guiding-Principles/.

2. Keeble, B. R. The Brundtland Report: "Our Common Future." *Med. War* **1988**, *4*, 17–25, doi:10.1080/07488008808408783.

3. European Technology Platform for Sustainable Chemistry SusChem Available online: http://www.suschem.org/.

4. Anastas, P. T.; Warner, J. C. *Green Chemistry: Theory and Practice*; New York: Oxford University Press, Ed.; New York: Oxford University Press, 1998;

5. Anastas, P. T.; Zimmerman, J. B. Design through the 12 principles of green engineering. *IEEE Eng. Manag. Rev.* **2007**, *35*, 16, doi:10.1109/EMR.2007.4296421.

6. Association of Plastics Manufacturers in Europe & European Association of Plastics Recycling and Recovery Plastics- the Facts 2017 2017, 1–44.

7. European Commission A European Strategy for Plastics in a Circular Economy. *COM(2018) 28 Final* 2018, *SWD(2018)*, 1–18.

8. Lubin, G. *Handbook of Composites*; Lubin, G., Ed.; Springer US: Boston, MA, 1982; ISBN 978-1-4615-7141-4.

9. Matthews, F. L.; Rawlings, R. D. Overview. In *Composite Materials*; Elsevier, 1999; pp. 1–28.

10. Rothon, R.; DeArmitt, C. Fillers (Including Fiber Reinforcements). In *Brydson's Plastics Materials*; Elsevier, 2017; pp. 169–204 ISBN 9780323358248.

11. Wang, R.-M.; Zheng, S.-R.; Zheng, Y.-P. Introduction to polymer matrix composites. In *Polymer Matrix Composites and Technology*; Elsevier, 2011; pp. 1–548 ISBN 9780857092212.

12. Sapuan, S. M. Composite Materials. In *Composite Materials*; Elsevier, 2017; Vol. 72, pp. 57–93 ISBN 9780128025079.

13. Ribeiro, M.; Fiúza, A.; Ferreira, A.; Dinis, M.; Meira Castro, A.; Meixedo, J.; Alvim, M. Recycling Approach towards Sustainability Advance of Composite Materials' Industry. *Recycling* **2016**, *1*, 178–193, doi:10.3390/recycling1010178.

14. Thomason, J.; Jenkins, P.; Yang, L. Glass Fibre Strength—A Review with Relation to Composite Recycling. *Fibers* **2016**, *4*, 18, doi:10.3390/fib4020018.

15. López, J. P.; Méndez, J. A.; El Mansouri, N. E.; Mutjé, P.; Vilaseca, F. Mean intrinsic tensile properties of stone groundwood fibers from softwood. *BioResources* **2011**, *6*, 5037–5049.

16. Kuciel, S.; Kuzniar, P.; Liber-Kneć, A. Polyamides from renewable sources as matrices of short fiber reinforced biocomposites. *Polimery* **2012**, *57*, 627–634, doi:10.14314/polimery.2012.627.

17. Thomason, J.; Jenkins, P.; Yang, L. Glass Fibre Strength—A Review with Relation to Composite Recycling. *Fibers* **2016**, *4*, 18, doi:10.3390/fib4020018.

18. Joshi, S.; Drzal, L.; Mohanty, A.; Arora, S. Are natural fiber composites environmentally superior to glass fiber reinforced composites? *Compos. Part A Appl. Sci. Manuf.* **2004**, *35*, 371–376, doi:10.1016/j.compositesa.2003.09.016.

19. Greenberg, M. I.; Waksman, J.; Curtis, J. Silicosis: A review. *Dm Dis.* **2007**, *53*, 394–416, doi:10.1016/j.disamonth.2007.09.020.

20. Donaldson, K.; Tran, C. L. An introduction to the short-term toxicology of respirable industrial fibres. *Mutat. Res. Mol. Mech. Mutagen.* **2004**, *553*, 5–9, doi:10.1016/j.mrfmmm.2004.06.011.

21. Akil, H.; Omar, M.; Mazuki, A.; Safiee, S.; Ishak, Z.; Abu Bakar, A. Kenaf fiber reinforced composites: A review. *Mater. Des.* **2011**, *32*, 4107–4121, doi:10.1016/j.matdes.2011.04.008.

22. Lopez, J.; Mendez, J.; Espinach, F.; Julian, F.; Mutjé, P.; Vilaseca, F. Tensile strength characteristics of polypropylene composites reinforced with stone groundwood fibres from softwood. *Bioresources* **2012**, *7*, 3188–3200.

23. Gourier, C.; Bourmaud, A.; Le Duigou, A.; Baley, C. Influence of PA11 and PP thermoplastic polymers on recycling stability of unidirectional flax fibre reinforced biocomposites. *Polym. Degrad. Stab.* **2017**, *136*, 1–9, doi:10.1016/j.polymdegradstab.2016.12.003.

24. Rong, M. Z.; Zhang, M. Q.; Liu, Y.; Yang, G. C.; Zeng, H. M. The effect of fiber treatment on the mechanical properties of unidirectional sisal-reinforced epoxy composites. *Compos. Sci. Technol.* **2001**, *61*, 1437–1447, doi:10.1016/S0266-3538(01)00046-X.

25. Bledzki, A. K.; Gassan, J. Composites reinforced with cellulose based fibres. *Prog. Polym. Sci.* **1999**, *24*, 221–274, doi:10.1016/S0079-6700(98)00018-5.

26. González-Sánchez, C.; Martínez-Aguirre, A.; Pérez-García, B.; Martínez-Urreaga, J.; de la Orden, M. U.; Fonseca-Valero, C. Use of residual agricultural plastics and cellulose fibers for obtaining sustainable eco-composites prevents waste generation. *J. Clean. Prod.* **2014**, *83*, 228–237, doi:10.1016/j.jclepro.2014.07.061.

27. Sanadi, A.; Caulfield, D.; Jacobson, R.; Rowell, R. Renewable agricultural fibers as reinforcing fillers in plastics: mechanical properties of kenaf fiber– polypropylene composites. *Ind. Eng. Chem.* **1995**, *34*, 1889–1896, doi:10.1021/ie00044a041.

28. Granda, L. A.; Espinach, F. X.; Méndez, J. A.; Vilaseca, F.; Delgado-Aguilar, M.; Mutjé, P. Semichemical fibres of Leucaena collinsii reinforced polypropylene composites: Flexural characterisation, impact behaviour and water uptake properties. *Compos. Part B Eng.* **2016**, *97*, 176–182, doi:10.1016/j.compositesb.2016.04.063.

29. Serra, A.; Tarrés, Q.; Claramunt, J.; Mutjé, P.; Ardanuy, M.; Espinach, F. X. Behavior of the interphase of dyed cotton residue flocks reinforced polypropylene composites. *Compos. Part B Eng.* **2017**, *128*, 200–207, doi:10.1016/j.compositesb.2017.07.015.

30. Aranberri-Askargorta, I.; Lampke, T.; Bismarck, A. Wetting behavior of flax fibers as reinforcement for polypropylene. *J. Colloid Interface Sci.* **2003**, *263*, 580–589, doi:10.1016/S0021-9797(03)00294-7.

31. Fuentes, C. A.; Brughmans, G.; Tran, L. Q. N.; Dupont-Gillain, C.; Verpoest, I.; Van Vuure, A. W. Mechanical behaviour and practical adhesion at a bamboo composite interface: Physical adhesion and mechanical interlocking. *Compos. Sci. Technol.* **2015**, *109*, 40–47, doi:10.1016/j.compscitech.2015.01.013.

32. Cui, Y.; Lee, S.; Noruziaan, B.; Cheung, M.; Tao, J. Fabrication and interfacial modification of wood/recycled plastic composite materials. *Compos. Part A Appl. Sci. Manuf.* **2008**, *39*, 655–661, doi:10.1016/j.compositesa.2007.10.017.

33. Akampumuza, O.; Wambua, P. M.; Ahmed, A.; Li, W.; Qin, X. H. Review of the applications of biocomposites in the automotive industry. *Polym. Compos.* **2017**, *38*, 2553–2569, doi:10.1002/pc.23847.

34. Granda, L. A.; Espinach, F. X.; Tarrés, Q.; Méndez, J. A.; Delgado-Aguilar, M.; Mutjé, P. Towards a good interphase between bleached kraft softwood fibers and poly(lactic) acid. *Compos. Part B Eng.* **2016**, *99*, 514–520, doi:10.1016/j.compositesb.2016.05.008.

35. Posch, W. Polyolefins. In *Applied Plastics Engineering Handbook*; Elsevier, 2011; pp. 23–48.

36. Sauter, D. W.; Taoufik, M.; Boisson, C. Polyolefins, a Success Story. *Polymers (Basel).* **2017**, *9*, 185, doi:10.3390/polym9060185.

37. Qiu, K.; Netravali, A. N. Fabrication and characterization of biodegradable composites based on microfibrillated cellulose and polyvinyl alcohol. *Compos. Sci. Technol.* **2012**, *72*, 1588–1594, doi:10.1016/j.compscitech.2012.06.010.

38. Halley, P. J.; Dorgan, J. R. Next-generation biopolymers: Advanced functionality and improved sustainability. *MRS Bull.* **2011**, *36*, 687–691, doi:10.1557/mrs.2011.180.

39. Jiménez, A. M.; Espinach, F. X.; Delgado-Aguilar, M.; Reixach, R.; Quintana, G.; Fullana-i-Palmer, P.; Mutjé, P. Starch-Based Biopolymer Reinforced with High Yield Fibers from Sugarcane Bagasse as a Technical and Environmentally Friendly Alternative to High Density Polyethylene. *BioResources* **2016**, *11*, 9856–9868, doi:10.15376/biores.11.4.9856-9868.

40. Espigulé, E.; Vilaseca, F.; Espinach, F. X.; Julian, F.; Mansouri, N.-E. El; Mutjé, P. Biocomposites from Starch-based Biopolymer and Rape Fibers. Part II: Stiffening, Flexural and Impact Strength, and Product Development. *Curr. Org. Chem.* **2013**, *17*, 1641–1646.

41. Averous, L.; Moro, L.; Dole, P.; Fringant, C. Properties of thermoplastic blends : starch – polycaprolactone. *Polymer (Guildf).* **2000**, *41*, 4157–4167.

42. Murariu, M.; Dubois, P. PLA composites: From production to properties. *Adv. Drug Deliv. Rev.* **2016**, *107*, 17–46, doi:10.1016/j.addr.2016.04.003.

43. Braskem I'm green™ PE 2013, 1–16.

44. Sarkar, N.; Ghosh, S. K.; Bannerjee, S.; Aikat, K. Bioethanol production from agricultural wastes: An overview. *Renew. Energy* **2012**, *37*, 19–27, doi:10.1016/j.renene.2011.06.045.

45. Haro, P.; Ollero, P.; Trippe, F. Technoeconomic assessment of potential processes for bio-ethylene production. *Fuel Process. Technol.* **2013**, *114*, 35–48, doi:10.1016/j.fuproc.2013.03.024.

46. Ogunniyi, D. S. Castor oil: A vital industrial raw material. *Bioresour. Technol.* **2006**, *97*, 1086–1091, doi:10.1016/j.biortech.2005.03.028.

47. Mutlu, H.; Meier, M. a. R. Castor oil as a renewable resource for the chemical

industry. *Eur. J. Lipid Sci. Technol.* **2010**, *112*, 10–30, doi:10.1002/ejlt.200900138.

48. Perret, P. *From castor oil to specialty polyamides: the success of the diversification*; Paris, 2014;

49. Bledzki, A. K.; Jaszkiewicz, A.; Scherzer, D. Mechanical properties of PLA composites with man-made cellulose and abaca fibres. *Compos. Part A Appl. Sci. Manuf.* **2009**, *40*, 404–412, doi:10.1016/j.compositesa.2009.01.002.

50. Bax, B.; Müssig, J. Impact and tensile properties of PLA/Cordenka and PLA/flax composites. *Compos. Sci. Technol.* **2008**, *68*, 1601–1607, doi:10.1016/j.compscitech.2008.01.004.

51. Frollini, E.; Bartolucci, N.; Sisti, L.; Celli, A. Biocomposites based on poly(butylene succinate) and curaua: Mechanical and morphological properties. *Polym. Test.* **2015**, *45*, 168–173, doi:10.1016/j.polymertesting.2015.06.009.

52. Frollini, E.; Bartolucci, N.; Sisti, L.; Celli, A. Poly(butylene succinate) reinforced with different lignocellulosic fibers. *Ind. Crops Prod.* **2013**, *45*, 160–169, doi:10.1016/j.indcrop.2012.12.013.

53. Delgado-Aguilar, M.; Reixach, R.; Tarrés, Q.; Espinach, F. X.; Mutjé, P.; Méndez, J. A. Bleached kraft eucalyptus fibers as reinforcement of polylactic acid for the development of high-performance fully biodegradable composites. *Polymers (Basel).*

54. Raj, G.; Balnois, E.; Baley, C.; Grohens, Y. Probing cellulose/polylactic acid interactions in model biocomposite by colloidal force microscopy. *Colloids Surfaces A Physicochem. Eng. Asp.* **2009**, *352*, 47–55, doi:10.1016/j.colsurfa.2009.09.048.

55. Huda, M. S.; Drzal, L. T.; Mohanty, A. K.; Misra, M. Effect of fiber surface-treatments on the properties of laminated biocomposites from poly(lactic acid) (PLA) and kenaf fibers. *Compos. Sci. Technol.* **2008**, *68*, 424–432, doi:10.1016/j.compscitech.2007.06.022.

56. Chun, K. S.; Husseinsyah, S.; Osman, H. Mechanical and thermal properties of coconut shell powder filled polylactic acid biocomposites: Effects of the filler content and silane coupling agent. *J. Polym. Res.* **2012**, *19*, doi:10.1007/s10965-012-9859-8.

57. Bledzki, A. K.; Feldmann, M. Bio-based polyamides reinforced with cellulosic fibres - Processing and properties. *Compos. Sci. Technol.* **2014**, *100*, 113–120.

58. Vilaseca, F.; Valadez-Gonzalez, A.; Herrera-Franco, P. J.; Pelach, M. A.; López, J. P.; Mutjé, P. Biocomposites from abaca strands and polypropylene. Part I: Evaluation of the tensile properties. *Bioresour. Technol.* **2010**, *101*, 387–395, doi:10.1016/j.biortech.2009.07.066.

59. Reixach, R.; Franco-Marquès, E.; El Mansouri, N. E.; Ramirez de Cartagena, F.; Arbat, G.; Espinach, F. X.; Mutjé, P. Micromechanics of mechanical, thermomechanical, and chemi-thermomechanical pulp from orange tree pruning as polypropylene reinforcement: a comparative study. *Bioresources* **2013**, *8*, 3231–3246.

60. Granda, L. A.; Espinach, F. X.; López, F.; García, J. C.; Delgado-Aguilar, M.; Mutjé, P. Semichemical fibres of Leucaena collinsii reinforced polypropylene: Macromechanical and micromechanical analysis. *Compos. Part B Eng.* **2016**, *91*, 384–391, doi:10.1016/j.compositesb.2016.01.035.

61. Naghmouchi, I.; Mutje, P.; Boufi, S. Polyvinyl Chloride Composites Filled with Olive Stone Flour: Mechanical, Thermal, and Water Absorption Properties. *J. Appl. Polym. Sci.* **2014**, *131*, 10, doi:10.1002/app.41083.

62. Kind, S.; Neubauer, S.; Becker, J.; Yamamoto, M.; Volkert, M.; Abendroth, G. von; Zelder, O.; Wittmann, C. From zero to hero - Production of bio-based nylon from renewable resources using engineered Corynebacterium glutamicum. *Metab. Eng.* **2014**, *25*, 113–123, doi:10.1016/j.ymben.2014.05.007.

63. Gilbert, M. Aliphatic Polyamides. In *Brydson's Plastics Materials (Eighth Edition)*; 2017; Vol. 5 ISBN 9780323358248.

64. Devaux, J.; Lê, G.; Pees, B. Application of Eco-Profile Methodology To Polyamide 11. 1–11.

65. Winnacker, M.; Rieger, B. Biobased Polyamides: Recent Advances in Basic and Applied Research. *Macromol. Rapid Commun.* **2016**, *37*, 1391–1413, doi:10.1002/marc.201600181.

66. Börås, L.; Gatenholm, P. Surface Composition and Morphology of CTMP Fibers. *Holzforschung* **1999**, *53*, doi:10.1515/HF.1999.031.

67. Sears, K. D.; Jacobson, R.; Caulfield, D. F.; Underwood, J. Reinforcement of Engineering Themoplastics with High Purity Wood Cellulose Fibers. In *The Sixth International Conference on Woodfiber- Plastic Composites*; Madison, Wisconsin (USA), 2001; pp. 27–34.

68. Ksouri, I.; De Almeida, O.; Haddar, N. Long term ageing of polyamide 6 and polyamide 6 reinforced with 30% of glass fibers: physicochemical, mechanical and morphological characterization. *J. Polym. Res.* **2017**, *24*, 133, doi:10.1007/s10965-017-1292-6.

69. Orzen, E.; Kiziltas, A.; Kiziltas, E. E.; Gardner, D. J. Natural fiber blends- filled engineering thermoplastic composites for the automobile industry. *12th Annu. Automot. Compos. Conf. Exhib. 2012 Unleashing Power Des. ACCE 2012 (pp 275-286)* **2012**, 1–12.

70. Aydemir, D.; Kiziltas, A.; Erbas Kiziltas, E.; Gardner, D. J.; Gunduz, G. Heat treated wood-nylon 6 composites. *Compos. Part B Eng.* **2015**, *68*, 414–423, doi:10.1016/j.compositesb.2014.08.040.

71. Xu, S.; Sun, L.; He, J.; Han, H.; Wang, H.; Fang, Y.; Wang, Q. Effects of LiCl on crystallization, thermal, and mechanical properties of polyamide 6/wood fiber composites. *Polym. Compos.* **2017**, *16*, 101–113, doi:10.1002/pc.24507.

72. Santos, P. A.; Spinacé, M. A. S.; Fermoselli, K. K. G.; De Paoli, M. A. Polyamide-6/vegetal fiber composite prepared by extrusion and injection molding. *Compos. Part A Appl. Sci. Manuf.* **2007**, *38*, 2404–2411, doi:10.1016/j.compositesa.2007.08.011.

73. Kiziltas, A.; Behzad, N.; Gardner, D. J.; Bousfield, D. W. Polyamide 6–Cellulose Composites: Effect of Cellulose Composition on Melt Rheology and Crystallization Behavior. *Polym. Eng. Sci.* **2014**, *54*, 739–746, doi:10.1002/pen.

74. Klason, C.; Kubát, J.; Strömvall, H.-E. The Efficiency of Cellulosic Fillers in Common Thermoplastics. Part 1. Filling without Processing Aids or Coupling Agents. *Int. J. Polym. Mater. Polym. Biomater.* **1984**, *10*, 159–187,

doi:10.1080/00914038408080268.

75. Paunikallio, T.; Suvanto, M.; Pakkanen, T. T. Viscose fiber/polyamide 12 composites: Novel gas-phase method for the modification of cellulose fibers with an aminosilane coupling agent. *J. Appl. Polym. Sci.* **2006**, *102*, 4478–4483, doi:10.1002/app.24789.

76. Semba, T.; Ito, A.; Kitagawa, K.; Nakatani, T.; Yano, H.; Sato, A. Thermoplastic composites of polyamide-12 reinforced by cellulose nanofibers with cationic surface modification. *J. Appl. Polym. Sci.* **2014**, *131*, n/a-n/a, doi:10.1002/app.40920.

77. Panaitescu, D. M.; Frone, A. N.; Nicolae, C. Micro- and nano-mechanical characterization of polyamide 11 and its composites containing cellulose nanofibers. *Eur. Polym. J.* **2013**, *49*, 3857–3866, doi:10.1016/j.eurpolymj.2013.09.031.

78. Panaitescu, D. M.; Gabor, R. A.; Frone, A. N.; Vasile, E. Influence of Thermal Treatment on Mechanical and Morphological Characteristics of Polyamide 11/Cellulose Nanofiber Nanocomposites. *J. Nanomater.* **2015**, *2015*, 1–11, doi:10.1155/2015/136204.

79. Feldmann, M.; Bledzki, A. K. Bio-based polyamides reinforced with cellulosic fibres – Processing and properties. *Compos. Sci. Technol.* **2014**, *100*, 113–120, doi:10.1016/j.compscitech.2014.06.008.

80. Feldmann, M.; Heim, H. P.; Zarges, J. C. Influence of the process parameters on the mechanical properties of engineering biocomposites using a twin-screw extruder. *Compos. Part A Appl. Sci. Manuf.* **2016**, *83*, 113–119, doi:10.1016/j.compositesa.2015.03.028.

81. Zierdt, P.; Theumer, T.; Kulkarni, G.; Däumlich, V.; Klehm, J.; Hirsch, U.; Weber, A. Sustainable wood-plastic composites from bio-based polyamide 11 and chemically modified beech fibers. *Sustain. Mater. Technol.* **2015**, *6*, 6–14, doi:10.1016/j.susmat.2015.10.001.

82. Cherizol, R.; Sain, M.; Tjong, J. Evaluation of the Influence of Fibre Aspect Ratio and Fibre Content on the Rheological Characteristic of High Yield Pulp Fibre Reinforced Polyamide 11 " HYP / PA11 " Green Composite. *J. Polym. Chem.* **2015**, *5*, 1–8.

83. Le Duigou, A.; Bourmaud, A.; Gourier, C.; Baley, C. Multi-scale shear properties of flax fibre reinforced polyamide 11 biocomposites. *Compos. Part A Appl. Sci. Manuf.* **2016**, *85*, 123–129, doi:10.1016/j.compositesa.2016.03.014.

84. Bourmaud, A.; Le Duigou, A.; Gourier, C.; Baley, C. Influence of processing temperature on mechanical performance of unidirectional polyamide 11 - flax fibre composites. *Ind. Crops Prod.* **2016**, *84*, 151–165, doi:10.1016/j.indcrop.2016.02.007.

85. Armioun, S.; Panthapulakkal, S.; Scheel, J.; Tjong, J.; Sain, M. Sustainable and lightweight biopolyamide hybrid composites for greener auto parts. *Can. J. Chem. Eng.* **2016**, *94*, 2052–2060, doi:10.1002/cjce.22609.

86. Armioun, S.; Panthapulakkal, S.; Scheel, J.; Tjong, J.; Sain, M. Biopolyamide hybrid composites for high performance applications. *J. Appl. Polym. Sci.* **2016**, *43595*, n/a-n/a, doi:10.1002/app.43595.

87. Pérez, J.; Muñoz-Dorado, J.; de la Rubia, T.; Martínez, J. Biodegradation and biological treatments of cellulose, hemicellulose and lignin: an overview. *Int. Microbiol.* **2002**, *5*, 53–63, doi:10.1007/s10123-002-0062-3.

88. Kelly, A.; Tyson, W. R. Tensile properties of fibre-reinforced metals-copper/tungsten and copper/molybdenum. *J. Mech. Phys. Solids* **1965**, *13*, 329in1339-338in2350, doi:10.1016/0022-5096(65)90035-9.

89. Bowyer, W. H.; Bader, M. G. On the re-inforcement of thermoplastics by imperfectly aligned discontinuous fibres. *J. Mater. Sci.* **1972**, *7*, 1315–1321, doi:10.1007/BF00550698.

90. Oliver-Ortega, H.; Granda, L. A.; Espinach, F. X.; Méndez, J. A.; Julian, F.; Mutjé, P. Tensile properties and micromechanical analysis of stone groundwood from softwood reinforced bio-based polyamide11 composites. *Compos. Sci. Technol.* **2016**, *132*, 123–130, doi:10.1016/j.compscitech.2016.07.004.

91. Hirsch, T. J. Modulus of Elasticity iof Concrete Affected by Elastic Moduli of Cement Paste Matrix and Aggregate. *J. Proc.* **1962**, *59*, 427–452.

92. Halpin, J. C.; Tsai, S. W. *Effects of environmental factors on composite materials.*

technical report; 1969;

93. Oliver-Ortega, H.; Granda, L. A.; Espinach, F. X.; Delgado-Aguilar, M.; Duran, J.; Mutjé, P. Stiffness of bio-based polyamide 11 reinforced with softwood stone ground-wood fibres as an alternative to polypropylene-glass fibre composites. *Eur. Polym. J.* **2016**, *84*, 481–489, doi:10.1016/j.eurpolymj.2016.09.062.

94. Oliver-Ortega, H.; Méndez, J. A.; Mutjé, P.; Tarrés, Q.; Espinach, F. X.; Ardanuy, M. Evaluation of Thermal and Thermomechanical Behaviour of Bio-Based Polyamide 11 Based Composites Reinforced with Lignocellulosic Fibres. *Polymers (Basel).* **2017**, *9*, 522, doi:10.3390/polym9100522.

95. Yang, H.; Yan, R.; Chen, H.; Lee, D. H.; Zheng, C. Characteristics of hemicellulose, cellulose and lignin pyrolysis. *Fuel* **2007**, *86*, 1781–1788, doi:10.1016/j.fuel.2006.12.013.

96. Arbelaiz, A.; Fernández, B.; Ramos, J. A.; Mondragon, I. Thermal and crystallization studies of short flax fibre reinforced polypropylene matrix composites: Effect of treatments. *Thermochim. Acta* **2006**, *440*, 111–121, doi:10.1016/j.tca.2005.10.016.

97. Zafeiropoulos, N. E.; Baillie, C. A.; Matthews, F. L. Study of transcrystallinity and its effect on the interface in flax fibre reinforced composite materials. *Compos. Part A Appl. Sci. Manuf.* **2001**, *32*, 525–543, doi:10.1016/S1359-835X(00)00058-0.

98. Ouchiar, S.; Stoclet, G.; Cabaret, C.; Gloaguen, V. Influence of the Filler Nature on the Crystalline Structure of Polylactide-Based Nanocomposites: New Insights into the Nucleating Effect. *Macromolecules* **2016**, acs.macromol.5b02746, doi:10.1021/acs.macromol.5b02746.

99. Nair, S. S.; Ramesh, C.; Tashiro, K. Crystalline phases in nylon-11: Studies using HTWAXS and HTFTIR. *Macromolecules* **2006**, *39*, 2841–2848, doi:10.1021/ma052597e.

100. Oliver-Ortega, H.; Méndez, J. A.; Reixach, R.; Espinach, F. X.; Ardanuy, M.; Mutjé, P. Towards More Sustainable Material Formulations: A Comparative Assessment of PA11-SGW Flexural Performance versus Oil-Based Composites. *Polymers (Basel).* **2018**, *10*, 440, doi:10.3390/polym10040440.

101. López, J. P.; Gironès, J.; Mendez, J. A.; Pèlach, M. A.; Vilaseca, F.; Mutjé, P. Impact and flexural properties of stone-ground wood pulp-reinforced polypropylene composites. *Polym. Compos.* **2013**, *34*, 842–848, doi:10.1002/pc.22486.

102. Hashemi, S.; Khamsehnezhad, A. Analysis of tensile and flexural strengths of single and double gated injection moulded short glass fibre reinforced PBT/PC composites. *Plast. Rubber Compos.* **2010**, *39*, 343–349, doi:10.1179/174328910X12647080902934.

103. Reuvers, N. J. W.; Huinink, H. P.; Fischer, H. R.; Adan, O. C. G. Quantitative water uptake study in thin nylon-6 films with NMR imaging. *Macromolecules* **2012**, *45*, 1937–1945, doi:10.1021/ma202719x.

104. Department of Trade and Industry *Tha Handbook of Measurements and capabilities of the Older Adult. Strength Data for Design Safety.*; London, 2002.

CAPÍTULO 2: RESULTADOS

2.1 Tensile properties and micromechanical analysis of stone groundwood from softwood reinforced bio-based polyamide11 composites

Publicada en *Composites Science and Technology*. Factor de impacto 2016: 4,873. Posición 1 de 25 en Materials Science, Composites. Primer cuartil.

Composites Science and Technology 132 (2016) 123–130

Contents lists available at ScienceDirect

Composites Science and Technology

journal homepage: http://www.elsevier.com/locate/compscitech

Tensile properties and micromechanical analysis of stone groundwood from softwood reinforced bio-based polyamide11 composites

H. Oliver-Ortega [a, *], L.A. Granda [a], F.X. Espinach [b], J.A. Mendez [a], F. Julian [b], P. Mutjé [a]

[a] Group LEPAMAP, Department of Chemical Engineering, University of Girona, C/M. Aurèlia Capmany, n°61, Girona 17071, Spain
[b] Design, Development and Product Innovation, Dpt. of Organization, Business Management and Product Design, University of Girona, C/M. Aurèlia Capmany, n°61, Girona 17071, Spain

ARTICLE INFO

Article history:
Received 12 May 2016
Received in revised form
1 July 2016
Accepted 4 July 2016
Available online 9 July 2016

Keywords:
Short-fibre composites
Mechanical properties
Interface
Injection moulding
Photoelectronic spectroscopy (XPS)

ABSTRACT

Bio-polyamides (BioPA) reinforced with natural fibres are one of the most promising bio-based composites. However the principal challenge of polyamides (PA) is their high melting temperature close to the degradation temperature of the natural fibres. Polyamide 11 (PA11) is a 100% BioPA with a melting point lower than cellulose temperature degradation. Nonetheless, few researches about PA11 reinforced with natural fibres composites had been performed. In this work, PA11 was reinforced with stone groundwood fibres (SGW) ranging 20% up to 60% of fibre contents. The composites were prepared, extruded, injected moulded and their tensile properties were characterised. An enhancement of 66.8% was obtained for the tensile strength of the composites, besides the strain and the toughness decreased as expected. The significant enhancement of the tensile strength leads to consider a relatively good interface between the fibre and the polymer matrix which was determined in the micromechanical studies. Moreover a morphology analysis of the fibre and its chemical composition study at surface were carried on, in order to discuss the micromechanical analysis results. The average orientation factor and intrinsic tensile strength of the fibres were also determined in the micromechanical analysis.

1. Introduction

Composites materials reinforced with natural fibres had been a common field of research in the last decades. The significant enhancement of the mechanical properties and low density of this composites are some of their attractiveness for the industry [1–3]. In order to reduce the petrol-based dependence, the use of bio-based polymers for the production of composite materials has become an increasing research topic in the last years [2,4,5]. One type of these bio-based polymers is biopolyamides (BioPA). BioPA are non biodegradable polymers that could be totally or almost completely bio-based. Some examples are polyamide 11 (PA11) which is 100% bio-based, polyamide 10.10 (PA10.10) which could have a bio-based content up to 99%, or polyamide 6.10 (PA6.10) which has a 62% of bio-content, depending on the carbon percentage from natural resources. BioPA has been successfully reinforced with synthetic cellulosic fibres [5]; however some special requirements are necessary for the processing of its composites caused by its melting which is close to the degradation temperature of the cellulose fibres. This hinders processing BioPA composites while conserving the natural fibres because short time processes are mandatory to preserve the natural fibres properties [6,7].

PA11 is a 100% bio-based polyamide biotechnologically obtained from 11-aminoundecanoic acid, derived from castor oil [8,9]. Additionally, PA11 has a smaller footprint in the global warming than other polymers [8,10]. PA11 is a thermoplastic polymer with a low melting point regarding other polyamides (about 200 °C). This allows PA11 to be natural fibre reinforced with relatively low or inexistent thermal degradation of the natural fibres and becoming a promising polymer matrix for composites. In addition, its non biodegradability, recyclability, good mechanical properties and high water and chemical resistance enables their use for long-life applications such as pipes, automotive, commodities, etc [2,11,12]. However, to the best knowledge of the authors, there is a lack of PA11 studies in the field of natural fibres reinforced composites [13].

Stone groundwood (SGW) is a commercial easily available pulp usually used in papermaking. SGW is obtained high yield process (about 98.5%) and at a relatively low price (less than 0.5€/kg). This

* Corresponding author.
E-mail address: helena.oliver@udg.edu (H. Oliver-Ortega).

http://dx.doi.org/10.1016/j.compscitech.2016.07.004
0266-3538/

methodology leads to lignocellulosic fibres with a chemical composition similar to the initial wood.

Tensile properties in composite materials are directly related with the capacity of transferring the stress between the polymer and the reinforcement. Probably the quality of the interface is the main parameter affecting these properties. A bad interface leads to a non-well bonded composite with a slightly increase of the mechanical properties against reinforcement content. However, when a good interface is obtained a significant enhancement of the composites tensile strength is observed regarding the polymer matrix. In order to obtain this good interface, the use of a coupling agent is usually required to compatible the highly hydrophilic natural fibres with the highly hydrophobic polymer matrix [14,15]. Nonetheless, in the case of polyamide-based composites, even though the available researches [5,16] show limited interactions between both components of the composites, it does not seem necessary the use of coupling agents to obtain a significant enhancement of mechanical properties. This could be related with the hydrogen bonding of the polyamide matrix structure [17] which probably could interact with the lignocellulosic fibres.

The aim of this work is to study the behaviour of the tensile properties (tensile strength, strain, toughness) of PA11 reinforced from 20 up to 60% of SGW fibres from softwood (*pinus radiata*). Some micromechanical properties such as the orientation factor, interfacial shear strength (τ) and the intrinsic tensile strength of fibres will be obtained in the micromechanics analysis of the composites. The materials will be produced without the use of coupling agents.

2. Experimental

2.1. Materials

A Rilsan® BMNO TL polyamide 11 provided by Arkema S.A. (Colombes, France) was used as a matrix. Its density is 1.03 g/cc and the melt flow index is 11 cc/10 min at 235 ºC/2.16 kg.

The mechanical fibre used as reinforcement was stone groundwood (SGW) from softwood (*pinus radiata*), supplied by Zubialde S.A. (Aizarnazabal, Spain). As a pulp produced and used at industrial scale, it's produced under high standards to ensure a high homogeneity in the different batches.

Dichloromethane (Extra Pure, stabilized with approx. 50 ppm of amylene, Pharmpur®) and formic acid (Extra Pure, 98–100%)both supplied by Scharlau (Sentmenat, Spain) were used for the extraction of the fibre from the composites.

2.2. Methods

2.2.1. Composite compounding

PA11 composites reinforced with 20%–60% w/w of SGW fibre were mixed using a Gelimat Kinetic Mixer. Both components were added at low speed (300 rpm). Afterwards, the speed was increased up to 2500 rpm. Once the blend reached 200 °C, the material was discharged, cooled and grinded in a knife mill.

2.2.2. Sample obtaining

Sample probes for mechanical characterization (ASTM D638-14 Type I) were obtained in accordance with the ASTM D638 standard through injection moulding in a Meteor-40 injection machine (Mateu&Solé, clamping pressure: 40 tons). The temperature profile used was 170–185–200 °C and the pressures were modified regarding the fibre content: 75 bar was the maximum pressure during the volumetric phase and 30 bar during the maintenance pressure phase for the PA11 + 60SGW composite. The cooling phase lasted 10 s.

2.2.3. Mechanical Characterization

Before the mechanical characterization, the tensile probes were placed in a climatic chamber at 23 °C and 50% RH during 48 h following the ASTM D618 standard. Subsequently, the PA11-SGW composites were tested in a DTC-10 Universal testing machine, supplied by IDM test, fitted with a 5 kN load cell at 2 mm/min deformation speed. Ten samples were tested for each material in order to obtain the experimental results. The water absorption of the samples has ranged from 0.1 to 0.3% (w/w).

2.2.4. Fibre extraction from composites

A Soxhlet apparatus was used to recover the fibres from the composites. The procedure is based in the solubilisation of the composite's matrix using a mixture of dichloromethane and formic acid (1:1 v/v) as solvent during 24 h. The dog-bone specimens were cut in small pieces and placed inside a cellulose filter set into the Soxhlet apparatus. Afterwards, the recovered fibres in the cellulose filter were cleaned and dried at 105 °C in an oven for 24 h.

2.2.5. Determination of the fibre lengths and diameters

The fibre length and diameter distributions were measured by means of a MorFi analyser (Techpap SAS. Grenoble, France). A suspension of 25 mg/L of fibre in water was measured in accordance with the procedure described in the ISO/FDIS 160652 standard.

The arithmetic average length (l^F) and diameter (d^F) were determined by:

$$l^F = \frac{\sum_i \cdot l_i^F}{\sum_i n} \tag{1}$$

$$d^F = \frac{\sum_i \cdot d_i^F}{\sum_i n} \tag{2}$$

where l_i^F is the length of a fibre and d_i^F its diameter and n is the number of fibres.

The weighted average length (l^{WF}) was calculated as:

$$l^{WF} = \frac{\sum_i n \cdot \left(l_i^F\right)^2}{\sum_i n \cdot l_i^F} \tag{3}$$

2.2.6. X-ray Photoelectron Spectroscopy (XPS) studies

The surface composition of the SGW was determined by XPS in the Sheffield Surface Analysis Centre. A Kratos Axis Ultra DLD equipment was used to scan between 1200 and 0e V binding energy at 1e V resolution. Additionally, high resolution scans were collected with a 0.05e V resolution for C1s signals.

2.2.7. Tensile strength modelling

The linear behaviour of the tensile strength versus the reinforcement content allows the application of lineal models such as the Rule of Mixtures (RoM) or the Kelly-Tyson equation. Kelly and Tyson [18] modelled the composite tensile strength as a function of the matrix and fibre strengths, the interfacial characteristics of the composites and the orientation of the fibres. Kelly-Tyson model for short and semi-oriented fibres is expressed as:

$$\sigma_t^C = \chi_1\left(\sum_{Lc}^{i=0}\left[\frac{\tau\cdot l_i^F\cdot V_i^F}{d^F}\right] + \sum_{\infty}^{j=Lc}\left[\sigma_j^F\cdot V_j^F\cdot\left(1-\frac{\sigma_j^F\cdot d^F}{4\cdot\tau\cdot l_j^F}\right)\right]\right) + \left(1-V^F\right)\cdot\sigma_t^{m*} \quad (4)$$

where σ_t^C and σ_t^F are the intrinsic tensile strength of the composite and the intrinsic tensile strength of the fibre, respectively; $\sigma_t^{m^*}$ is the tensile strength of the matrix in the breaking point of the composite; χ_1 is the orientation factor; τ is the interfacial shear strength; V^F is the volume fraction of the fibre in the composite which is calculated as $V^F = \rho^F\cdot weight_{fibre}$ and considering a fibre's density (ρ^F) of 1.4 g/cc. Natural fibres show a length and diameter distribution (l^F and d^F).

However, this equation has four unknowns: χ_1, σ_t^F, τ and the critical length (Lc). This makes necessary the use of numeric methods. Bowyer and Bader developed a methodology for solving the Kelly-Tyson equation.

2.2.8. Bowyer-Bader solution

Bowyer and Bader [19] considered that the tensile strength could be approximated to $\sigma_t^F = E_t^F\cdot\varepsilon_t^C$. The fibre Young's modulus was determined by the Hirsch model [20] as described in the literature [21–24].

The contributions of the subcritical length fibres, supercritical length fibres and the matrix can be expressed as X, Y and Z, respectively, consequently equation (4) can be rewritten as:

$$\sigma_t^C = \chi_1(X+Y)+Z \quad (5)$$

Then, the composite maximum strength is compared between two different strain levels, and express as a relation:

$$R = \frac{\sigma_{t1}^C - Z_1}{\sigma_{t2}^C - Z_2}; R^* = \frac{(X_1+Y_1)}{(X_2+Y_2)} \quad (6)$$

In that way, it is possible to discard χ_1 from the equation. However, the equation still presents two unknowns: τ and Lc. Numeric methods will be used to find values that fit $R = R^*$. Once determined τ and Lc, it will be possible to obtain χ_1 and σ_t^F.

2.2.9. Scanning electron microscopy (SEM)

Photography's of the fracture of tensile strength probes were made by scanning electron microscopy (SEM). A Zeiss DSM 960A was used to obtain the images and the samples were sputter coated with gold.

3. Results and discussion

3.1. Tensile strength behaviour

It is commonly agreed that the tensile strength of a composite material is mainly determined by the nature and properties of the matrix and the fibre, the reinforcement aspect ratio and orientation of the fibres, the fibre content and their dispersion inside the matrix and the interaction between the matrix and the fibre, also called interfacial shear strength (τ). Among these, the most important factor is the interface, which is related with the chemical composition of the fibre surface and the matrix chemical structure. When the interface is good the stress transmission from the matrix to the fibre increases and thus enhances the tensile strength of the composite. On the other hand, when the interactions between matrix and reinforcement fibre are low, the composite's tensile strength tends to remain similar to the matrix tensile strength possibly due to fibres sliding during testing [15,25].

Table 1 shows the tensile strength (σ_t^C), the strain at maximum strength (ε_t^C), the toughness (U_T) and the tensile strength of the matrix at breaking ($\sigma_t^{m^*}$)of the tested composites. The standard deviation of the values is presented in brackets.

$$\sigma_t^{m*} = 8.11\cdot10^{-5}\cdot\varepsilon^5 - 6.06\cdot10^{-4}\cdot\varepsilon^4 + 1.71\cdot10^{-1}\cdot\varepsilon^3 2.26\cdot\varepsilon^2 + 14.30\cdot\varepsilon - 0.52 \quad (7)$$

Under the sample column, PA11 + xSGW, x refers to the fibre content w/w. The $\sigma_t^{m^*}$ was calculated from equation (7) obtained by a polynomial regression of the PA11 stress-strain curve. A lineal increment of the tensile strength of the PA11-SGW composites was observed when increasing the fibre content up to 50% w/w. The maximum enhancement on the tensile strength was achieved with the PA11 + 50SGW composite with an increase about the 66.8% compared to PA11. Nevertheless, the addition of a 60% of SGW resulted in a diminution of the tensile strength regarding the PA11 + 50SGW.This might be caused by the matrix not wetting the fibre properly.

The tensile strength obtained in the PA11-SGW composites (63.8 MPa) was comparable with the obtained for polypropylene (PP) composites reinforced with SGW fibres using maleated polypropylene (MAPP) as a coupling agent (59.2 MPa) [26]. However, the literature points out the incompatibility of the PP matrix with the fibres and the necessity of a coupling agent to obtain a good interface [14]. This seemed not necessary in the case of PA11 matrix [16] as the capacity of the matrix to establish H-bonds was enough to obtain a significance enhancement of the tensile strength of composites materials. Indeed, this is in accordance with the 12 principles of the green chemistry [27], making the PA11-SGW composites a promising greener alternative.

The strain of composites materials was reduced drastically following an asymptotic tendency (Fig. 2). For instance, the addition of 20% SGW fibre in the PA11 matrix reduced the strain a 62%. The drop in the strain of composite materials is usually one of their disadvantages, as restricts is use to low deformation purposes. Besides, toughness, which was calculated as the area under the strain-stress curve (Fig. 1), decreased considerably when increasing the fibre content following a similar trend to the strain as is shown in Fig. 2.

3.2. Fibre morphology analysis

Fibres morphology inside the composite is one of the factors affecting the composites tensile strength. The SGW fibres morphological characterization was carried out with the PA11 + 30SGW, PA11 + 40SGW and the SGW fibres before the composite compounding.

The MorFi analyser considered the fibres with lengths lower than 90 μm as fines, excluding them from the fibre's length distribution. However, these fines can be present in a high content and their exclusion might cause an erratic calculus of the micromechanical properties analysis. The fibre's distribution considering

Table 1
Tensile properties of SGW reinforced PA11 composites.

Sample	V^F	σ_t^C (MPa)	ε_t^C (%)	U_T (KJ/m^3)	$\sigma_t^{m^*}$ (MPa)
PA11	0	38.3 (0.9)	25.0 (1.6)	–	–
PA11 + 20SGW	0.155	45.0 (0.8)	9.5 (0.8)	3926 (277)	34.9
PA11 + 30SGW	0.240	52.4 (0.8)	5.5 (0.4)	2196 (239)	33.1
PA11 + 40SGW	0.329	56.7 (0.6)	4.5 (0.3)	1638 (105)	31.3
PA11 + 50SGW	0.424	63.9 (1.8)	3.7 (0.2)	1334 (98)	29.0
PA11 + 60SGW	0.524	59.6 (2.1)	2.8 (0.2)	903 (46)	25.2

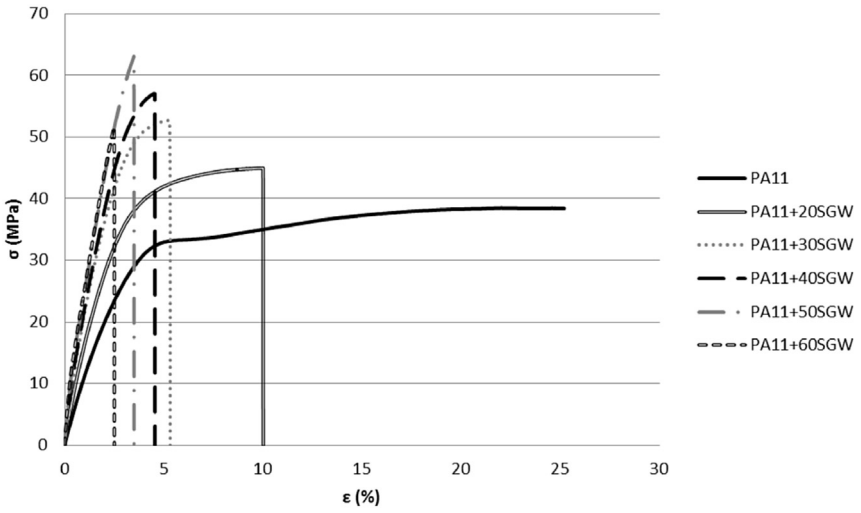

Fig. 1. Stress-Strain curves of PA11 and their composites.

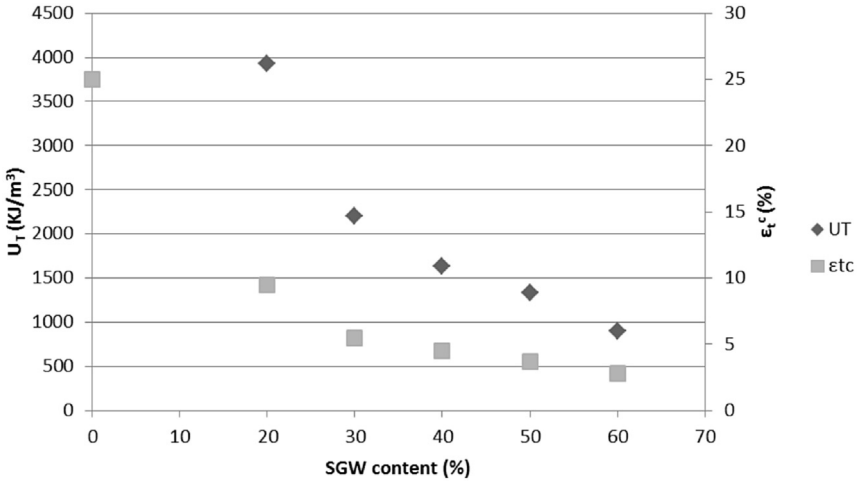

Fig. 2. Toughness and strain evolution regarding the fibre content of PA11-SGW composites.

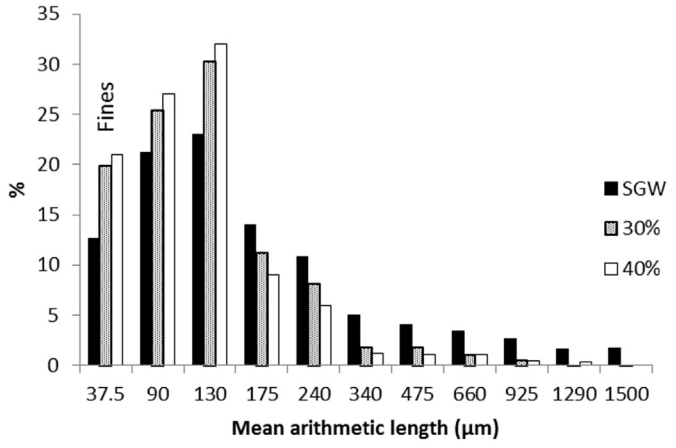

Fig. 3. Fibre length distributions obtained for PA11 + 30SGW, PA11 + 40SGW and SGW.

these fines is exposed in Fig. 3.

An attrition phenomenon was observed after the composite compounding and when the fibres content is raised. Moreover, the quantity of fines has a significant increment after the composite production and their content was considered relevant. Thus, a comparative micromechanical analysis including and excluding the fines was carried out to assess their impact in the final results.

3.3. Fibre surface characterization

Natural fibres are composed principally by lignin, hemicelluloses and cellulose. Their distribution is different through the different fibre structure layers (middle lamella, primary wall and secondary wall) [28]. Lignin content tends to decrease through the walls while the cellulose content increase. Moreover, defibrering techniques and other surface treatments could affect the chemical composition of the fibres walls. The stone groundwood process leads to high yield fibres with a high conservation of the chemical composition of the wood.

The surface chemical composition of the fibres was characterised using XPS technique that also was used in the LA Granda et al. [29] in order to offer an explanation about the interactions between the reinforcement and the matrix.

Initially, a survey scan was made to calculate the atomic composition of the fibre surface (Table 2). Cellulose is composed by

Table 2
XPS survey scan of SGW fibres. Elements observed, binding energy and atomic percentage is indicated.

Element	Binding energy (eV)	Atomic (%)
C	285	67.88
O	532	31.97
Na	1071	0.14

the repetition of the unit ($C_6H_{10}O_5$), so in a pure cellulose fibre the atomic percentage expected would be 45% for oxygen and 55% for carbon as hydrogen cannot be measured in the XPS. The SGW fibre analysis showed an atomic oxygen percentage of 32% and a 68% of carbon. This higher carbon quantity is related with lignin molecules [30–32], composed principally by hydrocarbon compounds. These results are in agreement with the literature [33] where lignin had been proved to be one of the superficial components of natural fibres [34,35]. A trace of sodium has been detected that could be related with extractive compounds.

A high resolution scan over the carbon peak was collected in order to clarify the fibre's surface composition. The scan results are exposed in Table 3. Four types of bonds were found: carbon-carbon, carbon-hydroxyl groups, acetals and carboxylic acid or esters, which could be related with esters bonds in lignin [36]. A pure cellulose sample would show a carbon-hydroxyl/acetal groups ratio of 5:1. However, SGW rendered a ratio of 3:1, caused mainly by the presence of lignin in the surface of the fibre [37]. This is in agreement with the apparition of a C–C band with a high area that is not expected in a pure cellulose sample and is related principally with the lignin macromolecules [38,39].

Lignin content characterised on fibre's surface was relatively high as expected in a non-bleached mechanical pulp. Its presence in the fibre's surface might decrease the polarity of lignocellulosic fibres that could favour the dispersion of fibres in the matrix. However, its high content in the surface may hinder intermolecular interactions established between polyamide matrix and cellulose fibres decreasing the enhancement of the mechanical properties of composites reinforced with natural fibres [40,41].

3.4. Micromechanical analysis

As presented in the methods section, the Kelly and Tyson equation and the solution provided by Bowyer and Bader were used to obtain the micromechanical properties. Table 4 shows the data used for the calculation of χ_1, σ_t^F, τ and Lc whenever the fines were included or excluded. All the calculations were performed using the morphological data obtained for PA11 + 30%SGW.

The outcome data is shown in Table 5. The inclusion of fines in the fibre distribution had a slight effect in the χ_1 computed value, as only a 2% of difference was observed (0.356 including fines and 0.348 without them). The obtained values of χ_1 were comprised between the expected values of 0.2 and 0.375 found in the literature [42].

Von Mises ($\sigma_t^C/3^{1/2}$) and Tresca ($\sigma_t^C/2$) criterion [41,43,44] are accepted to predict quite well the τ value for correctly bonded composites. The XPS results showed a high content of hydroxyl groups (provided from the lignin and in lower measure from the cellulose and hemicelluloses (Fig. 5)) on the surface that could interact with the PA11 matrix. Hence it was expected that τ value was close to them. Two different τ values were obtained after including and excluding fines (19.29 MPa and 16.52 MPa). It was found that the inclusion of the fines increase the τ value, rendering a close Tresca value (19.5 MPa) and 15% lower to the Von Mises value (22.11 MPa). Nevertheless, the calculated τ value discarding fines was the lowest. The higher τ value obtained by including the fines might be related with their higher specific surface, which could imply an enhancement on the fibre-matrix interactions. Even so higher τ values were found in the literature for PA11 reinforced with flax stalks (22.2 MPa) (flax stalks have a low lignin content and higher hemicelluloses and cellulose content on the surface) and close to the Von Mises criteria [16]. However the measurement techniques and fibre used were different.

On the other hand, a fibre's intrinsic tensile strength of 562 MPa was obtained when using a fibre length distribution including fines, and 542 MPa excluding them. Therefore, a 3.6% of difference was observed when the fines were disregarded. The obtained value for fines was slightly lower than the found from the literature for the same fibres [25]. However, the average intrinsic tensile strength of SGW fibres in the literature was performed with composites using polypropylene (PP) with a coupling agent (617.7 ± 20.1 MPa) where SGW fibres are covalent bonding plus entanglement to the polypropylene. In PA11-SGW composites the interaction between the fibres and the matrix are only intermolecular forces, mainly hydrogen bonding and Van der Waals forces which are energetically weaker. Finally, the calculated critical length are 344 and 453 μm including fines and excluding them, respectively.

In order to discuss the quality of the interface, a RoM [45] was used. The RoM is a lineal model used to predict composites strength. This model describes the obtained strength of the composite as:

$$\sigma_t^C = f_c \cdot V^F \cdot \sigma_t^F + \left(1 - V^F\right) \cdot \sigma_t^{m*} \tag{8}$$

where f_c is compatibility factor that in a well bonded composite has values near 0.2 [42,46]. The f_c of the PA11 + 30SGW was found to be 0.202, typical of a good quality interface. A mean value of f_c was computed using 562 MPa as intrinsic tensile strength and the experimental data for the composites ranging 20–50% w/w reinforcement contents. The average value was 0.193.

These results are in agreement with the SEM images of PA11 + 50SGW fractured tensile specimen (Fig. 4).

SEM images showed a good dispersion and individualization of the fibres, as there are not fibres bundles. A fibre with an approximately width of 20 μm could be observed. A correct wetting of the fibres is also observed, as there are no appreciable voids around the fibres. The observed voids are mainly caused by the slippage of the fibres during the tensile test. Nevertheless, the broken fibres observed in the SEM images indicate a good interface, showing a granular breaking mechanism and in lower quantity a fibrilar breaking mechanism that could be related with residual water content in the sample.

Finally, a composite tensile strength simulation was performed using the obtained results with the Kelly-Tyson equation (Fig. 5). The simulated values were similar including or excluding the fines and slightly higher than the obtained experimentally, especially for composites with fibre contents in the range from 30 to 50%. It is accepted that higher fibre contents leads to higher attrition phenomena and thus lower mean fibre length. The decrease obtained

Table 3
High resolution scans of SGW fibres with carbon environments, energy binding detected and bonds percentage.

Bond type	Binding energy (eV)	Bonds %
C–C	285.00	35.04
O=C*–OR	289.24	4.35
C–C*–O	286.61	45.18
O–C*–O	287.95	15.43

Table 4
Incoming data for Kelly-Tyson and Bowyer-Bader modelling.

	PA11-SGW including fines	PA11-SGW excluding fines
Reinforcement weight content (%)	30%	30%
Reinforcement volume fraction	0.240	0.240
Average length (μm)	193	221
Weighted average length (μm)	341	478
Average diameter (μm)	23.63	27.65
Composite strength (MPa)	52.41	52.41
Fibre modulus (GPa)	17.1	17.1
Elongation at break (%)	5.5	5.5
Strain level 1 analyzed (%)	0.55 (10%)	0.55 (10%)
Composite stress at strain level 1 (MPa)	12.3	12.3
Strain level 2 analyzed (%)	1.1 (20%)	1.1 (20%)
Composite stress at strain level 2 (MPa)	22.6	22.6
Matrix stress at strain level 1 (MPa)	6.5	6.5
Matrix stress at strain level 2 (MPa)	12.15	12.15
Matrix stress at break (MPa)	33.28	33.28

Table 5
Outcoming data of Bowyer-Bader modelling.

	PA11-SGW including fines	PA11-SGW excluding fines
Reinforcement content (%)	30%	30%
Orientation factor -χ_1	0.356	0.348
Interface shear strength -τ (MPa)	19.29	16.52
Fibre's tensile strength at maximum stress − σ_t^F (MPa)	562	542
Critical length − Lc (μm)	344	453

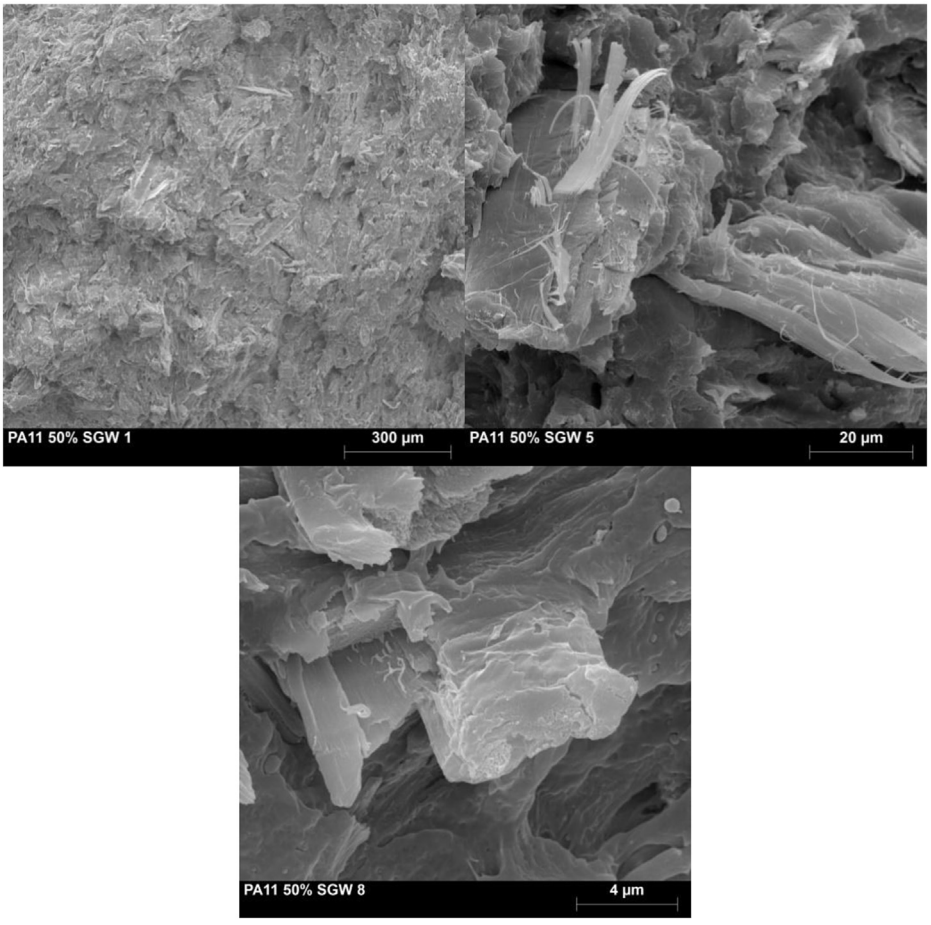

Fig. 4. SEM images of PA11 + 50%SGW composite.

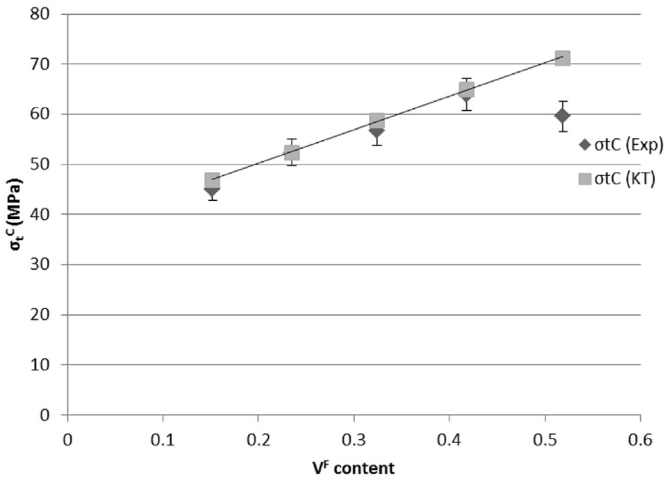

Fig. 5. Tensile strength experimentally obtained and simulated by Kelly-Tyson values.

4. Conclusions

PA11 was successfully reinforced with SGW fibres obtaining a significant enhancement on the mechanical properties. The tensile strength was increased to a maximum of 63.9 MPa when a 50% (w/w) of SGW fibre was added to the composite. This increment was obtained without the use of a coupling agent.

The morphological analysis determined a high quantity of fines in the recovered fibres. These fines were included in the fibre's distribution for modelling the tensile strength.

The surface's chemical composition suggested high lignin contents in the fibre's surface, as expected in a SGW fibre which was not subjected to any chemical treatment.

Micromechanical analysis using Kelly-Tyson model and Bowyer-Bader solution was carried. The results showed the impact of considering the contribution of the fines to the micromechanical properties. The measured τ for PA11-SGW composites including the fines in the fibre distribution rendered a value of 19.29 MPa, closer to the Tresca criterion value (22.11 MPa) than obtained disregarding the fines (16.52 MPa).

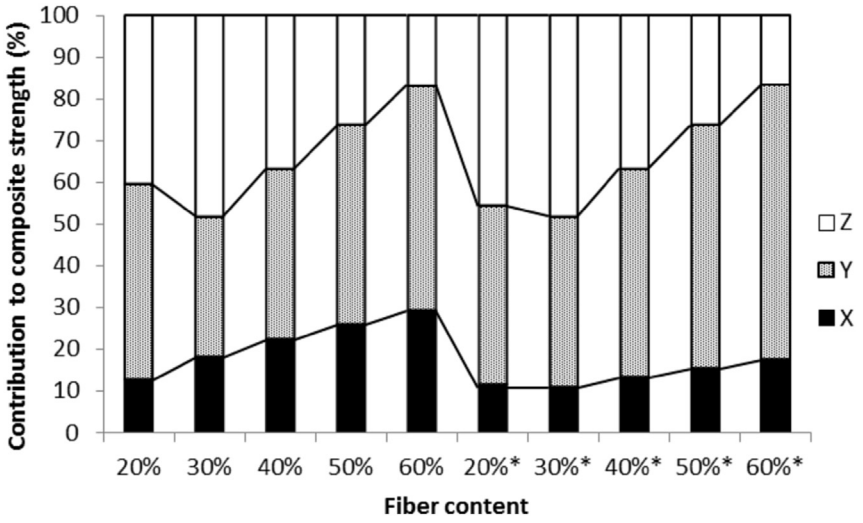

Fig. 6. Contributions to composite's tensile strength. Marked (*) fibre contents indicates the results excluding fines.

in the PA11 + 60SGW was probably related with the matrix not correctly wetting the SGW fibres or the fibre aggregates origination. Despite the 60% w/w fibre content composite, Kelly-Tyson's results agree with the experimental results making the Kelly-Tyson model a good for the tensile analysis [23].

A statistical analysis of t-student [47] was performed between the experimental results obtained and the Kelly-Tyson calculated, except in the 60% of fibre content where the calculated result not fit with the experimental. The *t*-student test showed a possibility of find both results without statistically differences in the 99% of confidence interval.

To further discuss the differences in the τ computed values, Fig. 6 shows the contribution the subcritical and supercritical fibres, and matrix to the composite's tensile strength.

It was found that the calculations performed disregarding fines showed an almost constant contribution of the subcritical fibres. Otherwise, the calculation including the fines showed a regular increment in the contribution of the subcritical fibres. The higher τ value obtained including fines is related with the increase contribution of the subcritical fibres. These values fit better with experimental results.

Tensile strength predictions from the 20 to the 60% reinforced PA11 composites were performed using PA11 + 30SGW data. The obtained values adjust well to the experimental values. The result showed no statistically significant differences in the 99% of the confidence interval.

SGW fibres showed its ability to reinforce PA11 successfully. Their composites can become an interesting and a greener alternative to replace composites materials produced with polypropylene, a petrol-based polymer.

Acknowledgments

We hereby thank Arkema for kindly supplying the polyamide 11 used in this work as well as for the technical information provided by Dr. Patrick Dang (Arkema France) and Mr. Pep Català (Arkema Spain).

References

[1] M.T. Heitzmann, M. Veidt, C.T. Ng, B. Lindenberger, M. Hou, R. Truss, et al.,

Single-plant biocomposite from ricinus communis: preparation, properties and environmental performance, J. Polym. Environ. 21 (2013) 366–374, http://dx.doi.org/10.1007/s10924-012-0517-3.
[2] A. Bourmaud, A. Le Duigou, C. Gourier, C. Baley, Influence of processing temperature on mechanical performance of unidirectional polyamide 11-flax fibre composites, Ind. Crops Prod. 84 (2016) 151–165, http://dx.doi.org/10.1016/j.indcrop.2016.02.007.
[3] P.A. Santos, M.A.S. Spinacé, K.K.G. Fermoselli, M.A. De Paoli, Polyamide-6/vegetal fiber composite prepared by extrusion and injection molding, Compos. Part A Appl. Sci. Manuf. 38 (2007) 2404–2411, http://dx.doi.org/10.1016/j.compositesa.2007.08.011.
[4] P. Zierdt, T. Theumer, G. Kulkarni, V. Däumlich, J. Klehm, U. Hirsch, et al., Sustainable wood-plastic composites from bio-based polyamide 11 and chemically modified beech fibers, Sustain. Mater. Technol. 6 (2015) 6–14, http://dx.doi.org/10.1016/j.susmat.2015.10.001.
[5] M. Feldmann, A.K. Bledzki, Bio-based polyamides reinforced with cellulosic fibres – processing and properties, Compos. Sci. Technol. 100 (2014) 113–120, http://dx.doi.org/10.1016/j.compscitech.2014.06.008.
[6] A. Kiziltas, N. Behzad, D.J. Gardner, D.W. Bousfield, Polyamide 6–Cellulose composites: effect of cellulose composition on melt rheology and crystallization behavior, Polym. Eng. Sci. 54 (2014) 739–746, http://dx.doi.org/10.1002/pen.
[7] D. Aydemir, A. Kiziltas, E. Erbas Kiziltas, D.J. Gardner, G. Gunduz, Heat treated wood-nylon 6 composites, Compos. Part B Eng. 68 (2015) 414–423, http://dx.doi.org/10.1016/j.compositesb.2014.08.040.
[8] P. Perret, From castor Oil to Specialty Polyamides: the Success of the Diversification, Journées Anuelles des Hydrocarbures, Paris, 2014.
[9] L. Martino, L. Basilissi, H. Farina, M.A. Ortenzi, E. Zini, G. Di Silvestro, et al., Bio-based polyamide 11: synthesis, rheology and solid-state properties of star structures, Eur. Polym. J. 59 (2014) 69–77, http://dx.doi.org/10.1016/j.eurpolymj.2014.07.012.
[10] D.M. Panaitescu, R.A. Gabor, A.N. Frone, E. Vasile, Influence of Thermal Treatment on Mechanical and Morphological Characteristics of Polyamide 11/Cellulose Nanofiber Nanocomposites, 2015.
[11] A. Salazar, A. Rico, J. Rodríguez, J. Segurado Escudero, R. Seltzer, F. Martin de la Escalera Cutillas, Monotonic loading and fatigue response of a bio-based polyamide Pa11 and a petrol-based polyamide Pa12 manufactured by selective laser sintering, Eur. Polym. J. 59 (2014) 36–45, http://dx.doi.org/10.1016/j.eurpolymj.2014.07.016.
[12] L. Mancic, R.F.M. Osman, A.M.L.M. Costa, J.R.M. d'Almeida, B.A. Marinkovic, F.C. Rizzo, Thermal and mechanical properties of polyamide 11 based composites reinforced with surface modified titanate nanotubes, Mater. Des. 83 (2015) 459–467, http://dx.doi.org/10.1016/j.matdes.2015.06.059.
[13] A. Bourmaud, A. Le Duigou, C. Gourier, C. Baley, Influence of processing temperature on mechanical performance of unidirectional polyamide 11-flax fibre composites, Ind. Crops Prod. 84 (2016) 151–165, http://dx.doi.org/10.1016/j.indcrop.2016.02.007.
[14] P. Mutjé, M.E. Vallejos, J. Gironès, F. Vilaseca, A. López, J.P. López, et al., Effect of maleated polypropylene as coupling agent for polypropylene composites reinforced with hemp strands, J. Appl. Polym. Sci. 102 (2006) 833–840, http://dx.doi.org/10.1002/app.24315.
[15] E. Franco-Marques, J.A. Mendez, M.A. Pelach, F. Vilaseca, J. Bayer, P. Mutje, Influence of coupling agents in the preparation of polypropylene composites reinforced with recycled fibers, Chem. Eng. J. 166 (2011) 1170–1178, http://dx.doi.org/10.1016/j.cej.2010.12.031.
[16] A. Le Duigou, A. Bourmaud, C. Gourier, C. Baley, Multi-scale shear properties of flax fibre reinforced polyamide 11 biocomposites, Compos. Part A Appl. Sci. Manuf. 85 (2016) 123–129, http://dx.doi.org/10.1016/j.compositesa.2016.03.014.
[17] F. Stempfle, P. Ortmann, S. Mecking, Long-chain aliphatic polymers to bridge the gap between semicrystalline polyolefins and traditional polycondensates, Chem. Rev. (2016), http://dx.doi.org/10.1021/acs.chemrev.5b00705 acs.chemrev.5b00705.
[18] A. Kelly, W.R. Tyson, Tensile properties of fibre-reinforced metals-copper/tungsten and copper/molybdenum, J. Mech. Phys. Solids 13 (1965), http://dx.doi.org/10.1016/0022-5096(65)90035-9, 329in1339–338in2350.
[19] W.H. Bowyer, M.G. Bader, On the re-inforcement of thermoplastics by imperfectly aligned discontinuous fibres, J. Mater. Sci. 7 (1972) 1315–1321, http://dx.doi.org/10.1007/BF00550698.
[20] T.J. Hirsch, Modulus of elasticity of concrete affected by elastic moduli of cement paste matrix and aggregate, J. Am. Concr. Inst. 59 (1962) 427–451.
[21] J.P. López, P. Mutjé, M. Angels Pèlach, N.E. El Mansouri, S. Boufi, F. Vilaseca, Analysis of the tensile modulus of polypropylene composites reinforced with stone groundwood fibers, BioResources 7 (2012) 1310–1323.
[22] R. Reixach, F.X. Espinach, E. Franco-Marques, F. Ramirez de Cartagena, N. Pellicer, J. Tresserras, et al., Modeling of the tensile moduli of mechanical, thermomechanical, and chemi-thermomechanical pulps from orange tree pruning, Polym. Compos (2013) 1840–1846.
[23] L.A. Granda, X. Espinach, F. López, J.C. García, M. Delgado-Aguilar, P. Mutjé, Semichemical fibres of Leucaena collinsii reinforced polypropylene: macro-mechanical and micromechanical analysis, Compos. Part B Eng. 91 (2016) 384–391, http://dx.doi.org/10.1016/j.compositesb.2016.01.035.
[24] M. Rodriguez, A. Rodriguez, J. Bayer R, F. Vilaseca, J. Gironès, P. Mutjé, Determination of corn stalk fibers' strength through modeling of the mechanical properties of its composites, BioResources 5 (2010) 2535–2546.
[25] J.P. López, J.A. Méndez, N.E. El Mansouri, P. Mutjé, F. Vilaseca, Mean intrinsic tensile properties of stone groundwood fibers from softwood, BioResources 6 (2011) 5037–5049.
[26] J.P. Lopez, J.A. Mendez, F.X. Espinach, F. Julian, P. Mutjé, F. Vilaseca, Tensile strength characteristics of polypropylene composites reinforced with stone groundwood fibres from softwood, Bioresources 7 (2012) 3188–3200.
[27] P.T. Anastas, J.C. Warner, Green Chemistry: Theory and Practice, Oxford University Press, New York, 1998.
[28] R. Reixach, E. Franco-Marquès, N.-E. El Mansouri, F.R. de Cartagena, G. Arbat, F.X. Espinach, et al., Micromechanics of mechanical, thermomechanical, and chemi-thermomechanical pulp from orange tree pruning as polypropylene reinforcement: a comparative study, BioResources 8 (2013) 3231–3246, http://dx.doi.org/10.15376/biores.8.3.3231-3246.
[29] L. Granda, F.X. Espinach, Q. Tarrés, J.A. Méndez, M. Delgado-Aguilar, P. Mutjé, Towards a good interphase between bleached kraft softwood fibers and poly(lactic) acid, Compos. Part B Eng. 99 (2016) 514–520, http://dx.doi.org/10.1016/j.compositesb.2016.05.008.
[30] J.S. Lupoi, S. Singh, R. Parthasarathi, B. a. Simmons, R.J. Henry, Recent innovations in analytical methods for the qualitative and quantitative assessment of lignin, Renew. Sustain. Energy Rev. 49 (2015) 871–906, http://dx.doi.org/10.1016/j.rser.2015.04.091.
[31] L.S. Johansson, J.M. Campbell, Reproducible XPS on biopolymers: cellulose studies, Surf. Interface Anal. 36 (2004) 1018–1022, http://dx.doi.org/10.1002/sia.1827.
[32] I.C. Hoeger, I. Filpponen, R. Martin-Sampedro, L.S. Johansson, M. Österberg, J. Laine, et al., Bicomponent lignocellulose thin films to study the role of surface lignin in cellulolytic reactions, Biomacromolecules 13 (2012) 3228–3240, http://dx.doi.org/10.1021/bm301001q.
[33] J. Pérez, J. Muñoz-Dorado, T. de la Rubia, J. Martínez, Biodegradation and biological treatments of cellulose, hemicellulose and lignin: an overview, Int. Microbiol. 5 (2002) 53–63, http://dx.doi.org/10.1007/s10123-002-0062-3.
[34] A. Serrano, F.X. Espinach, J. Tresserras, R. del Rey, N. Pellicer, P. Mutjé, Macro and micromechanics analysis of short fiber composites stiffness: the case of old newspaper fibers-polypropylene composites, Mater. Des. 55 (2014) 319–324, http://dx.doi.org/10.1016/j.matdes.2013.10.011.
[35] A.K. Bledzki, J. Gassan, Composites reinforced with cellulose based fibres, Prog. Polym. Sci. 24 (1999) 221–274, http://dx.doi.org/10.1016/S0079-6700(98)00018-5.
[36] A. Kumar, Y.S. Negi, V. Choudhary, N.K. Bhardwaj, Characterization of cellulose nanocrystals produced by acid-hydrolysis from sugarcane bagasse as agro-waste, J. Mater. Phys. Chem. 2 (2014) 1–8, http://dx.doi.org/10.12691/jmpc-2-1-1.
[37] G. Dorris, D. Gray, Surface analysis of paper and wood fibres by ESCA [electron spectroscopy for chemical analyses]. II. Surface composition of mechanical pulps, Cellul. Chem. Technol. 12 (1978) 721–734.
[38] L.S. Johansson, J. Campbell, K. Koljonen, M. Kleen, J. Buchert, On surface distributions in natural cellulosic fibres, Surf. Interface Anal. 36 (2004) 706–710, http://dx.doi.org/10.1002/sia.1741.
[39] L.S. Johansson, Monitoring fibre surfaces with XPS in papermaking processes, Mikrochim. Acta 138–139 (2002) 217–223, http://dx.doi.org/10.1007/s006040200025.
[40] M.Z. Rong, M.Q. Zhang, Y. Liu, G.C. Yang, H.M. Zeng, The effect of fiber treatment on the mechanical properties of unidirectional sisal-reinforced epoxy composites, Compos. Sci. Technol. 61 (2001) 1437–1447, http://dx.doi.org/10.1016/S0266-3538(01)00046-X.
[41] R. Reixach, E. Franco-Marquès, N.E. El Mansouri, F. Rodríguez de Cartagena, G. Arbat, F.X. Espinach, et al., Micromechanics of mechanical, thermo-mechanical, and chemi-thermomechanical pulp from orange tree pruning as polypropylene reinforcement: a comparative study, Bioresources 8 (2013) 3231–3246.
[42] a. R. Sanadi, R. a. Young, C. Clemons, R.M. Rowell, Recycled newspaper fibers as reinforcing fillers in thermoplastics: Part I-Analysis of tensile and impact properties in polypropylene, J. Reinf. Plast. Compos 13 (1994) 54–67, http://dx.doi.org/10.1177/073168449401300104.
[43] A. Pegoretti, C. Della Volpe, M. Detassis, C. Migliaresi, H.D. Wagner, Thermo-mechanical behaviour of interfacial region in carbon fibre/epoxy composites, Compos. Part A Appl. Sci. Manuf. 27 (1996) 1067–1073, http://dx.doi.org/10.1016/1359-835X(96)00065-6.
[44] F. Vilaseca, A. Valadez-Gonzalez, P.J. Herrera-Franco, M.A. Pelach, J.P. López, P. Mutjé, Biocomposites from abaca strands and polypropylene. Part I: evaluation of the tensile properties, Bioresour. Technol. 101 (2010) 387–395, http://dx.doi.org/10.1016/j.biortech.2009.07.066.
[45] J.L. Thomason, Interfacial strength in thermoplastic composites - at last an industry friendly measurement method? Compos. Part a-Applied Sci. Manuf. 33 (2002) 1283–1288, http://dx.doi.org/10.1016/s1359-835x(02)00150-1.
[46] S.Y. Fu, B. Lauke, Effects of fiber length and fiber orientation distributions on the tensile strength of short-fiber-reinforced polymers, Compos. Sci. Technol. 56 (1996) 1179–1190, http://dx.doi.org/10.1016/S0266-3538(96)00072-3.
[47] B.S. Everitt, G. Dunn, Applied Multivariate Data Analysis, Wiley, New York, 1995.

2.2 Stiffness of bio-based polyamide 11 reinforced with softwood stone ground-wood fibres as an alternative to polypropylene-glass fibre composites

Publicada en *European Polymer Journal*. Factor de impacto 2016: 3,531. Posición 13 de 86 en Polymer Science. Primer cuartil.

European Polymer Journal 84 (2016) 481–489

Contents lists available at ScienceDirect

European Polymer Journal

journal homepage: www.elsevier.com/locate/europolj

Stiffness of bio-based polyamide 11 reinforced with softwood stone ground-wood fibres as an alternative to polypropylene-glass fibre composites

H. Oliver-Ortega [a,*], L.A. Granda [a], F.X. Espinach [b], M. Delgado-Aguilar [a], J. Duran [c], P. Mutjé [a]

[a] Group LEPAMAP, Department of Chemical Engineering, University of Girona, C/M. Aurèlia Capmany, n°61, Girona 17003, Spain
[b] Design, Development and Product Innovation, Dpt. of Organization, Business Management and Product Design, University of Girona, C/M. Aurèlia Capmany, n°61, Girona 17003, Spain
[c] Chemistry Department, University of Girona, Campus Montilivi S-N, Girona 17003, Spain

ARTICLE INFO

Article history:
Received 18 August 2016
Received in revised form 26 September 2016
Accepted 29 September 2016
Available online 30 September 2016

Keywords:
Biopolymers
Biocomposites
Natural fibre reinforcements
Stiffness
Micromechanics

ABSTRACT

Polyolefin had been successfully reinforced with glass fibres and applied in the industry during the last decades. However there are unsolved processability and recyclability problems due to its fragility. There are also concerns related with the human health. This had promoted the interest towards more environmentally friendly and healthier reinforcements such as natural fibres. In addition, the oil origin of polyolefin increases the interest in researching greener polymer alternatives. This work proposes polyamide 11 (PA11) as a promising alternative to polypropylene or other commodity polyolefin. This paper studies the behaviour of the Young's modulus of natural fibre reinforced PA11 composites at different fibre contents. The composites were prepared, injection molded and characterized to tensile modulus. Afterwards a micromechanical modelling was performed using two models: Hirsch's and Tsai-Pagano's. The results allow proposing natural fibre reinforced PA11 composites as a suitable replacement to glass fibre reinforced polypropylene composites.

1. Introduction

Stiffness has a big impact on designing structural applications; one of the main objectives during the design process is choosing materials that ensure the appropriate stiffness and strain during the use of the designed good [1]. Stiffness is related with the necessary strength to deform a material, and it is associated to the Young's modulus which represents the average slope in the elastic region of the strain-stress diagram. Experimentally, the Young's modulus is measured in the strain interval comprehended between 0.05 and 0.25% [2].

Composite materials are produced by combining two or more phases. The main objective of this mixture is obtaining materials with combined properties [3]. The chemical structure and intrinsic properties of both phases, the aspect ratio of the reinforcement and its orientation against the loads, the volume content of fibre and its dispersion inside the matrix have a remarkable importance on such final properties [2,4].

* Corresponding author.
E-mail address: helena.oliver@udg.edu (H. Oliver-Ortega).

http://dx.doi.org/10.1016/j.eurpolymj.2016.09.062
0014-3057/

Polyolefins, such as polypropylene (PP), polyethylene (PE) or polyvinylchloride (PVC), commonly considered commodities, when reinforced with glass fibres or natural fibres show a high enhancement of its stiffness and are, nowadays, widely used in industrial scale [5,6]. Nevertheless, these polymer matrices are commonly obtained from oil and in the near future it will be interesting searching for more sustainable biodegradables or bio-based matrices such as bio-polyamides (BioPA) alternatives [7–9]. Nonetheless one of the main drawbacks of such composites is its poor ability to sustain high deformation without breaking. This is specially visible in starch based composites [10,11]. Therefore, one of the objectives in the development of bio-based composites should be obtaining materials which could achieve stiffness values similar to glass fibre reinforced polyolefin composites.

BioPA are biotechnologically obtained polyamides (PA), produced through different processes and raw materials [12,13]. The natural resource contents can differ between different BioPAs, like polyamide 11 (PA11) which is 100% bio-based and polyamide 6.10 (PA6.10) that only has a 62% of bio-based carbon. However, their melting point, higher than the cellulose degradation temperature, made PAs difficult to reinforce with lignocellulosic fibres [14]. Nonetheless, adapting the processes, it is possible to reinforce these higher melting point PAs with natural fibres [15,16].

PA11 is produced using 11-aminoundecanoic acid derived from castor oil [12]. Castor oil is extracted from the *Ricinus communis*, a common plant in Asia. The variety of fatty acids contained in the oil, with the appropriate refinery process, lead to obtain a huge variety of products used in the industry [17,18]. PA11 shows good oil and water resistance [19], fair biocompatibility [20] and it is non degradable. Furthermore PA11 has a lower melting point than other PA (above 190 °C) which made it an interesting matrix to be reinforced with natural fibres [21,22]. Although PA11 is not degradable, it is bio-based and has mechanical properties comparable to PP. This converts PA11 in a greener alternative to PP, especially as composite matrix.

Glass fibres (GF) are, nowadays, one of the most extended polyolefin reinforcements. The main reason is its high capacity to improve the strength and stiffness of the composites. Nevertheless, this properties enhancement is accompanied by an acceptable diminution of the toughness of the composites. However, the main drawback of GF is related with its fragility, which reduces the number of recyclability cycles, as each process subjects the reinforcement to shrinkage. Other disadvantages of GF are related with the healthiness: dermatitis and respiratory problems have been reported, related with the manipulation of such material [23–25]. On the other hand, natural reinforcements based on lignocellulosic fibres have shown reasonable capacities to increase the mechanical properties in composites, regardless the polymer matrix used [26]. Its use is highly limited by the degradative temperature of the natural fibres. Despite performing a lower relative reinforcing effect than GF, lignocellulosic fibres have high specific properties, they are less abrasive, non-toxic, recyclable and easier to process [27–29]. Those advantages made natural fibres an attractive reinforcement for applications such as automotive [30], construction [31] and industrial goods [32,33].

Stone ground-wood pulp (SGW), a natural fibre, mechanically produced from *Pinus radiata*, with a yield of 98.5%, was choosed as reinforcement in that study. SGW has been commonly used in the paper industry [34]. Besides, SGW reinforced PP composites showed good stiffness compared to GF sized and GF coupled PP composites [35–37].

Considering the European Union environmental goals for 2025 and 2035 [38], the scientific community is doing an effort in the research of fully bio-based or biodegradables composites materials [39,40]. In a previous work, some of the authors studied the effect of the SGW reinforcement in the tensile strengths of the composites [40]. Significant increases of such property against the SGW content were obtained. Nonetheless, it is known that, commonly, increases on the strength of the materials drive to decreases on its toughness [41]. In this work, PA11-SGW composites with 20–60% of SGW contents were prepared and its Young's modulus was analysed and discussed. To better understand the effect of the reinforcement, some micromechanic properties of the Young's modulus were modelled.

2. Experimental

2.1. Materials

The composites were prepared using polyamide 11 (PA11) (Rilsan® BMNO TL), with a density of 1.03 g/cc and a melt volumetric index of 11 cc/10 min at 235 °C/2.16 kg. The PA11 was kindly provided by Arkema S.A (Colombes, France) as the polymer matrix. Stoneground wood (SGW) derived from softwood (*Pinus radiata*) was supplied by Zubialde, S.A. (Aizarnazabal, Spain) and was used as lignocellulosic reinforcement.

Dichloromethane (Extra Pure, stabilized with approx. 50 ppm of amylene, Pharmpur®) and Formic acid (Extra Pure, 98–100%), both supplied by Scharlau (Sentmenat, Spain) were used to dissolve the PA11 matrix and recover the fibres from the composites.

2.2. Methods

2.2.1. Compounding

Five different PA11-based composites, incorporating from 20 up to 60% of SGW reinforcement were prepared. The compounding was performed using a Gelimat kinetic mixer. The SGW and the polymer were added at a low speed (300 rpm).

Once in the mixing chamber, the speed was increase up to 2500 rpm. The material was discharged when the blend reached 200 °C. Afterwards, the blends were pelletized in a knife mill.

2.2.2. Sample obtaining

Composites blends were mould injected in a Meteor-40 injection machine (Mateu&Solé, clamping pressure: 40 tons). The temperature profile was 170–185–200 °C. The injection pressure was 50 bar and the second pressure 20 bar. Samples were cooled 10 s before opening the mould. This process allowed the acquisition of specimens for mechanical characterization under tensile stress (ASTM D638).

2.2.3. Mechanical characterization

The obtained tensile samples were placed in a climatic chamber at 23 °C and 50% RH during 48 h prior to testing, in accordance with ASTM D618. Afterwards, composites were tested to tensile test at 2 mm/min with a DTC-10 Universal testing machine supplied by IDMtest, fitted with a 5 kN load cell. An extensometer was used in agreement with the ASTM D790 standard. Results were obtained from the average of 10 samples.

2.2.4. Fibre recovering from composites

Fibres from composites were recovered by solubilisation of composite's matrix using a Soxhlet apparatus and a mixture of dichloromethane and formic acid (1:1 v/v). Composite samples were grinded in small pieces and placed inside a specific cellulose filter and set into the Soxhlet equipment. The extraction was performed during 24 h. Then, fibres were cleaned and dried in an oven at 105 °C for 24 h more before analysis.

2.2.5. Determination of the fibre length and fibre diameter

The extracted SGW fibre length and diameter distributions were characterized by means of a MorFi analyser (Techpap SAS. Grenoble, France). An aqueous solution of 25 mg/L of fibre was analysed following the standard ISO/FDIS 160652.

3. Results and discussions

3.1. Effect of the fibre reinforcement on the Young's modulus

When a reinforcement is correctly dispersed, the composite material stiffness is directly linked to the intrinsic fibre's Young's modulus, the matrix Young's modulus, the reinforcement content and the fibre orientation against the applied loads [2]. Some of the authors found that the orientation of the fibres is highly affected by the processing equipment and the process parameters [2,36,42]. Contrarily to tensile strength, the interface quality has little effect on the Young's modulus [36,43,44].

PA11 reinforced with 20–60% w/w SGW contents composite materials, were characterized to obtain its Young's modulus. Table 1 (standard deviations between brackets), where V^F is the volume fraction of the fibre in the composite, E_t^C is the experimental Young's modulus of the composite, ε_t^C is the experimental elongation of the composite and ρ^C is the density of the composite, shows the experimental results.

It was found that the Young's modulus increased linearly with the reinforcement content, denoting a correct dispersion of the fibres inside the matrix. The 50% w/w SGW reinforced material showed a Young's modulus 3.51 times higher than the PP matrix. At the same time, this composite also showed a 3.7% strain at break point. Both properties compared good to a 30% w/w GF reinforced PP composite [36,32]. As expected the strain at break decreased when the fibre content was increased [45].

The lineal trend of the stiffness against the fibre content allowed the use of lineal models based on the RoM (Eq. (1)) [46].

$$E_t^c = \eta_e \cdot E_t^F \cdot V^F + (1 - V^F) \cdot E_t^m \quad (1)$$

where E_t^C, E_t^F and E_t^m are the Young's modulus of the composite, fibre and matrix, respectively. V^F is the fibre volumetric fraction and η_e is the efficiency factor. Having only the experimental data, the intrinsic Young's modulus and the efficiency factor are unknowns. The Young's modulus and strain of the PA11 –based composites reinforced with 50 and 60% w/w of

Table 1
Composites Young's moduli, strains and density values obtained experimentally against fibre content.

	V^F	E_t^C (GPa)	ε_t^C (%)	ρ^C (g/cm^3)
PA11	0.000	1.36 (0.04)	24.97 (1.64)	1.03
PA11 + 20%SGW	0.155	2.51 (0.08)	9.47 (0.82)	1.09
PA11 + 30%SGW	0.240	3.03 (0.09)	5.50 (0.38)	1.12
PA11 + 40%SGW	0.329	3.88 (0.08)	4.54 (0.27)	1.15
PA11 + 50%SGW	0.424	4.78 (0.10)	3.70 (0.22)	1.18
PA11 + 60%SGW	0.524	5.76 (0.15)	2.76 (0.22)	1.22

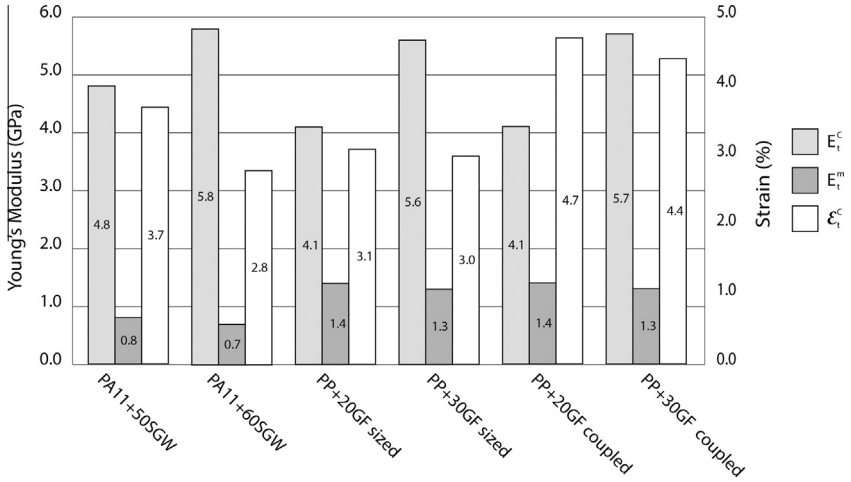

Fig. 1. Young's modulus and strain of PA11-SGW and PP-GF composites and the matrix contribution to the tensile modulus at each fibre contents.

SGW - were compared with literature data of PP-GF composites (Fig. 1) [36,32]. The matrix contributions were calculated using Eq. (1).

PA11-SGW composites at 50 and 60% w/w SGW contents showed similar Young's modulus values than PP-GF composites with 20 and 30% (w/w) GF contents (4.8 and 5.8 versus 4.1 and 5.7 GPa). Nonetheless, it was necessary a higher amount of natural fibre than glass fibre. This was due to the higher intrinsic Young's modulus of the glass fibres. It is possible to find such values in the literature, with an intrinsic Young's modulus of 18 GPa for SGW [35] and 72 GPa for glass fibre's [47]. Moreover, the strain of PA11-SGW composites rendered similar values than PP-GF sized composites (3.7 and 2.8 for PA11-SGW and 3.1 and 3.0 for PP-GF sized). The higher strains obtained in the PP-GF coupled composites was probably caused by the use of a coupling agent. It was also possible to compare the Young's modulus of the PA11-SGW composites with PP-SGW composites (5.2 GPa for a 50% SGW content) [36]. The similarity between PA11-SGW Young's modulus and that of the other composites leads to propose PA11 as a promising candidate to substitute PP [48].

The Specific Composite Young's moduli, calculated as E_t^C/ρ^C, (being ρ^C the density of the composite) were used to relate the effect of the reinforcement weight contents in the stiffness enhancements of the composite materials. Fig. 2 shows the results for some of the above discussed composites. According to the literature, besides the lower mechanical properties of natural fibres composites regarding GF composites, their specific properties could be better or equivalent [49,50]. However, the experimental results were in disagreement and an increase of the fibre content was necessary to achieve the same specific mechanical properties than PP-GF composites.

Then, with the objective of evaluating the net contribution of the reinforcement to the Young's modulus in the composites, a fibre tensile modulus factor (*FTMF*) was defined as:

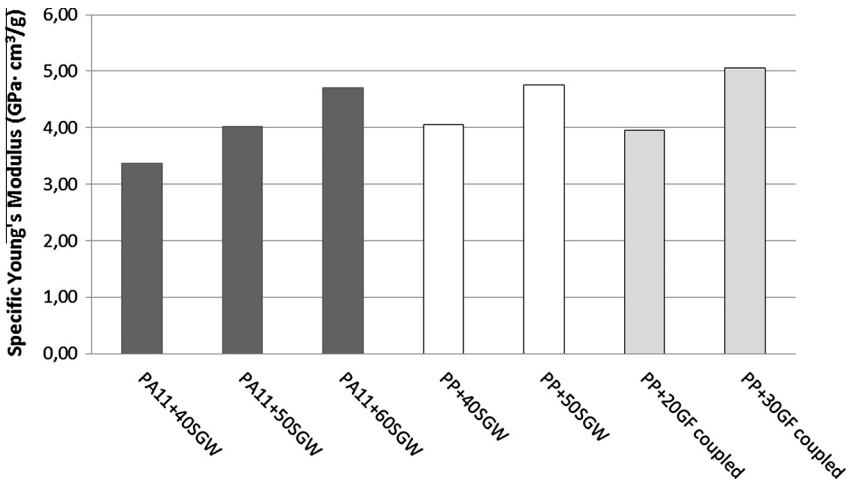

Fig. 2. Specific Young's Modulus of PP-GF, PP-SGW and PA11-SGW composites.

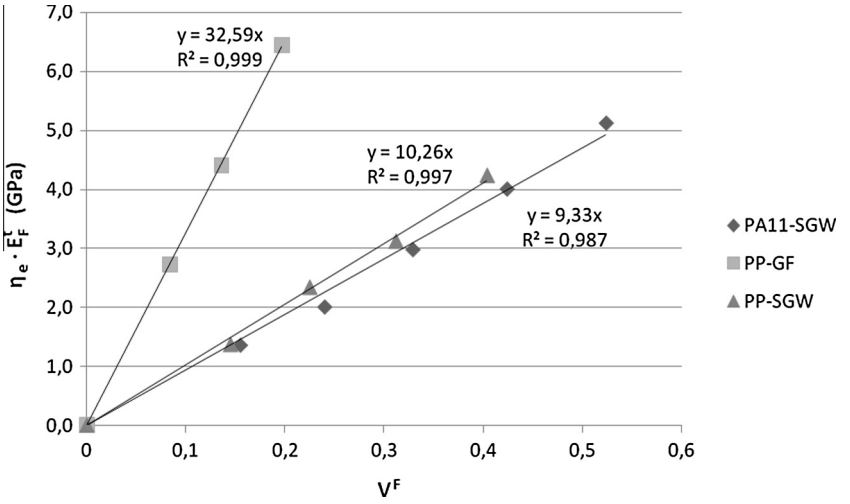

Fig. 3. *FTMF* of PA11-SGW, PP-SGW and PP-GF composites.

$$FTMF = \frac{E_t^c - \left(1 - V^F\right) \cdot E_t^m}{V^F} = \eta_e \cdot E_t^F \tag{2}$$

Fig. 3 presents the obtained results of *FTMF* of PA11-SGW composites and compares them with those for PP-SGW and PP-GF composites, obtained from the literature [36]. The determined *FTMF* for PA11-SGW composites was 9.33. This value was slightly lower than the obtained for PP-SGW composites (10.26) but distant from the obtained for PP-GF composites (32.59). The close *FTMF* values for the SGW reinforced composites might indicate a similar stiffening effect of such reinforcement despite the matrix.

3.2. Micromechanical modelling

As above mentioned, the RoM presented two unknowns making necessary the evaluation of the intrinsic Young's modulus of the fibre. The experimental evaluation of the intrinsic fibre's Young's modulus is difficult and expensive, mainly due the morphology of the reinforcements. As an alternative, it is possible to use micromechanical models to evaluate such property. In this case, the Hirsch model was used for calculating the fibre's intrinsic Young's modulus from the experimental data. The Hirsch model is expressed as [51]:

$$E_t^c = \beta \cdot \left(E_t^F \cdot V^F + E_t^m \cdot (1 - V^F)\right) + (1 - \beta) \cdot \frac{E_t^F \cdot E_t^m}{E_t^m \cdot V^F + E_t^F \cdot (1 - V^F)} \tag{3}$$

where β is a parameter related with the stress transfer between the fibre and the matrix. It is reported that the fibre orientation and the stress concentration effects at the end of the fibres has a strong influence on β. A value of 0.4 has been found to be accurate with experimental behaviour for natural short fibre semi oriented reinforced composites [52].

Once E_t^F was known, it was possible to calculate the efficiency factor (η_e) solving the RoM (Eq. (1)). At the same time the efficiency factor could be expressed as the multiplication of the orientation factor (η_o) and the length factor (η_l); $\eta_e = \eta_o \cdot \eta_l$. The length factor is defined by the Cox and Krenchel equation [53,54]:

$$\eta_l = 1 - \frac{\tanh\left(\frac{\beta \cdot l^F}{2}\right)}{\frac{\beta \cdot l^F}{2}} \tag{4}$$

Being l^F the mean fibre length and β the stress concentration rate at the end of the fibres coefficient, calculated with the following expression:

$$\beta = \frac{1}{r} \sqrt{\frac{E_t^m}{E_t^F \cdot (1 - v) \cdot \ln\left(\sqrt{\frac{\pi}{4 \cdot V^F}}\right)}} \tag{5}$$

where r is the mean radius of the fibres and v the Poisson's ratio of the matrix.

Natural fibres present a length and diameter distribution. However the MorFi analyser used to measure the fibre length and diameter considers the fibres with a length lower than 90 μm as fines. Therefore, and to include them into the modelling,

the fibre's length and diameter including fines was backcalculated. The calculated weighted average length was used to determine η_l by using Eq. (4). According to the literature, the Poisson's ratio for PA11 is 0.42 [55].

Once η_e and η_l were calculated, η_o was easily determined, as $\eta_e = \eta_o \cdot \eta_l$. The orientation coefficient is related with the mean fibre angle regarding the tested load direction. Considering a rectangular distribution of the fibres in the matrix [56,57], the mean angle of the fibres could be expressed as:

$$\eta_o = \frac{\sin(\alpha)}{\alpha} \cdot \left(\frac{3 - \nu}{4} \cdot \frac{\sin(\alpha)}{\alpha} + \frac{1 + \nu}{4} \cdot \frac{\sin(3\alpha)}{\alpha} \right) \tag{6}$$

where α is the mean fibre angle measured from the load direction.

The obtained results are shown in Table 2.

An average angle of 47.6° was measured for the SGW fibres. This angle was slightly higher than the 44.0° measured for PP-SGW composites [36]. Both angles are very similar in agreement with its above mentioned dependence on the used equipment and process parameters. Moreover the intrinsic Young's Modulus of the fibres are really similar between both matrices (17.8 GPa for PA11-SGW and 18.2 GPa for PP-SGW composites [35]). This slight difference could contribute to the lower slope of the Young's modulus progression when increasing the amount of reinforcement in the case of the PA11-based composites.

Despite the importance of the length and diameter of the reinforcements, the Hirsch model does not consider these parameters explicitly. On the other hand, the Tsai-Pagano model, using the Halpin-Tsai equations [58–60] includes the morphology on the fibres. This model showed useful for predicting the fibres' intrinsic Young's modulus in composites [61,62]. In addition, in previous works, the predicted Young's modulus of the PP-SGW determined by Tsai-Pagano model showed to be in agreement with the experimental results [36]. The Tsai-Pagano model is described as:

$$E_t^c = \frac{3}{8} E^{11} + \frac{5}{8} E^{22} \tag{7}$$

Being E^{11} and E^{22} the longitudinal and transversal elastic modulus determined by the Halpin-Tsai equations:

$$E^{11} = \frac{1 + 2 \cdot \left(\frac{l^F}{d^F} \right) \cdot \eta_L V^F}{1 - \eta_L V^F} \cdot E_t^m \tag{8}$$

$$E^{22} = \frac{1 + 2 \cdot \eta_T V^F}{1 - \eta_T V^F} \cdot E_t^m \tag{9}$$

where d^F is the average diameter of the fibres (23.63 μm) and η_L and η_T are parameters described by:

$$\eta_L = \frac{\left(\frac{E_t^F}{E_t^m} \right) - 1}{\left(\frac{E_t^F}{E_t^m} \right) + 2 \cdot \left(\frac{l^F}{d^F} \right)} \tag{10}$$

$$\eta_T = \frac{\left(\frac{E_t^F}{E_t^m} \right) - 1}{\left(\frac{E_t^F}{E_t^m} \right) + 2} \tag{11}$$

The results obtained using the Tsai-Pagano model are presented in Table 3. The determined intrinsic Young's Moduli were numerically different to those calculated using the Hirsch model (Table 2). Nonetheless, the intrinsic average Young's modulus determined by both equations was almost the same; 17.84 GPa for the Hirsch model and 18.04 GPa for the Tsai-Pagano. It seems that the lack of the implicit morphology of the fibres in the Hirsch model had little impact on the calculus.

New values of the efficiency, length and orientation factor (Table 3) were found using the intrinsic Young's modulus of the fibre calculated by Tsai-Pagano. The obtained efficiency, length and orientation factors were slightly different than the measured using the Hirsch model. The calculated fibre mean angle using the Tsai-Pagano Young's modulus renders $\alpha = 48.0°$. This

Table 2
Angle, efficiency, orientation and length factors calculated for the different fibre contents using the intrinsic Young's modulus of the SGW fibre determined by Hirsch model.

Fibre content (%)	V^F	E_t^F (GPa)	η_e	η_l	η_0	α
20	0.155	17.76	0.495	0.844	0.586	47.6°
30	0.240	16.44	0.508	0.859	0.592	47.2°
40	0.329	17.85	0.506	0.861	0.588	47.5°
50	0.424	18.45	0.511	0.877	0.583	47.8°
60	0.524	18.68	0.522	0.898	0.581	47.9°
Mean		**17.84**	0.508	0.868	0.586	47.6°
S.D.		**0.87**	0.01	0.02	0.01	0.3°

Table 3
Intrinsic Young's modulus of the fibre (E_t^F) obtained by Halpin-Tsai modelling, and fibres length (l^F) for PA11-SGW composites at different fibre contents. Efficiency, length and orientation factors obtained from the intrinsic Young's modulus of the fibre calculated using the Tsai-Pagano model.

Fibre content (%)	V^F	l^F (μm)	E_t^F (GPa)	η_e	η_l	η_0	α
20	0.155	377	19.48	0.451	0.837	0.539	51.4°
30	0.240	341	16.81	0.496	0.857	0.579	48.2°
40	0.329	310	18.40	0.491	0.859	0.572	48.8°
50	0.424	299	18.18	0.519	0.878	0.591	47.2°
60	0.524	295	17.32	0.566	0.902	0.625	44.5°
Mean			18.04	0.505	0.866	0.581	48.0°
S.D.			1.03	0.042	0.024	0.031	2.5°

value shows little differences with the obtained by Hirsch model (47.6°). It was found that the efficiency, length and orientation factors of the PP-SGW composites were higher than those of PA11-SGW composites [36]. An increase in the fibre's orientation was observed when the fibre quantity became higher than the matrix content. This effect was more appreciable with the Tsai-Pagano model approximation where it was found an angle of 44.52°, which was the lowest angle obtained for PA11-SGW composites.

However, a statistical hypothesis t-student test was performed to determine if the rendered results between the two models were statistically different. The obtained *p*-value for the 99% of confidence interval was higher than the 0.01 *p*-value corresponding to this interval. Hence, the probability that both methodologies rendered non-significant differences is 99% [63].

4. Conclusions

PA11-SGW composite materials were successfully produced with reinforcement contents ranging from 20 up to 60% w/w.

A lineal increase of the materials' Young's modulus was observed when increasing the SGW content. The Young's modulus of the 50% SGW composite was 3.51 times higher than the matrix.

The Young's moduli of PA11 + 50SGW and PA11 + 60SGW composites were compared with data from a previous work based on PP-GF composites. It was necessary to increase the fibre content up to 50% to obtain similar stiffness than PP-GF at 30% w/w GF content.

The *FTMF* obtained for PA11-SGW composites (9.33) was similar to that obtained for PP-SGW composites in the literature (10.26). This could indicate a similar effect of the reinforcement regardless the polymer matrix used.

The intrinsic Young's modulus was obtained through two different models: Hirsch and Tsai-Pagano. The Hirsch model rendered an intrinsic Young's modulus of 17.84 GPa, which was similar to the intrinsic Young's modulus found in the literature.

The intrinsic Young's modulus calculated by Tsai-Pagano was 18.04 GPa. This model takes into account explicitly the morphological characteristics of the fibre. Nonetheless, no significant differences were obtained. This effect was also reflected in the efficiency and orientation factors, finding numerically differences values but very close values when the Tsai-Pagano model was used. The efficiency factor rendered values comprehended between 0.451 and 0.566 by Tsai-Pagano modelling, while the obtained using Hirsch model resulted on 0.495–0.522. Both models rendered orientation angles around 48°; Tsai-Pagano model 48.0°, and Hirsch 47.6°. Moreover, it was observed an increase of the orientation of the fibres in the composite when the fibre content was increased.

It was found that the efficiency, length and orientation factors of the PP-SGW composites were higher than those of PA11-SGW composites.

In conclusion, it was thought that PA11 was an interesting material that could be under consideration for producing more sustainable composite materials. As it has been stated, the addition of SGW fibres had a similar stiffening effect with either PA11 or PP matrices. In addition, it was possible to obtain similar Young's modulus and strain than PP-GF composite ranging 20–30% w/w GF contents.

Acknowledgements

We hereby thank Arkema for kindly supplying the polyamide 11 used in this work as well as for the technical information provided by Dr. Patrick Dang (Arkema France) and Mr. Pep Català (Arkema Spain).

References

[1] R.C. Neagu, Stiffness contribution of various wood fibers to composite materials, J. Compos. Mater. 40 (2005) 663–699, http://dx.doi.org/10.1177/0021998305055276.
[2] R. Reixach, F.X. Espinach, E. Franco-Marques, F. Ramirez de Cartagena, N. Pellicer, J. Tresserras, P. Mutje, Modeling of the tensile moduli of mechanical, thermomechanical, and chemi-thermomechanical pulps from orange tree pruning, Polym. Compos. 34 (2013) 1840–1846, http://dx.doi.org/10.1002/pc.22589.
[3] G. Lubin, Handbook of Composites, Van Nostrand Reinhold Company, 1982.

[4] L.A. Granda, F.X. Espinach, J.A. Méndez, J. Tresserras, M. Delgado-Aguilar, P. Mutjé, Semichemical fibres of Leucaena collinsii reinforced polypropylene composites: Young's modulus analysis and fibre diameter effect on the stiffness, Compos. Part B: Eng. 92 (2016) 332–337, http://dx.doi.org/10.1016/j.compositesb.2016.02.023.
[5] C. Alves, P.M.C. Ferrão, A.J. Silva, L.G. Reis, M. Freitas, L.B. Rodrigues, D.E. Alves, Ecodesign of automotive components making use of natural jute fiber composites, J. Clean. Prod. 18 (2010) 313–327, http://dx.doi.org/10.1016/j.jclepro.2009.10.022.
[6] J. Holbery, D. Houston, Natural-fiber-reinforced polymer composites in automotive applications, Jom 58 (2006) 80–86, http://dx.doi.org/10.1007/s11837-006-0234-2.
[7] M.T. Heitzmann, M. Veidt, C.T. Ng, B. Lindenberger, M. Hou, R. Truss, C.K. Liew, Single-plant biocomposite from Ricinus communis: preparation, properties and environmental performance, J. Polym. Environ. 21 (2013) 366–374, http://dx.doi.org/10.1007/s10924-012-0517-3.
[8] L. Teuber, V.-S. Osburg, W. Toporowski, H. Militz, A. Krause, Wood polymer composites and their contribution to cascading utilisation, J. Clean. Prod. 110 (2015) 9–15, http://dx.doi.org/10.1016/j.jclepro.2015.04.009.
[9] J.L. Vold, C.A Ulven, B.J. Chisholm, Torrefied biomass filled polyamide biocomposites: mechanical and physical property analysis, J. Mater. Sci. 50 (2015) 725–732, http://dx.doi.org/10.1007/s10853-014-8632-2.
[10] F.X. Espinach, F. Julián, M. Alcalà, J. Tresserras, P. Mutjé, High stiffness performance alpha-grass pulp fiber reinforced thermoplastic starch-based fully biodegradable composites, BioResources 9 (2014) 738–755.
[11] J.P. Lopez, F. Vilaseca, L. Barberà, R.J. Bayer, M.A. Pèlach, P. Mutjé, Processing and properties of biodegradable composites based on Mater-Bi® and hemp core fibres, Resour. Conserv. Recycl. 59 (2012) 38–42, http://dx.doi.org/10.1016/j.resconrec.2011.06.006.
[12] L. Martino, L. Basilissi, H. Farina, M.A. Ortenzi, E. Zini, G. Di Silvestro, M. Scandola, Bio-based polyamide 11: synthesis, rheology and solid-state properties of star structures, Eur. Polym. J. 59 (2014) 69–77, http://dx.doi.org/10.1016/j.eurpolymj.2014.07.012.
[13] S. Kind, S. Neubauer, J. Becker, M. Yamamoto, M. Volkert, G. von Abendroth, O. Zelder, C. Wittmann, From zero to hero – production of bio-based nylon from renewable resources using engineered Corynebacterium glutamicum, Metab. Eng. 25 (2014) 113–123, http://dx.doi.org/10.1016/j.ymben.2014.05.007.
[14] M. Feldmann, A.K. Bledzki, Bio-based polyamides reinforced with cellulosic fibres – processing and properties, Compos. Sci. Technol. 100 (2014) 113–120, http://dx.doi.org/10.1016/j.compscitech.2014.06.008.
[15] P. Alvarez de Arcaya, A. Retegi, A. Arbelaiz, J.M. Kenny, I. Mondragon, Mechanical properties of natural fibers/polyamides composites, Polym. Compos. 30 (2009) 257–264.
[16] A.K. Bledzki, M. Feldmann, Bio-based polyamides reinforced with cellulosic fibres – processing and properties, Compos. Sci. Technol. 100 (2014) 113–120.
[17] H. Mutlu, M.A.R. Meier, Castor oil as a renewable resource for the chemical industry, Eur. J. Lipid Sci. Technol. 112 (2010) 10–30, http://dx.doi.org/10.1002/ejlt.200900138.
[18] D.S. Ogunniyi, Castor oil: a vital industrial raw material, Bioresour. Technol. 97 (2006) 1086–1091, http://dx.doi.org/10.1016/j.biortech.2005.03.028.
[19] T. Mazan, R. Berggren, J.K. Jørgensen, A. Echtermeyer, Aging of polyamide 11. Part 1: evaluating degradation by thermal, mechanical, and viscometric analysis, J. Appl. Polym. Sci. 132 (2015), http://dx.doi.org/10.1002/app.41971.
[20] M. Dhanalakshmi, Preparation and characterization of electrospun fibers of Nylon 11, Express Polym. Lett. 2 (2008) 540–545, http://dx.doi.org/10.3144/expresspolymlett.2008.65.
[21] A. Bourmaud, A. Le Duigou, C. Gourier, C. Baley, Influence of processing temperature on mechanical performance of unidirectional polyamide 11 – flax fibre composites, Ind. Crops Prod. 84 (2016) 151–165, http://dx.doi.org/10.1016/j.indcrop.2016.02.007.
[22] P. Zierdt, T. Theumer, G. Kulkarni, V. Däumlich, J. Klehm, U. Hirsch, A. Weber, Sustainable wood-plastic composites from bio-based polyamide 11 and chemically modified beech fibers, Sustain. Mater. Technol. 6 (2015) 6–14, http://dx.doi.org/10.1016/j.susmat.2015.10.001.
[23] B.J. Wang, J.Y. Lee, R.C. Wang, Fiberglass dermatitis: report of two cases, J. Formos. Med. Assoc. 92 (1993) 755–758.
[24] K. Donaldson, C.L. Tran, An introduction to the short-term toxicology of respirable industrial fibres, Mutat. Res. Mol. Mech. Mutagen. 553 (2004) 5–9, http://dx.doi.org/10.1016/j.mrfmmm.2004.06.011.
[25] M.I. Greenberg, J. Waksman, J. Curtis, Silicosis: a review, Dm Dis. 53 (2007) 394–416, http://dx.doi.org/10.1016/j.disamonth.2007.09.020.
[26] E. Bodros, I. Pillin, N. Montrelay, C. Baley, Could biopolymers reinforced by randomly scattered flax fibre be used in structural applications?, Compos Sci. Technol. 67 (2007) 462–470, http://dx.doi.org/10.1016/j.compscitech.2006.08.024.
[27] A.K. Bledzki, J. Gassan, Composites reinforced with cellulose based fibres, Prog. Polym. Sci. 24 (1999) 221–274, http://dx.doi.org/10.1016/S0079-6700(98)00018-5.
[28] H.M. Akil, M.F. Omar, A.A.M. Mazuki, S. Safiee, Z.A.M. Ishak, A. Abu Bakar, Kenaf fiber reinforced composites: a review, Mater. Des. 32 (2011) 4107–4121, http://dx.doi.org/10.1016/j.matdes.2011.04.008.
[29] Z.N. Azwa, B.F. Yousif, A.C. Manalo, W. Karunasena, A review on the degradability of polymeric composites based on natural fibres, Mater. Des. 47 (2013) 424–442, http://dx.doi.org/10.1016/j.matdes.2012.11.025.
[30] F.M. Al-Oqla, S.M. Sapuan, Natural fiber reinforced polymer composites in industrial applications: feasibility of date palm fibers for sustainable automotive industry, J. Clean. Prod. 66 (2014) 347–354, http://dx.doi.org/10.1016/j.jclepro.2013.10.050.
[31] A.M. Carus, A. Eder, L. Dammer, H. Korte, L. Scholz, R. Essel, E. Breitmayer, M. Barth, Wood-plastic composites (WPC) and natural fibre composites (NFC): European and global markets 2012 and future trends in automotive and construction, 2015. <http://www.sciencedirect.com/science/article/pii/S1464391X0280174X>.
[32] A. Serrano, F.X. Espinach, J. Tresserras, N. Pellicer, M. Alcala, P. Mutje, Study on the technical feasibility of replacing glass fibers by old newspaper recycled fibers as polypropylene reinforcement, J. Clean. Prod. 65 (2014) 489–496, http://dx.doi.org/10.1016/j.jclepro.2013.10.003.
[33] T.C. Rousakis, I.S. Tourtouras, RC columns of square section – passive and active confinement with composite ropes, Compos. Part B: Eng. 58 (2014) 573–581, http://dx.doi.org/10.1016/j.compositesb.2013.11.011.
[34] L. Salmén, M. Lucander, E. Härkönen, J. Sundholm, Fundamentals of mechanical pulping, Mechanical pulping, Fapet Oy, Jyväskylä, Finland, 1999.
[35] J.P. López, J.A. Méndez, N.E. El Mansouri, P. Mutjé, F. Vilaseca, Mean intrinsic tensile properties of stone groundwood fibers from softwood, BioResources 6 (2011) 5037–5049.
[36] J.P. López, P. Mutjé, M. Angels Pèlach, N.E. El Mansouri, S. Boufi, F. Vilaseca, Analysis of the tensile modulus of polypropylene composites reinforced with stone groundwood fibers, BioResources 7 (2012) 1310–1323.
[37] F. Julian, J.A. Méndez, F.X. Espinach, N. Verdaguer, P. Mutje, F. Vilaseca, Bio-based composites from stone groundwood applied to new product development, BioResources 7 (2012) 5829–5842.
[38] J. Martínez Urreaga, C. González-Sánchez, A. Martínez-Aguirre, C. Fonseca-Valero, J. Acosta, M.U. de la Orden, Sustainable eco-composites obtained from agricultural and urban waste plastic blends and residual cellulose fibers, J. Clean. Prod. 108 (2015) 1–8, http://dx.doi.org/10.1016/j.jclepro.2015.06.001.
[39] L. Granda, F.X. Espinach, Q. Tarrés, J.A. Méndez, M. Delgado-Aguilar, P. Mutjé, Towards a good interphase between bleached kraft softwood fibers and poly(lactic) acid, Compos. Part B: Eng. 99 (2016) 514–520, http://dx.doi.org/10.1016/j.compositesb.2016.05.008.
[40] H. Oliver-Ortega, L.A. Granda, F.X. Espinach, J.A. Mendez, F. Julian, P. Mutjé, Tensile properties and micromechanical analysis of stone groundwood from softwood reinforced bio-based polyamide11 composites, Compos. Sci. Technol. 132 (2016) 123–130, http://dx.doi.org/10.1016/j.compscitech.2016.07.004.
[41] R.O. Ritchie, The conflicts between strength and toughness, Nat. Mater. 10 (2011) 817–822, http://dx.doi.org/10.1038/nmat3115.
[42] F.X. Espinach, F. Julian, N. Verdaguer, L. Torres, M.A. Pelach, F. Vilaseca, P. Mutje, Analysis of tensile and flexural modulus in hemp strands/polypropylene composites, Compos. Part B: Eng. 47 (2013) 339–343, http://dx.doi.org/10.1016/j.compositesb.2012.11.021.

[43] R. Reixach, F.X. Espinach, G. Arbat, F. Julián, M. Delgado-Aguilar, J. Puig, P. Mutjé, Tensile properties of polypropylene composites reinforced with mechanical, thermomechanical, and chemi-thermomechanical pulps from orange pruning, BioResources 10 (2015) 4544–4556.
[44] M.D.H. Beg, K.L. Pickering, Mechanical performance of Kraft fibre reinforced polypropylene composites: Influence of fibre length, fibre beating and hygrothermal ageing, Compos. Part A – Appl. Sci. Manuf. 39 (2008) 1748–1755, http://dx.doi.org/10.1016/j.compositesa.2008.08.003.
[45] S.E. Vannan, S.P. Vizhian, Microstructure and mechanical properties of as cast aluminium alloy 7075/basalt dispersed metal matrix composites, J. Miner. Mater. Charact. Eng. 2 (2014) 182–193, http://dx.doi.org/10.4236/jmmce.2014.23023.
[46] J.L. Thomason, The influence of fibre properties on the properties of glass-fibre-reinforced polyamide 6,6, J. Compos. Mater. 34 (2000) 158–172, http://dx.doi.org/10.1177/002199830003400205.
[47] A. Bismarck, S. Mishra, T. Lampke, Plant fibers as reinforcement for green composites, in: Nat. Fibers, Biopolym. Biocomposites, 2005, pp. 37–108.
[48] P. Wambua, J. Ivens, I. Verpoest, Natural fibres: can they replace glass in fibre reinforced plastics?, Compos Sci. Technol. 63 (2003) 1259–1264, http://dx.doi.org/10.1016/S0266-3538(03)00096-4.
[49] I. Aranberri-Askargorta, T. Lampke, A. Bismarck, Wetting behavior of flax fibers as reinforcement for polypropylene, J. Colloid Interface Sci. 263 (2003) 580–589, http://dx.doi.org/10.1016/S0021-9797(03)00294-7.
[50] M.S. Islam, K.L. Pickering, N.J. Foreman, Influence of alkali treatment on the interfacial and physico-mechanical properties of industrial hemp fibre reinforced polylactic acid composites, Compos. Part A: Appl. Sci. Manuf. 41 (2010) 596–603, http://dx.doi.org/10.1016/j.compositesa.2010.01.006.
[51] T.J. Hirsch, Modulus of elasticity of concrete affected by elastic moduli of cement paste matrix and aggregate, J. Am. Concr. Inst. 59 (1962) 427–451.
[52] G. Kalaprasad, K. Joseph, S. Thomas, C. Pavithran, Theoretical modelling of tensile properties of short sisal fibre-reinforced low-density polyethylene composites, J. Mater. Sci. 32 (1997) 4261–4267, http://dx.doi.org/10.1023/a:1018651218515.
[53] H.L. Cox, The elasticity and strength of paper and other fibrous materials, Br. J. Appl. Phys. 3 (1952) 72.
[54] H. Krenchel, Fibre reinforcement, Alademisk Forl. (1964).
[55] G. Boisot, L. Laiarinandrasana, J. Besson, C. Fond, G. Hochstetter, Experimental investigations and modeling of volume change induced by void growth in polyamide 11, Int. J. Solids Struct. 48 (2011) 2642–2654, http://dx.doi.org/10.1016/j.ijsolstr.2011.05.016.
[56] H. Fukuda, K. Kawata, On Young's modulus of short fibre composites, Fibre Sci. Technol. 7 (1974) 207–222.
[57] Y. Sanomura, M. Kawamura, Fiber orientation control of short-fiber reinforced thermoplastics by ram extrusion, Polym. Compos. 24 (2003) 587–596, http://dx.doi.org/10.1002/pc.10055.
[58] J.C. Halpin, Stiffness and expansion estimates for oriented short fiber composites, J. Compos. Mater. 3 (1969) 732–734.
[59] J.C. Halpin, N.J. Pagano, The laminate approximation for randomly oriented fibrous composites, J. Compos. Mater. 3 (1969) 720–724.
[60] J.C. Halpin, Effects of environmental factors on composite materials, Ohio, 1969.
[61] C.L. Tucker, E. Liang, Stiffness predictions for unidirectional short-fiber composites: review and evaluation, Compos. Sci. Technol. 59 (1999) 655–671, http://dx.doi.org/10.1016/S0266-3538(98)00120-1.
[62] A. Serrano, F.X. Espinach, J. Tresserras, R. del Rey, N. Pellicer, P. Mutjé, Macro and micromechanics analysis of short fiber composites stiffness: the case of old newspaper fibers-polypropylene composites, Mater. Des. 55 (2014) 319–324, http://dx.doi.org/10.1016/j.matdes.2013.10.011.
[63] B.S. Everitt, G. Dunn, Applied Multivariate Data Analysis, Wiley, New York, 1995.

2.3 Evaluation of thermal and thermomechanical behaviour of bio-based polyamide 11 based composites reinforced with lignocellulosic fibres

Publicada en *Polymers*. Factor de impacto 2016: 3,364. Posición 16 de 86 en Polymer Science. Primer cuartil.

polymers

MDPI

Article

Evaluation of Thermal and Thermomechanical Behaviour of Bio-Based Polyamide 11 Based Composites Reinforced with Lignocellulosic Fibres

Helena Oliver-Ortega [1], José Alberto Méndez [1], Pere Mutjé [1], Quim Tarrés [1,*], Francesc Xavier Espinach [2] and Mònica Ardanuy [3]

1 Group LEPAMAP, Department of Chemical Engineering, University of Girona, C/M.Aurèlia Capmany, 61, 17003 Girona, Spain; helena.oliver@udg.edu (H.O.-O.); jalberto.mendez@udg.edu (J.A.M.); pere.mutje@udg.edu (P.M.)

2 Design, Development and Product Innovation, Dpt. Organization, Business Management and Product Design, University of Girona, C/M.Aurèlia Capmany, 61, 17003 Girona, Spain; francisco.espinach@udg.edu

3 Departament de Ciència dels Materials i Enginyeria Metal.lúrgica, Secció Enginyeria Tèxtil, Universitat Politècnica de Catalunya, C/Colom, 11, 08222 Terrassa, Barcelona, Spain; monica.ardanuy@upc.edu

* Correspondence: joaquimagusti.tarres@udg.edu; Tel.: +34-690-754-563

Received: 14 September 2017; Accepted: 16 October 2017; Published: 18 October 2017

Abstract: In this work, polyamide 11 (PA11) and stone ground wood fibres (SGW) were used, as an alternative to non-bio-based polymer matrices and reinforcements, to obtain short fibre reinforced composites. The impact of the reinforcement on the thermal degradation, thermal transitions and microstructure of PA11-based composites were studied. Natural fibres have lower degradation temperatures than PA11, thus, composites showed lower onset degradation temperatures than PA11, as well. The thermal transition and the semi-crystalline structure of the composites were similar to PA11. On the other hand, when SGW was submitted to an annealing treatment, the composites prepared with these fibres increased its crystallinity, with increasing fibre contents, compared to PA11. The differences between the glass transition temperatures of annealed and untreated composites decreased with the fibre contents. Thus, the fibres had a higher impact in the composites mechanical behaviour than on the mobility of the amorphous phase. The crystalline structure of PA11 and PA11-SGW composites, after annealing, was transformed to α' more stable phase, without any negative impact on the properties of the fibres.

Keywords: polyamide 11; lignocellulosic fibres; thermomechanical behaviour; annealing; microstructure

1. Introduction

Composites are produced to obtain new materials, designed to be used for a specific applications, with comparatively better properties than its phases [1]. In this sense, the literature shows that polymeric matrices with comparatively poor mechanical properties, such as polyolefin, have been successfully reinforced to obtain competitive materials. One example of these composites are glass fibre reinforced polypropylene (PP) materials, currently produced and used at industrial level [2]. Nonetheless, despite the high mechanical performance of these composites, there are health problems associated with the manipulation of glass fibres [3] and its poor recyclability. This justifies the search for more healthy and environmentally friend substitutive reinforcements. Moreover, the UE has fixed for 2025–2030 some recyclability goals [4] which are not possible to achieve using glass fibres as reinforcements.

Cellulosic or lignocellulosic reinforcing fibres have become a recyclable alternative to glass fibres. These fibres have been extensively studied since the 1980s showing good intrinsic properties

such as comparatively high tensile strengths [5]. Moreover, cellulosic fibres are fully bio-based and biodegradable [6]. Besides, the use of natural fibres accomplishes objectives proposed by green chemistry and sustainable production [7,8]. In addition, their use and manipulation is healthier.

Since the 1980s, the environmental awareness of the society has increased noticeably. The use of non-renewable resources and the high impact of oil-based polymers on the environment drive the research of more environmentally friendly alternatives to such resources. One of the proposed challenges is reducing the oil-based polymer dependence and replacing these polymers by bio-based or biodegradable ones [9], with lower environmental fingerprints [10]. Besides, the use of biodegradable polymers can also promote waste reduction, diminishing its environmental impact [11]. Therefore, the composite materials researchers have increased their interest on these materials as possible replacements to oil-based matrices [12].

Despite all the aforementioned advantages, cellulosic fibres have low thermal degradation temperatures, being this its main drawback that limits their use as reinforcement for polymer-based composites [12]. The degradation temperatures of cellulosic fibres are between 200 °C and 250 °C, and, therefore, the matrices must be able to be processed at such temperatures. Polyamide 11 (PA11), also called nylon 11, is a bio-based polyamide obtained from castor oil. Moreover, it is a non-biodegradable polymer matrix allowing its use for long-time applications, such as those needed in the construction or automotive sectors [12,13]. Besides, its melting temperature, around 190 °C, is low enough to avoid the thermal degradation of cellulosic fibres during composites manufacturing. Furthermore, PA11 is a recyclable thermoplastic matrix with mechanical properties similar to polypropylene. Thus, PA11 is a promising green alternative to polypropylene [14,15].

There are some studies in the about different nanomaterial reinforced PA11 nanocomposites [16,17]. More recently, there are works devoted to cellulosic fibres reinforced PA11 composites [15,18,19]. The analysis of the tensile and flexural properties of these cellulosic composites showed significant increases of its modulus and strength together with low reductions of its strains at break [15,19], compared to other fibre, like glass fibres (GF), based composites [14]. However, although the thermal properties and the structure of PA11-based composites reinforced with several micro- or nano-reinforcements have been extensively studied, there are only few studies about the effect of cellulosic fibres in a PA11 matrix [15].

In this study, Stone Groundwood (SGW) fibres from softwood were used as reinforcement for PA11 biocomposites. SGW fibres were obtained by high yield mechanical processes (98%) and, therefore, the chemical composition of such fibres and the wood from which they come were the same [19]. Moreover, SGW is produced in a sustainable way due to its use in the papermaking industry. The effect of these lignocellulosic fibres in the thermal stability, thermal transitions and thermomechanical behaviour of PA11 composites were analysed. In addition, an annealing treatment was applied to the fibres to study the impact of such treatment in the thermal properties of the composites.

2. Materials and Methods

2.1. Materials

Rilsan®BMNO TLD polyamide 11, kindly supplied by Arkema S.A. (Colombes, France), with a density of 1.03 g/cm^3 and a melt flow index (MFI) of 11 cc/10 min measured at 235 °C/2.16 kg, was used as polymer matrix.

Stone Groundwood (SGW), a mechanically defibrated pulp from softwood (*Pinus radiata*), provided by Zubialde S.A. (Aizarnazabal, Spain), was used as reinforcement. The length and diameter distributions of SGW fibres were studied in a previous work [19]. In the mentioned study, the density of fibre was determined to be 1.40 g/cm^3.

2.2. Composite Compounding

Composites reinforced with 10%, 20% and 50% *w*/*w* fibre content were produced in a Gelimat Kinetic Mixer (model G5S, Draiswerke, Mahaw, New Jersey, NJ, USA). The fibres and the polymer matrix were firstly added and premixed at low speed (300 rpm) and then the speed was increased up to 2500 rpm. When the mixture reached 200 °C, the material was discharged, cooled and pelletized with a knives mill. To produce the specimens, the composites were mould injected in a Meteor-40 injection machine (Mateu & Solé, Barcelona, Spain). The processing temperature profile was 170–185–200 °C and the pressures were modified regarding the fibre content to a maximum of 75 bars for the volumetric phase and 30 bars for the pressure maintenance phase. The samples were stored in a climatic chamber at 23 °C and 50% RH before their analysis, according to ASTM D618 standard specifications.

2.3. Annealing Treatment

The annealing treatment, based previous publications, was performed following the conditions that led to a maximum crystallinity enhancement [20,21]. This treatment consisted of heating the matrix or the composites in an oven at 165 °C for 1 h followed by cooling them at room temperature (23 °C).

2.4. Composite Characterization

Thermogravimetrical analysis (TGA) was performed in a Mettler Toledo SDTA 851 thermobalance (Mettler Toledo, L'Hospitalet de Llobregat, Spain). Samples were heated from 30 to 700 °C at a heating rate of 10 °C/min under nitrogen atmosphere at a flow rate of 40 mL/min.

Differential Scanning Calorimetry analysis (DSC) was performed using a Mettler Toledo DSC822e calorimeter (Mettler Toledo, L'Hospitalet de Llobregat, Spain) following ASTM E 1269.01 standard specification. The samples were initially heated from 40 to 210 °C to erase their thermal history. Afterwards, the samples were cooled and heated again using the same temperature range. All runs were performed at heating or cooling rates of 10 °C/min under 40 mL/min flow of nitrogen atmosphere.

Dynamic mechanical thermal analysis (DMTA) was carried out in a Mettler Toledo DMA/SDTA 861 (Mettler Toledo, L'Hospitalet de Llobregat, Spain) using dual cantilever configuration. Specimens of 65 × 13 × 3 mm^3 were cut from the flexural specimens obtained following the ASTM D3641. The tests were performed at a frequency of 1 Hz and a preload of 3 N. The temperature range was −40 °C to 120 °C with a heating rate of 3 °C/min and the analysis was performed in air atmosphere.

X-ray diffraction measurements were performed on a Bruker D8 Advance diffractometer (Bruker, Madrid, Spain) with a Cu-Kα radiation (λ = 0.15406 nm). Data were collected on the 2θ range from 5° to 40° operating at 40 KV and 40 mA.

A Fourier Transformed infrared spectroscopy (FT-IR) using a Bruker Alpha FT-IR spectrometer (FT-IR) (Bruker, Madrid, Spain) was performed in the PA11 and PA11 composites.

3. Results and Discussion

3.1. Thermal Stability of the Composites

As mentioned in the Introduction, the comparatively low degradation temperature of natural fibres limits its use with a broad set of polymeric matrices. The matrices must have melting temperatures in the order of 200 °C. Moreover, the fibre degradation could have a negative effect on the thermal degradation of the polymer matrix.

The TGA profiles and the first derivate of the PA11 and the composites reinforced with a 20% and 50% *w*/*w* of SGW are shown in Figure 1.

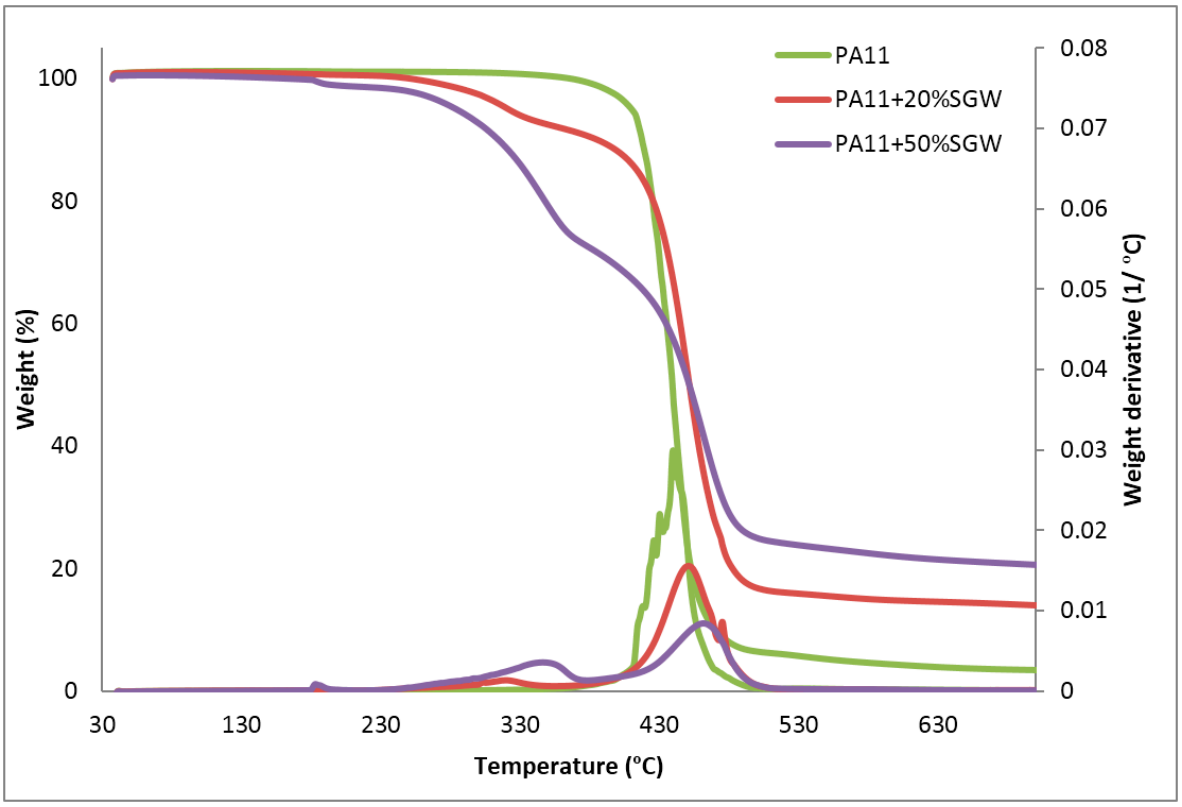

Figure 1. TGA curves and first derivate of the TGA curve for neat PA11 and PA11-SGW composites.

As shown in Figure 1, neat PA11 presents a TGA trend with one main decomposition step starting around 400 °C. PA11 composites started degrading before, and presented two main decomposition steps, as was expected for cellulose reinforced composite materials. Table 1 shows the onset temperatures for the 5% and 10% of weight loss ($T_{5\%}$ and $T_{10\%}$) in PA11 and PA11-SGW composites.

Table 1. Onset temperatures for the 5% and 10% of weight loss and temperature in the maximum decomposition rate.

Temperatures (°C)	PA11	PA11 + 20% SGW	PA11 + 50% SGW
$T_{5\%}$	409	322	307
$T_{10\%}$	417	386	336
T_{max}	439	451	461

Although the degradation of PA11-SGW composites seemed to start around 200 °C, the weight loss did not surpass 5% until 300 °C. This first decomposition step was related to the reinforcement degradation, and gained importance when the fibre contents were increased. During this step, the degradation of the O-glucosidic bonds of the cellulose and hemicelluloses occurred [22,23]. The degradation of the other component of the fibres, lignin and extractives occurred in a broader temperature range from around 200 °C to 900 °C [24,25]. SGW fibres showed high lignin contents [19,26], thus, a high degradation range was expected. It was considered that the slight differences obtained in the fibres length, produced by attrition phenomena during composite preparation of the fibres [14,19], had little influence in its decomposition. Moreover, it was possible to measure the onset temperature for the 95% weight loss ($T_{95\%}$) for the matrix (560 °C) but it was impossible for the composites. An inflection point in the curve, where a second degradation step started, was observed at around 350 °C and 375 °C for PA11 + 20% SGW and PA11 + 50% SGW, respectively. This was related with the degradation of the polymeric phase. This inflection point in

the curve indicated that the matrix started degrading before the fibre degradation was finished [22]. The first derivative of the TGA curve was performed to evaluate this effect (Figure 1). As expected, only one peak was obtained for the PA11 matrix, while two peaks, corresponding with the degradation of the fibres and polymer matrix, were found in PA11-SGW composites. Moreover, these peaks appeared overlapped indicating that there was a range of temperatures where fibres and matrix degraded simultaneously.

On the other hand, a shift of the maximum temperature of the decomposition step (T_{max}) of the polymer from 439 °C for pure PA11 to 451 °C and 461 °C for PA11 + 20% SGW and PA11 + 50% SGW composites, respectively, was observed. From these results, it was concluded that, although the cellulose fibres had a negative effect on the onset decomposition temperature of the composites, their presence contributed to thermally stabilize the composite once the degradation started. The literature shows similar thermal stabilizations in the case of cellulose nanofiber (CNF) reinforced PA11 [27] and other thermoplastic matrices reinforced with lignocellulosic fibres [28]. This phenomenon has been explained as an inhibiting effect of the char obtained from the fibres decomposition to the diffusion of volatile and radical compounds implied in PA11 decomposition.

Another important effect of the fibre addition was related to the residue found at 700 °C. It was observed that the addition of fibre enhanced its content from 3.4%, obtained in monolithic PA11, up to 20.5% when 50% SGW fibres were added to the composite material. This increase on the residue was related with the extractives and inorganic compounds contents in the lignocellulosic reinforcement, and lignin molecules which did not totally degrade [24,25,29]. Finally, from these TGA curves, it was observed that the degradation of the fibres occurred at higher temperatures than the processing temperatures of the corresponding composites, allowing the preparation of these composites.

3.2. Thermal Transitions and Structure of the Composites

The melting and crystallization behaviours of the polymer matrix and the composites were studied by means of DSC. The thermographs obtained during the second heating, after erasing the thermal history, are shown in Figure 2.

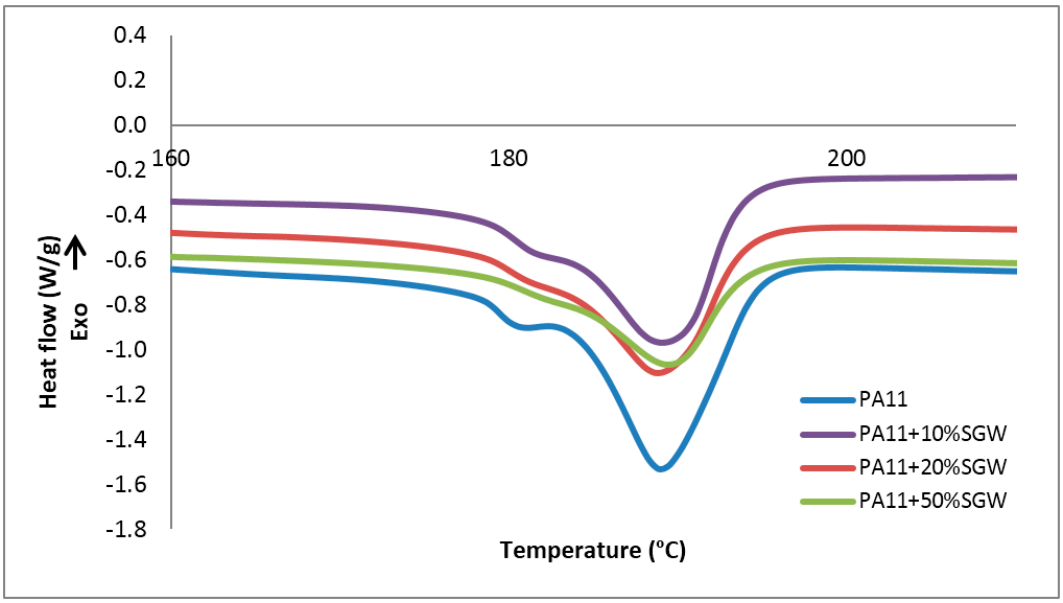

Figure 2. DSC thermographs of the melting point of PA11 and PA11 composites.

It was observed that PA11 presented a main peak at around 189 °C, preceded by a shoulder with a maximum at around 181 °C as a rearrangement in the structure [30]. PA11 has different crystalline structures which can be transformed from one to another depending on temperature,

cooling conditions and pressure, among others [31–33]. This shoulder peak corresponded to the melt-crystallization process of the γ phase to the α′ crystalline form of PA11 [30,34]. The secondary peak seemed to decrease and the main peak became broader when the fibre content was increased in the composite material. This effect has also been found when CNF were used as reinforcement, indicating that the fibres promoted the α′ crystalline form instead of the γ form observed in the neat PA11 [27,34]. On the other hand, it was found that the melting temperature (T_m) was not affected by SGW presence (189 °C for all the studied materials).

The degree of crystallinity of the polymer matrix was calculated as the ratio between the enthalpy of main melting endotherm and the theoretical enthalpy for a fully crystalline polymer matrix ($\Delta\hat{H}$ m = 226.4 J/g) [27,35]. The obtained degree of crystallinities for the composites materials were 26.4%, 26.4% and 27.2% for PA11 + 10% SGW, PA11 + 20% SGW and PA11 + 50% SGW, respectively. These values were very similar to the pure matrix (26.7%), indicating no significant effect of the fibres on the degree of crystallinity of the PA11 matrix. In the literature, a slight increase (around 3%) in the degree of crystallinity for CNF reinforced PA11 composites with contents lower than 5% has been reported [27]. However, for higher contents of CNF, the crystallinity decreased. This could be related with a disruption of the PA11 structure by the effect of the CNF [27]. Moreover, the chemical surface's composition of SGW fibres is different to CNF studied in the literature, mainly due to the presence of lignin in the fibre surface. This could inhibit the nucleating effect of the fibres, as it also inhibited the interactions between the polymer matrix and the fibre [15,19,29]. On the other hand, cellulose nanocrystals (CNC) and modified CNC also obtained no significant changes in crystallinity when they were used as reinforcement in PA11 [36]. This is the opposite effect to that observed in other polymer matrices, where the cellulosic fibres acted as nucleating agents, increasing the polymer crystallinity [22,37,38]. Nonetheless, these matrices had weaker interactions with cellulose fibres than PA11. The capacity of this polymer to establish H-bonds with cellulose [19] can explain this disruption in the polymer matrix, and hence no considerable nucleating effect was observed. Moreover, this capacity can inhibit the formation of the γ crystalline phase on the composites.

Concerning the crystallization behaviour, a peak with a maximum crystallization temperature (T_c) at 164 °C was observed for the PA11 and the composites. The crystallinity of PA11 matrix was also measured as the ratio between the enthalpy of the polymer crystallization and the theoretical value of the crystalline polymer matrix. The obtained values were not different from those obtained during the melting except for the PA11 + 10% SGW composite, where a lower degree of crystallinity (22.8%) was measured.

The results allowed concluding that, as found in the literature for other cellulose reinforced PA11 and PP composites, the presence of SGW fibres did not affect the main transition temperatures of the crystalline polymer phase [22,33,37].

The DMTA thermograms of the PA11 composite materials was performed to observe other processes in which the material loss energy take place, as well as to understand the behaviour of the stiffness of the materials with the temperature. In this sense, a softening is usually experimented when thermoplastic materials overpass the glass transition (T_g) as the amorphous chains of the polymer suffers an important gain of mobility.

As shown in Figure 3, the evolution of the loss modulus (E″) of pure PA11 and the composites with respect to the temperature showed a unique transition in the studied range, related with the T_g of the polymer matrix.

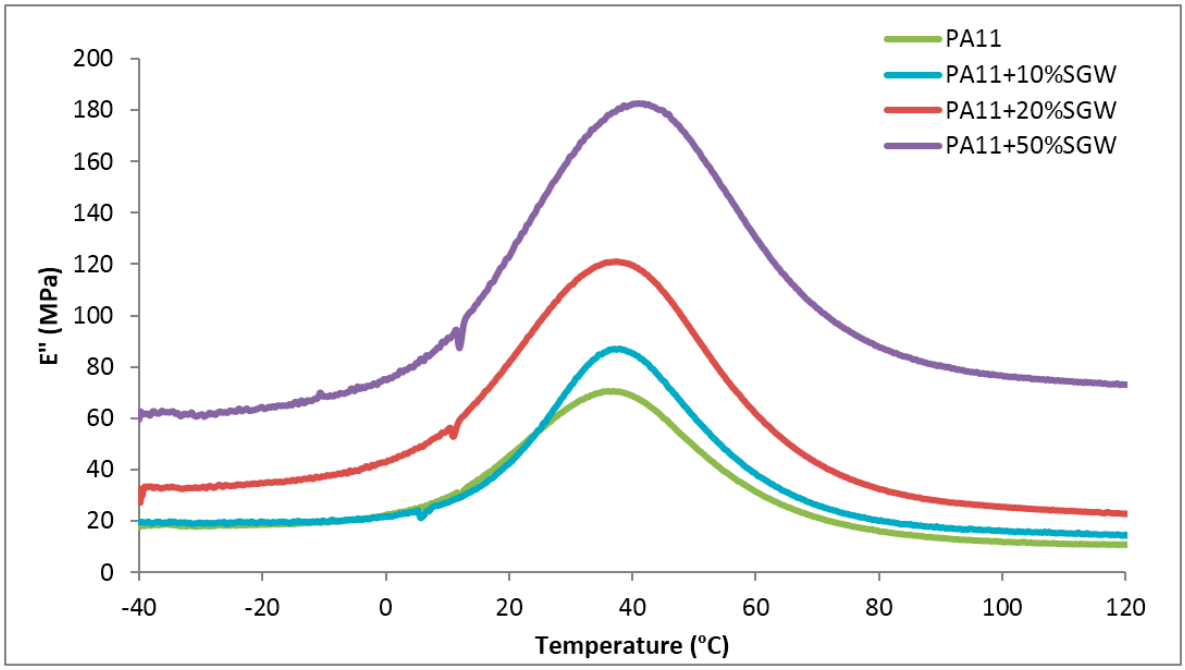

Figure 3. Loss Modulus of the PA11, PA11 + 20% SGW and PA11 + 50% SGW with respect to the temperature.

Figure 4 represents the evolution of the values of storage modulus (E') and tan δ of PA11 and the composites with the temperature. The measured values of the T_g obtained from the tan δ curve shifted from 53.1 °C for neat PA11 °C to 50.0 °C, 51.0 °C and 53.2 °C for the PA11 + 10% SGW, PA11 + 20% SGW and PA11 + 50% SGW, respectively. No considerable differences were observed in the T_g of the composites by the effect of SGW content. This was related with the same crystallinity values of the materials. Thus, no changes were observed in the amorphous phase of the PA11 matrix in the composite materials. It was observed that tan δ decreased with SGW contents as a consequence of the enhancement of the loss moduli.

As expected, higher values of storage moduli were obtained for the composite materials due to the stiffening effect of the reinforcing material [39,40]. For all materials, a slight decrease was observed when the temperature was raised in the analysis below 20 °C, as a result of a slight mobility gain in the polymer chain, and a drastic drop was observed when the T_g was overpass. Once the temperature was over the T_g, the storage modulus values were really low, indicating a high mobility of the polymer molecules corresponding to the amorphous phase of the PA11. However, the presence of SGW fibres stiffened the material, achieving higher values of storage modulus due to the higher stiffness of cellulosic fibres and counteracting the reduction of the modulus when the T_g was exceeded. It must be noted that the presence of lignocellulosic fibres in the composite material significantly reduced the mobility of the polymer chains for temperatures higher than its T_g. The influence of SGW fibres is clearly observed in Figure 4, where the modulus of PA11 + 50% SGW at 80 °C is 10 times higher than the PA11 modulus at the same temperature and slightly higher than the PA11 matrix at 20 °C.

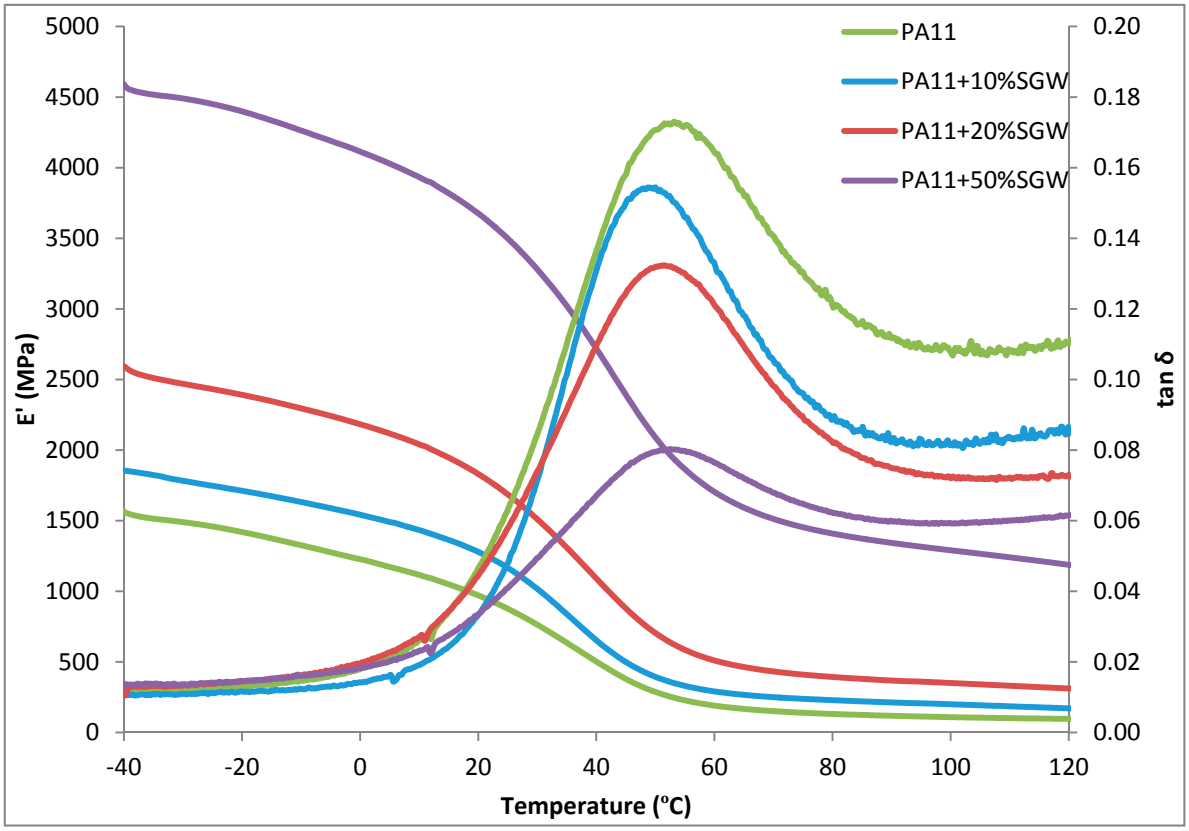

Figure 4. Storage modulus and tan δ results of PA11, PA11 + 10% SGW, PA11 + 20% SGW and PA11 + 50% SGW.

The crystalline structure of PA11 and PA11-SGW composites was analysed using an X-ray diffractometer (Figure 5). It is known that PA11 shows polymorphism that highly influences its properties [41,42]. The DSC study showed two different structures during the second melting (γ and α′ forms), for PA11 and the composite with 10% of SGW. However, it must be noted that these structures were obtained after a melting process and controlled crystallization with a cooling rate of 10 °C/min. The obtained samples produced by injection-moulding were not cooled under the same conditions and can have a different structure. As can be seen in Figure 5, the samples after injection-moulding process showed a broad peak at 2θ = 21°, corresponding to the δ′ phase produced from quenching from the melt [35,43,44], which is similar to the process produced during injection-moulding. The controlled crystallization of the DSC led to obtaining the α′ crystalline form that was produced by melt crystallization [44]. Moreover, a small content of γ phase is typically obtained during this analysis and is transformed to the α′ more stable form [21]. Nonetheless, the γ phase or was impossible to be observed at room temperature [43] or its content was low and was difficult to identify. Thus, its formation simultaneously with the δ′ phase was not observed in the X-ray diffractograms.

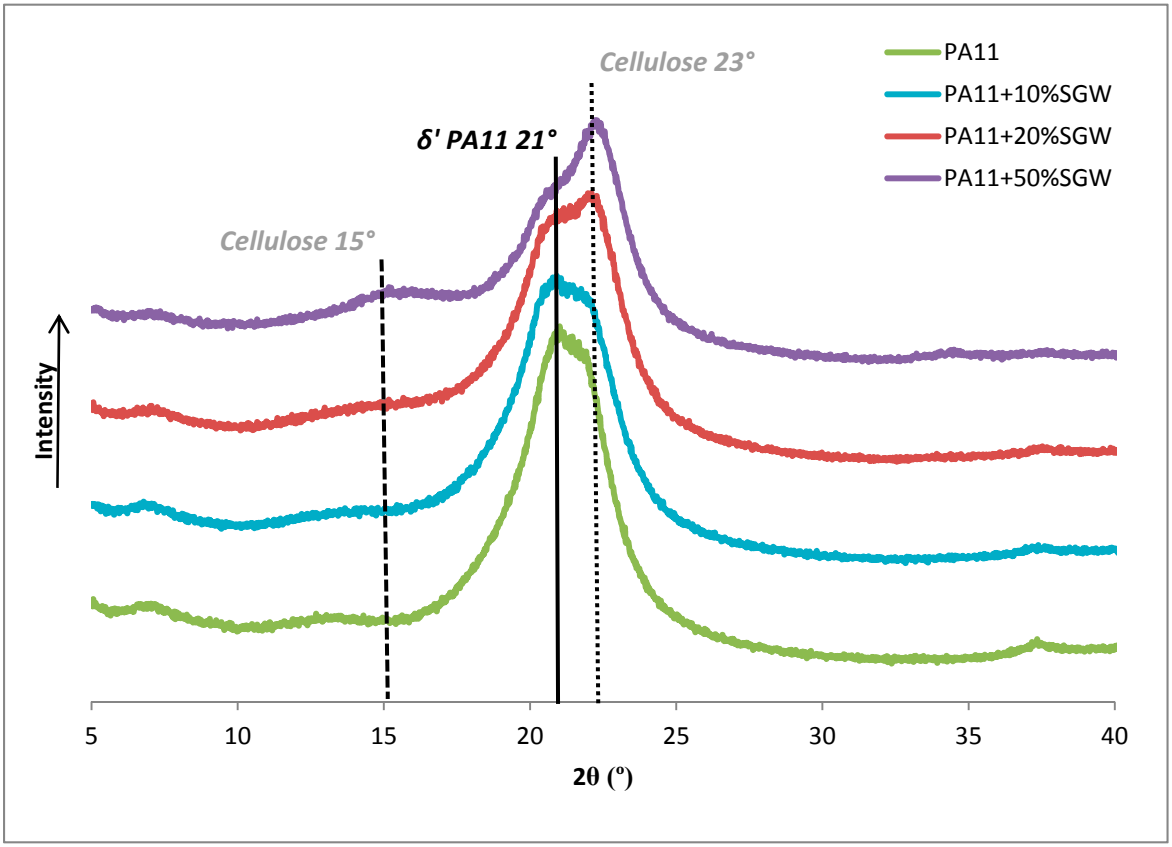

Figure 5. X-ray diffractograms of PA11 and PA11-SGW composites.

The broad peak of PA11 and composites related with the PA11 δ′ crystalline form was similar to that obtained in the literature for this PA11 structure [17]. Despite this, two more peaks at 22.3° and 15° of 2θ appeared for PA11 + 20% SGW and PA11 + 50% SGW composites and were related with cellulose [29]. These peaks can only be appreciated in the composites with higher fibre contents due to the low crystallinity of the fibre: 48.5% measured with the X-ray diffractometer and calculated as the ratio between the intensity at the peak at 22°–23° and the minimum at 15°–18°, as has been described in the literature [45]. This low crystallinity of the SGW fibres is in agreement with the values obtained for untreated pine fibres [29]. These results differ from those found on the literature for PA11 nanocomposites, where, usually, the α′ structure is observed [21,36,44]. However, the reinforcement content with respect to the matrix for these nanocomposites was significantly lower. Moreover, the formation of the different phases is strongly influenced by the cooling process, which could be different than the performed in this work [35,44].

Nonetheless, although γ phase is difficult to identify in the diffractograms at room temperature, FT-IR can serve as a complementary technique to determine the presence of this crystalline phase [39,45]. Figure 6 shows the FT-IR normalized for PA11 and PA11-SGW composites. There are some differences in the main bands observed regarding the crystal phase. Nevertheless, usually the difference in the wavelength is really small. One of the most differentiated bands in the FT-IR profiles was in the fingerprint zone of the FT-IR spectrum. The bands comprised in the range 500–800 cm^{-1} were related with amide V and VI amide bands (marked in the Figure 6). When the γ phase was present, a shoulder peak was observed in the 721 cm^{-1} peak, while in other forms a double peak at 721 and 686 cm^{-1} was shown. In PA11 and PA11 + 10% SGW a broad peak was observed while a double peak 721 and 681 cm^{-1} was appreciated in 20% and 50% of SGW fibre reinforced composites. Moreover, a small peak was observed around 627 cm^{-1} in the FT-IR of the PA11 and PA11 + 10% SGW composites and the band of 581 shifted to higher wavelengths, usually found in in the γ phase [45].

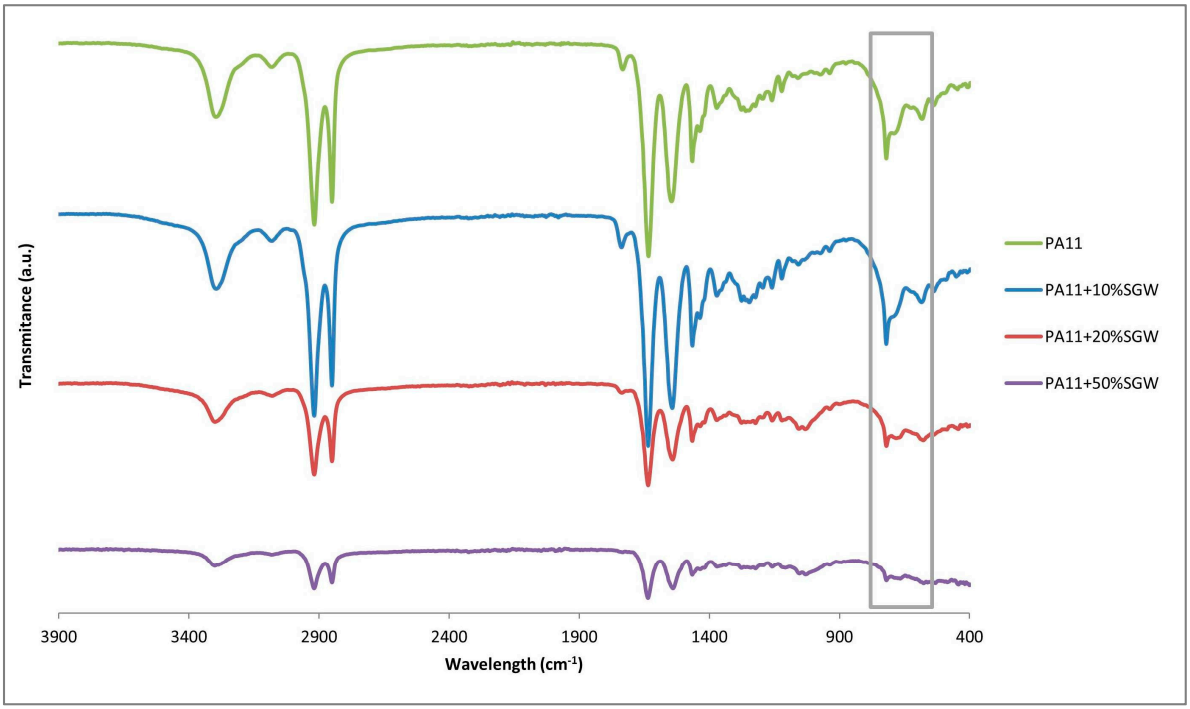

Figure 6. FT-IR PA11 and PA11-SGW composites.

3.3. Effect of Annealing on the Structure and Thermal Transitions

Thermal annealing treatment is used in polymers to obtain a specific crystallinity form, to increase their crystallinity reducing the softening effect when the T_g is overpassed or as a useful form to remove residual stresses, which could appear during the extrusion, injection or other processing procedures [17,42,46]. Thermal annealing has growing importance in PA11 thermal studies because of its piezoelectric and ferroelectric properties. However, these studies usually involved the use of nanomaterials in the case of composite materials [21,34].

In this case, the objective of the annealing was to enhance the crystallinity of the samples to study the influence of SGW fibres during this process. As mentioned above, no considerable increase of the crystallinity was obtained in the DSC of PA11-SGW composites while a nucleating effect of the fibre was observed for PP-SGW composites [23]. As mentioned above, using CNF at low reinforcement contents increased the crystallinity of PA11. Otherwise, high contents of fibre seemed to inhibit the crystalline production, probably due to the H-bonds established between the fibres and the matrix. Crystalline structures in PA11 have a large dependence of the H-bond orientation [32]. In the literature, it can be found that, after an annealing process, the PA11 structure shows higher crystallinity [17,35]. However, the fibres and their capacity to interact with PA11 can impact this process.

As explained before, the PA11, PA11 + 10% SGW, PA11 + 20% SGW and PA11 + 50% SGW samples were annealed at 165 °C for 1 h and studied using DSC, DMTA and X-Ray diffraction.

The DSC results showed an increase of the degree of the crystallinity in the first heat by the effect of the annealing, which increased considerably when the fibre content was augmented. In particular, the crystallinity of PA11 after the annealing treatment increased from 26.7% to 28.9%, and, in the composites, from 26.4%, 26.4% and 27.2% to 27.5%, 30.7% and 40.5% for PA11 + 10% SGW, PA11 + 20% SGW and PA11 + 50% SGW, respectively. It seems that SGW fibres can act as nucleating agent during the annealing process. Trans-crystallinity process between fibres and matrix are highly dependent on the characteristics of the fibre, matrix and their interactions [47]. PA11 requires higher time and temperature than PP due to the high intermolecular interactions, which can be produced between PA11 and fibres, explaining the increments produced during the annealing. The highest crystallinity

was observed for the highest fibre content, with a difference in the crystallinity up to 10%, compared with the neat annealed PA11.

Furthermore, a secondary crystal formation was observed in all the samples after annealing (Figure 7). PA11 showed a small peak around the temperature of the annealing treatment (165 °C) corresponding to the polymer chains crystallized during the annealing. In the composites, this small peak increased and was shifted to higher temperatures, indicating higher T_m of the crystals produced during the annealing process. In the case of PA11 + 50% SGW, the secondary crystal formation merged with the peak of the melting temperature at 189 °C. This phenomenon can be related with a nucleating effect of the fibre which has been observed in other polymers [22]. Moreover, the enhancement of the T_m of the crystals obtained after the annealing was also observed in the literature when the annealing time was increased for PA11 matrix [31]. The addition of SGW shortened the annealing treatment to achieve similar crystallinities.

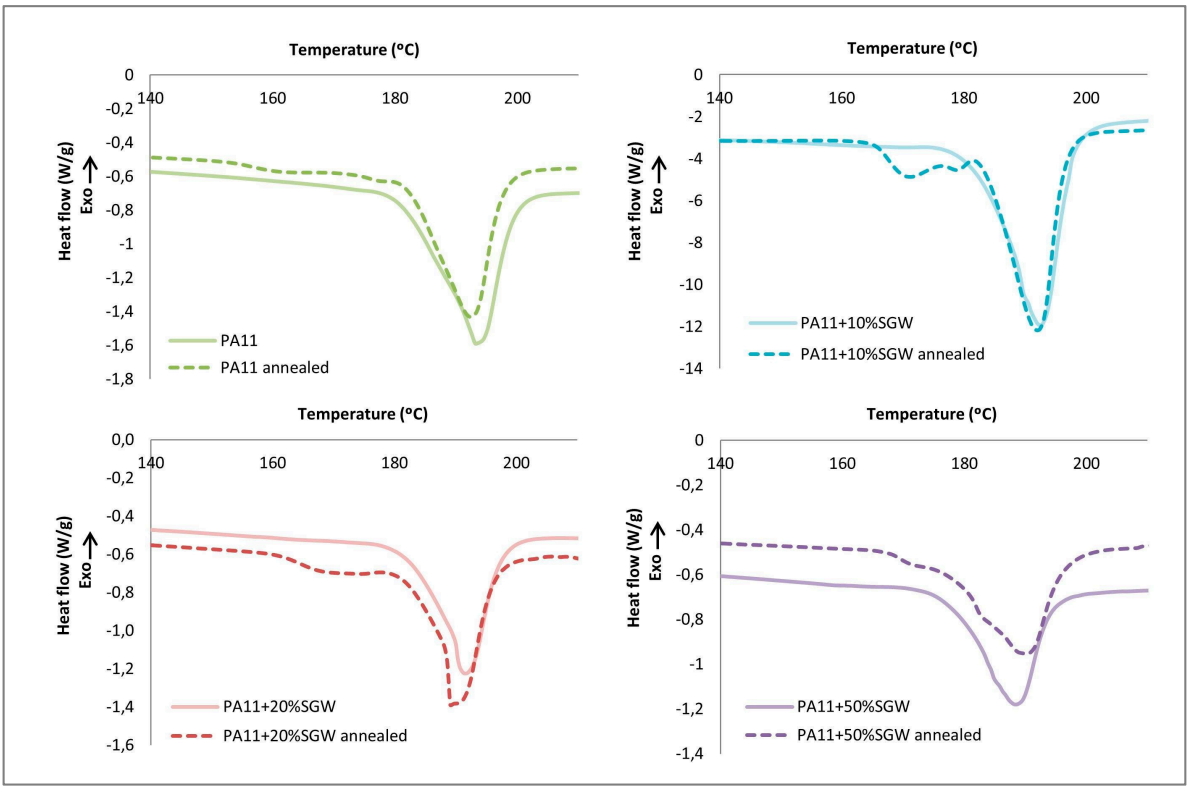

Figure 7. DSC thermographs of the firsts heating comparing annealed and not annealed samples.

Although an improvement in the crystallinity due the secondary crystal growth obtained during annealing was observed, only slight differences in the T_m values were found by the effect of the annealing treatment.

A change in the T_g was expected, as this transition temperature is directly related with the amorphous phase in the material. After the annealing, the amorphous phase of the polymer matrix was reduced, thus the crystalline phase was increased, diminishing the mobility of the chains. This can imply a higher T_g temperature. DMTA was performed in the annealed PA11 and their composites and the results were compared to the untreated ones.

In the loss modulus (Figure 8), the annealed samples achieved higher values due to the higher crystalline phase in the polymer. Nonetheless, this increment in the modulus was reduced as the fibre content increased. Moreover, again, a unique transition corresponding to the T_g was observed in the studied range. However, the peaks were shifted to higher temperatures, except for the PA11 + 50% SGW.

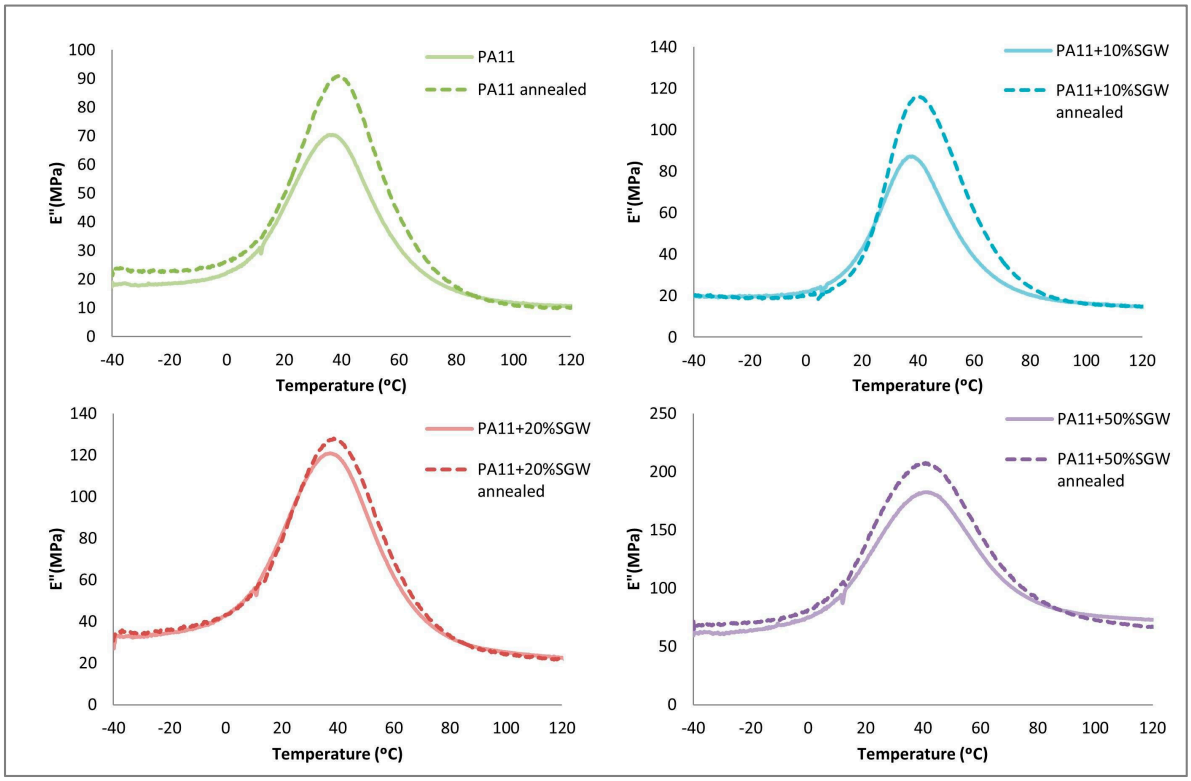

Figure 8. Loss modulus obtained by DMTA of the treated and untreated samples.

As aforementioned, the tan δ was used to determine the T_g of the composite materials. Figure 9 shows the T_g obtained for untreated and treated samples.

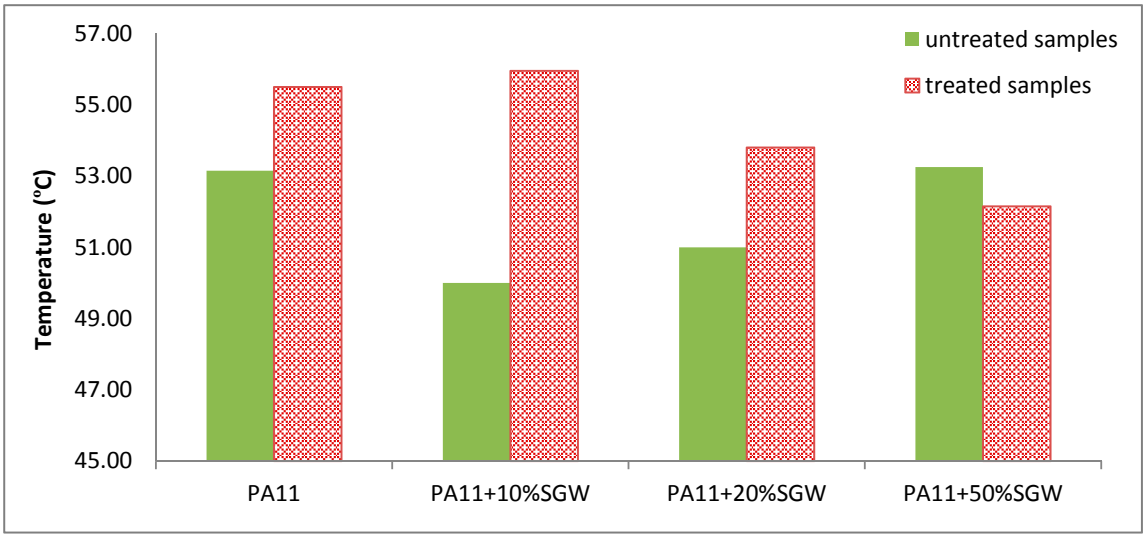

Figure 9. T_g measured values for treated and untreated samples.

The T_g temperatures increased for all the samples, except for the PA11 + 50% SGW, where similar T_g values were found for the untreated and annealed samples. On the other hand, the effect of the annealing in the T_g decreased as the fibre contents increased. This can be due to higher impact of the stiffness of the fibres in the modulus and in the reduction of the chain mobility than to the increase of crystallinity produced by the annealing treatment.

Figure 10 shows the results obtained for the evolution of the storage modulus with the temperature analysed by DMTA. Higher moduli were obtained in the annealed samples due to the higher crystalline phase in the polymer. Nevertheless, as was observed, this effect was higher in the neat PA11 than in PA11-SGW composites.

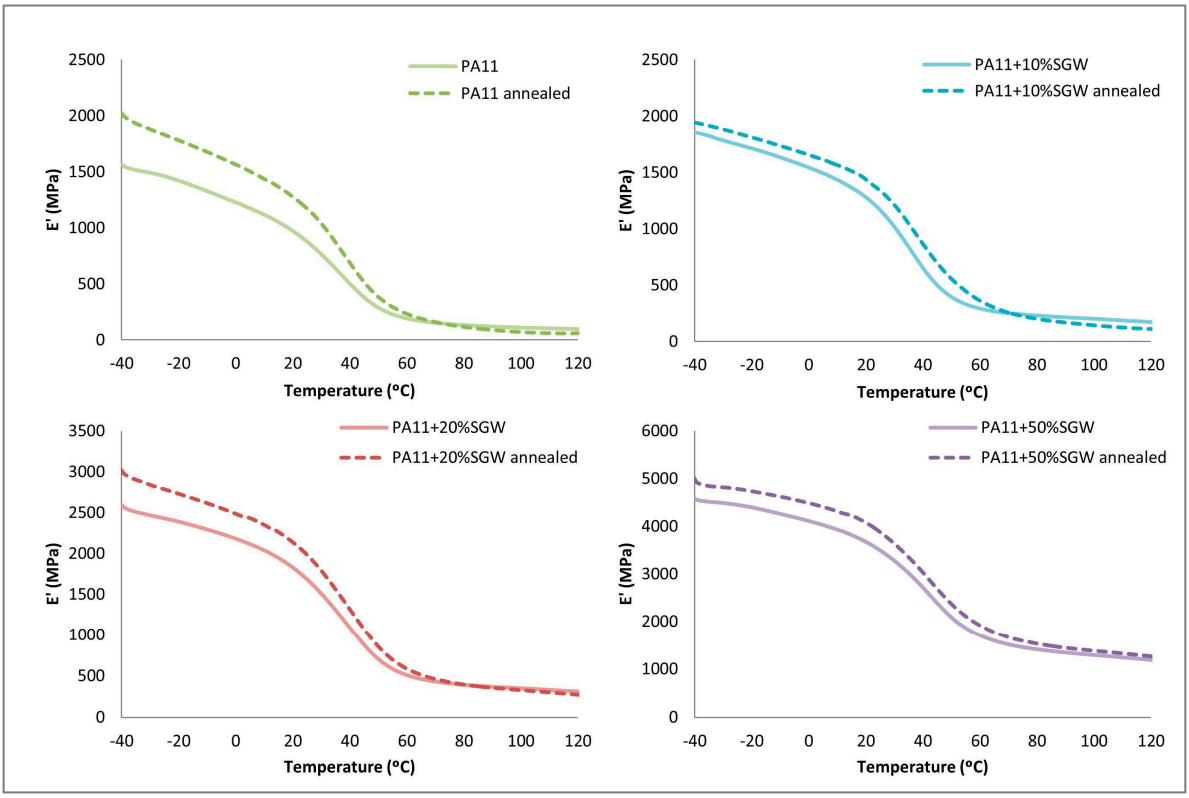

Figure 10. Storage modulus of treated and untreated samples obtained by DMTA.

Finally, the annealed samples were also studied by X-ray diffraction. As shown, the α′ form was observed in the neat PA11 and PA11-based composites (Figure 11). The annealing treatment produced a change in the polymer structure from the δ′ obtained after the injection-moulding process to the triclinic α′ structure, which is more thermodynamically stable [17,35]. The broad peak of the δ′ phase observed at 2θ = 21° was transformed in two well defined peaks at room temperature which shifted to 20.3° and 22.7°. The γ phase can be also obtained but is not usually observed under 100 °C [43].

Moreover, in the FT-IR of the PA11 annealed sample (Figure 12), the peaks shifted to α′ reported wavelengths [45] and their presence can be discarded or really reduced. In the composite materials, when the fibre content were augmented, the intensity of the second peak intensity corresponding to α′ form did the same, and exceeded the intensity of the first peak in the PA11 + 20% SGW and PA11 + 50% SGW composites. This effect, can be related with the overlap of this second peak with the cellulose peak and also with higher crystallinity [21] in the material which was in accordance with the obtained data in the DSC.

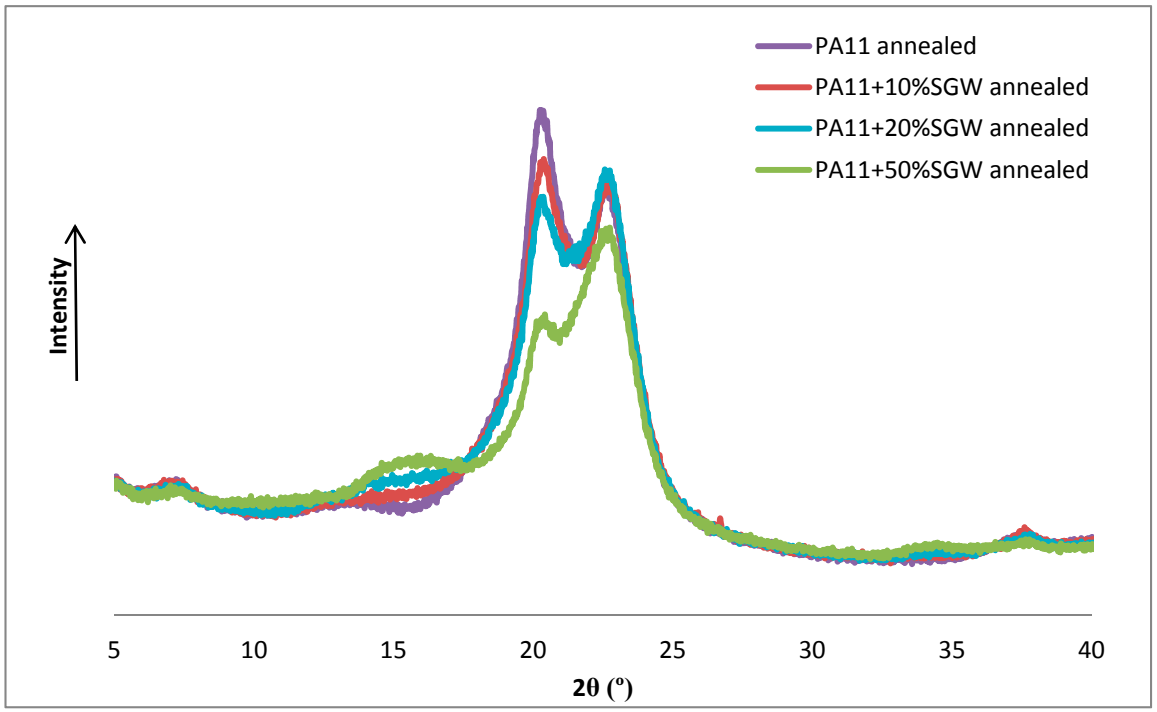

Figure 11. X-ray diffractograms of annealed samples.

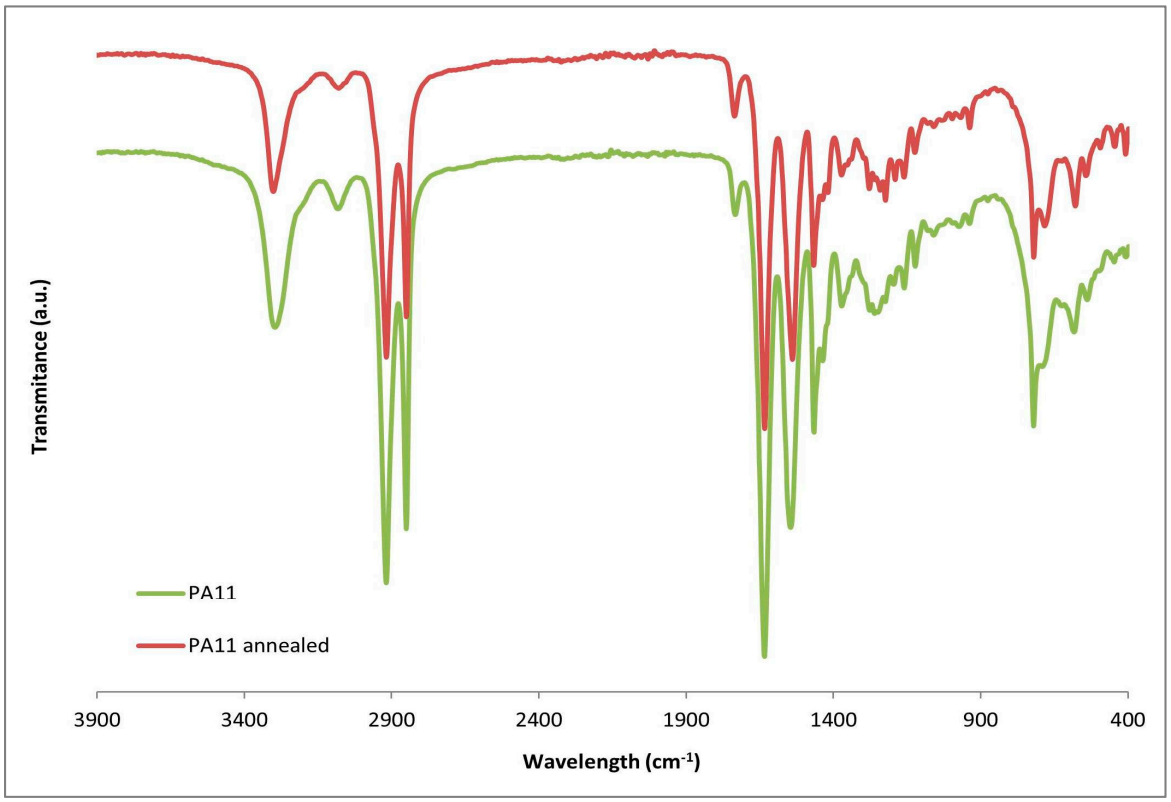

Figure 12. FT-IR of PA11 and annealed PA11.

The use of an annealing treatment has interest in lignocellulosic reinforced PA11 materials to increase the stiffness and the mechanical properties of the composite materials if working temperatures do not overpass T_g.

4. Conclusions

A thermal and structural characterization of PA11 and its composites reinforced with SGW was performed by means of TGA, DSC, DMTA and X-ray diffractionto determine the effect of the lignocellulosic reinforcement on the thermal transitions and morphology of the polymer matrix. A lower onset degradation temperature of PA11 by the effect of the fibres was found; however, once the decomposition temperature was started, the cellulosic fibres contributed to thermally stabilize the composites. No differences in T_m and T_c, the main melting and crystallization peaks, and the crystallinity degree (26–27%) were found by the incorporation of SGW. Nonetheless, fibres promoted the α' crystalline form instead of the both γ and α' forms observed in the neat PA11. DMTA results revealed no considerable differences in the T_g of the composites with the fibre content attributed to the formation of an amorphous phase with more restricted mobility caused by the presence of the reinforcement. An improvement on the storage modulus was observed when increasing the fibre content throughout all the measured temperature range.

Some samples were subjected to an annealing treatment during 1 h at 165 °C. The effect of the annealing on the materials was analysed by means of DSC and DMTA. The matrix crystallinity increased after the treatment. Moreover, higher crystal growth was also observed when the fibre content was augmented in the materials, achieving crystallinities increments around 13% for PA11 + 50% SGW. A slight increase of the T_g was observed, which can be related with the different crystal growths during the annealing treatment. A lower effect was obtained when the fibre content increased, probably due to the higher melting temperature of these crystals, similar to the PA11 melting point in the case of PA11 + 50% SGW composite. Slightly higher storage modulus values were obtained in the annealed samples, although the effect of the annealing in the stiffness seemed to decrease when the reinforcement content were increased. Finally, a different structure was observed before and after annealing in all samples. X-ray diffractograms showed a δ' phase in the samples after the injection moulding process. However, in the annealed sample, this phase was transformed to a more stable α' form. Moreover, FT-IR detected a small part of γ phase in neat PA11 and low fibre contents, which was not shown after the annealing.

Acknowledgments: The authors hereby thank Arkema for kindly supplying the polyamide 11 that was used in this work, and Patrick Dang (Arkema France) and Pep Català (Arkema Spain) for the technical information provided. The authors are also grateful to Luis Angel Granda for the technical support and helpful discussion.

Author Contributions: Helena Oliver-Ortega performed the experimental part and wrote the first version of the paper. José Alberto Méndez and Mònica Ardanuy conceived and designed the experiments. Francesc Xavier Espinach and Quim Tarrés analysed and represented the data. Pere Mutjé guided the project. All the authors contributed to write and correct the paper.

Conflicts of Interest: The authors declare no conflict of interest.

References

1. Lubin, G. *Handbook of Composites*; Lubin, G., Ed.; Springer: Boston, MA, USA, 1982; ISBN 978-1-4615-7141-4.
2. Bodros, E.; Pillin, I.; Montrelay, N.; Baley, C. Could biopolymers reinforced by randomly scattered flax fibre be used in structural applications? *Compos. Sci. Technol.* **2007**, *67*, 462–470. [CrossRef]
3. Donaldson, K.; Tran, C.L. An introduction to the short-term toxicology of respirable industrial fibres. *Mutat. Res. Mol. Mech. Mutagen.* **2004**, *553*, 5–9. [CrossRef] [PubMed]
4. Martino, L.; Basilissi, L.; Farina, H.; Ortenzi, M.A.; Zini, E.; Di Silvestro, G.; Scandola, M. Bio-based polyamide 11: Synthesis, rheology and solid-state properties of star structures. *Eur. Polym. J.* **2014**, *59*, 69–77. [CrossRef]
5. Lefeuvre, A.; Bourmaud, A.; Morvan, C.; Baley, C. Elementary flax fibre tensile properties: Correlation between stress-strain behaviour and fibre composition. *Ind. Crops Prod.* **2014**, *52*, 762–769. [CrossRef]
6. Bledzki, A.K.; Gassan, J. Composites reinforced with cellulose based fibres. *Prog. Polym. Sci.* **1999**, *24*, 221–274. [CrossRef]
7. Anastas, P.T.; Zimmerman, J.B. Design through the 12 principles of green engineering. *IEEE Eng. Manag. Rev.* **2007**, *35*, 16. [CrossRef]

8. Anastas, P.T.; Kirchhoff, M.M. Origins, current status, and future challenges of green chemistry. *Acc. Chem. Res.* **2002**, *35*, 686–694. [CrossRef] [PubMed]
9. Mohanty, A.K.; Misra, M.; Drzal, L.T. Sustainable Bio-Composites from renewable resources: Opportunities and challenges in the green materials world. *J. Polym. Environ.* **2002**, *10*, 19–26. [CrossRef]
10. Winnacker, M.; Rieger, B. Biobased Polyamides: Recent Advances in Basic and Applied Research. *Macromol. Rapid Commun.* **2016**, *37*, 1391–1413. [CrossRef] [PubMed]
11. Heitzmann, M.T.; Veidt, M.; Ng, C.T.; Lindenberger, B.; Hou, M.; Truss, R.; Liew, C.K. Single-plant biocomposite from ricinus communis: Preparation, properties and environmental performance. *J. Polym. Environ.* **2013**, *21*, 366–374. [CrossRef]
12. Ashori, A. Wood–plastic composites as promising green-composites for automotive industries! *Bioresour. Technol.* **2008**, *99*, 4661–4667. [CrossRef] [PubMed]
13. Bourmaud, A.; Le Duigou, A.; Gourier, C.; Baley, C. Influence of processing temperature on mechanical performance of unidirectional polyamide 11-flax fibre composites. *Ind. Crops Prod.* **2016**, *84*, 151–165. [CrossRef]
14. Oliver-Ortega, H.; Granda, L.A.; Espinach, F.X.; Delgado-Aguilar, M.; Duran, J.; Mutjé, P. Stiffness of bio-based polyamide 11 reinforced with softwood stone ground-wood fibres as an alternative to polypropylene-glass fibre composites. *Eur. Polym. J.* **2016**, *84*, 481–489. [CrossRef]
15. Zierdt, P.; Theumer, T.; Kulkarni, G.; Däumlich, V.; Klehm, J.; Hirsch, U.; Weber, A. Sustainable wood-plastic composites from bio-based polyamide 11 and chemically modified beech fibers. *Sustain. Mater. Technol.* **2015**, *6*, 6–14. [CrossRef]
16. Hu, Y.; Shen, L.; Yang, H.; Wang, M.; Liu, T.; Liang, T.; Zhang, J. Nanoindentation studies on Nylon 11/clay nanocomposites. *Polym. Test.* **2006**, *25*, 492–497. [CrossRef]
17. Zhang, X.; Yang, G.; Lin, J. Crystallization behavior of nylon 11/montmorillonite nanocomposites under annealing. *J. Appl. Polym. Sci.* **2006**, *102*, 5483–5489. [CrossRef]
18. Le Duigou, A.; Bourmaud, A.; Gourier, C.; Baley, C. Multi-scale shear properties of flax fibre reinforced polyamide 11 biocomposites. *Compos. Part A Appl. Sci. Manuf.* **2016**, *85*, 123–129. [CrossRef]
19. Oliver-Ortega, H.; Granda, L.A.; Espinach, F.X.; Méndez, J.A.; Julian, F.; Mutjé, P. Tensile properties and micromechanical analysis of stone groundwood from softwood reinforced bio-based polyamide11 composites. *Compos. Sci. Technol.* **2016**, *132*, 123–130. [CrossRef]
20. Zhang, Q.; Mo, Z.; Liu, S.; Zhang, H. Influence of annealing on structure of Nylon 11. *Macromolecules* **2000**, *33*, 5999–6005. [CrossRef]
21. Panaitescu, D.M.; Gabor, R.A.; Frone, A.N.; Vasile, E. Influence of Thermal Treatment on Mechanical and Morphological Characteristics of Polyamide 11/Cellulose Nanofiber Nanocomposites. *J. Nanomater.* **2015**, *2015*, 1–11. [CrossRef]
22. Granda, L.A.; Méndez, J.A.; Espinach, F.X.; Puig, J.; Delgado-Aguilar, M.; Mutjé, P. Polypropylene reinforced with semi-chemical fibres of Leucaena collinsii: Thermal properties. *Compos. Part B Eng.* **2016**, *94*, 75–81. [CrossRef]
23. López, J.P.; Gironés, J.; Méndez, J.A.; El Mansouri, N.E.; Llop, M.; Mutjé, P.; Vilaseca, F. Stone-ground wood pulp-reinforced polypropylene composites: Water uptake and thermal properties. *BioResources* **2012**, *7*, 5478–5487. [CrossRef]
24. Yang, H.; Yan, R.; Chen, H.; Lee, D.H.; Zheng, C. Characteristics of hemicellulose, cellulose and lignin pyrolysis. *Fuel* **2007**, *86*, 1781–1788. [CrossRef]
25. Azwa, Z.N.; Yousif, B.F.; Manalo, A.C.; Karunasena, W. A review on the degradability of polymeric composites based on natural fibres. *Mater. Des.* **2013**, *47*, 424–442. [CrossRef]
26. Lopez, J.P.; Mendez, J.A.; Espinach, F.X.; Julian, F.; Mutjé, P.; Vilaseca, F. Tensile strength characteristics of polypropylene composites reinforced with stone groundwood fibres from softwood. *BioResources* **2012**, *7*, 3188–3200. [CrossRef]
27. Panaitescu, D.M.; Frone, A.N.; Nicolae, C. Micro- and nano-mechanical characterization of polyamide 11 and its composites containing cellulose nanofibers. *Eur. Polym. J.* **2013**, *49*, 3857–3866. [CrossRef]
28. Ardanuy, M.; Antunes, M.; Velasco, J.I. Vegetable fibres from agricultural residues as thermo-mechanical reinforcement in recycled polypropylene-based green foams. *Waste Manag.* **2012**, *32*, 256–263. [CrossRef] [PubMed]

29. Aydemir, D.; Kiziltas, A.; Erbas Kiziltas, E.; Gardner, D.J.; Gunduz, G. Heat treated wood-nylon 6 composites. *Compos. Part B Eng.* **2015**, *68*, 414–423. [CrossRef]
30. Stoclet, G.; Sclavons, M.; Devaux, J. Relations between structure and property of polyamide 11 nanocomposites based on raw clays elaborated by water-assisted extrusion. *J. Appl. Polym. Sci.* **2013**, *127*, 4809–4824. [CrossRef]
31. Castagnet, S.; Thilly, L. High-pressure dependence of structural evolution in polyamide 11 during annealing. *J. Polym. Sci. Part B Polym. Phys.* **2009**, *47*, 2015–2025. [CrossRef]
32. Stempfle, F.; Ortmann, P.; Mecking, S. Long-chain aliphatic polymers to bridge the gap between semicrystalline polyolefins and traditional polycondensates. *Chem. Rev.* **2016**, *116*, 4597–4641. [CrossRef] [PubMed]
33. Mancic, L.; Osman, R.F.M.; Costa, A.M.L.M.; d'Almeida, J.R.M.; Marinkovic, B.A.; Rizzo, F.C. Thermal and mechanical properties of polyamide 11 based composites reinforced with surface modified titanate nanotubes. *Mater. Des.* **2015**, *83*, 459–467. [CrossRef]
34. Mago, G.; Kalyon, D.M.; Fisher, F.T. Nanocomposites of polyamide-11 and carbon nanostructures: Development of microstructure and ultimate properties following solution processing. *J. Polym. Sci. Part B Polym. Phys.* **2011**, *49*, 1311–1321. [CrossRef]
35. Pepin, J.; Miri, V.; Lefebvre, J.-M. New Insights into the Brill Transition in Polyamide 11 and Polyamide 6. *Macromolecules* **2016**, *49*, 564–573. [CrossRef]
36. Peng, S.X.; Shrestha, S.; Youngblood, J.P. Crystal structure transformation and induction of shear banding in Polyamide 11 by surface modified Cellulose Nanocrystals. *Polymer* **2017**, *114*, 88–102. [CrossRef]
37. Reixach, R.; Puig, J.; Méndez, J.A.; Gironès, J. Orange Wood Fiber Reinforced Polypropylene Composites: Thermal Properties. *BioResources* **2015**, *10*, 2156–2166. [CrossRef]
38. Joseph, P.V.; Joseph, K.; Thomas, S.; Pillai, C.K.S.; Prasad, V.S.; Groeninckx, G.; Sarkissova, M. The thermal and crystallisation studies of short sisal fibre reinforced polypropylene composites. *Compos. Part A Appl. Sci. Manuf.* **2003**, *34*, 253–266. [CrossRef]
39. Mancic, L.; Pontón, P.I.; Letichevsky, S.; Costa, A.M.; Marinkovic, B.A.; Rizzo, F.C. Application of silane grafted titanate nanotubes in reinforcing of polyamide 11 composites. *Compos. Part B Eng.* **2016**, *93*, 153–162. [CrossRef]
40. Semba, T.; Ito, A.; Kitagawa, K.; Nakatani, T.; Yano, H.; Sato, A. Thermoplastic composites of polyamide-12 reinforced by cellulose nanofibers with cationic surface modification. *J. Appl. Polym. Sci.* **2014**, *131*. [CrossRef]
41. Rhee, S.; White, J.L. Crystalline structure and morphology of biaxially oriented polyamide-11 films. *J. Polym. Sci. Part B Polym. Phys.* **2002**, *40*, 2624–2640. [CrossRef]
42. Frübing, P.; Kremmer, A.; Gerhard-Multhaupt, R.; Spanoudaki, A.; Pissis, P. Relaxation processes at the glass transition in polyamide 11: From rigidity to viscoelasticity. *J. Chem. Phys.* **2006**, *125*. [CrossRef] [PubMed]
43. Nair, S.S.; Ramesh, C.; Tashiro, K. Crystalline phases in nylon-11: Studies using HTWAXS and HTFTIR. *Macromolecules* **2006**, *39*, 2841–2848. [CrossRef]
44. Naffakh, M.; Shuttleworth, P.S.; Ellis, G. Bio-based polymer nanocomposites based on nylon 11 and WS 2 inorganic nanotubes. *RSC Adv.* **2015**, *5*, 17879–17887. [CrossRef]
45. Nair, S.S.; Ramesh, C.; Tashiro, K. Polymorphism in nylon-11: Characterization using HTWAXS and HTFTIR. *Macromol. Symp.* **2006**, *242*, 216–226. [CrossRef]
46. Pérez-Fonseca, A.A.; Robledo-Ortíz, J.R.; González-Núñez, R.; Rodrigue, D. Effect of thermal annealing on the mechanical and thermal properties of polylactic acid-cellulosic fiber biocomposites. *J. Appl. Polym. Sci.* **2016**, *133*, 1–10. [CrossRef]
47. Quan, H.; Li, Z.M.; Yang, M.B.; Huang, R. On transcrystallinity in semi-crystalline polymer composites. *Compos. Sci. Technol.* **2005**, *65*, 999–1021. [CrossRef]

2.4 Towards more sustainable material formulations: A comparative assessment of PA11-SGW flexural performance versus Oil-based composites

Publicada en *Polymers*. Factor de impacto 2016: 3,364. Posición 16 de 86 en Polymer Science. Primer cuartil.

polymers

MDPI

Article

Towards More Sustainable Material Formulations: A Comparative Assessment of PA11-SGW Flexural Performance versus Oil-Based Composites

Helena Oliver-Ortega [1,*], José Alberto Méndez [1], Rafel Reixach [2], Francesc Xavier Espinach [3], Mònica Ardanuy [4] and Pere Mutjé [1]

1 Group LEPAMAP, Department of Chemical Engineering, University of Girona, C/M. Aurèlia Capmany, 61, 17003 Girona, Spain; jalberto.mendez@udg.edu (J.A.M.); pere.mutje@udg.edu (P.M.)
2 Department of Architecture and Construction Engineering, University of Girona, C/M. Aurèlia Capmany, 61, 17003, Girona, Spain; rafel.reixach@udg.edu
3 Design, Development and Product Innovation, Department Organization, Business Management and Product Design, University of Girona, C/M. Aurèlia Capmany, 61, 17003 Girona, Spain; francisco.espinach@udg.edu
4 Departament de Ciència dels Materials i Enginyeria Metal·lúrgica, Secció Enginyeria Tèxtil, Universitat Politècnica de Catalunya, C/Colom, 11, 08222 Terrassa, Barcelona, Spain; monica.ardanuy@upc.edu
* Correspondence: helena.oliver@udg.edu; Tel.: +34-669-996-998

Received: 24 February 2018; Accepted: 12 April 2018; Published: 14 April 2018

Abstract: The replacement of commodity polyolefin, reinforced with glass fiber (GF), by greener alternatives has been a topic of research in recent years. Cellulose fibers have shown, under certain conditions, enough tensile capacities to replace GF, achieving competitive mechanical properties. However, if the objective is the production of environmentally friendlier composites, it is necessary to replace oil-derived polymer matrices by bio-based or biodegradable ones, depending on the application. Polyamide 11 (PA11) is a totally bio-based polyamide that can be reinforced with cellulosic fibers. Composites based on this polymer have demonstrated enough tensile strength, as well as stiffness, to replace GF-reinforced polypropylene (PP). However, flexural properties are of high interest for engineering applications. Due to the specific character of short-fiber-reinforced composites, significant differences are expected between the tensile and flexural properties. These differences encourage the study of the flexural properties of a material prior to the design or development of a new product. Despite the importance of the flexural strength, there are few works devoted to its study in the case of PA11-based composites. In this work, an in-depth study of the flexural strength of PA11 composites, reinforced with Stoneground wood (SGW) from softwood, is presented. Additionally, the results are compared with those of PP-based composites. The results showed that the SGW fibers had lower strengthening capacity reinforcing PA11 than PP. Moreover, the flexural strength of PA11-SGW composites was similar to that of PP-GF composites.

Keywords: flexural properties; polyamide 11; lignocellulosic fibers; polypropylene composites; fiber/matrix bond

1. Introduction

Flexural strength and strain are of great interest in the design and product development fields [1–5]. In short-fiber-reinforced composite materials, the in-depth study of these properties is relevant to the different fiber orientations in the skin, the shell, and the core of injected specimens regarding the load axis [5]. Consequently, a significant gap between the tensile and flexural properties of such composites

is expected [6,7]. From an engineering point of view, depending on constraints and loads applied to a geometry, the failure point will be defined by the tensile and flexural properties of the material [8]. In addition, one of the most common applications for wood polymer composites are decking profiles, supporting the flexural loads between the points that hold them [5].

A schematic evolution of composite materials from synthetic fibers, such as glass fibers (GF), to greener materials, is represented in Figure 1.

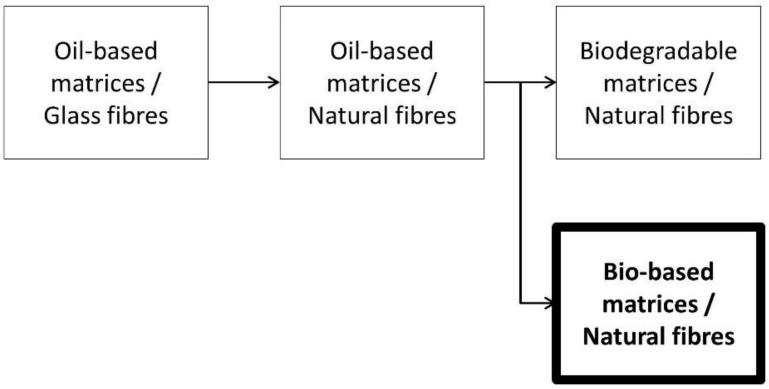

Figure 1. Evolution of composite materials in recent years.

In view of environmental awareness, one of the goals of this evolution is the production of totally bio-based and biodegradable composites. GF has been one of the most often used reinforcements for petroleum-based matrices, due to its high capacity to increase the strength and modulus of the resulting composite materials [1], combined with a low production cost and availability. Nowadays, 98% of the whole composites' production in Europe are reinforced with GF [9,10]. However, one of the main drawbacks of the use of GF is related to its high stiffness, which leads to a drop of the toughness of the materials, giving rise to a reduction of the recyclability of these materials [11]. This reduced recyclability does not agree with the European Union (EU) solid waste treatment targets for 2025 and 2030 related to the improvement of the performance of recycled plastics [12]. In this sense, many tons of GF waste from composite materials are deposited in landfills [9]. Otherwise, another disadvantage of the use of GF is related to its health risks, as dermatitis and respiratory diseases can be caused by the manipulation of this material [13,14].

In order to avoid these drawbacks derived from the use of GF, efforts have been devoted to substitute GF by environmentally friendlier reinforcements. An example of these greener reinforcements are cellulosic or lignocellulosic fibers, which have successfully replaced GF as reinforcement for oil-based polymers in some industrial fields such as automotive, construction, and clinical fields [15–17]. Cellulose is a natural and sustainable polymer that has the potential to become a raw material for energy production (incineration) and a source of reinforcement for polymer matrices [1,5,7,18].

Despite their availability and widespread use in the industry, the use of oil-based polymers, such as polypropylene (PP), as the matrix in composite materials is not desirable. In recent years, research centers and actors in industry have focused on the research and development of more sustainable materials using biopolymers as matrices, such as thermoplastic starch [19] or polylactic acid (PLA) [20]. Nonetheless, the relatively fast biodegradability of these materials becomes a drawback for their long-term applications, being considered as a greener solution. One promising example of bio-based matrices are bio-polyamides (BioPA). Polyamides (PA), including BioPA and oil-based PA, show good mechanical and insulation properties as well as thermal resistance [21,22]. Moreover, depending on their chemical structure and the raw materials required for their production, BioPA can be totally or partially bio-based. Some examples are polyamide 11 (PA11), which is 100% bio-based, polyamide 10.10 (PA10.10), which is up to 99% bio-based, or polyamide 6.10 (PA6.10), which only contains 62% of carbon from renewable resources [23]. Besides, PA overcomes the

problems related to the hydrophobic nature of PP, which penalizes the quality of its interface with hydrophilic reinforcements [24–27]. The hydrophilic behavior of polyamide matrices [28,29] allows their reinforcement with natural fibers and the achievement of significant improvements to their mechanical properties without the use of coupling agents [23,30–32]. Moreover, PA11, which is 100% bio-based (obtained from castor oil) and non-biodegradable, shows a low melting temperature when compared with other PAs [11,33]. This phenomenon is very interesting when cellulose fibers are considered as reinforcement due to their relatively low decomposition temperature ($T \approx 200$ °C) [34,35].

Stoneground wood (SGW) from pine is a commercially and sustainable fiber produced for the paper industry. Its low cost, high-yield process, and continuous production made it an interesting alternative to GF as a composite reinforcement [36,37]. These fibers have been widely researched as a composite reinforcement, and the mechanical properties of SGW-based composites reveal its competitiveness. According to the literature, the intrinsic tensile strength of SGW in the case of PP-SGW coupled composites is 618 MPa [36]. The presence of coupling agents guarantees a well-bonded system. A slight difference was obtained when the SGW tensile strength was calculated for PA11-SGW composites, which was found to be 562 MPa [38].

The literature on natural fiber-reinforced PA11 composites is scarce. The natural fibers used in such researches are mainly short wood fibers like pine, beech, or commercial pulps and injection molding processes [35,38–42]. The tensile properties obtained with chemically modified beech fiber-reinforced PA11 composites were similar to those of SGW-reinforced composites [35,38]. Nonetheless, the chemical treatment of the beech fibers can increase the cost of the composites compared to those that employ SGW. Armioun, Shaghayegh et al. obtained lower results with commercial wood fiber-reinforced PA11. The lower results were probably due to processing parameters that allowed the presence of noticeable percentages of voids inside the composite. Other works used flax fibers and flax tape [34,43]. These studies obtained high tensile strengths, but they used long aligned fibers and molding press processes. Anyhow, such properties are difficult to obtain with mold injected specimens. Additionally, flax is a comparatively expensive source for reinforcing fibers. Only Armioun, Shaghayegh et al. researched the flexural properties of the composites [41]. Thus, to the best knowledge of the authors, the literature devoted to the flexural properties of PA11-natural fiber composites is scarce.

The present work provides an in-depth analysis of the flexural strength and deformation of SGW-reinforced PA11 composites. Five different materials with SGW contents, ranging from 20% to 60% (w/w), were prepared by injection-molding and characterized to obtain their experimental flexural performance. These results were compared with the tensile properties obtained in previous studies [38,44]. Then, a fiber flexural strength factor was used to study the neat contribution of the fibers to the flexural strength and such values were compared to their tensile counterparts. Micromechanics models were used to compute the intrinsic flexural strength and modulus of the reinforcement. Finally, the flexural properties of the PA11-based materials were compared with those of GF-reinforced PP commercial composites.

2. Materials and Methods

2.1. Materials

Polyamide 11 (PA11) (Rilsan® BMNO TL, Colombes, France) was used as a polymer matrix, kindly supplied by Arkema S.A (Colombes, France), with a density of 1.030 g/cm^3 and a melting temperature around 189 °C.

Stoneground wood (SGW) was used as lignocellulosic reinforcement. SGW was derived from softwood (*Pinus radiata*) and supplied by Zubialde, S.A. (Aizarnazabal, Spain).

2.2. Composite Compounding and Sample Obtaining

PA11 was reinforced with five different fiber contents, ranging from 20 up to 60% w/w of SGW. The compounding process was performed using a Gelimat kinetic mixer (model G5S, Draiswerke,

Mahaw, NJ, USA). PA11 and SGW were added at a low speed (300 rpm) and then the speed was raised up to 2500 rpm. The polymeric phase blended when it reached 200 °C, after which the blend was discharged. The extraction of the composite from the kinetic mixer was achieved by gravity discharge.

Afterwards, all of the blends were pelletized by means of a mill equipped with a set of blades. The obtained blends were injected into a Meteor-40 injection machine (Mateu and Solé, Barcelona, Spain; clamping pressure: 40 tons) to obtain the standard specimens for the bending test (ASTM D3641). The samples were conditioned in a climatic chamber at 23 °C and 50% Relative Humidity (RH) before the mechanical test in accordance with ASTM D618.

2.3. Mechanical Characterization

Composites were tested under three-point bend configuration in accordance with ASTM D790 standard specifications, using a Universal testing machine supplied by IDMtest (Instron™ 1122, Mark-10 Corporation, Copiague, New York, NY, USA), equipped with a 5-kN load cell. Flexural strength and deformation at the maximum load were obtained from an average of at least five samples.

2.4. Composite Density Determination

The composite's density (ρ^C) was obtained using a pycnometer. A certain weight of the composite was introduced into the pycnometer and the pycnometer was raised to the calibrated volume with distilled water. The density was calculated using the following equation:

$$\rho^C = \frac{Weight_{\text{composite}}}{V_{\text{total}} - Weight_{\text{water}} \cdot (\rho_{\text{water}})^{-1}} \quad (1)$$

where V_{total} is the total volume of the pycnometer, and ρ_{water} is the water density, also calculated experimentally with the pycnometer. The composite samples used were obtained after the injection molding process.

3. Results and Discussion

3.1. Flexural Properties of PA11-SGW Composites

The results of the flexural tests are shown in Table 1, where V^F is the fiber volume fraction regarding the total volume in the composite, ρ^C is the experimental values of the composite density, ${\sigma_f}^C$ is the flexural strength, ${\sigma_f}^{m^*}$ is the flexural strength of the matrix at the maximum composite strength, D is the experimental deflection of the tested materials, ${\varepsilon_f}^C$ is the strain of composites at the maximum flexural strength, and U_r is the resilience of the composites regarding the fiber content in weight percentage (w/w) in the composite material. ${\varepsilon_f}^C$ was measured as ${\varepsilon_f}^C = (6 \cdot D \cdot d)/L^2$, were d is the specimen depth and L is the length of the support span. The contribution of the matrix ${\sigma_f}^{m^*}$ was obtained by a curve fit of the experimental stress and deflection values. The values returned by the equation agreed with the experimental data with very low deviations that did not impact the results of the mathematical operations.

Table 1. Flexural properties of Polyamide 11-Stone Groundwood fibers (PA11-SGW) composites.

Fiber content (% w/w)	V^F	ρ^C (g/cm^3)	${\sigma_f}^C$ (MPa)	${\sigma_f}^{m^*}$ (MPa)	D (mm)	${\varepsilon_f}^C$ (%)	U_r (KJ/m^3)
0	0.000	1.03	40.0 ± 1.52	40.0	11.0 ± 0.32	7.39	78.18
20	0.155	1.09	55.0 ± 2.22	39.2	9.5 ± 0.51	6.39	57.77
30	0.240	1.12	68.7 ± 1.79	38.5	8.6 ± 0.45	5.78	49.65
40	0.329	1.15	77.5 ± 1.28	36.8	7.8 ± 0.38	5.24	42.73
50	0.424	1.18	92.6 ± 3.12	32.3	6.3 ± 0.51	4.24	37.05
60	0.524	1.22	102.7 ± 4.75	26.5	4.8 ± 0.47	3.23	29.79

The ${\sigma_f}^C$ of the composites increased linearly up to 60% w/w SGW contents, obtaining a linear fitting with the following equation: ${\sigma_f}^C = 123.11 \cdot V^F + 38.44$, and a correlation coefficient (r^2) of 0.99.

The increases of the flexural strength of the composites with the addition of 20 to 60% w/w SGW, compared to the matrix, were 37.5%, 71.7%, 93.7%, 131.5%, and 156.7%, respectively. It is reported in the literature that such linear behavior is indicative of an optimal interface between the fibers and the matrix as well as a good dispersion of the reinforcements in the matrix [3,45,46]. When the tensile strength of the same composites was investigated, a maximum tensile strength was found for 50% w/w SGW content, and further increases of the reinforcement content produced a noticeable decrease in this property [38]. One possible explanation for this phenomena could be a poor wetting process of the fibers for high reinforcement contents or the creation of fiber bundles [47,48]. The results show that the effect of such phenomena on the flexural strength is less apparent than in the tensile strength. In short-fiber-reinforced composites, the strength property depends on the fiber and polymer natures and volumes, the fiber morphology and orientation inside the matrix, and the interaction between the fiber and the matrix [49]. These interactions allow for matrix-fiber stress transfer and can be determined by the interfacial shear strength (IFSS). The IFSS, together with the fiber's orientation, are the most important factors in the strength performance of the composites. Nonetheless, the orientation of the fibers is highly dependent of the mold in injected-molded samples and it cannot be modified. Thus, IFSS could be considered as the main factor of the reinforcement effect of the fibers in the composite strength. In turn, the IFSS is affected by the properties of the reinforcement fiber, the type of bond established between the polymer and the fiber, and the quantity of these bonds [50].

A higher enhancement of the flexural strength than that observed for tensile strength of the same composites has been observed [38]. This difference between tensile and flexural strength enhancements is related to the specimens working at tensile and compression loads during the bending test as opposed to pure tensile loads (Figure 2).

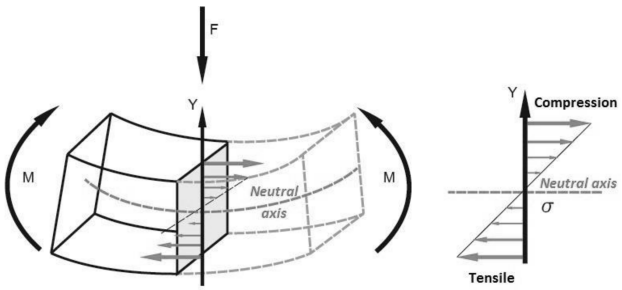

Figure 2. Scheme of load forces acting during the bending test.

During the bending test, the load force is produced in a perpendicular direction over the surface of the sample bar. This force produces a response in the extreme points of the bar to counteract it. The sample response in the vertical axis, where the force is loaded, produced different loads: tensile and compression. Thus, it is expected to find fibers working under tensile or compression stresses. However, as mentioned above, the main factor affecting the stress transmission, and thus the strength property, is the interface. To obtain an enhancement in the flexural strength it is necessary to ensure an optimal interface in the composite material.

The flexural strength and its evolution, with respect to the reinforcement content, are related to the formation of a suitable interface. In PA11-SGW composites, this interface is produced by the capacity of the PA11 to interact with the SGW fibers by H-bonds and other intermolecular forces in addition to mechanical anchorage. The SGW fibers used in this work are mechanical fibers from pine, obtained through high-yield processes, and the chemical composition of such fibers (i.e., the carbohydrates, lignin, and extractives) and their distribution along the section is slightly affected by the process. Lignin and extractives are usually found in the most superficial layers of the fiber and can inhibit the interaction between the cellulosic chains and the polymer [51,52]. Böras and Gantenholm [53] proposed a simple schematic model for the chemical distribution on the surface of a mechanical fiber (Figure 3).

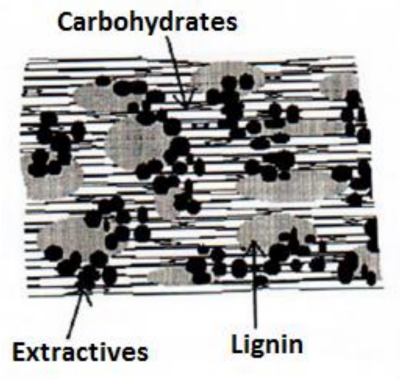

Figure 3. Chemical composition of a lignocellulosic fiber [53].

In this model, the largest area corresponded to lignin (28%) and extractives (32%), and only 40% of the available surface was covered by carbohydrates (cellulose and hemicellulose). In the case of SGW fibers, the cellulose and hemicellulose surface available could be slightly reduced. The lignin content on the surface was expected to be slightly higher than that obtained for thermomechanical treated fibers from softwood [54]. Apart from cellulose and hemicellulose, lignin has also a considerable percentage of hydroxyl groups in its structure, allowing its interaction with the PA11 matrix. A scheme of the interface of PA11 and SGW fibers is proposed in Figure 4. The figure describes a fiber surface with hydroxyl groups from lignin (phenol groups) and carbohydrates available at the fiber surface that can interact with the PA11 matrix.

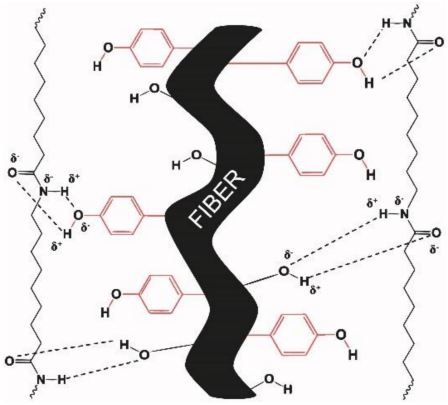

Figure 4. Schematic interaction of PA11 chains with a lignocellulosic fiber. The phenol groups (marked in red) represent the hydroxyl groups provided by lignin and the others represent the hydroxyls groups from the hemicellulose and cellulose.

The capacity of the PA11 to interact at the same time with lignin and cellulose hydroxyls could explain the good mechanical performance obtained for PA11-SGW composites [35]. Without this interaction and due to the moderate number of available hydroxyl groups from cellulose and hemicellulose in the surface as a result of the high presence of lignin in the surface (Figure 3), the composite strengths would probably be reduced. Moreover, the lignin content probably contributes to the enhancement of the fiber dispersion in the PA11 matrix, inhibiting the creation of fiber agglomerates [38,55]. Furthermore, the use of SGW fibers reduced the cost and the production time of the composite materials as it was not necessary to submit the fiber to higher energy- and time-consuming processes. In addition, their use agrees with the postulates of green chemistry and engineering proposed by Anastas et al. [56,57].

Figure 5 shows the stress-strain curves of the composites and the matrix up to the maximum flexural strength. As expected, the deformation of the materials decreased when the fiber content was

increased due to the higher stiffness of the fiber. The strain at the maximum flexural strength for the composite with 60% *w*/*w* SGW content was 44% of the matrix. The behavior of the flexural strain of the PA11-based composites was similar to that of the SGW-reinforced PP with the use of a coupling agent [37]. Nonetheless, the values of the PA11-based composites were slightly higher, probably due to the higher strain obtained for this matrix.

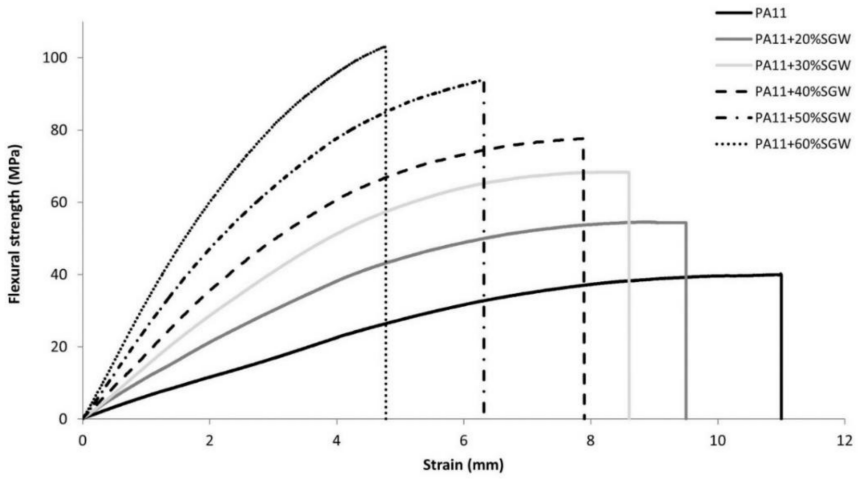

Figure 5. Stress-curves of PA11 and PA11 composites up to the maximum flexural strength of the composites.

A reduction of the $\sigma_f{}^{m^*}$ and, consequently, of the matrix contribution was observed (Table 1) due to the increasing fiber content, a stiffer phase, and the reduction of the strain of the composite materials [58].

The toughness of a material is understood as the energy which a material can absorb before collapsing. In the case of the flexural toughness of PA11 and PA11 + 20% SGW, the specimens did not collapse during the bending test, so the determination of their toughness was not possible. Nevertheless, the resilience, understood as the ability of a material to absorb energy and release it without suffering permanent deformation, was calculable for all tested materials. The resilience was calculated as the area under the linear or elastic zone of the stress-strain curve. The highest resilience was obtained for PA11 and decreased as the fiber content was increased. The resilience was reduced by 62%, regarding the matrix, at 60% fiber content.

A linear increment of the density was observed for increasing fiber contents, as was expected due to the high density of the fiber (1.40 g/cm^3) compared to that of PA11 (1.03 g/cm^3). The density of PA11-SGW composites was slightly higher than that of PP-SGW composites, which was attributed to the higher density of the PA11 matrix compared to that of PP (0.905 g/cm^3) [59]. In natural fiber-reinforced composites, the polymer density is a key factor due to the similar densities of natural fibers [60,61]. The density of SGW was in the range of other natural fibers, as reported in the literature [15,62], and significantly lower than GF (2.45 g/cm^3).

3.2. Analysis of the Flexural Strength: Fiber Flexural Strength Factor and Average Fiber Intrinsic Flexural Strength

In order to assess the competitiveness of PA11-based composites, it is important to compare their flexural strength with those commercially available materials, such as PP-GF and PP-natural fiber composites. PP-GF composites, processes by injection-molding, are usually reinforced up to 20–30% *w*/*w*. In the Figure 6, the flexural strength of PA11-SGW was compared with the values obtained in previous works for PP-SGW [37] and PP-GF [63] composites at the same fiber contents (20–30%). The difference between PP-GF-sized and -coupled composites is the use of GF surface

modifications in the case of GF-sized composites and the addition of a coupling agent in the formulation of coupled composites.

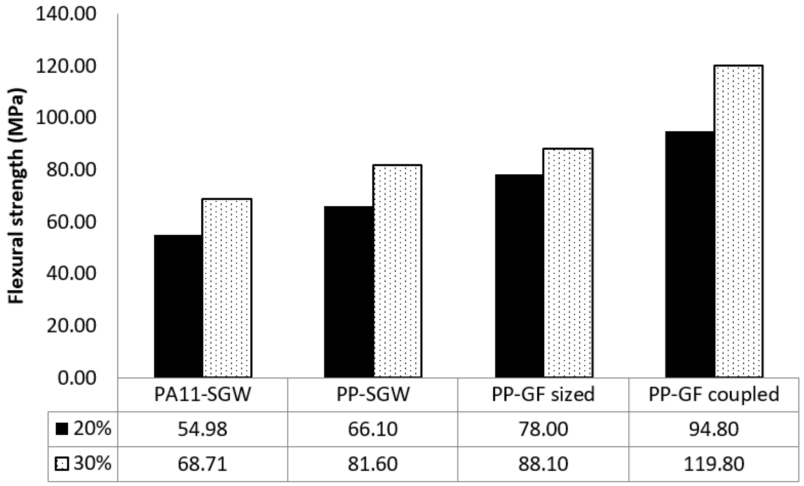

Figure 6. Comparison between PA11- and polypropylene (PP)-based composites at same the fiber content.

A noticeable gap between the flexural strengths of all of the composites reinforced with a 30% w/w was observed, especially when compared with the GF-coupled reinforced PP composite. The composites reinforced with 30% w/w of SGW exhibited flexural strengths that were 43% and 32% lower, for PA11 and PP matrices, than the GF-coupled reinforced composite.

The analysis of the flexural strength behavior can help the understanding of the differences between reinforced PA11- and PP-based composites. The use of a model such as the modified rule of mixtures (mRoM) was proposed to model the behavior of the flexural strength of the composites (Equation (2)) [64].

$$\sigma_f^C = f_c^f \cdot V^F \cdot \sigma_f^F + \left(1 - V^F\right) \cdot \sigma_f^{m*} \quad (2)$$

where $\sigma_f{}^F$ is the average fiber's intrinsic flexural strength and $f_c{}^f$ is the flexural coupling factor. The flexural coupling factor incorporated the impacts of the mean orientations of the fibers, the morphology of such fibers, and the quality of the interface. In fact, the flexural coupling factor is defined as the product of an orientation factor and a length and interface factor ($f_c{}^f = X^f{}_1 \cdot X^f{}_2$). The mRoM models the flexural strength of a composite as the sum of the contributions of the reinforcement and the matrix. Figure 7 shows the contributions of the matrix ($(1 - V^F) \cdot \sigma_f{}^{m*}$) to the flexural strength of reinforced PA11- and PP-based composites.

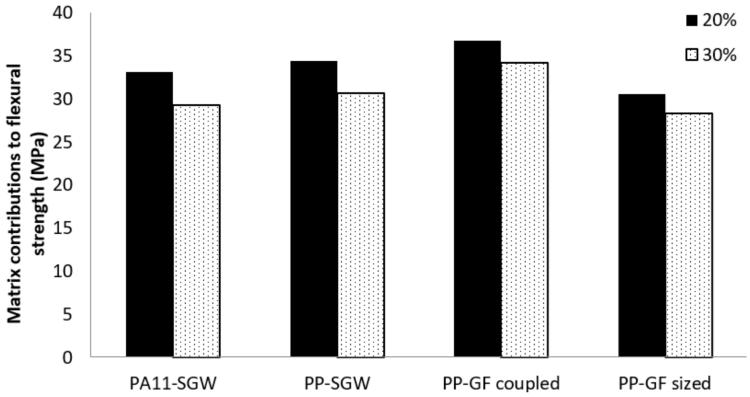

Figure 7. Matrix contribution of PA11-SGW and PP-based composites with 20% and 30% fiber content.

It was found that the matrix contribution values were all in similar ranges. Thus, the $f_c^f \cdot \sigma_f^F$ term of the mRoM (Equation (3)) was responsible for the main differences between the flexural strengths of the composites. In the mRoM, f_c^f and σ_f^F remained as unknown parameters. A fiber flexural strength factor (*FFSF*) was proposed as an useful way to evaluate the neat contribution of the reinforcement to the composite strength [65]. *FFSF* was defined by rearranging the mRoM and isolating these unknown parameters:

$$FFSF = \frac{\sigma_f^C - (1 - V^F) \cdot \sigma_f^{m*}}{V^F} = f_c^f \cdot \sigma_f^F \quad (3)$$

In the above, the *FFSF* is the slope of the regression curve obtained from the representation of $\sigma_f - (1 - V^F) \cdot {\sigma_f}^{m^*}$ vs. V^F [1]. The value of *FFSF* is unique for a family of composites, as its value does not change with the amount of reinforcement due to its dependence on the fiber properties and its interaction with the matrix. The *FFSF* of PA11-SGW composites was calculated and compared with those of PP-based composites obtained from the literature [1,36,63,66] (Figure 8).

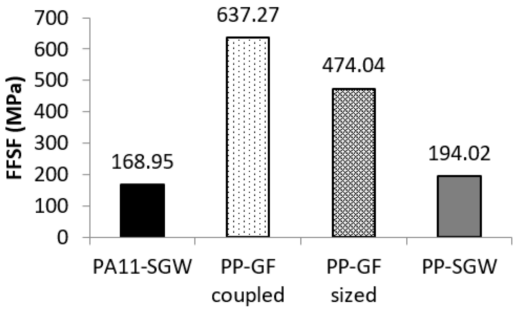

Figure 8. The fiber flexural strength factor (FFSF) of PA11 and PP composites.

The *FFSF* for PA11-SGW was 3.7 and 2.8 times lower than that for PP-GF-coupled and -sized composites, respectively. In the case of SGW composites, a higher value was obtained for the PP-based composites. These differences between SGW-reinforced composites indicated a higher strengthening effect of these fibers in PP. This was also observed between coupled and sized GF-based composites. As mentioned above, f_c^f is dependent on the quality of the interface, the morphological characteristics of the fibers, and their orientation against the loads. Usually, the orientation of the fibers is related to the equipment used to fabricate the specimens via inject-molding, and it was the same for all of the composites. Thus, the differences between the flexural strengths of the composites depend mainly on the fiber properties and the quality of the interface.

The difficulties in measuring the intrinsic properties of the fibers led us to consider the calculation of these properties using theoretical models. One of the methodologies proposed to compute the average intrinsic flexural strength uses the *FFSF* and the *FTSF* (fiber tensile strength factor) [1,37,46]. The proposed relation is $\sigma_f^F = FFSF/FTSF \cdot \sigma_t^F$ [1,37]. The ratio between *FFSF*/*FTSF* for PA11-SGW composites was 1.57, which is lower than those obtained for other natural fiber-reinforced thermoplastic composites, with ratios in the range of 1.7–1.9 [1,37,61]. Using this ratio, the computed mean theoretical intrinsic flexural strength of SGW in PA11-based composites was 888 MPa. This value was lower than 1095 MPa, a value found in the literature for SGW as a reinforcement for PP [37]. However, some studies showed that the intrinsic strength of the fibers changes with matrix chemical families [19,46]. In that sense, the value of the intrinsic strength is also a measurement of the exploitation of the strengthening capabilities of the reinforcing fibers. These strengthening capabilities can also be related to the interface type, the quantity of bonds, and their energy value [50]. Because our investigation made use of the same fiber, the differences were related to the interface quality. PP cannot establish strong chemical interactions and a coupling agent was required to do so. The coupling agent used in PP-SGW composites was maleate polypropylene. The maleate part of the coupling agent established covalent bonds and intermolecular forces with the fibers, and its polyolefinic chain became entangled

with the polymer matrix [67]. The energetic value of H-bonds may be different depending on the atoms involved and the distance between them, but these bonds are energetically weaker than covalent bonds [68,69]. This explains the lower interface of the PA11-SGW composites in comparison with the PP-SGW composites. However, the presence of this H-bond in the interface produced a difference of 13 MPa, while in the case of uncoupled PP-SGW composites the difference was around 30 MPa [37].

The literature showed that the strengthening effect of wood fibers on polyamide 6 (PA6) composites was also lower than that observed in PP-based composites [30,70,71]. All of these arguments reinforce the hypothesis of a good but not optimal interphase in PA11-based composites. Nevertheless, these intrinsic flexural strengths values were obtained using a back-calculation and the results obtained may differ from experimental results [72].

The intrinsic flexural strengths of GF, sized and coupled, were evaluated at 3787 and 4237 MPa, respectively. These values were 4 times higher than those achieved using SGW as a PA11 reinforcement. Nonetheless, the *FFSF* of the same reinforcements was only 3 times higher. According to the definition of *FFSF* (Equation (4)), these differences were probably related to the values of the coupling factors.

3.3. Flexural Strength Performance of PA11-SGW Composites versus Oil-Based Composites

The coupling factor can be considered as an indication of the quality of the interface, the morphological characteristics of the fibers, and their orientation against the loads in the composite. Once the ${\sigma_f}^F$ was obtained, the use the mRoM to calculate ${f_c}^f$ for PA11-SGW composites was possible. In a previous work, the mean coupling factor for the tensile strength (${f_c}^t$) was evaluated at 0.186 [38]. Using the ${\sigma_f}^F$ obtained in the relation between the *FFSF* and *FTSF*, the coupling factor for the flexural strength was computed to a mean of 0.183. The tensile and flexural coupling factors were very similar, showing that the differences between the tensile and flexural tests had little effect in such parameters [37,66,73]. The same coupling factor computed for the 50% w/w SGW-reinforced PP coupled composite materials was computed to be 0.173, which was slightly inferior to that of the PA11-based composites (Table 2). This lower result could be related to the lower orientation factor (${X^f}_1$) found in PP-SGW composites [36,38] as ${f_c}^f = {X^f}_1 \cdot {X^f}_2$ and assuming no differences obtained between the flexural and tensile strength's ${X^f}_1$. This assumption was made because the orientation of the fibers in the composed material mainly depended on the injection-molding equipment employed in the fabrication process [1].

Table 2. Coupling factor for the flexural strength.

Composite	Fiber content	V^F	${\sigma_f}^F$ (MPa)	$(1 - V^F) \cdot {\sigma_f}^{m*}$ (MPa)	${f_c}^f$
PA11-SGW	20%	0.155	888	33.16	0.159
	30%	0.240	888	29.29	0.185
	40%	0.329	888	24.69	0.181
	50%	0.424	888	18.82	0.196
	60%	0.524	888	12.59	0.194
PP-SGW	50%	0.404	1095	20.98	0.173
$PP\text{-}GF_{sized}$	20%	0.084	3787	30.60	0.137
	30%	0.136	3787	28.31	0.116
$PP\text{-}GF_{coupled}$	20%	0.084	4237	30.60	0.163
	30%	0.136	4237	28.31	0.150

As mentioned above, GF is more prone to decrease its length as the fiber content increases. This impact was reflected when the coupling factor for the sized GF-reinforced PP composites decreased by 18% when the reinforcement contents were changed from 20 to 30% w/w. In the case of the coupled GF-based composites, this decrease was 9%. Despite its high intrinsic flexural strengths, GF was penalized due to its fragility. Finally, the literature agrees on values of f_c around 0.2 as an indication of a well-bonded system for semi-aligned short-fiber composites [38,74,75]. The mean ${f_c}^f$ for PA11-SGW composites was near to this value, indicating a quite good interface.

After the study of the intrinsic properties of the fiber and its interaction with the matrix, a lower reinforcement effect was observed in PA11-SGW compared to PP-SGW composites. This difference was mainly attributed to the lower energetic interface bonds in the PA11-SGW composites. Thus, the interface obtained in both composites was mainly related to the interactions between the polymers and the fibers. In PP-GF composites, the GF surface was modified to obtain a hydrophobic behavior that enhanced the dispersion and produced some interaction between the fiber and the polymer. In GF-coupled composites, the mechanism was the same as that detailed above for SGW fibers. Although the strength of the GF-based composites was higher due to the higher mechanical performance of GF, the sized GF-based composites showed an interface with scarce and probably quite low intermolecular interactions, obtaining flexural strengths slightly higher than PP + 30% SGW and 31 MPa lower than coupled GF-based composites. These results are in agreement with the values of f_c^f observed in both GF composites.

Finally, Figure 9 compares the flexural strength performance of SGW-based composites with higher reinforcement contents vs oil-based composites.

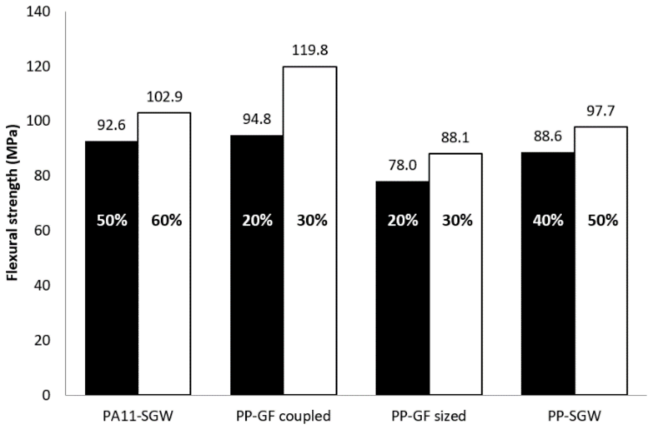

Figure 9. PA11-SGW and PP-SGW composites with high fiber contents versus PP-GF composites.

It was found that the 50–60% SGW-reinforced PA11 composites compared well with the remaining composites, excluding the coupled 30% GF-reinforced PP composite. In fact, to obtain the same flexural strength as the PA11-based composite, a 0.66 volume fraction of SGW was needed. This volume fraction corresponds to a fiber content of around 73%. For PP-SGW composites, the V^F required is 0.583, along with a fiber content of 65% [37]. In both cases, these fiber fractions cannot be achieved due to the bad dispersion and poor wettability of the matrix over the fibers. Moreover, the strength of these hypothetical composites is directly related to the fiber due to the low volume of the matrix and the high stiffness and content of fibers, which drastically reduce their strain at break. Nonetheless, the PA11 + 50% SGW composite can replace almost all of the compared materials (Figure 6). Moreover, the strains of SGW-reinforced composites were similar to or higher than those achieved for PP-GF composites, although the fiber volume fractions were at least 3 times higher [8,37]. These results displayed the suitability of PA11-SGW composites to replace commercial materials as a greener and more sustainable alternative. Furthermore, nowadays PA11 is comparatively quite expensive, but its capacity to be reinforced with high fiber contents in composite materials will reduce drastically the cost of these materials and enable the achievement of competitive commercial prices.

4. Conclusions

Fully bio-based composites from bio-based PA11 and high-yield mechanical SGW fibers were successfully formulated and prepared. The PA11-SGW composites were characterized by means of a three-point bending test, as well as calculation of the *FFSF* and the average σ_f^F. Their competitiveness, in terms of flexural performance, was evaluated against three different oil-based composites: PP-GF

coupled and sized, and PP-SGW. The use of a bio-based matrix such as PA11 reinforced with SGW instead of oil-based composites followed the principles of green chemistry.

The flexural strength of PA11-SGW composites evolved linearly up to a maximum value of 102.7 MPa, when 60% SGW content was added to the composite. The PA11-SGW composites with high fiber content (PA11 + 50% SGW and PA11 + 60% SGW) were shown to be able to replace some oil-based composites. Moreover, the strain values of all PA11-SGW composites remained higher than those of the oil-based ones. The competitive results of the PA11-SGW composites and the linear evolution of the results indicated a good interface between PA11 and SGW fibers. This interface was obtained without the modification of any phase and without the use of coupling agents, due to the capacity of PA11 to establish H-bonds.

The strengthening capabilities of SGW fibers were studied using the *FFSF*. SGW showed a lower performance in PA11 than in PP. The differences between SGW-based composites were related to a lower exploitation of the strengthening capabilities of the fiber in PA11-SGW due to a weaker interface (H-bonds versus covalent bonds and entanglement). This weaker interface was also reflected in the lower $\sigma_f{}^F$ of SGW fibers in PA11-SGW compared to that obtained in PP-SGW composites. The slightly higher value of $f_c{}^f$ of PA11-SGW composites than PP-SGW was related to the higher orientation factor in PA11-SGW. On the other hand, the differences from GF were mainly related to its higher $\sigma_f{}^F$. Moreover, in the case of the GF-coupled composite, the high FFSF value was obtained by the combination of the GF's $\sigma_f{}^F$ and the effect of the coupling agent.

Finally, GF reported higher strengthening capabilities than SGW. This implies the necessity of increasing the V^F of SGW up to 3.7 times to achieve a similar fiber contribution to that achieved by GF coupled in the composite strength. However, the use of GF as a reinforcement is limited by its fragility. In terms of processability and sustainability, SGW fibers, especially as reinforcement of PA11, provide better options.

Acknowledgments: We hereby thank Arkema for kindly supplying the polyamide 11 used in this work as well as for the technical information provided by Patrick Dang and Pep Català.

Author Contributions: Helena Oliver-Ortega performed the experiments and wrote the first version of the manuscript. José Alberto Méndez and Mònica Ardanuy conceived and designed the experiments. Francesc Xavier Espinach and Rafel Reixach performed the calculus and represented the data. Pere Mutjé guided the project. All of the authors contributed to write and correct the document.

Conflicts of Interest: The authors declare no conflict of interest.

References

1. Gironès, J.; Lopez, J.P.; Vilaseca, F.; Bayer, R.; Herrera-Franco, P.J.; Mutjé, P. Biocomposites from Musa textilis and polypropylene: Evaluation of flexural properties and impact strength. *Compos. Sci. Technol.* **2011**, *71*, 122–128. [CrossRef]
2. Bledzki, A.K.; Franciszczak, P.; Osman, Z.; Elbadawi, M. Polypropylene biocomposites reinforced with softwood, abaca, jute, and kenaf fibers. *Ind. Crop. Prod.* **2015**, *70*, 91–99. [CrossRef]
3. Espigulé, E.; Vilaseca, F.; Espinach, F.X.; Julian, F.; El Mansouri, N.-E.; Mutjé, P. Biocomposites from Starch-based Biopolymer and Rape Fibers. Part II: Stiffening, Flexural and Impact Strength, and Product Development. *Curr. Org. Chem.* **2013**, *17*, 1641–1646. [CrossRef]
4. Singh, V.K.; Bansal, G.; Negi, P.; Bisht, A. Characterization of Flexural and Impact Strength of Jute/Almond Hybrid Biocomposite. *J. Test. Eval.* **2017**, *45*. [CrossRef]
5. Granda, L.A.; Espinach, F.X.; Méndez, J.A.; Vilaseca, F.; Delgado-Aguilar, M.; Mutjé, P. Semichemical fibres of Leucaena collinsii reinforced polypropylene composites: Flexural characterisation, impact behaviour and water uptake properties. *Compos. Part B* **2016**, *97*, 176–182. [CrossRef]
6. Arrakhiz, F.Z.; Malha, M.; Bouhfid, R.; Benmoussa, K.; Qaiss, A. Tensile, flexural and torsional properties of chemically treated alfa, coir and bagasse reinforced polypropylene. *Compos. Part B* **2013**, *47*, 35–41. [CrossRef]
7. Espinach, F.X.; Julian, F.; Verdaguer, N.; Torres, L.; Pelach, M.A.; Vilaseca, F.; Mutje, P. Analysis of tensile and flexural modulus in hemp strands/polypropylene composites. *Compos. Part B* **2013**, *47*, 339–343. [CrossRef]

8. Serrano, A.; Espinach, F.X.; Tresserras, J.; Pellicer, N.; Alcala, M.; Mutje, P. Study on the technical feasibility of replacing glass fibers by old newspaper recycled fibers as polypropylene reinforcement. *J. Clean. Prod.* **2014**, *65*, 489–496. [CrossRef]
9. Mäder, E. Glass Fibers: Quo Vadis? *Fibers* **2017**, *5*, 10. [CrossRef]
10. Shuaib, N.A.; Mativenga, P.T. Effect of Process Parameters on Mechanical Recycling of Glass Fibre Thermoset Composites. *Procedia CIRP* **2016**, *48*, 134–139. [CrossRef]
11. Heitzmann, M.T.; Veidt, M.; Ng, C.T.; Lindenberger, B.; Hou, M.; Truss, R.; Liew, C.K. Single-plant biocomposite from ricinus communis: Preparation, properties and environmental performance. *J. Polym. Environ.* **2013**, *21*, 366–374. [CrossRef]
12. Martínez Urreaga, J.; González-Sánchez, C.; Martínez-Aguirre, A.; Fonseca-Valero, C.; Acosta, J.; de la Orden, M.U. Sustainable eco-composites obtained from agricultural and urban waste plastic blends and residual cellulose fibers. *J. Clean. Prod.* **2015**, *108*, 1–8. [CrossRef]
13. Wang, B.J.; Lee, J.Y.; Wang, R.C. Fiberglass dermatitis: report of two cases. *J. Formos. Med. Assoc.* **1993**, *92*, 755–758. [PubMed]
14. Donaldson, K.; Tran, C.L. An introduction to the short-term toxicology of respirable industrial fibres. *Mutat. Res. Mol. Mech. Mutagen.* **2004**, *553*, 5–9. [CrossRef] [PubMed]
15. Alves, C.; Ferrão, P.M.C.; Silva, A.J.; Reis, L.G.; Freitas, M.; Rodrigues, L.B.; Alves, D.E. Ecodesign of automotive components making use of natural jute fiber composites. *J. Clean. Prod.* **2010**, *18*, 313–327. [CrossRef]
16. Reixach, R.; Del Rey, R.; Alba, J.; Arbat, G.; Espinach, F.X.; Mutjé, P. Acoustic properties of agroforestry waste orange pruning fibers reinforced polypropylene composites as an alternative to laminated gypsum boards. *Constr. Build. Mater.* **2015**, *77*, 124–129. [CrossRef]
17. Claramunt, J.; Fernández-Carrasco, L.J.; Ventura, H.; Ardanuy, M. Natural fiber nonwoven reinforced cement composites as sustainable materials for building envelopes. *Constr. Build. Mater.* **2016**, *115*, 230–239. [CrossRef]
18. Shibata, S.; Cao, Y.; Fukumoto, I. Study of the flexural modulus of natural fiber/polypropylene composites by injection molding. *J. Appl. Polym. Sci.* **2006**, *100*, 911–917. [CrossRef]
19. Jiménez, A.M.; Espinach, F.X.; Delgado-Aguilar, M.; Reixach, R.; Quintana, G.; Fullana-i-Palmer, P.; Mutjé, P. Starch-Based Biopolymer Reinforced with High Yield Fibers from Sugarcane Bagasse as a Technical and Environmentally Friendly Alternative to High Density Polyethylene. *BioResources* **2016**, *11*, 9856–9868. [CrossRef]
20. Faruk, O.; Bledzki, A.K.; Fink, H.P.; Sain, M. Biocomposites reinforced with natural fibers: 2000-2010. *Prog. Polym. Sci.* **2012**, *37*, 1552–1596. [CrossRef]
21. Winnacker, M.; Rieger, B. Biobased Polyamides: Recent Advances in Basic and Applied Research. *Macromol. Rapid Commun.* **2016**, *37*, 1391–1413. [CrossRef] [PubMed]
22. Xu, X. *Cellulose Fiber Reinforced Nylon 6 or Nylon 66*; Georgia Institute of Technology: Atlanta, GA, USA, 2008; pp. 1–228.
23. Bledzki, A.K.; Feldmann, M. Bio-based polyamides reinforced with cellulosic fibres—Processing and properties. *Compos. Sci. Technol.* **2014**, *100*, 113–120.
24. Unterweger, C.; Duchoslav, J.; Stifter, D.; Fürst, C. Characterization of carbon fiber surfaces and their impact on the mechanical properties of short carbon fiber reinforced polypropylene composites. *Compos. Sci. Technol.* **2015**, *108*, 41–47. [CrossRef]
25. Fuentes, C.A.; Brughmans, G.; Tran, L.Q.N.; Dupont-Gillain, C.; Verpoest, I.; Van Vuure, A.W. Mechanical behaviour and practical adhesion at a bamboo composite interface: Physical adhesion and mechanical interlocking. *Compos. Sci. Technol.* **2015**, *109*, 40–47. [CrossRef]
26. Ayaz, M.; Daneshpayeh, S.; Noroozi, A. Enhancing the impact and flexural strength of PP/LLDPE/TiO2/SEBS nano-composites by using Taguchi methodology. *Compos. Sci. Technol.* **2016**, *129*, 61–69. [CrossRef]
27. Ding, Y.; Yu, Z.; Zheng, J. Rational design of adhesion promoter for organic/inorganic composites. *Compos. Sci. Technol.* **2017**, *147*, 1–7. [CrossRef]
28. Gilbert, M. Aliphatic Polyamides. In *Brydson's Plastics Materials*, 8th ed.; William Andrew: Norwich, NY, USA, 2017; Volume 5, ISBN 9780323358248.
29. Reuvers, N.J.W.; Huinink, H.P.; Fischer, H.R.; Adan, O.C.G. Quantitative water uptake study in thin nylon-6 films with NMR imaging. *Macromolecules* **2012**, *45*, 1937–1945. [CrossRef]

30. Orzen, E.; Kiziltas, A.; Kiziltas, E.E.; Gardner, D.J. Natural fiber blends- filled engineering thermoplastic composites for the automobile industry. In Proceedings of the 12th Automotive Composites Conference & Exhibition (ACCE 2012), Troy, MI, USA, 11–13 September 2012; pp. 275–286.
31. Panaitescu, D.M.; Gabor, R.A.; Frone, A.N.; Vasile, E. Influence of Thermal Treatment on Mechanical and Morphological Characteristics of Polyamide 11/Cellulose Nanofiber Nanocomposites. *J. Nanomater.* **2015**, *2015*, 1–11. [CrossRef]
32. Santos, P.A.; Spinacé, M.A.S.; Fermoselli, K.K.G.; De Paoli, M.A. Polyamide-6/vegetal fiber composite prepared by extrusion and injection molding. *Compos. Part A* **2007**, *38*, 2404–2411. [CrossRef]
33. Martino, L.; Basilissi, L.; Farina, H.; Ortenzi, M.A.; Zini, E.; Di Silvestro, G.; Scandola, M. Bio-based polyamide 11: Synthesis, rheology and solid-state properties of star structures. *Eur. Polym. J.* **2014**, *59*, 69–77. [CrossRef]
34. Bourmaud, A.; Le Duigou, A.; Gourier, C.; Baley, C. Influence of processing temperature on mechanical performance of unidirectional polyamide 11-flax fibre composites. *Ind. Crops Prod.* **2016**, *84*, 151–165. [CrossRef]
35. Zierdt, P.; Theumer, T.; Kulkarni, G.; Däumlich, V.; Klehm, J.; Hirsch, U.; Weber, A. Sustainable wood-plastic composites from bio-based polyamide 11 and chemically modified beech fibers. *Sustain. Mater. Technol.* **2015**, *6*, 6–14. [CrossRef]
36. López, J.P.; Méndez, J.A.; El Mansouri, N.E.; Mutjé, P.; Vilaseca, F. Mean intrinsic tensile properties of stone groundwood fibers from softwood. *Bio Resources* **2011**, *6*, 5037–5049.
37. López, J.P.; Gironès, J.; Mendez, J.A.; Pèlach, M.A.; Vilaseca, F.; Mutjé, P. Impact and flexural properties of stone-ground wood pulp-reinforced polypropylene composites. *Polym. Compos.* **2013**, *34*, 842–848. [CrossRef]
38. Oliver-Ortega, H.; Granda, L.A.; Espinach, F.X.; Méndez, J.A.; Julian, F.; Mutjé, P. Tensile properties and micromechanical analysis of stone groundwood from softwood reinforced bio-based polyamide11 composites. *Compos. Sci. Technol.* **2016**, *132*, 123–130. [CrossRef]
39. Zierdt, P.; Kulkarni, G.; Theumer, T. Mechanical and Thermo-Mechanical Properties of Discontinuously and Continuously Processed Biogenic Wood-Plastic Composites from Polyamide 11 and Chemically Modified Beech Particles. *Macromol. Symp.* **2017**, *373*, 1600118. [CrossRef]
40. Armioun, S.; Panthapulakkal, S.; Scheel, J.; Tjong, J.; Sain, M. Biopolyamide hybrid composites for high performance applications. *J. Appl. Polym. Sci.* **2016**, *133*. [CrossRef]
41. Armioun, S.; Panthapulakkal, S.; Scheel, J.; Tjong, J.; Sain, M. Sustainable and lightweight biopolyamide hybrid composites for greener auto parts. *Can. J. Chem. Eng.* **2016**, *94*, 2052–2060. [CrossRef]
42. Oliver-Ortega, H.; Méndez, J.A.; Mutjé, P.; Tarrés, Q.; Espinach, F.X.; Ardanuy, M. Evaluation of Thermal and Thermomechanical Behaviour of Bio-Based Polyamide 11 Based Composites Reinforced with Lignocellulosic Fibres. *Polymers* **2017**, *9*, 522. [CrossRef]
43. Gourier, C.; Bourmaud, A.; Le Duigou, A.; Baley, C. Influence of PA11 and PP thermoplastic polymers on recycling stability of unidirectional flax fibre reinforced biocomposites. *Polym. Degrad. Stab.* **2017**, 1–9. [CrossRef]
44. Oliver-Ortega, H.; Granda, L.A.; Espinach, F.X.; Delgado-Aguilar, M.; Duran, J.; Mutjé, P. Stiffness of bio-based polyamide 11 reinforced with softwood stone ground-wood fibres as an alternative to polypropylene-glass fibre composites. *Eur. Polym. J.* **2016**, *84*, 481–489. [CrossRef]
45. Huber, T.; Bickerton, S.; Müssig, J.; Pang, S.; Staiger, M.P. Flexural and impact properties of all-cellulose composite laminates. *Compos. Sci. Technol.* **2013**, *88*, 92–98. [CrossRef]
46. Espinach, F.X.; Delgado-Aguilar, M.; Puig, J.; Julian, F.; Boufi, S.; Mutjé, P. Flexural properties of fully biodegradable alpha-grass fibers reinforced starch-based thermoplastics. *Compos. Part B* **2015**, *81*, 98–106. [CrossRef]
47. Valadez-Gonzalez, A.; Cervantes-Uc, J.M.; Olayo, R.; Herrera-Franco, P.J. Effect of fiber surface treatment on the fiber-matrix bond strength of natural fiber reinforced composites. *Compos. Part B* **1999**, *30*, 309–320. [CrossRef]
48. Yang, H.S.; Wolcott, M.P.; Kim, H.S.; Kim, S.; Kim, H.J. Effect of different compatibilizing agents on the mechanical properties of lignocellulosic material filled polyethylene bio-composites. *Compos. Struct.* **2007**, *79*, 369–375. [CrossRef]
49. Vilaseca, F.; Valadez-Gonzalez, A.; Herrera-Franco, P.J.; Pelach, M.A.; López, J.P.; Mutjé, P. Biocomposites from abaca strands and polypropylene. Part I: Evaluation of the tensile properties. *Bioresour. Technol.* **2010**, *101*, 387–395. [CrossRef] [PubMed]

50. Marais, A.; Wågberg, L. The use of polymeric amines to enhance the mechanical properties of lignocellulosic fibrous networks. *Cellulose* **2012**, *19*, 1437–1447. [CrossRef]
51. Johansson, L.S. Monitoring fibre surfaces with XPS in papermaking processes. *Mikrochim. Acta* **2002**, *138–139*, 217–223. [CrossRef]
52. Bledzki, A.K.; Gassan, J. Composites reinforced with cellulose based fibres. *Prog. Polym. Sci.* **1999**, *24*, 221–274. [CrossRef]
53. Börås, L.; Gatenholm, P. Surface Composition and Morphology of CTMP Fibers. *Holzforschung* **1999**, *53*. [CrossRef]
54. Johansson, L.S.; Campbell, J.; Koljonen, K.; Kleen, M.; Buchert, J. On surface distributions in natural cellulosic fibres. *Surf. Interface Anal.* **2004**, *36*, 706–710. [CrossRef]
55. Granda, L.A.; Espinach, F.X.; Tarrés, Q.; Méndez, J.A.; Delgado-Aguilar, M.; Mutjé, P. Towards a good interphase between bleached kraft softwood fibers and poly(lactic) acid. *Compos. Part B* **2016**, *99*, 514–520. [CrossRef]
56. Anastas, P.T.; Warner, J.C. *Green Chemistry: Theory and Practice*; Oxford University Press: New York, NY, USA, 1998.
57. Anastas, P.T.; Zimmerman, J.B. Design through the 12 principles of green engineering. *IEEE Eng. Manag. Rev.* **2007**, *35*, 16. [CrossRef]
58. Vannan, S.E.; Vizhian, S.P. Microstructure and mechanical properties of as cast aluminium alloy 7075/basalt dispersed metal matrix composites. *J. Miner. Mater. Charact. Eng.* **2014**, *2*, 182–193. [CrossRef]
59. López, J.P.; Mutjé, P.; Angels Pèlach, M.; El Mansouri, N.E.; Boufi, S.; Vilaseca, F. Analysis of the tensile modulus of polypropylene composites reinforced with stone groundwood fibers. *BioResources* **2012**, *7*, 1310–1323. [CrossRef]
60. Van de Velde, K.; Kiekens, P. Biopolymers: overview of several properties and consequences on their applications. *Polym. Test.* **2002**, *21*, 433–442. [CrossRef]
61. Espinach, F.X.; Julián, F.; Alcalà, M.; Tresserras, J.; Mutjé, P. High stiffness performance alpha-grass pulp fiber reinforced thermoplastic starch-based fully biodegradable composites. *BioResources* **2014**, *9*, 738–755. [CrossRef]
62. Ashori, A. Wood–plastic composites as promising green-composites for automotive industries! *Bioresour. Technol.* **2008**, *99*, 4661–4667. [CrossRef] [PubMed]
63. Julian, F.; Méndez, J.A.; Espinach, F.X.; Verdaguer, N.; Mutje, P.; Vilaseca, F. Bio-based composites from stone groundwood applied to new product development. *BioResources* **2012**, *7*, 5829–5842. [CrossRef]
64. del Rey, R.; Serrat, R.; Alba, J.; Perez, I.; Mutje, P.; Espinach, F.X. Effect of sodium hydroxide treatments on the tensile strength and the interphase quality of hemp core fiber-reinforced polypropylene composites. *Polymers* **2017**, *9*, 377. [CrossRef]
65. Thomason, J.L. Interfacial strength in thermoplastic composites—At last an industry friendly measurement method? *Compos. Part A* **2002**, *33*, 1283–1288.
66. Hashemi, S.; Khamsehnezhad, A. Analysis of tensile and flexural strengths of single and double gated injection moulded short glass fibre reinforced PBT/PC composites. *Plast. Rubber Compos.* **2010**, *39*, 343–349. [CrossRef]
67. Park, J.M.; Quang, S.T.; Hwang, B.S.; DeVries, K.L. Interfacial evaluation of modified Jute and Hemp fibers/polypropylene (PP)-maleic anhydride polypropylene copolymers (PP-MAPP) composites using micromechanical technique and nondestructive acoustic emission. *Compos. Sci. Technol.* **2006**, *66*, 2686–2699. [CrossRef]
68. Grunenberg, J. Direct assessment of interresidue forces in Watson-Crick base pairs using theoretical compliance constants. *J. Am. Chem. Soc.* **2004**, *126*, 16310–16311. [CrossRef] [PubMed]
69. Chundawat, S.P.S.; Bellesia, G.; Uppugundla, N.; Da Costa Sousa, L.; Gao, D.; Cheh, A.M.; Agarwal, U.P.; Bianchetti, C.M.; Phillips, G.N.; Langan, P.; Balan, V.; Gnanakaran, S.; Dale, B.E. Restructuring the crystalline cellulose hydrogen bond network enhances its depolymerization rate. *J. Am. Chem. Soc.* **2011**, *133*, 11163–11174. [CrossRef] [PubMed]
70. Aydemir, D.; Kiziltas, A.; Erbas Kiziltas, E.; Gardner, D.J.; Gunduz, G. Heat treated wood-nylon 6 composites. *Compos. Part B* **2015**, *68*, 414–423. [CrossRef]

71. Sears, K.D.; Jacobson, R.; Caulfield, D.F.; Underwood, J. Reinforcement of Engineering Themoplastics with High Purity Wood Cellulose Fibers. In Proceedings of the Sixth International Conference on Woodfiber-Plastic Composites, Madison, WI, USA, 15–16 May 2001.
72. Shah, D.U.; Nag, R.K.; Clifford, M.J. Why do we observe significant differences between measured and "back-calculated" properties of natural fibres? *Cellulose* **2016**, *23*, 1481–1490. [CrossRef]
73. Hashemi, S. Strength of single- and double-gated injection moulded short glass fibre reinforced polycarbonate. *J. Thermoplast. Compos. Mater.* **2013**, *26*, 276–295. [CrossRef]
74. Fu, S.Y.; Lauke, B. Effects of fiber length and fiber orientation distributions on the tensile strength of short-fiber-reinforced polymers. *Compos. Sci. Technol.* **1996**, *56*, 1179–1190. [CrossRef]
75. Sanadi, A.R.; Young, R.A.; Clemons, C.; Rowell, R.M. Recycled newspaper fibers as reinforcing fillers in thermoplastics: Part I-Analysis of tensile and impact properties in polypropylene. *J. Reinf. Plast. Compos.* **1994**, *13*, 54–67. [CrossRef]

2.5 Study of the flexural modulus of lignocellulosic fibres reinforced bio-based polyamide11 green composites

Enviado y en revisión en *Composites Part B: Engineering.* Factor de impacto 2016: 4,727. Posición 2 de de 25 en Materials Science, Composites. Primer cuartil.

Manuscript Details

Manuscript number	JCOMB_2018_1313
Title	Study of the flexural modulus of lignocellulosic fibres reinforced bio-based polyamide11 green composites
Article type	Full Length Article

Abstract

The stiffness of a material has high impact in its industrial use. Moreover, this property has interest in the case of short fibre reinforced materials due to its dependence on the orientation of the fibres against the loads. Due to environmental concerns, nowadays greener alternatives are being developed as an alternative to common oil-based composites. In this work, polyamide 11 reinforced with lignocellulosic fibres are evaluated as sustainable alternatives. Previous works showed the suitability of PA11-based composites to replace glass fibre reinforced polypropylene. Nonetheless, there is a lack of information about the flexural modulus behaviour of these composites. This is of interest because, under some conditions, flexural modulus is more representative of a material behaviour than Young's modulus. The flexural modulus of the composites was analysed by a three point bending test and the results were evaluated from macro and micromechanical points of view. The increment of the modulus with the fibre contents implied a good dispersion of the reinforcements. Nonetheless, the results were lower than those observed for the tensile modulus. This was unexpected due to the anisotropy of the bending test. The micromechanics analysis showed a lower performance of the fibre during the flexural test. These lower results were related with a non-optimal interface or with the non-adequate compression of the fibres. Additionally, the calculus of the void volume showed low void contents.

Keywords	Fibres; interface; Micromechanics;Injection molding
Manuscript region of origin	Europe

Corresponding Author	F.X. Espinach
Corresponding Author's Institution	Universitat de Girona, Escola Politècnica Superior
Order of Authors	Helena Oliver-Ortega, Miquel Llop, F.X. Espinach, Quim Tarres, Monica Ardanuy, Pere Mutje
Suggested reviewers	Nour-Eddine El Mansouri, sami boufi, Fernando Julian, Carlos Negro

Submission Files Included in this PDF

File Name [File Type]

cover letter.doc [Cover Letter]

modul flex_v2.docx [Manuscript File]

To view all the submission files, including those not included in the PDF, click on the manuscript title on your EVISE Homepage, then click 'Download zip file'.

Research Data Related to this Submission

There are no linked research data sets for this submission. The following reason is given:
No data was used for the research described in the article

Girona, May 3rd, 2018

Dear Editor,

Please find attached our manuscript for publication in *Composites Part B: Engineering*:

Study of the flexural modulus of lignocellulosic fibres reinforced bio-based polyamide11 green composites.

By: H. Oliver-Ortega, M.F. Llop, F.X. Espinach, Q. Tarrés, M. Ardanuy, P. Mutjé

This work analyses the flexural modulus of stoneground wood from softwood reinforced polyamide 11 (PA11) and their suitability to replacement commercial composites materials as glass fibre (GF) reinforced polypropylene (PP).

Environmental concern is a highly topic in the scientific research. In the field of composites materials one of the main objectives is replacing non-renewable raw materials by renewable and sustainable materials, while maintaining good mechanical properties. PA11 is totally obtained from castor oil and can be reinforced with natural fibres due to their low melting point regarding other polyamides. In addition, PA11 can be reinforced with natural fibres without the use of a coupling agent, typical used in polyolefin, due to the capacity of PA11 to stablish H-bonds.

Although tensile modulus of these composites has been widely studied, there is a lack of studies about the flexural modulus. However, flexural modulus is quite relevant for the development and application of composite materials due to the clear anisotropy of its mechanical properties. Moreover, their study is necessary in the design and product development fields. The aim of this paper is to examine flexural modulus of PA11-SGW composites and compares the results with PP-GF commodities to analyse the suitability of PA11-SGW composites to replace them as a greener and sustainable alternative.

We therefore believe that our work, as described in this manuscript, would be very much of interest to Scientifics. Our aim is to show the scientific community how they can benefit from the use of a new matrix with easily obtainable natural fibres and their competitiveness to replace commercial composites by sustainable ones.

We confirm that this manuscript has not been published elsewhere and is not under consideration by another journal, and all authors have approved the manuscript and agree with its submission to *Composites Part B: Engineering*.

In case of any questions please do not hesitate to contact us anytime.

The corresponding author is

Francesc X. Espinach

PRODIS
Escola Politècnica Superior. C/M. Aurèlia Capmany, n°61, Girona 17003, Spain
Phone : 34 669 996 998,
FAX +34 972 418 399
E-mail: Francisco.espinach@udg.edu

Study of the flexural modulus of lignocellulosic fibres reinforced bio-based polyamide11 green composites

H. Oliver-Ortega[a], M.F. Llop[a], F.X. Espinach[b*], Q. Tarrés[a] , M. Ardanuy[c], P. Mutjé[a]

[a] Group LEPAMAP, Department of Chemical Engineering, University of Girona, C/M. Aurèlia Capmany, nº61, Girona 17003, Spain.

[b] Design, Development and Product Innovation, Dpt. of Organization, Business Management and Product Design, University of Girona, C/M. Aurèlia Capmany, nº61, Girona 17003, Spain.

[c] Departament de Ciència dels Materials i Enginyeria Metal.lúrgica, Secció Enginyeria Tèxtil, Universitat Politècnica de Catalunya. C/ Colom,11, 08222 Terrassa (Barcelona), Spain.

*Corresponding author

ABSTRACT

The stiffness of a material has high impact in its industrial use. Moreover, this property has interest in the case of short fibre reinforced materials due to its dependence on the orientation of the fibres against the loads. Due to environmental concerns, nowadays greener alternatives are being developed as an alternative to common oil-based composites. In this work, polyamide 11 reinforced with lignocellulosic fibres are evaluated as sustainable alternatives. Previous works showed the suitability of PA11-based composites to replace glass fibre reinforced polypropylene. Nonetheless, there is a lack of information about the flexural modulus behaviour of these composites. This is of interest because, under some conditions, flexural modulus is more representative of a material behaviour than Young's modulus. The flexural modulus of the composites was

analysed by a three point bending test and the results were evaluated from macro and micromechanical points of view. The increment of the modulus with the fibre contents implied a good dispersion of the reinforcements. Nonetheless, the results were lower than those observed for the tensile modulus. This was unexpected due to the anisotropy of the bending test. The micromechanics analysis showed a lower performance of the fibre during the flexural test. These lower results were related with a non-optimal interface or with the non-adequate compression of the fibres. Additionally, the calculus of the void volume showed low void contents.

Keywords: A, Fibres; B, interface; C, Micromechanics; D, Injection molding

1 INTRODUCTION

Stiffness is a milestone for the processability and application of materials [1,2]. This property gains interest in short-fibre reinforced composites where the orientation of the reinforcing fibres in the composite material and against the load plays a major role [3,4]. Young's modulus is commonly used as reference of material stiffness [5]. However, its results are less representative than flexural modulus due to the unique load direction in tensile test.

The higher performance and lower weight of composites materials, principally polymeric ones, made them typical material in our lives. Thus it is common to find these composites in quotidian objects like cars, windows, furniture, etc. Their use in cars or planes reduced the weight, and as consequence fuel consumption, while the mechanical characteristics were maintained or enhanced. One of the most used composite materials are glass fibre (GF) reinforced polypropylene [6]. The mechanical enhancement obtained by the GF combined with the chemical resistance and the toughness of polypropylene made them almost a commodity in the market. However,

the poor recyclability of GF and the health problems derived from its manipulation led to take under consideration greener and more sustainable composites [7,8].

Lignocellulosic fibres have become a greener and sustainable reinforcement for composites materials [9]. There is a large quantity of literature about different fibres and treatments with polypropylene [10–12]. Moreover, these composites are nowadays available in commercial products [13,14]. However, society environmental awareness has increased in the last decades and oil derived products demand is reducing every day [15]. In this sense, there is a perceived need to replace polypropylene matrices by bio-based and/or biodegradables polymers, both as virgin materials or as composite matrices.

Polyamide 11 (PA11) is a well-stablish bio-based polymer in the market since the 50's [16]. However, it has not attracted the attention of the composite researchers up to the last years. Polyamide 11 is considered an engineering plastic because is recyclable and non-biodegradable and has the typical polyamide properties [17,18]. PA11 are interesting for long-time application which is desirable in some fields such as the automotive industry [19]. Moreover, the low melting point regarding other polyamides allows reinforcing it with lignocellulosic fibres without any or really low degradation of such fibres [20].

Previous works showed the competitiveness of PA11-lignocellulosic fibres to replace PP composites [19,21–23]. However, these works have been focused on the tensile properties and the processability of PA11-based composites and a lack of literature on flexural properties has been detected. Thus, the flexural modulus of stone groundwood fibres (SGW) reinforced PA11 and its micromechanics are studied in this work (Figure 1). The experiments returned some unexpected results, regarding the author's

experience, which led them to consider the presence of void volumes as the cause of the collapse of the fibres.

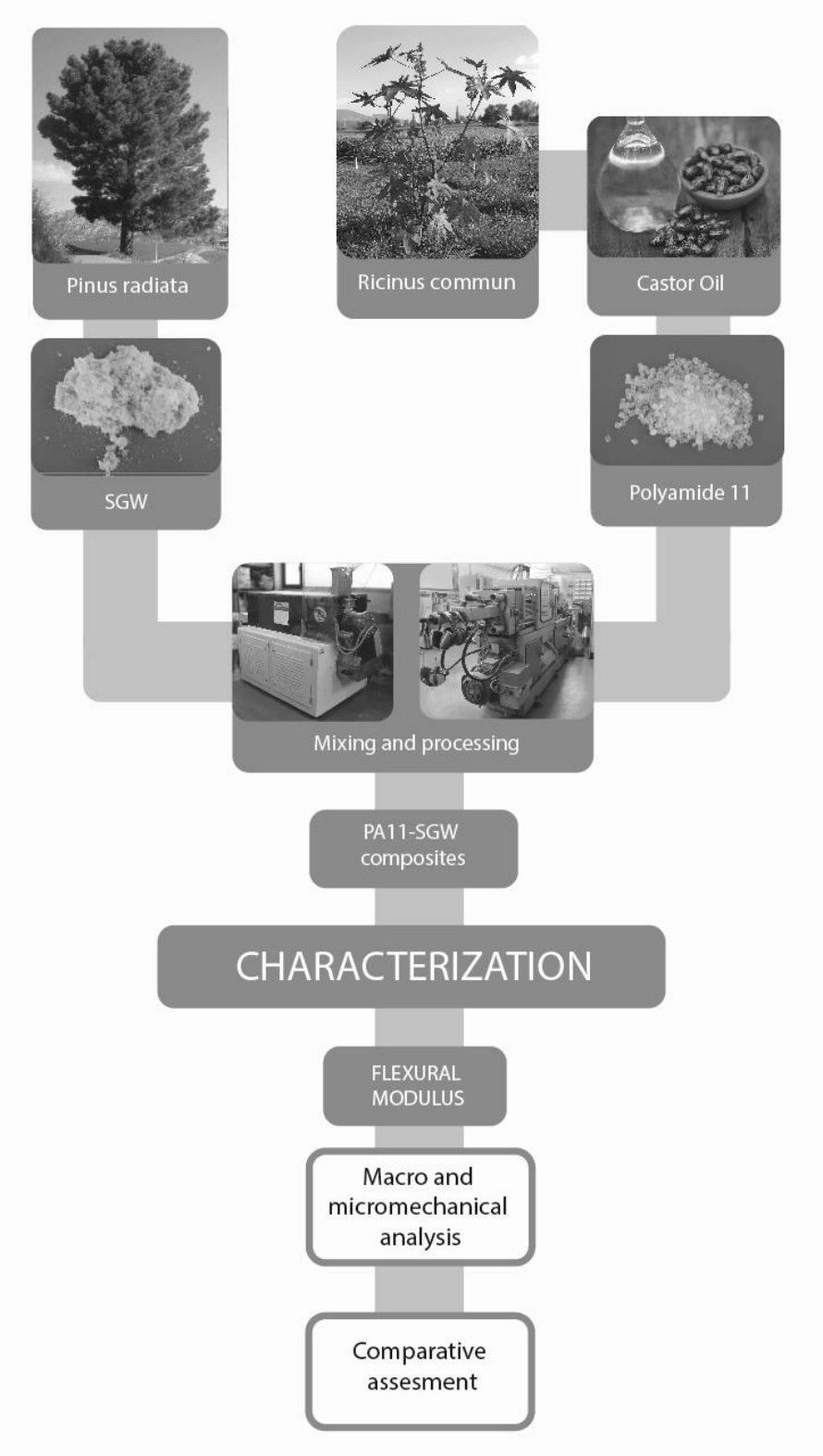

Figure 1. Scheme of the composite production and experimental workflow of the research.

2 MATERIALS AND METHODS

2.1 Materials

The polymeric matrix used to produce the composites was a Polyamide 11 (PA11) Rilsan® BMNO TL kyndly supplied by Arkema S.A (Colombes, France). Its melting point was around 189ºC and had a density of 1.03g/cc. The reinforcement fibre was Stoneground wood (SGW) from pine supplied by by Zubialde, S.A. (Aizarnazabal, Spain).

Dichloromethane (Extra Pure, stabilized with approx. 50ppm of amylene, Pharmpur®) and Formic acid (Extra Pure, 98-100%), both supplied by Scharlau (Sentmenat, Spain) were used to dissolve the PA11 matrix and recover the fibres.

2.2 Methods

Composite compounding and sample obtaining

Five different reinforced composites were obtained with SGW fibre contents ranging from 20 to 60%. The compounding process was performed using a Gelimat kinetic mixer as accordingly to previous works [21,22]. The specimens for the flexural characterization (ASTM D638) were obtained by means of a Meteor-40 injection machine (Mateu&Solé, clamping pressure: 40 tons). The samples were conditioned following the ASTM D618 at 23ºC and 50%RH before the mechanical tests.

Mechanical characterization

An Universal testing machine by IDMtest fitted with a 5kN load cell was used for the mechanical characterization. The composite materials were tested under a three points bending configuration following ASTM D790. The results were obtained from an average of at least 5 samples.

100 The strain (ε_f^C) of the samples was determined following ASTM D790:

$$\varepsilon_f^C = \frac{6 \cdot D \cdot d}{L^2} \quad [1]$$

101 Where D is the experimental deflection at the centre of the beam observed, d is the
102 thickness of the sample and L is the length of the support span.

103 *Composites and fibre density*

104 The experimental density of the composites (ρ^C) was obtained using a pycnometer. An
105 exact weight of an injected-moulding sample of the composite was measured in the
106 pycnometer and was bring to the volume with distilled water. The density was
107 calculated as:

$$\rho^C = \frac{Weight_{composite}}{V_{total} - Weight_{water} \cdot \rho_{water}} \quad [2]$$

108 Where V_{total} is the total volume of the pycnometer, and ρ_{water} is the water density
109 determined experimentally. Fibre density (ρ^F) used for the fibre volumetric fraction
110 calculus (V^F) was back-calculated from ρ^C from:

$$\rho^F = \frac{Weight_{fibre} \cdot \rho^C \cdot \rho^m}{\left(\left(Weight_{matrix} + Weight_{fibre}\right) \cdot \rho^m\right) - Weight_{matrix} \cdot \rho^C} \quad [3]$$

111 Where ρ^m is the polymeric matrix density.

112 *Fibre extraction from composites and morphological analysis*

113 Knowing the mean lengths and diameters of the fibres was necessary to model the
114 mechanical behaviour of the composites. As it is known that the morphology of the
115 fibres changes during the composites preparation the data was obtained from the
116 processed materials. For this purpose, the extraction of the fibres was performed in a

Soxhlet apparatus with a mixture of dichloromethane and formic acid (1:1 v/v) for PA11-SGW composites. Composite samples were grinded in small pieces and placed inside a specific cellulose filter and set into the Soxhlet equipment. The extraction was performed during 24 hours. Then, the fibres were cleaned and dried in an oven at 105ºC for 24 hours more before analysis. The analysis of the length and width were characterized by means of a MorFi analyser (Techpap SAS. Grenoble, France) following the standard ISO/FDIS 160652.

Mechanical modelling

A modified Rule of Mixtures (mRoM) was used to model the flexural modulus of the composites materials:

$$E_f^C = \eta_e \cdot E_f^F \cdot V^F + (1 - V^F) \cdot E_f^m \quad [4]$$

Where E_f^C, E_f^F and E_f^m are the flexural modulus of the composite, fibre and matrix, respectively and η_e is an efficiency factor. However, in this formula η_e and E_t^F are unknown values which depend on the fibre stiffness and morphology and its orientation inside the composite material. The neat fibre contribution in the composite can be analysed using a Fibre Flexural Modulus Factor *(FFMF)*, rearranging Eq. 3 as:

$$FFMF = \frac{E_f^C - (1 - V^F) \cdot E_f^m}{V^F} = \eta_e \cdot E_f^F \quad [5]$$

FFMF led to determine the fibre neat contribution but not the intrinsic properties of the fibre. Fibre properties are usually difficult and expensive to measure. In this sense, Hirsch model [24] has been successfully applied to calculate E_f^F :

$$E_f^C = \beta \cdot (E_f^F \cdot V^F + E_f^m(1 - V^F) + (1 - \beta)\frac{E_f^F \cdot E_t^m}{E_f^F \cdot V^F + E_f^m(1 - V^F)} \quad [6]$$

135 Where β is a parameter related with the stress transference between both phases of the
136 composite material and in natural fibres has a value of 0.4 [25].

137 Once the intrinsic flexural modulus is known, η_e is obtained from the mRoM. Moreover,
138 the η_e could be subdivided in two efficiency factors, one related with the length and
139 another with the orientation; the length and orientation efficiency factors (η_l and η_0,
140 respectively). The length efficiency factor was calculated with the Cox and Krenchel
141 equations (Eq. 6 and 7). Equation 8 shows the relation between the efficiency factors.

$$\eta_l = 1 - \frac{tanh\left(\frac{\beta \cdot l^F}{2}\right)}{\frac{\beta \cdot l^F}{2}} \quad [7]$$

$$\beta = \frac{1}{r}\sqrt{\frac{E_f^m}{E_f^F \cdot (1 - \upsilon) \cdot Ln\left(\sqrt{\frac{\pi}{4 \cdot V^F}}\right)}}\beta\beta \quad [8]$$

$$\eta_e = \eta_l \cdot \eta_o \quad [9]$$

142 Where l^F and r are the mean length and radius of the fibres, respectively, obtained from
143 the MorFi analysis and a correction was performed in order to include the fines (fibres
144 with lengths lower than 90μm). Some of the authors had shown the impact of include
145 and discard the fines in the fibre's morphology analysis [22]. v is the Poisson's ratio of
146 the matrix

Once the η_0 was obtained, the mean orientation angle of the fibres was calculated considering a rectangular distribution of the fibres in the polymer matrix [21,26,27].

3 RESULTS AND DISCUSSION

The flexural modulus (E_f^C) of the PA11-SGW composites was analysed due to the importance stiffness for its application [3,28]. The experimental results for E_f^C and strain at the maximum flexural strength (ε_f^C) against the fibre volume content (V^F) are shown in Table 3. A lineal tendency of the modulus was obtained with a r^2=0.986 correlation. This linearity was an indicative of a correct dispersion of the reinforcement in the PA11 matrix. Composite stiffness depends on the fibre and matrix properties, fibre content and its dispersion inside the matrix. In the case of the flexural modulus, the interface between polymer and matrix has little effect as it has been observed before in different thermoplastic reinforced composites [21,29–31].

Table 1. Flexural modulus and strain at the maximum strength of PA11 and PA11-SGW composites.

	Fibre Content (%)	V^F	E_f^C (GPa)	ε_f^C (%)
PA11-SGW	0	0.000	0.9 ± 0.1	7.39
	20	0.155	1.7 ± 0.1	6.39
	30	0.240	2.1 ± 0.1	5.78
	40	0.329	2.6 ± 0.2	5.24
	50	0.424	3.3 ± 0.3	4.24
	60	0.524	4.1 ± 0.3	3.23

The composites moduli were 0.9, 1.3, 1.9, 2.6 and 3.6 times higher than the PA11 matrix when the fibre content was raised from 20 to 60%. The specimens deformation was reduced, as expected, caused by the addition of the stiffer reinforcement. Nonetheless, the reduction was smothering in comparison with the obtained in the tensile properties of the materials. In the case of 20% 30% of SGW fibre the test specimens did not break and continued deforming after the maximum strength.

In previous works, PA11-SGW composites were proposed as greener alternative to GF reinforced PP composites. Although PP has been successfully reinforced with natural fibres, as aforementioned in the introduction, there is a need to replace oil-based products. Figure 2 shows a comparison between PA11-SGW composites with reinforced PP available products. Flexural results from PP-GF composites were obtained from the literature and PP-SGW composites were choose as natural reinforced PP composites due the use of the same fibre [32–34]. High contents of natural fibre were used for the comparison as it was necessary to increase the fibre contents to obtain competitive properties [21,29]. The PA11-based composites moduli were lower than the obtained for PP-SGW composites at 40 and 50% of fibre content and PP-GF composites with 30% of reinforcement. Nonetheless, the PA11+50%SGW composite can replace PP+20%GF coupled or sized in terms of flexural stiffness. The PP+30%GF values were only 0.6GPa higher than PA11+60%SGW. In addition, the strain of PA11-SGW composites was the same or higher than PP-GF and PP-SGW composites [32,34,35]. The significant differences found between SGW-based composites were not expected. This effect was not observed for the Young's Moduli were PA11-SGW achieved similar values than PP-SGW at the same fibre contents and were considered a competitive alternative for PP-based composites [41]. Nevertheless, there is a lack of flexural properties literature for PA11-based composites to evaluate if the values were to be considered too low. To the authors knowledge, only *Armioun et al.* [36] studied the flexural modulus of PA11 reinforced with 30% of wood flour and the obtained result was slightly lower than the obtained for PA11+30%SGW composite. *Takeshi et al.* [37] also performed the bending test with cellulose nanofibers (CNF) reinforced PA11, and although with only 10% of CNF they achieved values similar to the 20 and 30% of PA11-SGW composites, the results can be related directly with the better properties of

CNF. Moreover, a poor effect of the CNF was observed regarding the tensile results reported by *Panaitescu et al.*[38], where the tensile modulus with 5% of CNF was the same than the flexural modulus of the 10% CNF reinforced PA11.

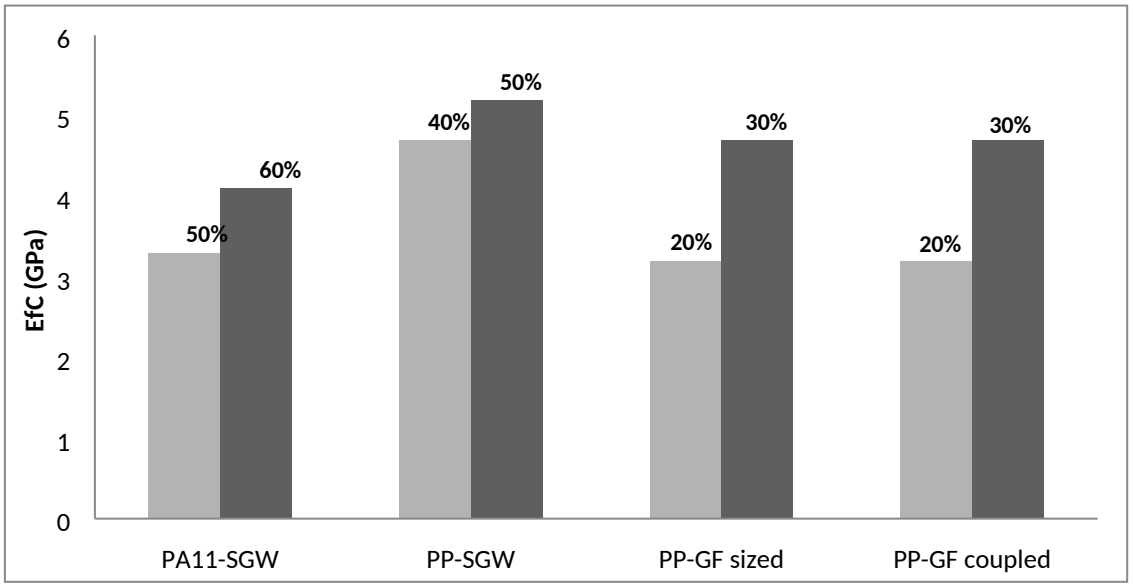

Figure 2. PA11-SGW moduli versus PP-based composites

The micromechanical analysis of the PA11-SGW was proposed to explain this effect. The lineal behaviour of the flexural modulus allowed the use of a mRoM (Eq.3) and the *FFMF*. In Figure 3 the *FFMF* of the PA11-based composites is shown and compared with PP reinforced materials. The use of GF as reinforcement resulted in higher *FFMF* due to the intrinsic properties of GF, higher than natural fibres [1]. Besides, the low effect of the interface as GF coupled and sized had almost the same neat contribution to the flexural modulus was noticeable. The *FFMF* of the SGW-based composites showed a higher stiffening effect using PP as polymer matrix than using PA11. This value was not expected as almost the same stiffening effect of SGW was observed in the fibre tensile modulus factor (*FTMF*) despite if a PP or PA11 matrix was used[21,29].

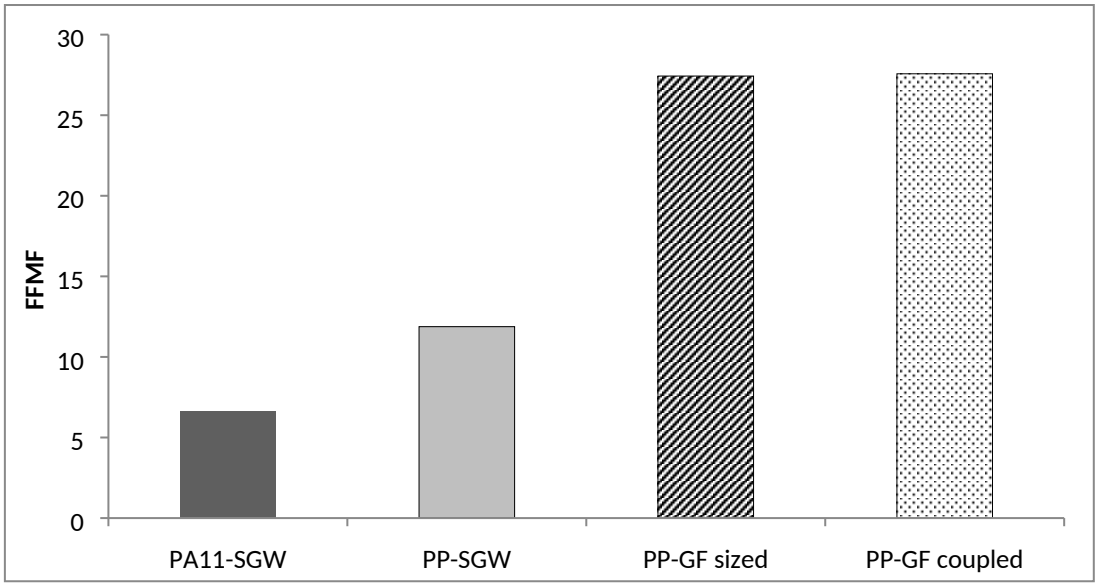

Figure 3. FFMF of PA11 and PP composites.

The observed differences between the *FTMF* and the *FFMF* indicated a lower performance of the SGW fibres in the flexural modulus of the PA11-based composites. These results were quite characteristic because due to the load configuration of the bending test, flexural values are usually higher than tensile ones. The Hirsch model was applied in order to calculate E_f^F and η_e. The results are shown in Table 2.

Table 2. Flexural modulus of PA11 composites

Fibre Content (%)	V^F	E_f^F (GPa)	η_e	η_l	η_0	α (°)
0	0.000	-	-	-	-	-
20	0.155	12.0	0.491	0.841	0.584	47.7
30	0.240	11.7	0.498	0.851	0.585	47.6
40	0.329	12.1	0.502	0.858	0.585	47.6
50	0.424	13.1	0.502	0.871	0.577	48.3
60	0.524	13.9	0.508	0.891	0.570	48.9
Mean	-	**12.6**	**0.500**	**0.862**	**0.580**	**48.0**
S.D.	-	**0.9**	**0.006**	**0.019**	**0.007**	**0.6**

The E_f^F of the SGW fibres rendered a mean value of 12.6MPa. The literature shows higher values for the same reinforcement used with PP [34]. Furthermore, the E_f^F of SGW fibre in PA11 was lower than the fibres intrinsic Young's modulus (E_t^F). This phenomena is opposite to the obtained in PP-SGW composites, where E_f^F was 1.35 times higher than the $E_t{}^F$ calculated using Hirsch model [34,39]. Although the different E_f^F, the obtained η_e rendered a mean value of 0.5. The results were similar to the η_e obtained in the tensile properties of PA11-SGW composites and other short-fibre composites using natural and man-made fibres, where the values ranged between 0.4-0.5 [21,34,40,41]. This result agreed with the *FFMF*, where a lower reinforcement effect of the fibre was observed for PA11. The η_l and η_0 were almost the same than the obtained in the study of the micromechanics of the tensile modulus for PA11-SGW composites [21]. Observing the higher values of the length efficiency factor in front of the orientation efficiency factor, a higher impact of the length of the reinforcement fibres in the η_e than its orientation was concluded. In addition, a mean orientation angle calculated as described in a previous work [21], was the similar to the obtained before for PA11-SGW tensile properties. There was a little difference from the 39.5º mean orientation angle the obtained from the micromechanics of the flexural strength. The difference of 9º was related with the cosinus form of the equation where little difference in the η_0 rendered high differences of the obtained angle.

Considering the obtained performance for tensile properties of PA11-SGW, a possible explanation for the low E_f^F obtained can be a lower impact of the reinforcement due to the fibres working poorly at compression. Bending test subjects the section of the specimens to tensile and compression loads. During the tensile strength analysis work, some scanning electronic microscope (SEM) micrographs showed the presence of voids in the material structure, mainly related with the slip-out of fibres when were submitted

to tensile stress [22]. Moreover a similar lower contribution of the fibre to the flexural strength was observed in PA11-SGW composites [42]. The adequate but not good interface of PA11-SGW can produce the apparition of some gaps during the bending test which could make the loaded fibres collapse, reducing the impact of the fibre in the flexural properties [43]. Thus, unlike short fibre reinforced polyolefin, the interface has a high impact on the stiffness of PA11-SGW composites. On the other hand, *Shibata S. et al.* [44] described the effect of the fibre compression on the Young's and flexural modulus in different natural fibre reinforce PP. It was found that a correct compression of the fibres rendered in better performance of the fibres inside the composite material. The poor work of SGW fibres inside the PA11-SGW composites can be also related with a no correct compression of the fibres which led to void volume in the composite material.

The void volume fraction was computed to establish its possible impact on the stiffness of the composites. V^m and V^F used in the Hirsch model were obtained from the densities of the phases. The density of the fibre (ρ^F) was not measured directly; it was back-calculated from the composite density (ρ^C) as:

$$\rho^C = \frac{W^m + W^F}{V^m + V^C} \quad [10]$$

Where W^m and W^F were the polymer and fibre weights, respectively. Volumes can be easily replaced by the relation between the weight and the density of each phase. It was observed that the density of SGW fibres was 1.401g/cc in PA11-SGW composites and 1.335g/cc in PP-SGW composites [39]. Considering that PP-SGW composites have a better interface due to the use of a coupling agent which stablishes covalent bonds with the fibres, there was an error in the calculation of the density of the PA11-SGW fibres.

The ρ^F of PP-SGW was used to compute V^F and the intrinsic flexural modulus of SGW were recomputed by using the Hirsch model. Nonetheless, the obtained values were not noticeably different from the original ones (E_f^F was 11.8 and η_e was 0.506). It was difficult to input the effect of the void volume in the ρ^C, as the air weight in the gaps was depreciable but not its volume. The void volume was considered as the difference in the V^F obtained using both densities (Table 5).

Table 2. Volume fractions of fibre and polymer matrix depending of the fibre density used and the volume of air estimated.

ρ^F= 1.401		ρ^F= 1.335		*Difference in volume*	*Percentage of void volume in the composite* (%)	*Percentage of void volume in the composite by Armioun et al. method* [36] (%)
V^F	V^m	V^F	V^m	V^{air}		
0.155	0.845	0.162	0.838	0.006	0.643	0.981
0.240	0.760	0.248	0.752	0.009	0.890	1.299
0.329	0.671	0.340	0.660	0.011	1.074	1.438
0.424	0.576	0.436	0.564	0.012	1.182	1.463
0.524	0.476	0.536	0.464	0.012	1.202	2.222

The percentage of void volume estimated increased when the fibre content increases up to a maximum of 1.20% of the total volume. Arminoun et al. [36] estimated the void volume in the PA11 composites as a relation between the theoretical and the experimental density of the composites. Applying their estimation and using 1.335g/cc as ρ^F, the obtained results increased. However, both results were lower than the reported in the literature, probably due to the different methods of composite compounding and injection conditions. This assumption was reinforced by the differences in the tensile strength results between the literature and the author's results [19,21,22].

279 Other authors obtained composites with different fibre compression rates, due to the
280 morphology of the fibre, that achieved differences in the modulus [28]. A different
281 compression performance in PP and PA11 matrices can be another explanation for the
282 obtained difference in the densit. Further researcher will be necessary to understand the
283 lower flexural stiffening impact of the reinforcement.

284 ## 4 CONCLUSIONS

285 In this work, the flexural modulus of PA11-SGW composites was analysed and a
286 micromechanics study was performed. The flexural modulus of the PA11-SGW
287 composites improved the PA11 matrix modulus. SGW fibres used as reinforcement
288 were correctly dispersed in the composite obtaining an enhancement of the modulus. A
289 composite with a 60% of SGW fibre content showed a 3.6 times higher flexural
290 modulus than PA11. Moreover, the minimum strain of the composites was 3.23% for
291 the 60% of fibre content.

292 The results were compared with PP-GF and PP-SGW composites. The PP-based
293 composites showed higher flexural moduli at the same fibre contents. It was necessary
294 to increase the fibre content up to 50% to obtain competitive results. PA11-SGW
295 composites with high content of fibre can replace PP-GF sized and coupled.
296 Nonetheless, the PA11-SGW composites modulus results are lower than the observed at
297 the same fibre contents for PP-SGW composites. A lower neat contribution of the SGW
298 fibre in the PA11-based composites was observed in the *FFMF*. This result differs from
299 the *FTMF* where no considerable differences were observed between PA11 and PP
300 composites reinforced with SGW. Hirsch model was applied to calculate the fibre's
301 intrinsic flexural modulus and the obtained value (12.6GPa) was lower than values
302 reported in the literature for SGW fibres. The η_e, η_l and η_0 were remained similar than in

303 the tensile modulus and it was observed a higher influence of the length of the fibres in
304 the flexural modulus of the composite material than the orientation of these fibres. The
305 flexural behaviour of PA11-SGW composites was related with the presence of voids in
306 the structure of the composites. This can prevent a correct behaviour of the
307 reinforcement under compression loads, leading to its collapse. An approximation of the
308 void volume was performed by the difference of the SGW fibre's density back-
309 calculated from PA11 and PP-based composites. The maximum void volume was
310 determined to be 1.2% of the total volume. Another methodology proposed in the
311 literature rendered to a maximum of 2.22% the void volume in the composites
312 materials.

313 ## 5 REFERENCES

314 [1] Bledzki AK, Franciszczak P, Osman Z, Elbadawi M. Polypropylene
315 biocomposites reinforced with softwood , abaca , jute , and kenaf fibers. Ind Crop
316 Prod 2015;70:91–9. doi:10.1016/j.indcrop.2015.03.013.

317 [2] Espigulé E, Vilaseca F, Espinach FX, Julian F, Mansouri N-E El, Mutjé P.
318 Biocomposites from Starch-based Biopolymer and Rape Fibers. Part II:
319 Stiffening, Flexural and Impact Strength, and Product Development. Curr Org
320 Chem 2013;17:1641–6.

321 [3] Granda LA, Espinach FX, Méndez JA, Vilaseca F, Delgado-Aguilar M, Mutjé P.
322 Semichemical fibres of Leucaena collinsii reinforced polypropylene composites:
323 Flexural characterisation, impact behaviour and water uptake properties. Compos
324 Part B Eng 2016;97:176–82. doi:10.1016/j.compositesb.2016.04.063.

325 [4] Singh VK, Bansal G, Negi P, Bisht A. Journal of Testing and Evaluation

Characterization of Flexural and Impact Strength of Jute/Almond Hybrid Biocomposite 2017;45. doi:10.1520/JTE20150414.

[5] Granda LA, Espinach FX, Méndez JA, Tresserras J, Delgado-Aguilar M, Mutjé P. Semichemical fibres of Leucaena collinsii reinforced polypropylene composites: Young's modulus analysis and fibre diameter effect on the stiffness. Compos Part B Eng 2016;92:332–7. doi:10.1016/j.compositesb.2016.02.023.

[6] Joshi S. V, Drzal L. T, Mohanty a. . K, Arora S. Are natural fiber composites environmentally superior to glass fiber reinforced composites? Compos Part A Appl Sci Manuf 2004;35:371–6. doi:10.1016/j.compositesa.2003.09.016.

[7] Bledzki AK, Faruk O, Sperber VE. Cars from Bio-Fibres. Macromol Mater Eng 2006;291:449–57. doi:10.1002/mame.200600113.

[8] Greenberg MI, Waksman J, Curtis J. Silicosis: A review. Dm Dis 2007;53:394–416. doi:10.1016/j.disamonth.2007.09.020.

[9] Faruk O, Bledzki AK, Fink HP, Sain M. Biocomposites reinforced with natural fibers: 2000-2010. Prog Polym Sci 2012;37:1552–96. doi:10.1016/j.progpolymsci.2012.04.003.

[10] Franco-Marquès E, Méndez JA, Pèlach MA, Vilaseca F, Bayer J, Mutjé P. Influence of coupling agents in the preparation of polypropylene composites reinforced with recycled fibers. Chem Eng J 2011;166:1170–8. doi:10.1016/j.cej.2010.12.031.

[11] Bledzki AK, Faruk O. Creep and impact properties of wood fibre-polypropylene composites: Influence of temperature and moisture content. Compos Sci Technol 2004;64:693–700. doi:10.1016/S0266-3538(03)00291-4.

[12] Aranberri-Askargorta I, Lampke T, Bismarck A. Wetting behavior of flax fibers as reinforcement for polypropylene. J Colloid Interface Sci 2003;263:580–9. doi:10.1016/S0021-9797(03)00294-7.

[13] Koronis G, Silva A, Fontul M. Green composites: A review of adequate materials for automotive applications. Compos Part B Eng 2013;44:120–7. doi:10.1016/j.compositesb.2012.07.004.

[14] Holbery J, Houston D. Natural-fiber-reinforced polymer composites in automotive applications. Jom 2006;58:80–6. doi:10.1007/s11837-006-0234-2.

[15] Alves C, Ferrão PMC, Silva a. J, Reis LG, Freitas M, Rodrigues LB, et al. Ecodesign of automotive components making use of natural jute fiber composites. J Clean Prod 2010;18:313–27. doi:10.1016/j.jclepro.2009.10.022.

[16] Arkema. Polyamide family 2017.

[17] Mancic L, Osman RFM, Costa AMLM, d'Almeida JRM, Marinkovic BA, Rizzo FC. Thermal and mechanical properties of polyamide 11 based composites reinforced with surface modified titanate nanotubes. Mater Des 2015;83:459–67. doi:10.1016/j.matdes.2015.06.059.

[18] Salazar A, Rico A, Rodríguez J, Segurado Escudero J, Seltzer R, Martin de la Escalera Cutillas F. Monotonic loading and fatigue response of a bio-based polyamide PA11 and a petrol-based polyamide PA12 manufactured by selective laser sintering. Eur Polym J 2014;59:36–45. doi:10.1016/j.eurpolymj.2014.07.016.

[19] Zierdt P, Theumer T, Kulkarni G, Däumlich V, Klehm J, Hirsch U, et al. Sustainable wood-plastic composites from bio-based polyamide 11 and

chemically modified beech fibers. Sustain Mater Technol 2015;6:6–14. doi:10.1016/j.susmat.2015.10.001.

[20] Oliver-Ortega H, Méndez JA, Mutjé P, Tarrés Q, Espinach FX, Ardanuy M. Evaluation of Thermal and Thermomechanical Behaviour of Bio-Based Polyamide 11 Based Composites Reinforced with Lignocellulosic Fibres. Polymers (Basel) 2017;9:522. doi:10.3390/polym9100522.

[21] Oliver-Ortega H, Granda LA, Espinach FX, Delgado-Aguilar M, Duran J, Mutjé P. Stiffness of bio-based polyamide 11 reinforced with softwood stone ground-wood fibres as an alternative to polypropylene-glass fibre composites. Eur Polym J 2016;84:481–9. doi:10.1016/j.eurpolymj.2016.09.062.

[22] Oliver-Ortega H, Granda LA, Espinach FX, Méndez JA, Julian F, Mutjé P. Tensile properties and micromechanical analysis of stone groundwood from softwood reinforced bio-based polyamide11 composites. Compos Sci Technol 2016;132:123–30. doi:10.1016/j.compscitech.2016.07.004.

[23] Bourmaud A, Le Duigou A, Gourier C, Baley C. Influence of processing temperature on mechanical performance of unidirectional polyamide 11-flax fibre composites. Ind Crops Prod 2016;84:151–65. doi:10.1016/j.indcrop.2016.02.007.

[24] Hirsch TJ. Modulus of Elasticity iof Concrete Affected by Elastic Moduli of Cement Paste Matrix and Aggregate. J Proc 1962;59:427–52.

[25] Kalaprasad G, Joseph K, Thomas S, Pavithran C. Theoretical modelling of tensile properties of short sisal fibre-reinforced low-density polyethylene composites. J Mater Sci 1997;32:4261–7. doi:10.1023/a:1018651218515.

[26] Sanomura Y, Kawamura M. Fiber Orientation Control of Short-Fiber Reinforced

Thermoplastics by Ram Extrusion. Polym Compos 2003;24:587–96. doi:10.1002/pc.10055.

[27] Fukuda H, Kawata K. On Young's modulus of short fibre composites. Fibre Sci Technol 1974;7:207–22.

[28] Shibata S, Cao Y, Fukumoto I. Flexural modulus of the unidirectional and random composites made from biodegradable resin and bamboo and kenaf fibres. Compos Part A Appl Sci Manuf 2008;39:640–6. doi:10.1016/j.compositesa.2007.10.021.

[29] López JP, Mutjé P, Angels Pèlach M, El Mansouri NE, Boufi S, Vilaseca F. Analysis of the tensile modulus of polypropylene composites reinforced with stone groundwood fibers. BioResources 2012;7:1310–23.

[30] Thomason JL. The influence of fibre properties on the properties of glass-fibre-reinforced polyamide 6,6. J Compos Mater 2000;34:158–72. doi:10.1177/002199830003400205.

[31] Cui Y, Lee S, Noruziaan B, Cheung M, Tao J. Fabrication and interfacial modification of wood/recycled plastic composite materials. Compos Part A Appl Sci Manuf 2008;39:655–61. doi:10.1016/j.compositesa.2007.10.017.

[32] Gironès J, Lopez JP, Vilaseca F, Bayer R, Herrera-Franco PJ, Mutjé P. Biocomposites from Musa textilis and polypropylene: Evaluation of flexural properties and impact strength. Compos Sci Technol 2011;71:122–8. doi:10.1016/j.compscitech.2010.10.012.

[33] Julian F, Méndez JA, Espinach FX, Verdaguer N, Mutje P, Vilaseca F. Bio-based composites from stone groundwood applied to new product development.

418 BioResources 2012;7:5829–42.

419 [34] López JP, Gironès J, Mendez JA, Pèlach MA, Vilaseca F, Mutjé P. Impact and
420 flexural properties of stone-ground wood pulp-reinforced polypropylene
421 composites. Polym Compos 2013;34:842–8. doi:10.1002/pc.22486.

422 [35] Méndez JA, Vilaseca F, Pèlach MA, López JP, Barberà L, Turon X, et al.
423 Evaluation of the reinforcing effect of ground wood pulp in the preparation of
424 polypropylene-based composites coupled with maleic anhydride grafted
425 polypropylene. J Appl Polym Sci 2007;105:3588–96. doi:10.1002/app.26426.

426 [36] Armioun S, Panthapulakkal S, Scheel J, Tjong J, Sain M. Sustainable and
427 lightweight biopolyamide hybrid composites for greener auto parts. Can J Chem
428 Eng 2016;94:2052–60. doi:10.1002/cjce.22609.

429 [37] Takeshi S, Kunio T, Masataka T, Akihiro I. Biocomposites Composed of
430 Polyamide 11 and Cellulose Nanofibers Pretreated with a Cationic Reagents. J
431 Soc Rheol 2017;45:39–47.

432 [38] Panaitescu DM, Frone AN, Nicolae C. Micro- and nano-mechanical
433 characterization of polyamide 11 and its composites containing cellulose
434 nanofibers. Eur Polym J 2013;49:3857–66. doi:10.1016/j.eurpolymj.2013.09.031.

435 [39] López JP, Méndez JA, Mansouri NE El, Mutjé P, Vilaseca F. Mean intrinsic
436 tensile properties of stone groundwood fibers from softwood. BioResources
437 2011;6:5037–49.

438 [40] Espinach FX, Delgado-Aguilar M, Puig J, Julian F, Boufi S, Mutjé P. Flexural
439 properties of fully biodegradable alpha-grass fibers reinforced starch-based
440 thermoplastics. Compos Part B Eng 2015;81:98–106.

doi:10.1016/j.compositesb.2015.07.004.

[41] Hashemi S. Hybridisation effect on flexural properties of single- and double-gated injection moulded acrylonitrile butadiene styrene (ABS) filled with short glass fibres and glass beads particles 2008:4811–9. doi:10.1007/s10853-008-2683-1.

[42] Oliver-Ortega H, Méndez JA, Reixach R, Espinach FX, Ardanuy M, Mutjé P. Towards More Sustainable Material Formulations: A Comparative Assessment of PA11-SGW Flexural Performance versus Oil-Based Composites. Polymers (Basel) 2018;10:440. doi:10.3390/polym10040440.

[43] Meek N, Penumadu D, Hosseinaei O, Harper D, Young S, Rials T. Synthesis and characterization of lignin carbon fi ber and composites. Compos Sci Technol 2016;137:60–8. doi:10.1016/j.compscitech.2016.10.016.

[44] Shibata S, Cao Y, Fukumoto I. Study of the flexural modulus of natural fiber/polypropylene composites by injection molding. J Appl Polym Sci 2006;100:911–7. doi:10.1002/app.22609.

2.6 Fully bio-based composites from PA11-SGW: Notable impact strength and water uptake

Enviado y en revisión en el *International Journal of Biological Macromolecules*. Factor de impacto 2016: 3,671. Posición 12 de 86 en Polymer Science. Primer cuartil.

Manuscript Details

Manuscript number	IJBIOMAC_2018_1585
Title	Fully bio-based composites from PA11-SGW: Notable impact strength and water uptake.
Article type	Research Paper

Abstract

Composite materials have attracted the attention of some industrial fields like due to their enhanced relative mechanical properties. Impact properties are essential to ensure the processability and engineering application of these materials. On the other hand, the plasticizing effect of water in polymer and polymer composites is critical for some applications. This effect worsens when a hydrophilic reinforcement is used. In this work, the impact and water uptake behaviour of totally bio-based composites from polyamide 11 (PA11) and lignocellulosic fibres of pine from a mechanical stone groundwood (SGW) process were studied. The impact resistance of PA11 and its composites were higher than expected, obtaining better results than common polyolefin-based results. The evaluated mechanical properties as like as the microphotographies showed an adequate interface. The water uptake test showed that PA11 had a non-Fickian behaviour and its composites a Fickian case I. Moreover, the maximum water absorbance was similar to SGW reinforced polypropylene.

Keywords	fully bio-based composites; Impact strength; Water uptake
Manuscript category	Carbohydrates, Natural Polyacids and Lignins

Corresponding Author	Helena Oliver-Ortega
Corresponding Author's Institution	University of Girona
Order of Authors	Helena Oliver-Ortega, José Alberto Méndez, Xavier Espinach, Quim Tarres, Monica Ardanuy, Pere Mutje

Suggested reviewers	sami boufi, Philippe Evon, Zeki Candan

Submission Files Included in this PDF

File Name [File Type]

cover letter.pdf [Cover Letter]

abstract.docx [Abstract]

manuscript.docx [Manuscript File]

Figures.docx [Figure]

Tables.docx [Table]

To view all the submission files, including those not included in the PDF, click on the manuscript title on your EVISE Homepage, then click 'Download zip file'.

Girona, April 9, 2018

Dear Editor,

Please find attached our manuscript for publication in International Journal of Biological Macromolecules:

Fully bio-based composites from PA11-SGW: Notable impact strength and water uptake.

By: H. Oliver-Ortega, J. A. Méndez, F.X. Espinach, Q. Tarrés, M. Ardanuy, P. Mutjé.

This work analyses the impact and water uptake of totally bio-based composites from stone groundwood fibres (SGW) and polyamide 11 (PA11). The results were totally unexpected showing better impact strength and similar water uptake behaviour than common PP-based composites. These results were obtained without the use of a coupling agent in the composite formulation.

Bio-based polyamides are promising matrices for composite production. PA11 is a 100% bio-based polyamide obtained from castor oil. Its small carbon footprint, low melting point, and mechanical properties made it an attractive matrix to be reinforced with SGW as greener alternative in the composite materials field.

The competitiveness of composite materials is usually studied through the tensile and flexural strength and stiffness. However, composites materials can be subjected to collisions during their lifespan and their response to the collisions it's crucial for some applications. In composites materials, the impact strength usually decreases with the increment of fibre content. The decrease can be mitigated by ensuring a good interface. On the other hand, it is well-known the plasticising effect of water in polymeric materials. Moreover, when a high hydrophilic reinforcement is used this process is accelerated.

We therefore believe that our work, as described in this manuscript, would be very much of interest to Scientifics. Our aim is to show the scientific community how they can benefit from the use of a new matrix with easily obtainable natural fibers, obtaining composite materials good mechanical properties and achieving a good interface without the necessity of a coupling agent.

We confirm that this manuscript has not been published elsewhere and is not under consideration by another journal, and all authors have approved the manuscript and agree with its submission to International Journal of Biological Macromolecules.

In case of any questions please do not hesitate to contact us anytime.

The corresponding author is

Helena Oliver Ortega

For all the authors.

Group LEPAMAP, Department of Chemical Engineering

Escola Politecnica Superior. Avda. Lluis Santalo, s/n, 17071 Girona, Spain

Phone : 34 972 419 889,

FAX +34 972 418 39

E-mail: helena.oliver@udg.edu

Fully bio-based composites from PA11-SGW: Notable impact strength and water uptake.

H. Oliver-Ortega[a*], J. A. Méndez[a], F.X. Espinach[b], Q. Tarrés[a], M. Ardanuy[c], P. Mutjé[a]

[a] Group LEPAMAP, Department of Chemical Engineering, University of Girona, C/M. Aurèlia Capmany, n°61, Girona 17071, Spain.

[b]Design, Development and Product Innovation, Dpt. of Organization, Business Management and Product Design, University of Girona, C/M. Aurèlia Capmany, n°61, Girona 17071, Spain.

[c] Departament de Ciència dels Materials i Enginyeria Metal.lúrgica, Secció Enginyeria Tèxtil, Universitat Politècnica de Catalunya

*Corresponding author

ABSTRACT

Composite materials have attracted the attention of some industrial fields like due to their enhanced relative mechanical properties. Impact properties are essential to ensure the processability and engineering application of these materials. On the other hand, the plasticizing effect of water in polymer and polymer composites is critical for some applications. This effect worsens when a hydrophilic reinforcement is used. In this work, the impact and water uptake behaviour of totally bio-based composites from polyamide 11 (PA11) and lignocellulosic fibres of pine from a mechanical stone groundwood (SGW) process were studied. The impact resistance of PA11 and its composites were higher than expected, obtaining better results than common polyolefin-based results. The evaluated mechanical properties as like as the microphotographies showed an adequate interface. The water uptake test showed that PA11 had a non-Fickian behaviour and its composites a Fickian case I. Moreover, the maximum water absorbance was similar to SGW reinforced polypropylene.

Fully bio-based composites from PA11-SGW: Notable impact strength and water uptake.

H. Oliver-Ortega[a*], J. A. Méndez[a], F.X. Espinach[b], Q. Tarrés[a], M. Ardanuy[c], P. Mutjé[a]

[a] Group LEPAMAP, Department of Chemical Engineering, University of Girona, C/M. Aurèlia Capmany, n°61, Girona 17071, Spain.

[b]Design, Development and Product Innovation, Dpt. of Organization, Business Management and Product Design, University of Girona, C/M. Aurèlia Capmany, n°61, Girona 17071, Spain.

[c] Departament de Ciència dels Materials i Enginyeria Metal.lúrgica, Secció Enginyeria Tèxtil, Universitat Politècnica de Catalunya

*Corresponding author

ABSTRACT

Composite materials have attracted the attention of some industrial fields like due to their enhanced relative mechanical properties. Impact properties are essential to ensure the processability and engineering application of these materials. On the other hand, the plasticizing effect of water in polymer and polymer composites is critical for some applications. This effect worsens when a hydrophilic reinforcement is used. In this work, the impact and water uptake behaviour of totally bio-based composites from polyamide 11 (PA11) and lignocellulosic fibres of pine from a mechanical stone groundwood (SGW) process were studied. The impact resistance of PA11 and its composites were higher than expected, obtaining better results than common polyolefin-based results. The evaluated mechanical properties as like as the microphotographies showed an adequate interface. The water uptake test showed that PA11 had a non-Fickian behaviour and its composites a Fickian case I. Moreover, the maximum water absorbance was similar to SGW reinforced polypropylene.

KEYWORDS: Fully bio-based composites; Impact strength; Water uptake

1 INTRODUCTION

Materials like polymers and polymer composites able to show competitive mechanical properties and lower densities have attracted the interest of industries like automotive and construction. A clear example are fibre reinforced polymers. These materials show high strength and stiffness, allowing higher loads and showing lower deformations than the neat polymer under normal use conditions. The most common properties used to evaluate the possible application of these materials are their strength and stiffness [1], and hence lots of papers evaluate these properties under flexural or tensile conditions.

Besides, in most of the applications, the composites can be subjected to collisions during their lifespan, and the response of the materials to such collisions has security concerns. Thus, knowing the impact behaviour of the materials is of crucial importance for the industries. The impact behaviour of a composite material is mainly influenced by the reinforcement content and the quality of the reinforcement-matrix interphase [2]. Usually, the impact strength decreases with the percentage of reinforcement [3]. This decrease can be balanced with a good fibre-matrix interphase allowing a good transmission and dissipation of the energy [4,5].

Automotive and construction industries are interested in materials with better relative properties, but also in greener or more sustainable ones. In this sense, bio-based polymers and reinforcements are very interesting options. Polyamide 11 (PA11), obtained from castor oil, with comparatively high mechanical performance, good chemical resistance and durability, is a promising alternative to oil-based polymers in composite materials [6–8]. Moreover, previous studies reported that PA11 reinforced with natural fibres showed competitive mechanical and thermomechanical performance with respect to commodity polymers like polypropylene, without using coupling agents [9,10]. Unlike polyolefin, PA11 can stablish H-

bonds with the cellulosic fibres allowing obtaining a good interface [11]. This interface can be strong enough to allow a good energy transfer under impact loading, but, to the best knowledge of the authors, the literature about this subject is scarce and generic [9].

On the other hand, the applications for automotive or construction purposes involves uses under humid environments. The reduction of the mechanical properties of polymeric materials due to moisture adsorption is well stablished in the literature [12]. This is because the small size and mobility of water molecules facilitates their diffusion to the amorphous phase of the polymers. Moreover, the polar groups in the polymer chains interact with water [13,14]. In the case of natural fibre reinforced composites, the hydrophilic behaviour of natural fibres accelerates the process due to their high capacity to absorb water [15].

Polyamides are hygroscopic polymers due to the presence of amide groups [16]. Nonetheless, among polyamides, PA11 has a low hydrophilic behaviour due to its lower content of amide groups [17]. The relatively high glass transition temperature (T_g) of PA11, around 50ºC, can also contribute to inhibit its water absorption at room temperature due to the low mobility of PA11 chains at temperatures under the T_g. Moreover, the stiffness enhancement of the composite materials provided by the reinforcing fibres can decrease the mobility, reducing also the diffusion of the water molecules in the material.

In this work, the flexural modulus, the impact properties and the water absorption behaviour of PA11 reinforced with different contents of stone groundwood fibres (SGW) are investigated. The impact properties were evaluated using Charpy impact energy specimens. Micromechanical models were used to stablish the energy devoted to create the fracture and its propagation in the impact test. The water absorption behaviour was analysed determining the water uptake of the composite materials under water immersion. Two different water

immersion temperatures were studied and the kinetic parameters of the absorption phenomena were determined.

2 MATERIALS AND METHODS

Materials

Polyamide 11 (Rilsan® BMNO TL) used as bio-based matrix was kindly provided by Arkema S.A. (Colombes, France). Its density is 1.03 g/cm3 and its melt volumetric index is 11 cc/10 min at 235ºC and 2.16 kg

The mechanical pulp used as reinforcement (SGW), supplied by Zubialde S.A. (Aizarnazabal, Spain), was obtained from pine fibres through a stone groundwood process.

Composite compounding

Composites with reinforcement content ranging from 20 to 60% were produced in a Gelimat Kinetic Mixer. The compounding and injection processes have been described in previous works [6,11]. Specimens for the Charpy impact test were obtained by injection-molding following the ASTM D3641 standard. For the water uptake test, tensile samples Type I described in the ASTM D638 standard were also obtained by injection-molding. The injection process was performed in a Meteor-40 injection- molding machine (Mateu&Solé. Barcelona, Spain).

All the samples were conditioned in a climatic chamber at 23ºC and 50%RH according to ISO D618 previously to the test.

Impact characterization

Charpy impact tests were performed on notched and un-notched specimens using a hammer Resil 5,5 Ceast instrument (Pianezza, Italy) following ISO 178 standard. The absorbed

energy of the material during crack formation and fracture propagation was also determined for the un-notched samples. For each test, five specimens were tested.

Scanning electron microscopy (SEM)

Micrographs of the fractured surface of the impact test samples were obtained by scanning electron microscopy (SEM). The images were taken in a Zeiss DSM 960A and the sample preparation required coating them with gold.

Hydrophilic behaviour: Water contact angle

The hydrophilic behaviours of the studied PA11 and PA11 reinforced with 20, 50 and 60% of SGW were determined by means of water contact angle. A DSSA25 drop-shape analyser from Krüss GmbH (Germany) was used to observe the angle and was controlled with the Krüss Advance Software. Two measurements each second during one minute were predetermined for each sample and the assay was performed at room temperature.

Immersion water uptake test

The composites were dried at 105ºC for 2 h before their immersion to remove any residual moisture. Afterwards, the samples were immersed in distilled water. Two sets were prepared, one at 23ºC and other at 40ºC. The specimens remained under immersion until its saturation. The water uptake was calculated by weight difference of the samples and the saturation point was determined by constant weight of the samples.

3 RESULTS AND DISCUSSION

Impact strength

Impact strength was obtained by means of Charpy test. In this test a hammer is thrown at a measured height to a sample bar. The difference in height, or in potential energy, is translated

as the transferred energy to the sample. In a composite material, this absorbed energy is dissipated by; the work necessary to create a fracture, by the different phases of the composite and by the interface created by both materials, as shown in Equation 3 [18]:

$$w \approx w_i + w_f + w_m + \sum w_{fm} \quad [1]$$

where w is the total work of fracture, w_i, w_f and w_m are the work dissipated by the creation of the fracture by the fibre and the matrix, respectively, and finally, w_{fm} is the mechanical work of the interactions between fibre and matrix (physical interactions, chemical bonds, etc.). The difference between the results of the notched and un-notched samples allows the calculation of the w_i.

Table 1 shows the experimental results of PA11 and PA11-SGW composites for notched and un-notched samples. PA11 matrix showed a lower Charpy impact strength than other thermoplastics like PP [4,18]. This difference with PP can be principally related to the glass transition temperature (T_g) of PA11. It is well-known that semi-crystalline polymers have higher impact strengths when the test is performed at temperatures above their T_g [19]. PA11's T_g has been determined around 50ºC while PP is around -10ºC.

TABLE 1

As expected, the Charpy impact strength decreased when the fibre content increased. It should be noted that the strength of the interface between the polymer matrix and the fibres defines the behaviour of the fracture. The quality of the interface and the dispersion of the filler has shown to be significant in other fibre reinforced thermoplastics like PP, where the impact strength values increased by the effect of coupling agents [4,20–22]. Moreover, the presence of SGW fibres contributes to further limiting the mobility of the PA11 chains, making the composites more fragile. In an ongoing research it was found that this

phenomenon occurred also when the temperature was raised due the stiffness of the fibres. This effect was also observed in the tensile properties of PA11-SGW composites, where the toughness of the material decreased showing a similar tendency [11]. However, the obtained results were better than those obtained for coupled cellulose reinforced PP composites [4,18,23], PP reinforced with glass fibre (GF) [22] and some polyamides reinforced with GF [24]. This result can be related with the achievement of a well-balanced fibre-matrix interaction on PA11/SGW system even avoiding the use of coupling agents.

SEM pictures of the PA11+50%SGW composite tested with Charpy impact test are presented in Figure 1. Although some voids are observed in the microphotographies, they were mainly related with slip-out of fibres during the impact. Nevertheless, broken fibres are also found (Figure 1) indicating a not perfect but suitable interface between PA11 and SGW fibres [9,11,25].

FIGURE 1

The addition of SGW fibres in the PA11 decreased the total work of fracture to the 32% of the work of the matrix for the un-notched samples (Eq. 1). However, in the case of the notched samples, the work was reduced 24% versus the matrix, because the higher part of the energy was consumed during the fracture production (w_i, value), and also because polyamides are notch sensitive [26,27]. This explained the lower results of the notched samples of the PA11 and the reduction in the composites materials due to the low energy dissipated by the matrix and the interface interactions.

Values of w_i are represented in Figure 2. As shown, the w_i value decreased when fibre content was increased. Nonetheless, it was observed that the tendency was logarithmic instead of linear. This indicated that the addition of SGW had higher impact than the amount of SGW in the composite material. The presence of SGW in the PA11 produced a discontinuity in the

PA11. Thus, higher contents will produce more discontinuities in the polymer matrix. Nonetheless, the w_i values in the composite materials decreased linearly with a low slope. The addition of 20% of SGW reduced the work 46%. Meanwhile an increasing the SGW up to 40% led to a reduction of 58%. The addition of 20% more in the composite material only represented an additional loss of 12%. These results indicated a higher impact produced by low fibre contents.

FIGURE 2

Hydrophility and Water Uptake behaviour at 23ºC and 40ºC

It is generally accepted that water acts as plasticizer in polymers. Water penetrates in the amorphous phases of the polymer [28] affecting their mobility. Moreover, in some polar polymers like polyamide 6 (PA6) the crystalline phase can be also affected by water absorption [29,30]. Polyamides have higher polar character than other polymers due to the presence of amide bonds. The capacity of the amide group to stablish H-bonds leads to PA to absorb higher water that other polymer matrixes since it is necessary to consider not only the adsorption phenomena on the amorphous phase, also the absorption due the H-bond capacity.

On the other hand, although lignocellulosic fibres have lower hydrophilic behaviour than pure cellulose, due to lignin presence in the surface of the fibre, their capacity to adsorb/desorb water is huge compared with a PA11 matrix. Then, it is expected that increments of fibre contents in the composite will increase the hydrophilic behaviour of the PA11-SGW composites. One simple technique to determine this hydrophilic behaviour is to measure the water contact angle. The mean contact angle determined is shown in Table 2.

TABLE 2

PA11 achieved an average water contact angle around 77.1º, indicating its hydrophilic behaviour, since hydrophobic materials are considered for angles around 100º [31]. In the case of its composites the water contact angle decreased until around 68.8º and 65.9º for the composites containing 20 and 50% SGW, respectively. The unexpected higher value found for PA11+60%SGW composite (69.3º) can be related with a lower homogeneity of the samples making difficult its correct characterization.

The values of contact angle are an average of the contact angles observed during 60 seconds. Although this angle reduced slightly with the time, due to the polarity of the samples, it was possible to determine the wetting energy (E_w) using the average angle obtained during the measure. The E_w is defined as the energy required to wet the material and is considered to be exothermic. E_w was calculated from the contact angle [32] as $E_w = \gamma \cos \theta$, been θ the contact angle and γ the surface tension of water (72.8 mJ/m^2). The E_w values obtained for the PA11 and its composites are shown in Table 2. As expected, E_w increased at lower angles due to the exothermic behaviour of the process.

The water uptake tests were performed at room temperature (23ºC) and at 40ºC. Although the T_g of the PA11 and composites was determined around 50ºC, the start of the chains mobility in the modulus was around 40ºC. The water uptake profiles obtained from the water uptake test at 23ºC and 40ºC performed were similar to the obtained for other natural fibre reinforced thermoplastic polymers [15,33,34]. The water uptake capacities increased with the fibre content in the composite material. The samples with higher fibre quantity needed less time to reach saturation, probably due to the higher content of the lignocellulosic reinforcement. In the case of the 40ºC the saturation time was also reduced due to the higher mobility of the amorphous chains of PA11 matrix from the beginning of the test, enhancing the mobility of the water molecules. Moreover, their higher content in the composite implies a higher fibre presence on the surface of the specimen which can facilitate the dispersion of the water

molecules throw the material. Nonetheless, the literature reports lower water uptake values for composites with PA11 at similar beech fibre contents [9]. This difference can be related with the aspect ratio and thus, the higher specific surface of SGW fibres with respect to beech fibres, leading to higher availability of the hydroxyl groups of cellulose, and, hence higher interaction with the water molecules. On the other hand, the water uptake at the saturation point (M_∞) observed for PA11 and PP reinforced with SGW at 50% of reinforcement content was almost the same [33]. The result was unexpected due the higher hydrophilicity of PA11 and the use of a coupling agent in the PP-SGW formulation. At 20% of SGW content, the result in PA11 is slightly superior and similar to the PP-SGW composite without the use of a coupling agent. Nonetheless, similar results were observed in other PP-cellulose reinforced composites [15].

The water uptake kinetics can be modelled by Fick's dispersion theory. The experimental results can be linearized by the logarithm of the water uptake (M_t) divided by the M_∞, represented regarding the logarithm of the time (t). The regressions of the results allows obtaining Equation 2:

$$\log\left(\frac{M_t}{M_\infty}\right) = n\log(t) + \log K \qquad [2]$$

Where n and K are kinetic constants. Another important parameter in the kinetics model is the diffusion coefficient (D), obtained from the Fick's Law and related with the ability of the solvent, in this case water, to penetrate in solid materials. As higher is D value, higher is the facility of the water to penetrate throws the solid. D was calculated at low times of immersion, when $M_t/M_\infty \leq 0.5$, as:

$$\frac{M_t}{M_\infty} = \frac{4}{L}\cdot\left(\frac{D}{\pi}\right)^{1/2}\cdot t^{1/2} \qquad [3]$$

Where *L* are the thickness of the studied samples. The measured values of these constants for 23 and 40ºC are shown in Table 3.

TABLE 3

The *n* values of the PA11 and composites materials at 23 and 40ºC increased with the fibre content of composite material. However, no considerable differences were obtained between both temperatures. The values of *n,* lower than 0.5, indicated a pseudo-Fickian dispersion case for PA11 and PA11+20%SGW composites [35]. Nonetheless, increasing the fibre contents in the composite materials, the PA11+50%SGW and PA11+60%SGW, produced a shift in the Pseudo-Fickian behaviour to a Fickian dispersion case I [15]. A Fickian dispersion case I is related with solvents with lower mobility than polymers chains and a pseudo-Fickian behaviour is related with a similar mobility of the solvent and the polymer chains. The *n* value is related with the time necessary to reach the saturation point. The slightly differences obtained in the *n* values at both temperatures indicated a high mobility of the PA11 chains at low temperatures, probably produced by the high diffusion of the water in the PA11, enhanced by the polar groups. Its decrease when the fibre contents increased can be related to the stiffness of the fibres, inhibiting the polymer chains mobility. On the other hand, *K* is a constant related with the system. The increment of the temperature of the system was reflected as an increment of *K* at 40ºC. The presence of the fibres reduced this constant around 50% in the composites at 23ºC and around 66% at 40ºC, regarding the PA11 constant. A clear dependence of the fibre content on *K* was not obtained, although it can be determined that the reduction of the PA11 chains due to the fibres presence had an impact in this constant.

The *D* results obtained for PA11 and its composites showed, in both temperatures, a lower ability of the solvent to penetrate in the 20 and 50% of reinforced composites regarding

PA11. This is in concordance with the *n* values obtained and the shift from to pseudo-Fickian to Fickian diffusion. The lower *D* values in the 20 and 50% of SGW reinforced composites were related with the lower mobility of the PA11 chains inhibited by the lignocellulosic reinforcement. Moreover, the H-bond interaction between the fibres and the PA11 can also have some negative effect in the diffusion of the water through the composite. As expected, the *D* values increased with the temperature due to the enhancement in the mobility of PA11 chains with temperature. Nonetheless, the higher effect of the temperature was obtained for pure PA11 sample, where the *D* value increased up to 5 times. In the case of the PA11+20%SGW and PA11+50%SGW, the increased was moderate. Thus, a positive impact was obtained in the composite materials by the fibres, even at temperatures near the T_g of the polymeric phase. Besides, the *D* results were in the same range than the obtained for PA11 and other polyamides in the literature [28,36].

Otherwise, the water diffusion through polymer materials is considered to be in the amorphous part of the polymer [28]. Nonetheless, the effect of the water in the crystalline part it is not well stablished [13]. In this sense, the crystalline structure of the PA11 can have some effect in the absorption and diffusion processes. These processes can be also affected by the different structures of the PA11, which depend on the H-bond disposition in the space between the PA11 chains. In the studied samples, the predominant phase was the δ' [37] and other phases showed to be more thermodynamically stable [38] which can reduce its *D* coefficient. Nevertheless, more research is required to stablish a possible relation. Another remark is the similar

The M_∞ of the materials were slightly higher at 40ºC. These increments were related with the higher temperature of the process. It can be expected that higher M_∞ had to be obtained due to the enhancement of the mobility by the plasticise effect of the water molecules which decreased the T_g of the materials [36].

In the case of the PA11+60%SGW composite, a higher value of D than PA11 matrix was obtained at 23ºC. This was related with the high content of fibres and the poor wettability of the fibres in the composites, previously observed [11]. A similar effect was observed in PP without the use of a coupling agent were higher D and M_∞ were obtained, due to the PP not wetting correctly the fibre [33]. At 40ºC, the D was lower than PA11 but around two times the obtained with the 20 and 50% reinforced composites. This effect was related with the enhancement in the mobility of the amorphous chains of the PA11 while in the composite material it is more limited due to the stiffness of the SGW fibres. Nevertheless, the presence of voids in the material produced its higher D regarding the other composites.

As expected, the D increased along with the temperature. In Fickian dispersion cases, and also can be applied in pseudo-Fickian causes, the dependency of D regarding the temperature followed an Arrhenius law [15]:

$$D = D_0 e^{\left(\frac{-E_d}{RT}\right)} \quad [4]$$

where D_0 is the permeability index, E_d is the starting energy for the diffusion process, T is the temperature and R is the gas constant. The linearization of the Eq. 4 allowed calculating the E_d value of PA11 and their composites (Table 4).

TABLE 4

The E_d value found for PA11 is in agreement with previous studies with PA11 and other PA [39,40]. A reduction in the E_d was observed in the composite materials regarding the PA11 matrix. This result can be expected and it is related with hydrophilic behaviour of the fibre, its higher presence in the surface of the specimens and the reduction of the polymeric matrix content in the composite, which can facilitate the beginning of the diffusion process.

On the other hand, the E_d obtained for PA11 was lower than the activation energy (E_a) calculated for the hydrolysis of PA11 [40–42], indicating no degradation process of the PA11 used in the composites materials at the studied temperatures. This was expected, and the literature reports that the hydrolysis degradation only occurs for temperatures higher than 90ºC. Besides, the fibre content it's not supposed to have any effect in the PA11 hydrolysis, at least at the studied temperatures. Nonetheless, more research, at temperatures ranging from 90 to140ºC, where hydrolysis of the amide group for PA11 is observed, has to be done to ensure any effect of the fibre in the hydrolysis of PA11.

4 CONCLUSIONS

Impact strength and water uptake behaviour of PA11 and PA11-SGW were analysed in this work. The un-notched and notched Charpy test showed a reduction of the PA11 impact strength due to the addition of reinforcements. The interface created between the PA11 matrix and SGW fibres was the point more favourable to be broken during the impact. This is in concordance with the slip-out fibres observed in the SEM photography's.

The difference between the un-notch and notch samples led to determine the necessary work to produce a fracture in the material. PA11 shows high strength although the test was carried out on a temperature lower than its T_g. The obtained results were higher than commercial fibre reinforced thermoplastics. Nonetheless, the matrix and the composites samples showed low resistance to the propagation of a fracture. This was related with PA's notch-sensitive behaviour and the discontinuity produced in the matrix by the fibres.

The hydrophilicity of PA11 and PA11-SGW composites was studied by their water contact angle. The results showed a hydrophilic behaviour for the PA11 which was enhanced by the addition of SGW fibres. The E_w reflected a more exothermic value for the composites materials in accordance with the observed contact angle.

The water uptake tests were carried out at room temperature (23ºC) and at 40ºC, a temperature near the T_g of PA11. An increase of the M_∞ was observed when the fibre content was increased, caused by the hydrophilic behaviour of lignocellulosic fibres. Although the hydrophilicity of PA11, the M_∞ observed for PA11 and PP composites were similar at high fibre content. The model of the water uptake curve led to determine some Fick's parameters. The PA11 matrix showed a pseudo-Fickian diffusion behaviour while the composites materials shifted to a Fickian one. The same behaviour was obtained at 23 and 40ºC. D showed lower values for PA11+20%SGW and PA11+50%SGW composites than the obtained for PA11, again for both temperatures. This was related with the reduced mobility of the polymer chains due to the fibres stiffness. As expected, the D coefficient was increased at 40ºC regarding the 23ºC value. However, enhancement of the diffusion process was reduced by the fibres presence. In the case of PA11+60%SGW composite, high D values were obtained because fibre was not correctly wetted by the matrix and some voids were identified, enhancing the diffusion. Finally, the E_d for PA11 and PA11-SGW composites were determined. In the composites material their energy was reduced favouring the start of the process.

5 AKNOWLEDGEMENTS

The authors hereby thank Arkema for kindly supplying the polyamide 11 which was used in this work and especially to Dr. Patrick Dang (Arkema France) and Mr. Pep Català (Arkema Spain).

6 BIBLIOGRAPHY

[1] V.N. Hristov, R. Lach, W. Grellmann, Impact fracture behavior of modified polypropylene/wood fiber composites, Polym. Test. 23 (2004) 581–589. doi:10.1016/j.polymertesting.2003.10.011.

[2] S. Shibata, Y. Cao, I. Fukumoto, Study of the flexural modulus of natural fiber/polypropylene composites by injection molding, J. Appl. Polym. Sci. 100 (2006) 911–917. doi:10.1002/app.22609.

[3] J.P. López, J. Gironés, J. Alberto, N.E. El Mansouri, M. Llop, P. Mutjé, F. Vilaseca, Stone-ground wood pulp-reinforced polypropylene composites: Water uptake and thermal properties, BioResources. 7 (2012) 5478–5487.

[4] J.P. López, J. Gironès, J.A. Mendez, M.A. Pèlach, F. Vilaseca, P. Mutjé, Impact and flexural properties of stone-ground wood pulp-reinforced polypropylene composites, Polym. Compos. 34 (2013) 842–848. doi:10.1002/pc.22486.

[5] K. Oksman, C. Clemons, Mechanical properties and morphology of impact modified polypropylene-wood flour composites, J. Appl. Polym. Sci. 67 (1998) 1503–1513. doi:10.1002/(SICI)1097-4628(19980228)67:9<1503::AID-APP1>3.0.CO;2-H.

[6] H. Oliver-Ortega, L.A. Granda, F.X. Espinach, M. Delgado-Aguilar, J. Duran, P. Mutjé, Stiffness of bio-based polyamide 11 reinforced with softwood stone ground-wood fibres as an alternative to polypropylene-glass fibre composites, Eur. Polym. J. 84 (2016) 481–489. doi:10.1016/j.eurpolymj.2016.09.062.

[7] L. Mancic, P.I. Pontón, S. Letichevsky, A.M. Costa, B.A. Marinkovic, F.C. Rizzo, Application of silane grafted titanate nanotubes in reinforcing of polyamide 11 composites, Compos. Part B Eng. 93 (2016) 153–162. doi:10.1016/j.compositesb.2016.03.028.

[8] D.M. Panaitescu, R.A. Gabor, A.N. Frone, E. Vasile, Influence of Thermal Treatment on Mechanical and Morphological Characteristics of Polyamide 11/Cellulose Nanofiber Nanocomposites, J. Nanomater. 2015 (2015) 1–11. doi:10.1155/2015/136204.

[9] P. Zierdt, T. Theumer, G. Kulkarni, V. Däumlich, J. Klehm, U. Hirsch, A. Weber, Sustainable wood-plastic composites from bio-based polyamide 11 and chemically modified beech fibers, Sustain. Mater. Technol. 6 (2015) 6–14. doi:10.1016/j.susmat.2015.10.001.

[10] L. Marrot, A. Bourmaud, P. Bono, C. Baley, Multi-scale study of the adhesion between flax fibers and biobased thermoset matrices, Mater. Des. 62 (2014) 47–56. doi:10.1016/j.matdes.2014.04.087.

[11] H. Oliver-Ortega, L.A. Granda, F.X. Espinach, J.A. Méndez, F. Julian, P. Mutjé, Tensile properties and micromechanical analysis of stone groundwood from softwood reinforced bio-based polyamide11 composites, Compos. Sci. Technol. 132 (2016) 123–130. doi:10.1016/j.compscitech.2016.07.004.

[12] S. Acierno, P. Van Puyvelde, Rheological behavior of polyamide 11 with varying initial moisture content, J. Appl. Polym. Sci. 97 (2005) 666–670. doi:10.1002/app.21810.

[13] V. Miri, O. Persyn, J.-M. Lefebvre, R. Seguela, Effect of water absorption on the plastic deformation behavior of nylon 6, Eur. Polym. J. 45 (2009) 757–762. doi:10.1016/j.eurpolymj.2008.12.008.

[14] I. Merdas, F. Thominette, A. Tcharkhtchi, J. Verdu, Factors governing water absorption by composite matrices, Compos. Sci. Technol. 62 (2002) 487–492. doi:10.1016/S0266-3538(01)00138-5.

[15] A. Espert, F. Vilaplana, S. Karlsson, Comparison of water absorption in natural cellulosic fibres from wood and one-year crops in polypropylene composites and its influence on their mechanical properties, Compos. Part A Appl. Sci. Manuf. 35 (2004) 1267–1276. doi:10.1016/j.compositesa.2004.04.004.

[16] A. Salazar, A. Rico, J. Rodríguez, J. Segurado Escudero, R. Seltzer, F. Martin de la Escalera Cutillas, Monotonic loading and fatigue response of a bio-based polyamide PA11 and a petrol-based polyamide PA12 manufactured by selective laser sintering, Eur. Polym. J. 59 (2014) 36–45. doi:10.1016/j.eurpolymj.2014.07.016.

[17] Arkema, Polyamide family, (2017).

[18] L.A. Granda, F.X. Espinach, J.A. Méndez, F. Vilaseca, M. Delgado-Aguilar, P. Mutjé, Semichemical fibres of Leucaena collinsii reinforced polypropylene composites: Flexural characterisation, impact behaviour and water uptake properties, Compos. Part B Eng. 97 (2016) 176–182. doi:10.1016/j.compositesb.2016.04.063.

[19] D.W. Van Krevelen, K. Te Nijenhuis, Product Properties (I): Mechanical Behaviour and Failure, in: Prop. Polym., Elsevier, 2009: pp. 819–845. doi:10.1016/B978-0-08-054819-7.00025-X.

[20] Z. Liu, Effects of coupling agent and morphology on the impact strength of high density polyethylene/CaCO3 composites, Polymer (Guildf). 43 (2002) 2501–2506. doi:10.1016/S0032-3861(02)00048-4.

[21] L. Cilleruelo, E. Lafranche, P. Krawczak, P. Pardo, P. Lucas, Injection moulding of long glass fibre reinforced poly(ethylene terephtalate): Influence of carbon black and nucleating agents on impact properties, Express Polym. Lett. 6 (2012) 706–718. doi:10.3144/expresspolymlett.2012.76.

[22] F. Julian, J.A. Méndez, F.X. Espinach, N. Verdaguer, P. Mutje, F. Vilaseca, Bio-based composites from stone groundwood applied to new product development, BioResources. 7 (2012) 5829–5842.

[23] J. Gironès, J.P. Lopez, F. Vilaseca, R. Bayer, P.J. Herrera-Franco, P. Mutjé, Biocomposites from Musa textilis and polypropylene: Evaluation of flexural properties and impact strength, Compos. Sci. Technol. 71 (2011) 122–128. doi:10.1016/j.compscitech.2010.10.012.

[24] A.K. Bledzki, M. Feldmann, Bio-based polyamides reinforced with cellulosic fibres - Processing and properties, Compos. Sci. Technol. 100 (2014) 113–120.

[25] A. Le Duigou, A. Bourmaud, C. Gourier, C. Baley, Multi-scale shear properties of flax fibre reinforced polyamide 11 biocomposites, Compos. Part A Appl. Sci. Manuf. 85 (2016) 123–129. doi:10.1016/j.compositesa.2016.03.014.

[26] M. Feldmann, A.K. Bledzki, Bio-based polyamides reinforced with cellulosic fibres – Processing and properties, Compos. Sci. Technol. 100 (2014) 113–120. doi:10.1016/j.compscitech.2014.06.008.

[27] M. Mehrabzadeh, P. Science, N.S. Wales, Impact Modification of Polyamid 11, (n.d.) 2305–2314.

[28] P. Wu, H.W. Siesler, Fourier transform NIR study of liquid diffusion processes in Nylon 11 films: Comparison of water with alcohols, Chem. Mater. 15 (2003) 2752–2756. doi:10.1021/cm0208307.

[29] I. Boukal, Effect of water on the mechanism of deformation of nylon 6, J. Appl. Polym. Sci. 11 (1967) 1483–1494. doi:10.1002/app.1967.070110811.

[30] G. Hinrichsen, The role of water in polyamides, Colloid Polym. Sci. 256 (1978) 9–14. doi:10.1007/BF01746685.

[31] A. Gandini, Polymers from renewable resources: A challenge for the future of macromolecular materials, Macromolecules. 41 (2008) 9491–9504. doi:10.1021/ma801735u.

[32] J.-W. Rhim, K. a. Mohanty, S.P. Singh, P.K.W. Ng, Preparation and Properties of Biodegradable Multilayer Films Based on Soy Protein Isolate and Poly(lactide), Ind. Eng. Chem. Res. 45 (2006) 3059–3066. doi:10.1021/ie051207+.

[33] J.P. López, J. Gironés, J.A. Méndez, N.E. El Mansouri, M. Llop, P. Mutjé, F. Vilaseca, Stone-ground wood pulp-reinforced polypropylene composites: Water uptake and thermal properties, BioResources. 7 (2012) 5478–5487.

[34] J.. Lagarón, E. Giménez, R. Gavara, J.. Saura, E. Gime, Study of the influence of water sorption in pure components and binary blends of high barrier ethylene–vinyl alcohol copolymer and amorphous polyamide and nylon-containing ionomer, Polymer (Guildf). 42 (2001) 9531–9540. doi:10.1016/S0032-3861(01)00496-7.

[35] H. Ventura, J. Claramunt, M.A. Rodríguez-Pérez, M. Ardanuy, Effects of hydrothermal aging on the water uptake and tensile properties of PHB/flax fabric biocomposites, Polym. Degrad. Stab. 142 (2017) 129–138. doi:10.1016/j.polymdegradstab.2017.06.003.

[36] N.J.W. Reuvers, H.P. Huinink, H.R. Fischer, O.C.G. Adan, Quantitative water uptake study in thin nylon-6 films with NMR imaging, Macromolecules. 45 (2012) 1937–1945. doi:10.1021/ma202719x.

[37] H. Oliver-Ortega, J.A. Méndez, P. Mutjé, Q. Tarrés, F.X. Espinach, M. Ardanuy, Evaluation of Thermal and Thermomechanical Behaviour of Bio-Based Polyamide 11 Based Composites Reinforced with Lignocellulosic Fibres, Polymers (Basel). 9 (2017) 522. doi:10.3390/polym9100522.

[38] J. Pepin, V. Miri, J.-M. Lefebvre, New Insights into the Brill Transition in Polyamide 11 and Polyamide 6, Macromolecules. (2016) acs.macromol.5b01701. doi:10.1021/acs.macromol.5b01701.

[39] S. Goudeau, M. Charlot, F. Müller-Plathe, Mobility Enhancement in Amorphous Polyamide 6,6 Induced by Water Sorption: A Molecular Dynamics Simulation Study, J. Phys. Chem. B. 108 (2004) 18779–18788. doi:10.1021/jp046461e.

[40] B. Jacques, M. Werth, I. Merdas, F. Thominette, J. Verdu, Hydrolytic ageing of polyamide 11. 1. Hydrolysis kinetics in water, Polymer (Guildf). 43 (2002) 6439–

6447. doi:10.1016/S0032-3861(02)00583-9.

[41] A. Meyer, N. Jones, Y. Lin, D. Kranbuehl, Characterizing and modeling the hydrolysis of polyamide-11 in a pH 7 water environment, Macromolecules. 35 (2002) 2784–2798. doi:10.1021/ma010541o.

[42] G. Serpe, N. Chaupart, J. Verdu, Ageing of polyarnide 11 in acid solutions, Polymer (Guildf). 38 (1997) 1911–1917. doi:10.1016/S0032-3861(96)00705-7.

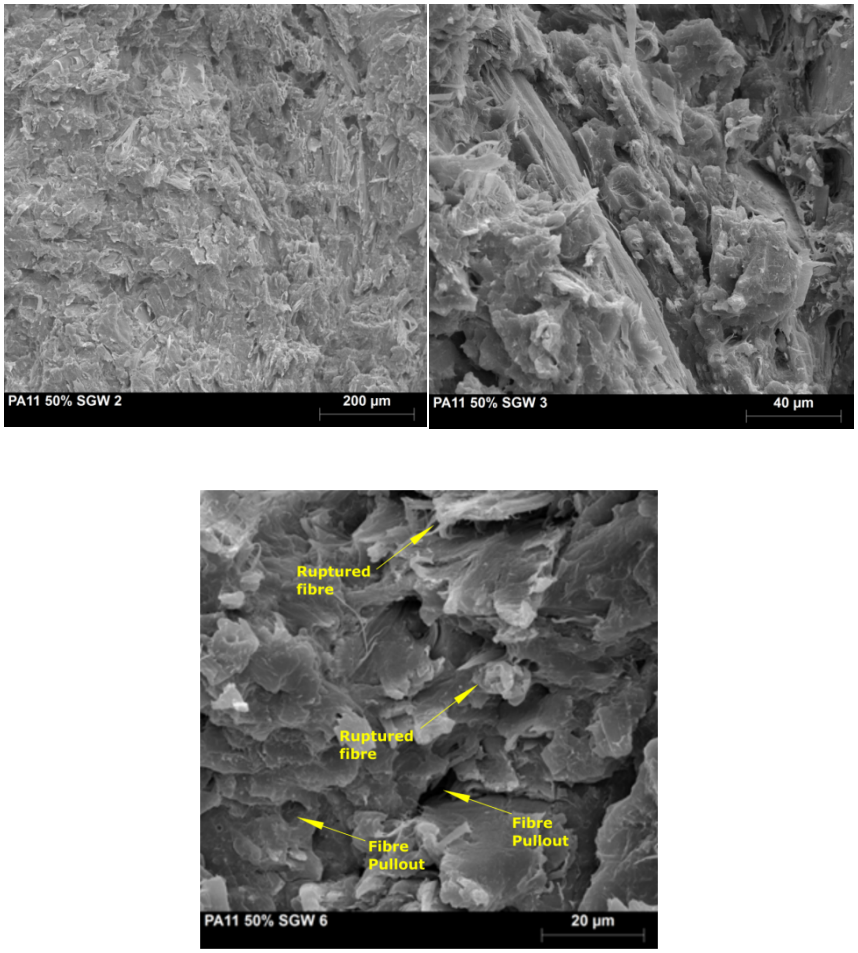

Figure 1. SEM photographs of PA11+50%SGW composite at different resolutions.

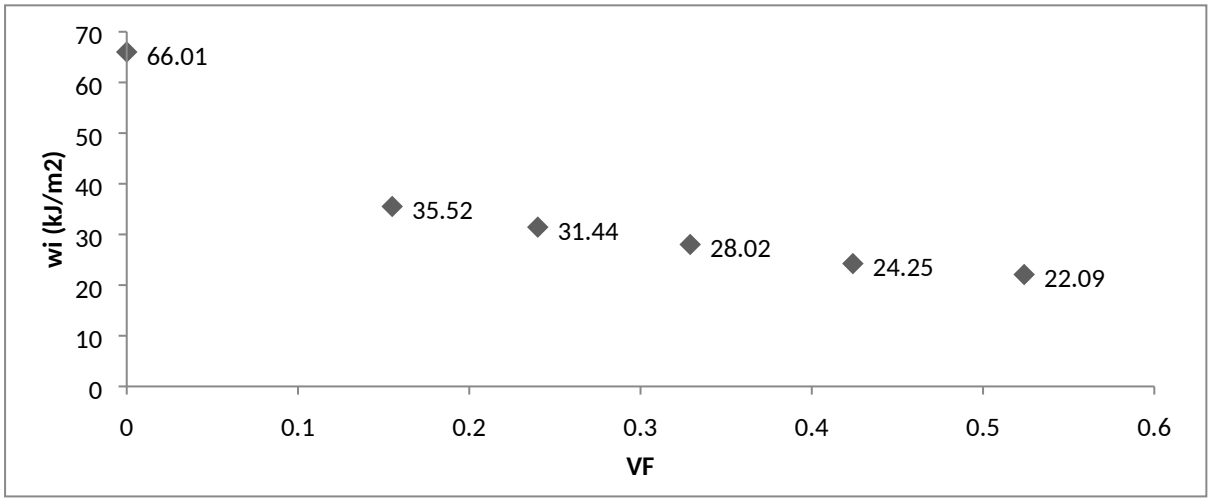

Figure 2. w_i for PA11 and PA11-SGW composites regarding fibre volume fraction.

Table 1. Charpy impact strength for un-notched and notched samples of PA11-SGW composites. (V^F indicate the fibre's volume fraction).

Fibre Content (%)	V^F	Charpy impact strength	
		un-notched (kJ/m²)	notched (kJ/m²)
0	0.000	77.52 ± 8.52	11.51 ± 1.91
20	0.155	40.75 ± 7.57	5.23 ± 0.21
30	0.240	35.79 ± 7.71	4.35 ± 0.18
40	0.329	31.35 ± 2.86	3.33 ± 0.16
50	0.424	27.43 ± 1.44	3.18 ± 0.15
60	0.524	24.80 ± 1.22	2.71 ± 0.11

Table 2. Average water contact angles and wetting Energy (E_w) for PA11 and PA11 composites.

Sample	Average contact angle (°)	E_w (mJ/m²)
PA11	77.1	16.3
PA11+20%SGW	68.8	26.3
PA11+50%SGW	65.9	29.7
PA11+60%SGW	69.3	25.7

Table 3. Fick's parameters and diffusion coefficient at 23 and 40°C regarding the fibre content.

Temperature (°C)	Fibre content (%)	M_∞ (%)	n	K	D (10^{-13} m²•s^{-1})
23	0	1.430	0.305	0.088	4.949
	20	3.423	0.371	0.044	2.192
	50	10.009	0.428	0.034	2.700
	60	12.512	0.453	0.043	5.812
40	0	1.580	0.272	0.155	21.998
	20	4.549	0.387	0.059	6.016
	50	11.098	0.419	0.057	8.048
	60	13.197	0.481	0.055	14.437

Table 4. E_d of PA11 and PA11 composites.

Fibre content (%)	E_d (kJ/mol)
0	67.66
20	45.79
50	49.53
60	41.26

2.7 Research on the use of bio-polyamide 11 reinforced with lignocellulosic fibers composites in automotive parts. The case of a car doors handle.

Enviado y en revisión en el *Journal of Cleaner Production*. Factor de impacto 2016: 5,715. Posición 5 de 31 en Green and Sustainable Science and Technology. Primer cuartil.

Elsevier Editorial System(tm) for Journal of Cleaner Production

Manuscript Draft

Manuscript Number:

Title: Research on the use of bio-polyamide 11 reinforced with lignocellulosic fibers composites in automotive parts. The case of a car doors handle.

Article Type: Original article

Keywords: Natural fiber composites; Mechanical properties; Product design; bio polymers; automotive

Corresponding Author: Dr. Xavier Xavier Espinach, Ph. D.

Corresponding Author's Institution: Universitat de Girona

First Author: Helena Oliver-Ortega

Order of Authors: Helena Oliver-Ortega; Fernando Julian; Xavier Xavier Espinach, Ph. D.; Quim Tarres; Monica Ardanuy; Pere Mutje

Abstract: A great effort is being devoted to the formulation and testing of presumably more environmentally friendly materials. Adjectives like bio-based, recyclable or biodegradable are commonly used as synonyms of greener. Nonetheless, if such materials cannot be used in real cases, as substitutes of currently used oil-based materials the greener advantages are lost in the path. Additionally, reaching competitive mechanical properties is not enough, as an analysis of the carbon footprint or the energy needed to obtain a product are necessary to assess the environmentally friendliness of any bio-based, recyclable or biodegradable material. This work tests replacing a glass fiber reinforced polypropylene composite with wood fiber reinforced bio-based polyamide 11 materials. The study compares the mechanical and environmental performance of the materials when used to produce a car interior door handle.

Suggested Reviewers: Sami Boufi
sami.boufi@fss.rnu.tn

Jose Tresserras
jose.tresserras@udg.edu

Nour Eddine El mansouri
elmansouri.noureddine@gmail.com

Research on the use of bio-polyamide 11 reinforced with lignocellulosic fibers composites in automotive parts. The case of a car doors handle.

Helena Oliver-Ortega[a], Fernando Julian[b], Francesc X. Espinach[b,*], Quim Tarres[a], Monica Ardanuy[c], Pere Mutjé[a]

[*]Escola Politecnica Superior. Avda. Lluis Santalo, s/n, 17003 Girona, Spain. Francisco.espinach@udg.edu, Tlf. +34 972 418 920, FAX +34 972 418 399

[a] Laboratory of Paper Engineering and Polymer Materials, Dpt. Of Chemical Engineering, University of Girona (Spain). Helena.oliver@udg.edu; joaquimagusti.tarres@udg.edu; pere.mutje@udg.edu

[b] Design, Development and Product Innovation, Dpt. Of Organization, Business Management and Product Design, (Spain). Fernando.julian@udg.edu; Francisco.espinach@udg.edu

[c] Materials Science and Metallurgic Engineering Dept., Polytechnic University of Catalunya, Barcelona 08019 (Spain). Monica.ardanuy@upc.edu

Abstract

A great effort is being devoted to the formulation and testing of presumably more environmentally friendly materials. Adjectives like bio-based, recyclable or biodegradable are commonly used as synonyms of greener. Nonetheless, if such materials cannot be used in real cases, as substitutes of currently used oil-based materials the greener advantages are lost in the path. Additionally, reaching competitive mechanical properties is not enough, as an analysis of the carbon footprint or the energy needed to obtain a product are necessary to assess the environmentally friendliness of any bio-based, recyclable or biodegradable material. This work tests replacing a glass fiber reinforced polypropylene composite with wood fiber reinforced

bio-based polyamide 11 materials. The study compares the mechanical and environmental performance of the materials when used to produce a car interior door handle.

Keywords: Natural fiber composites; Mechanical properties; Product design; bio polymers; automotive.

CAPÍTULO 3: *DISCUSIÓN GENERAL DE LOS RESULTADOS*

3.1 Discusión general de los resultados

Los resultados de esta tesis doctoral incluyen desde la capacidad de producción de los compuestos de PA11-SGW mediante un equipamiento semi-industrial, como es el caso del mezclador cinético Gelimat, y su procesado mediante inyección, hasta su caracterización mecánica y modelización de su comportamiento, caracterización térmica y de absorción de agua con el fin de demostrar su capacidad para reemplazar de forma sostenible materiales empleados actualmente en el mercado menos sostenibles.

En el primer artículo del compendio, "*Tensile properties and micromechanical analysis of stone groundwood from softwood reinforced bio-based polyamide11 composites"*, se analizaron las propiedades a tracción de los compuestos de PA11-SGW, exceptuando su E_t^C. No obstante, es necesario remarcar que el primer resultado positivo de dicho estudio es la correcta extrusión e inyección de los materiales de PA11-SGW (figura 6), contrariamente a los resultados obtenidos previamente con fibras blanqueadas donde es posible apreciar a simple vista diversas zonas de las probetas con aglomeraciones de fibras. Los resultados obtenidos, mostraron un aumento de la σ_t^C al incrementar el contenido de fibra en los compuestos. Este incremento lineal, puede ser asociado a una buena dispersión del refuerzo y, principalmente, con una muy buena interfase en entre la matriz y el refuerzo [1,2]. El valor máximo alcanzado de 63,9 MPa, supuso un incremento del 67% respecto a la matriz de PA11. El aumento significativo obtenido en los compuestos de PA11-SGW hasta el 50% w/w de fibra, reflejó una más que probable buena interfase en los compuestos de PA11 sin la necesidad de un agente de acoplamiento [3,4]. Por otra parte, en el caso del compuesto de PA11+60%SGW se produjo un descenso de la resistencia. Este fenómeno se encuentra relacionado con una inadecuada impregnación de las fibras por parte de la matriz y a una pobre dispersión, que probablemente, causó la formación de agregados de fibra. Todo ello, fue consecuencia del alto contenido de refuerzo utilizado para la preparación del material compuesto. Por otra parte, la ε_t^C y en consecuencia la U_T de los materiales compuestos experimento una caída drástica debido a la mayor rigidez de las fibras de SGW empleadas como refuerzo.

Figura 6. Muestras de los especímenes inyectados. De izquierda a derecha, PA11, PA11+20%SGW, PA11+50%SGW y PA11+60%SGW.

La morfología de las fibras y su composición química superficial fueron analizadas con el objetivo de determinar su influencia en los resultados experimentales. Ambos factores tienen un impacto significativo en la transmisión de los esfuerzos a través de las diferentes fases del material compuesto. La morfología de las fibras mostró una considerable cantidad de finos (fibras menores a 90μm de longitud), que se incrementaba tras los procesos de fabricación y transformación de los materiales compuestos debido a la reducción de longitud que sufren las fibras durante la fabricación. A pesar de ello, y teniendo en cuenta que las fibras largas presentan una mayor capacidad de refuerzo, la mayor superficie especifica de los finos podría tener un efecto positivo en la resistencia del material compuesto. Por otra parte, la composición química superficial de las fibras de SGW fue estudiada mediante XPS. El ratio carbono/oxigeno (tabla 4) obtenido, fue superior al esperado para la celulosa pura [5] y se mostró en consonancia con los valores bibliográficos de una fibra con un alto contenido superficial en lignina [6,7]. El ensayo de XPS a alta resolución confirmó este resultado y mostró una gran cantidad de grupos hidroxilos en la superficie de las fibras, muchos de los cuales provenían de la lignina. Estos grupos hidroxilo son capaces de establecer enlaces de

hidrogeno con las cadenas de PA11 produciendo una interfase adecuada, ello explica también el incremento en la resistencia de los compuestos obtenidos.

Tabla 4. Energías de enlace y porcentaje atómico en la superficie de las fibras de SGW.

Elemento	Energía de enlace (eV)	Porcentaje atómico (%)
Carbono	285	67.88
Oxígeno	532	31.97
Sodio	1071	0.14

Finalmente, la σ_t^C del compuesto con un contenido del 30% w/w de SGW se modelizó utilizando el modelo de Kelly y Thyson [8] y se resolvió mediante la ecuación de Bowyer y Bader [9]. Esta modelización permitió la obtención de los valores de σ_t^F de la SGW y la τ, indicador de la calidad de la interfase en el compuesto. Además, se modelizó con y sin la incorporación de los finos en la morfología de las fibras para observar el efecto de la mayor área de los finos. La inclusión de estos produjo una variación en la aportación de las fibras sub-críticas y alcanzó resultados superiores de τ y σ_t^F. La σ_t^F obtuvo un valor muy similar a la obtenida previamente con PP (562 respecto 617) [2]. La τ, con un valor de 19,29 MPa, fue casi idéntica al criterio de Tresca (19,5 MPa) y ligeramente inferior a Von Mises (22,1 MPa) [10–12].

El valor del f_c se calculó en 0,193, muy próximo al 0,2 de la literatura [10,13]. A partir de los resultados de τ, σ_t^F y f_c obtenidos se modelizaron los demás compuestos obteniendo valores sin diferencias significativas con los valores experimentalmente excepto en el caso del 60% w/w de SGW.

Los resultados obtenidos en los ensayos de resistencia a tracción mostraron los compuestos de PA11-SGW como una alternativa viable a compuestos comerciales de PP reforzados con GF y con fibras naturales. Además de la importancia de la resistencia a tracción, la rigidez y la deformación son factores claves para la producción y aplicación de los compuestos desarrollados en esta tesis. Es por ello por lo que en el artículo "*Stiffness of bio-based polyamide 11 reinforced with softwood stone ground-wood fibres as an alternative to*

polypropylene-glass fibre composites" se analizaron estas propiedades y la competitividad de los compuestos de PA11-SGW para el remplazo de los compuestos basados en PP.

El E_t^C es un indicativo de la rigidez de un material por lo que su análisis es de gran interés en la industria. La rigidez de un material compuesto depende en gran parte de la rigidez de las fases que lo conforman, de la morfología y volumen de refuerzo y sobre todo de la dispersión de este en la matriz. Una mala dispersión conlleva valores no lineales del E_t^C al aumentar la cantidad de fibra en el compuesto. Este no fue el caso en los compuestos de PA11-SGW, donde a pesar de la no linealidad en la σ_t^C cuando se incluye el material compuesto al 60% w/w. Se obtuvieron incrementos de hasta el 3,51 veces mayores que los de la matriz con un 50% w/w de fibra en el compuesto y 4,23 veces para el compuesto con un 60% w/w de SGW.

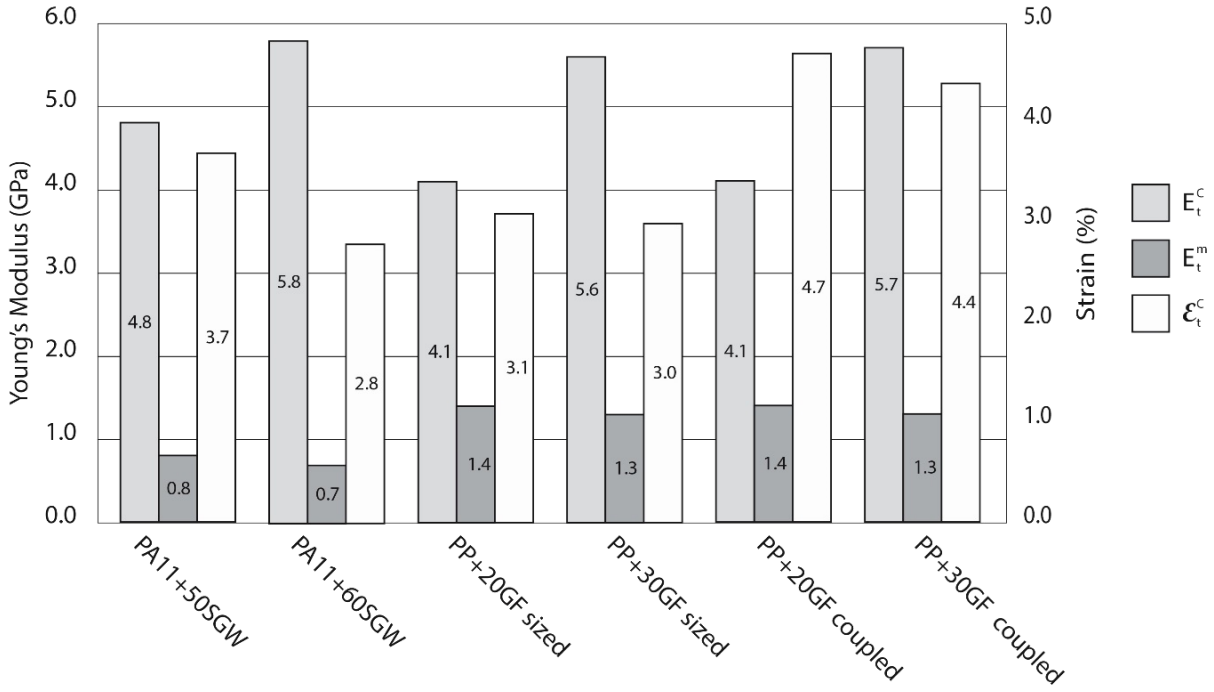

Figura 7. Comparativa PA11-SGW con PP-GF. En la figura se representan el Módulo de Young del compuesto y la contribución de la matriz al módulo, así como las deformaciones de los compuestos.

Los compuestos con porcentajes elevados de fibra mostraron valores similares de E_t^C a los alcanzados con PP reforzado con GF (figura 7). Aunque las ε_t^C de los compuestos de PA11-SGW fueron similares a las obtenidas con GF sin agente de acoplamiento (GF *sized*), los

valores experimentales no alcanzaron los de GF *coupled*. Las ε_t^C obtenidas en los compuestos de GF *coupled* se pueden relacionar con el menor volumen de fibra utilizado y el uso de un agente de acoplamiento. Por otro lado, se observó la necesidad de incrementar el volumen de refuerzo en los compuestos de PA11-SGW para lograr la misma rigidez que los compuestos de PP-GF. Ello es debido al menor E_t^F de las fibras naturales en comparación con las GF.

El análisis del módulo específico de Young, que se define como el E_t^C respecto a la densidad del material compuesto (ρ^C), demostró de nuevo la necesidad en el caso de las fibras naturales de aumentar su contenido para obtener propiedades similares a las de los compuestos de GF.

La contribución de la fibra sobre el E_t^C, fue analizada mediante el uso de la RoM. Inicialmente, se calculó el FTMF, mediante la reordenación de la RoM, ya que el E_t^F y el η_e son desconocidos. La FTMF demostró una misma eficiencia de las fibras de SGW en las matrices de PA11 y PP [14], pero alrededor de tres veces inferior a la obtenida con GF. Este resultado era esprado debido a las mayores propiedades mecánicas de las GF.

Para el cálculo de E_t^F y en consecuencia η_e, se utilizaron dos modelos lineales: el modelo de Hirsch y el de Tsai-Pagano [15,16]. La diferencia principal entre ellos se encuentra en la inclusión de la morfología de las fibras implícitamente en el caso de Tsai-Pagano y las ecuaciones de Halpin-Tsai [16,17] mientras que en el caso de Hirsch no se contempla y se emplean solamente en la resolución de Cox-Krenchel [18,19]. Los resultados desprendidos del uso de los dos modelos (tabla 5) fueron muy similares con valores medios de E_t^F de 17,84 para Hirsch y de 18,04 para Tsai-Pagano. Sin embargo, se apreciaron ligeras diferencias en los η_e, η_l, y η_0 que conllevaron valores ligeramente inferiores en Tsai-Pagano teniendo entonces un impacto más significativo la inclusión de la morfología de las fibras en el cálculo. Además, se observó una mayor tendencia a la orientación de las fibras cuando el contenido de estas aumenta en el material, representado por una disminución en el ángulo de las fibras en el modelo de Tsai-Pagano. No obstante, un ensayo estadístico *t-student* demostró que los resultados obtenidos mediante los dos modelos no mostraban diferencias significativas en el 99% del intervalo de confianza.

Tabla 5. Resultados de E_t^F y α en de los compuestos de PA11-SGW.

Material	E_t^C (GPa)	E_t^F Hirsch (GPa)	E_t^F Tsai-Pagano (GPa)	*α* Hirsch (º)	*α* Tsai-Pagano (º)
PA11+20%SGW	2,51	17,76	19,48	47,6	51,4
PA11+30%SGW	3,03	16,44	16,81	47,2	48,2
PA11+40%SGW	3,88	17,85	18,40	47,5	48,8
PA11+50%SGW	4,78	18,45	18,18	47,8	47,2
PA11+60%SGW	5,76	18,68	17,32	47,9	44,5
Promedio		**17,84**	**18,04**	**47,6**	**48,0**
Desviación estándar		**0,87**	**1,03**	**0,3**	**2,5**

Aunque las propiedades mecánicas definen la aplicación y viabilidad de los compuestos desarrollados, el estudio de las propiedades térmicas y termomecánicas es necesario para garantizar su correcto procesado y estabilidad térmica, que limitan el rango de temperatura en el que los materiales pueden ser utilizados. Además, el principal impedimento para el uso de fibras celulósicas como refuerzo de matrices poliméricas es su baja temperatura de degradación. Esto limita su uso como refuerzo de polímeros con temperaturas de fusión alrededor de 200ºC. En este caso, la PA11 tienen una temperatura de fusión de alrededor de 190ºC que permite que las fibras no sufran ninguna degradación durante el procesado.

En el tercer artículo del compendio "*Evaluation of Thermal and Thermomechanical Behaviour of Bio-Based Polyamide 11 Based Composites Reinforced with Lignocellulosic Fibres"* se estudiaron todos los parámetros anteriormente mencionados y se incluyó el efecto de un tratamiento térmico de *annealing*.

La presencia de las fibras puede tener alguna influencia en la estructura cristalina, las transiciones térmicas y la temperatura de descomposición de la PA11. La PA11, como otras PA, tiende a cristalizar en mayor o menor grado y en diferentes estructuras en función de la disposición del enlace por enlace de hidrogeno entre las cadenas [20,21]. No obstante, la capacidad de las fibras SGW de establecer enlaces de hidrogeno con la matriz [4] puede

afectar al porcentaje de regiones cristalinas formadas así como la estructura cristalina de la PA11.

La degradación de la PA11 y de los compuestos con diferentes porcentajes de fibra se evaluó mediante TGA. A pesar de que los compuestos de PA11-SGW se degradan antes que la PA11 debido a la presencia de las fibras, se observó una estabilización de la degradación de la matriz una vez iniciada debido a la presencia de las fibras de SGW. El carbón formado por la degradación de las fibras impide la dispersión de componentes volátiles y radicales relacionados en la degradación de la matriz [22,23]. La T_m y la temperatura de cristalización (T_c) de la PA11 y sus compuestos fueron determinadas mediante DSC, donde a pesar de no observarse cambios por efecto de las fibras, (con valores de 189ºC y 164ºC para la T_m y T_c respectivamente en todos los compuestos) si se observó una disminución de la fase cristalina γ durante la segunda fusión al incrementar el contenido de fibra (figura 8).

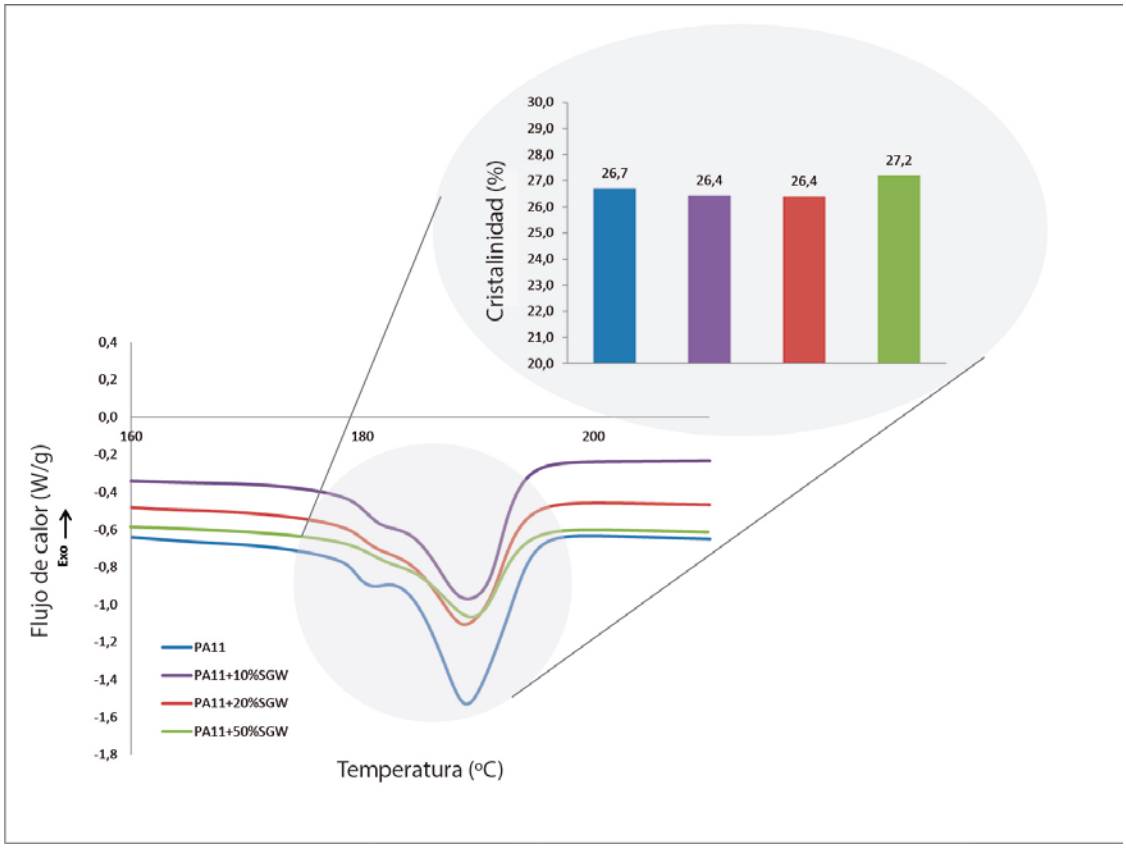

Figura 8. Termograma de la segunda fusión en el DSC de los compuestos de PA11-SGW. En el termograma se aprecia la disminución de la fase γ, pero las cristalinidades obtenidas son casi idénticas.

No obstante, y tal como se aprecia en la figura 8, no se obtuvo ningún incremento en la cristalinidad a diferencia de lo que ocurre con otras matrices termoplásticas al ser reforzadas con fibras celulósicas o lignocelulósicas [24,25]. Este efecto está relacionado con la formación de enlaces de hidrogeno entre la fibra y la matriz, que limitan la formación de regiones cristalinas.

El ensayo térmico dinamomecánico (DMTA) tampoco mostró efectos significativos de las fibras en la temperatura de transición vítrea (T_g) de los materiales compuestos. En cambio, se apreciaron incrementos en los módulos de pérdida (E") y almacenamiento (E') que se mantienen una vez sobrepasada la T_g debido a la rigidez de las fibras. El estudio de su microestructura mediante XRD mostró una fase δ' para todos los compuestos. Aun y así, es posible que la fase γ también se encuentre presente, pero en menores contenidos y que sea enmascarada en el XRD. El FT-IR de los compuestos mostró la presencia de la fase γ para la PA11 y como disminuye o desaparezca al aumentar el contenido de fibra.

Posteriormente, se estudió el efecto de un tratamiento térmico, un *annealing*, en los materiales compuestos. Se observó un incremento de la de la cristalinidad para todas las muestras por efecto de este tratamiento, pero de forma más pronunciada en el compuesto con un alto contenido de SGW: PA11+50% SGW. El mayor grado de cristalinidad obtenido fue del 40,5% en el compuesto con el 50% w/w de fibras SGW, lo que supone más de un 10% de incremento respecto a la cristalinidad inicial de la matriz de PA11 (26.7%).

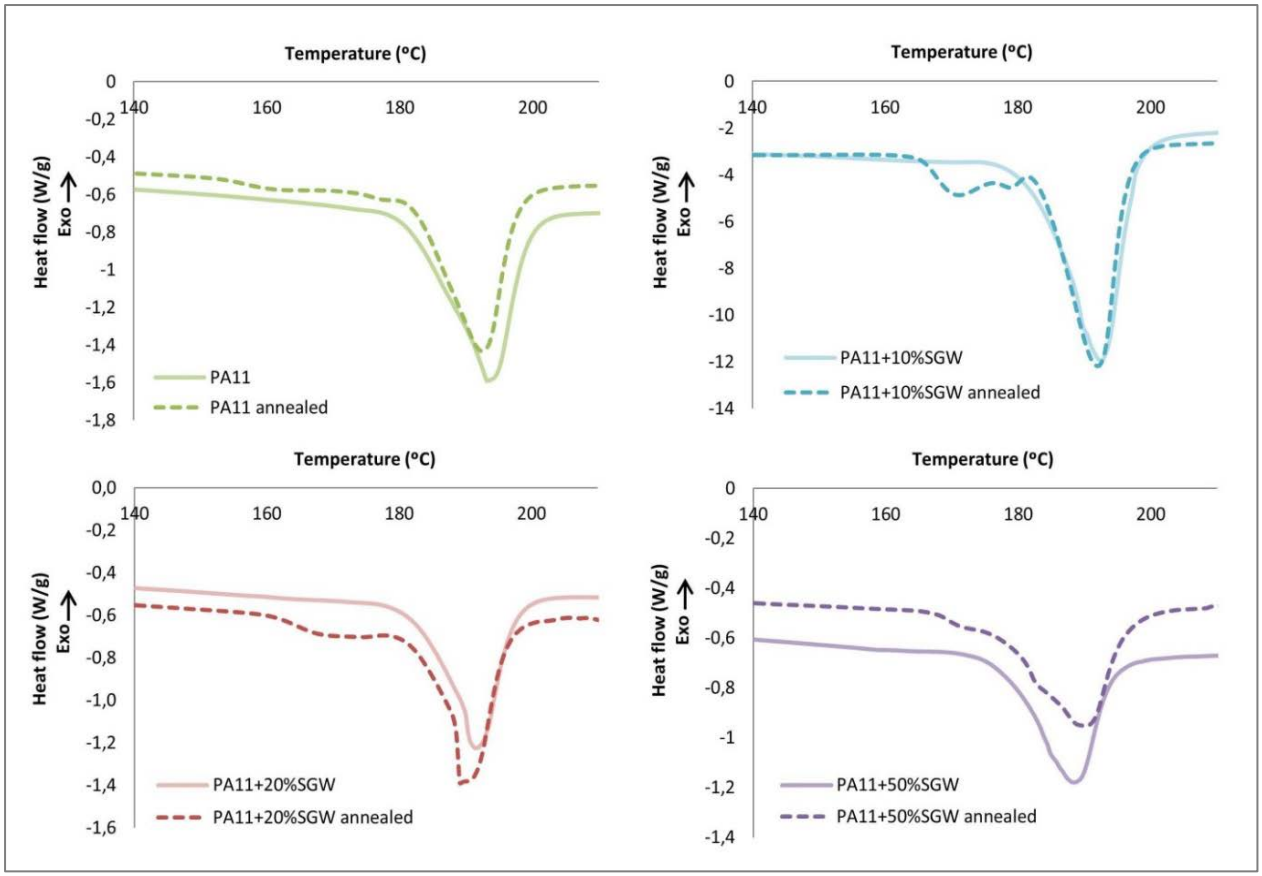

Figura 9. Termogramas de DSC de la PA11 y sus compuestos antes y tras el *annealing*.

Además, en los termogramas se apreció la aparición de cristales a la temperatura del *annealing* y como estos se desplazaron hacia mayores temperaturas al incrementar el contenido de fibra (figura 9).

Los ensayos de DMTA de las muestras tratadas mostraron un ligero incremento en los módulos debido al incremento de la cristalinidad, pero el efecto se vio reducido al aumentar el contenido de fibra igual que en el caso de las T_g, dónde la PA11 monolítica obtuvo el mayor valor mientras que en el caso del compuesto de PA11+50%SGW no varió. En el caso de los módulos, se apreciaron ligeros incrementos a menor contenido de fibra. Finalmente, el XRD demostró un cambio de estructura cristalina, obteniéndose la fase α', típica en muestras con *annealing* y termodinámicamente más estable. El FT-IR de la PA11 tratada demostró que la fase γ no estaba presente o su contenido era insuficiente como para observarse.

El análisis de la resistencia a flexión de los compuestos de PA11-SGW se realizó mediante el ensayo de tres puntos. Las propiedades a flexión pueden ser incluso de mayor interés que las propiedades a tracción en según qué ámbitos de desarrollo y aplicación de materiales [26–28]. En materiales compuestos reforzados con fibras, la orientación de las fibras en el material y la dirección de la fuerza aplicada tienen un impacto determinante en el resultado final [29]. En el artículo: "*Towards more sustainable material formulations: A comparative assessment of PA11-SGW flexural performance versus Oil-based composites"* se estudió y evaluó la σ_f^C de los compuestos de PA11-SGW y su idoneidad como alternativa a compuestos de PP-GF (tabla 6).

Tabla 6. Propiedades a flexión de los compuestos de PA11-SGW respecto al contenido de fibra.

Material	ρ^C ($g \cdot cm^{-3}$)	σ_f^C (MPa)	ε_f^C (%)	U_R ($kJ \cdot m^{-3}$)
PA11	1,03	40,0	7,39	78,18
PA11+20%SGW	1,09	55,0	6,39	57,77
PA11+30%SGW	1,12	68,7	5,78	49,65
PA11+40%SGW	1,15	77,5	5,24	42,73
PA11+50%SGW	1,18	92,6	4,24	37,05
PA11+60%SGW	1,22	102,7	3,23	29,79

Al igual que en el caso de la σ_t^C, la evolución lineal de la resistencia respecto al contenido de fibra, permite suponer una correcta interfase entre la matriz y la fibra debido a la capacidad de la PA11 a establecer enlaces de hidrogeno con las fibras. Por otra parte, el mayor incremento obtenido respecto a la σ_t^C se produce a consecuencia de la suma del trabajo a tracción y compresión que realizan las fibras y la matriz en el ensayo a flexión (figura 10).

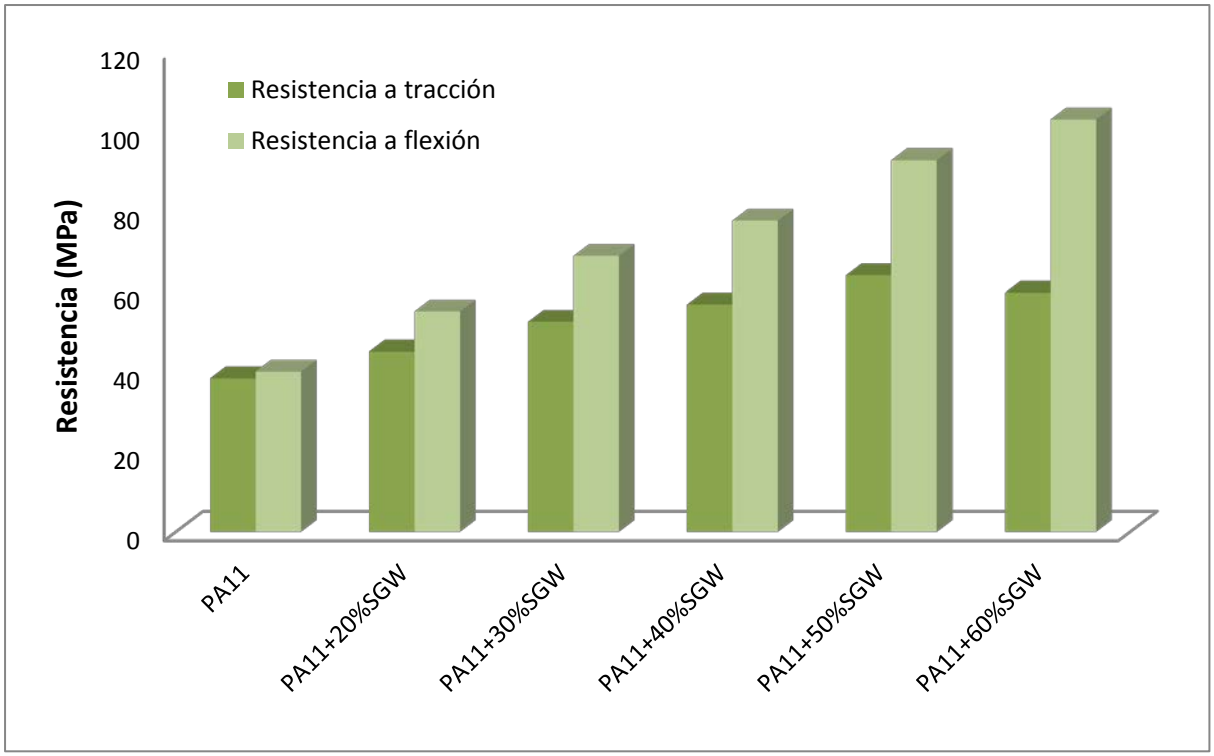

Figura 10. Comparación entre la σ_t^C y la σ_f^C de los materiales compuestos de PA11-SGW.

Esta relación entre la σ_t^C y la σ_f^C se incrementó al aumentar el contenido de fibra en el material. En el caso de la PA11 no se obtuvo apenas variación (1,02), mientras que en los materiales compuestos la relación aumenta de 1,22 para el compuesto PA11+20%SGW a 1,45 para el compuesto PA11+50%SGW. En el caso del compuesto PA11+60%SGW esta relación aumenta hasta un 1,72, pero es debido a que la resistencia a tracción se reduce debido a la incorrecta impregnación de las fibras por parte de la matriz y a la formación de aglomeraciones de fibras en el material. En la σ_f^C no se apreció este efecto.

Como es de esperar, la ε_f^C se redujo al aumentar el contenido de fibra en el material, pero en este caso, solamente las probetas a partir del 30% w/w de contenido de fibra rompieron durante el ensayo. La U_R mostró una tendencia similar a la deformación, reduciéndose hasta un 62% del valor inicial de PA11 con el material compuesto con un 60% w/w de fibras de SGW. Por otro lado, también se examinó la evolución de la ρ^C, incrementándose ligeramente con el contenido de fibra debido a la mayor densidad de ésta. No obstante, solo los

compuestos con contenidos superiores al 40% w/w muestran densidades superiores a los compuestos de PP-GF.

A efectos de comparar los compuestos de PA11-SGW con productos fabricados con PP-GF y PP-fibras naturales (en este caso, SGW), se compararon las σ_f^C de los compuestos con contenidos similares de refuerzo (figura 11).

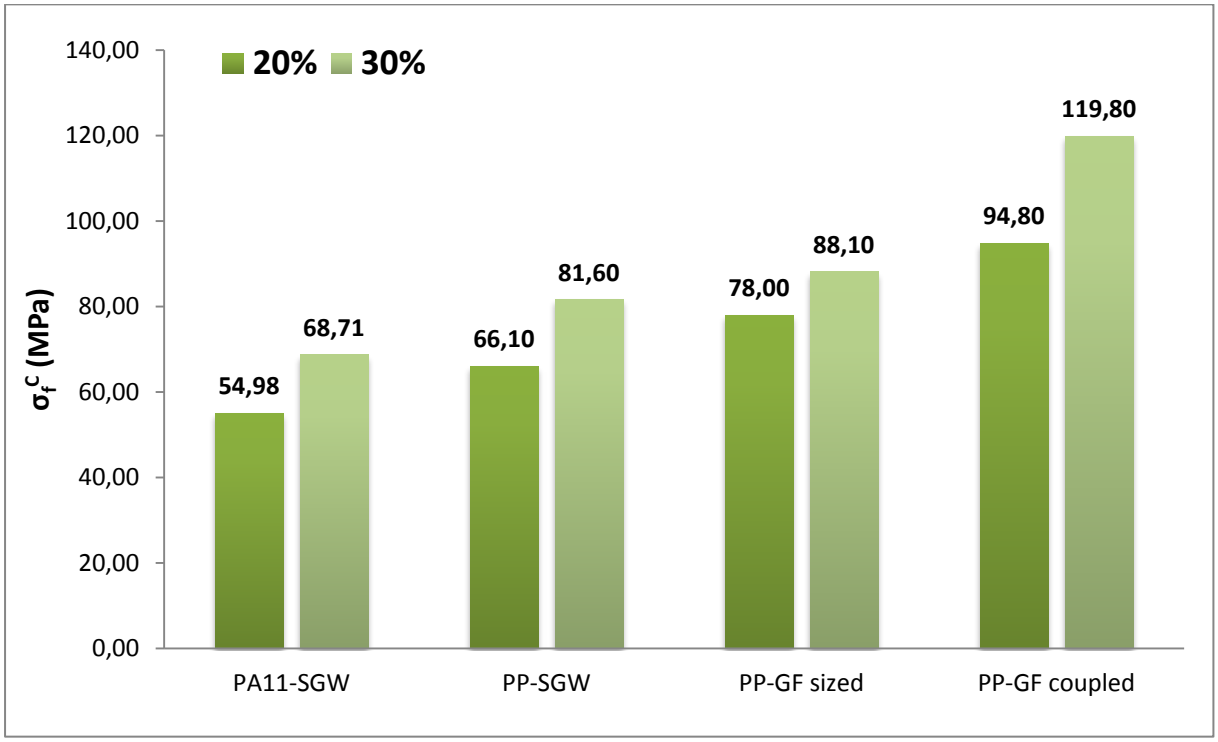

Figura 11. Comparación de entre los materiales compuestos de PA11-SGW y los de PP-GF y PP-SGW con el mismo contenido en peso de fibra.

Los materiales compuestos de PA11-SGW mostraron una menor σ_f^C que los compuestos de PP-GF, tal y como era esperable debido a las mayores propiedades mecánicas de las GF. No obstante, se apreció una diferencia considerable entre los materiales de PA11 y PP reforzados con SGW. Debido a esta diferencia, se analizó el FFSF (figura 12). La FFSF es una característica propia de cada material que depende de las propiedades de las fibras y de otros factores como la orientación y la morfología de las fibras y la interfase de los materiales.

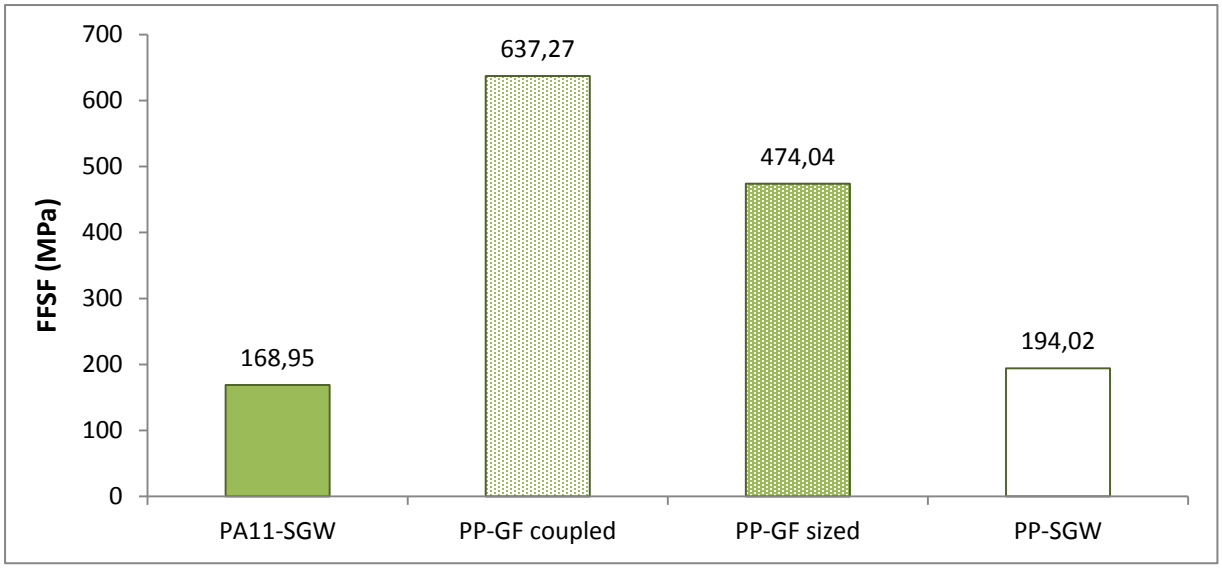

Figura 12. FFSF de los materiales de PA11-SGW y de los materiales compuestos de PP utilizados para comparación.

La FFSF de los materiales de PA11-SGW obtuvo un menor valor que los compuestos de PP. El menor resultado respecto a las GF era esperable debido a las propiedades de las GF, pero no era de esperar en el caso de los compuestos de PP-SGW ya que la fibra es la misma. Éste menor resultado se relacionó con una menor calidad de la interfase en el caso de los compuestos de PA11. La FFSF, como se menciona anteriormente, depende de las propiedades mecánicas y del aspecto de las fibras, de su orientación en el material y de la interfase. Entre los compuestos de PA11 y PP reforzados con SGW el único factor que podría tener un gran impacto es la interfase, ya que las fibras son las mismas y la orientación de las fibras en el material tienen una gran dependencia por el equipo de inyección y en ambos casos fue el mismo.

Por otro lado, y considerando la gran diferencia entre la FFSF de la PA11-SGW y los materiales compuestos de PP-GF (de 3,7 veces mayor para los compuestos de PP-GF *coupled* y 2,8 para los de PP-GF *sized*), se podría esperar un mayor rendimiento de estas fibras en la σ_f^C. La diferencia se debe al menor volumen de fibra (V^F) de las GF debido a su mayor densidad.

A través de la FFSF y de su análoga en las propiedades a tracción, la FTSF (Fibre Tensile Strength Factor), se determinó la σ_f^F en 888 MPa [26], valor inferior al obtenido con PP y en la literatura en general [30], probablemente debido a la menor calidad de la interfase que se

obtiene. Cabe recordar, que en el caso de los compuestos de PP-SGW, la interfase se obtiene mediante enlaces covalentes y un enredado de las cadenas de PP, mientras que en los compuestos de PA11-SGW la interfase se produce mediante enlaces por enlaces de hidrogeno que son fuerzas intermoleculares débiles en comparación con los enlaces covalentes. Además, estos enlaces de hidrogeno no se establecen solo con la celulosa sino que también con la lignina y las hemicelulosas (figura 13). Estos menores rendimientos de fibras lignocelulósicas también se han observado en otras poliamidas donde la interfase también se consigue mediante enlaces de hidrogeno [31,32].

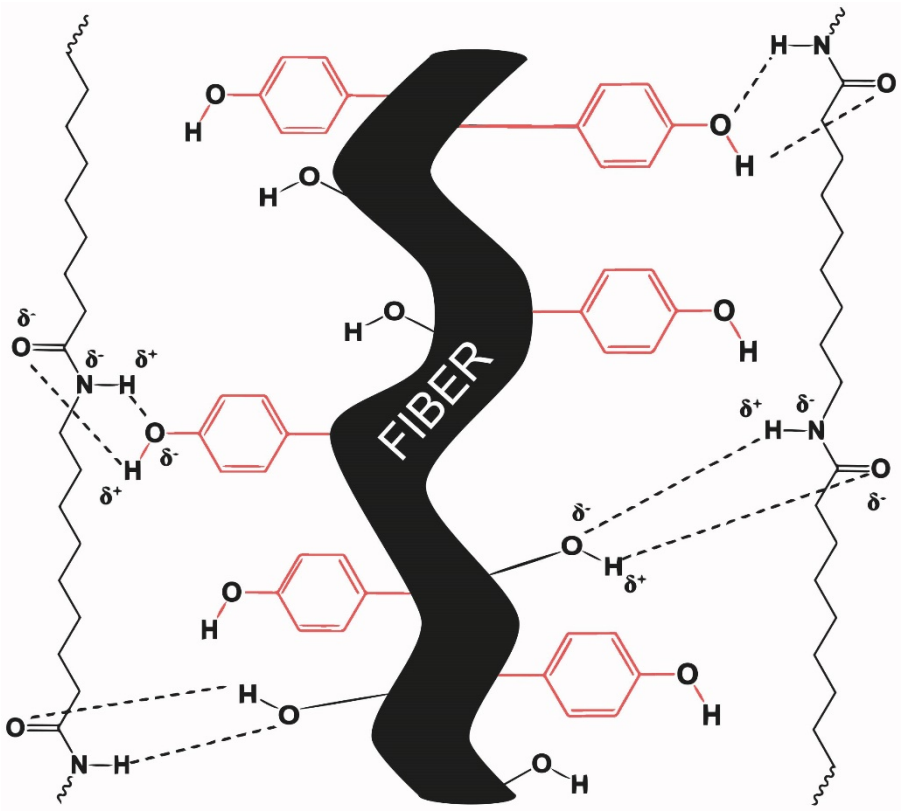

Figura 13. Representación de las interacciones en la interfase entre las fibras de SGW y la PA11. Los grupos fenoles de color rojo indican los grupos con hidroxilos que tiene la lignina.

El valor de σ_f^F de las SGW es muy reducido en comparación con las GF, que alcanzan σ_f^F de 3787 y 4237 MPa cuando se usa un agente de acoplamiento [33,34]. Utilizando las σ_f^F calculadas y mediante la RoM, se obtuvo el factor de acoplamiento f_c^f. El factor de los

compuestos de PA11-SGW resultó de 0,183, similar al obtenido a tracción y ligeramente superior al del compuesto de PP+50%SGW (0,173). Respecto a los compuestos de GF, se observaron mayores diferencias ya que durante el procesado la longitud de las fibras se reduce considerablemente debido a la mayor fragilidad de las GF.

Finalmente, se compararon los compuestos de PA11 con alto contenido de fibra (50 y 60% w/w) con los de PP y se observó la capacidad de reemplazarlos a todos excepto en el caso del PP+30%GF. Se estimó que sería necesario un compuesto de PA11 con un 73% w/w de SGW para reemplazarlo, pero no es posible producir estos compuestos de tan elevado contenido de fibra.

El E_f^C de los materiales compuestos de PA11 y SGW se examinó en el artículo "*Study of the flexural modulus of lignocellulosic fibres reinforced bio-based polyamide11 green composites"*. Similar a la σ_f^C, el E_f^C tiene una mayor relevancia en el desarrollo de nuevos materiales y su aplicación, sobre todo en el caso de materiales compuestos donde la orientación, longitud y tipo de fibra tiene un gran impacto en el módulo. En la tabla 7 se muestran los resultados obtenidos de la caracterización de los materiales compuestos.

Tabla 7. Resultados del E_f^C y ε_f^C de los compuestos de PA11 reforzados con SGW.

Material	V^F	E_f^C (GPa)	ε_f^C (%)
PA11	0,000	0,9	7,39
PA11+20%SGW	0,155	1,7	6,39
PA11+30%SGW	0,240	2,1	5,78
PA11+40%SGW	0,329	2,6	5,24
PA11+50%SGW	0,424	3,3	4,24
PA11+60%SGW	0,524	4,1	3,23

Se obtuvo un incremento de hasta 3,7 y 4,5 veces para los compuestos de PA11+50%SGW y PA11+60%SGW, a la vez que se mantenía una considerable deformación. Además, el comportamiento del E_f^C de los materiales compuestos de PA11-SGW era lineal al aumentar

la cantidad de fibra en el material, por lo que se podía asumir una correcta dispersión de las fibras en la matriz de PA11, al igual que ocurría en el E_t^C.

Cuando los E_f^C de los compuestos de PA11-SGW se comparaban con los compuestos de PP-GF, los compuestos de PA11 con elevado contenido de SGW mostraban resultados similares confirmando su competitividad para reemplazarlos. No obstante, cuando los resultados se compararon con los de compuestos de PP-SGW, éstos eran significativamente menores a los alcanzados en los compuestos de PP-SGW [30,35].

Los valores considerablemente menores de E_f^C de los compuestos de PA11-SGW respecto a los compuestos de PP-SGW indicaban un menor efecto de las SGW al módulo de los materiales compuestos, similar al obtenido anterioremente en la σ_f^C. Este efecto se examinó mediante el FFMF, dónde los compuestos de PA11-SGW obtuvieron el menor FFMF (figura 14). El FFMF de los compuestos de PP-SGW resultó casi el doble del de los compuestos de PA11-SGW.

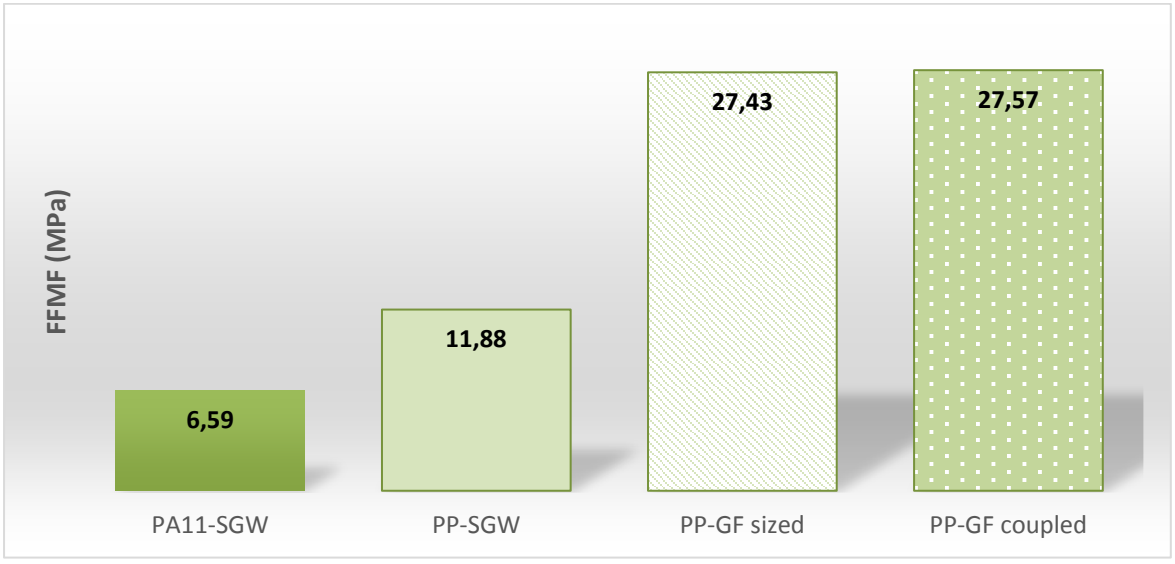

Figura 14. FFMF de los compuestos de PA11-SGW, PP-SGW y PP-GF.

En el caso de los compuestos de PP-GF, los resultados eran muy superiores a los de los compuestos reforzados con fibras naturales debido a la mayor rigidez de las GF. Por otra

parte, también se apreció que el FFMF de los PA11-SGW era menor incluso que su análogo el FTMF, cosa extraña ya que debido a la anisotropía del ensayo a flexión, donde se suman los esfuerzos a tracción y compresión, el valor a flexión se incrementa. Respecto a los materiales de PP-GF, el valor era muy inferior, pero era de esperar debido a las mayores propiedades de las GF.

En el análisis micromecánico mediante el modelo de Hirsch, el E_f^F alcanzó un valor de 12,6 MPa. Este resultado era menor que los anteriormente reportados para las fibras de SGW en PP y distantes de los obtenidos en las propiedades a tracción [30]. En cambio, los η_e, η_l, y η_0 e el ángulo de orientación fueron similares. Esta tendencia es consecuente con lo observado anteriormente en el FFMF y se relacionó con un pobre trabajo de las fibras a compresión por el colapso de éstas debido a la presencia de volumen vacío o de una interfase no del todo adecuada. No obstante, la interfase tiene usualmente poca repercusión en el módulo, por lo que se consideró que la presencia de volumen vació era una probabilidad más factible.

El volumen vacío fue estimado de forma teórica. El valor máximo de volumen vació se halló para el compuesto de PA11+60%SGW y fue del 2.22% [36]. Se consideró que los valores de volumen vacío eran muy reducidos y tenía probablemente poco impacto en el pobre trabajo de compresión que se observó para las SGW en la PA11.

La resistencia al impacto permite conocer el comportamiento de un material cuando este es golpeado por un cierto objeto de forma espontánea y puntual. A diferencia de los ensayos a tracción y flexión, la fuerza no se aplica de forma continuada, sino que el impacto y la respuesta del material se producen en apenas unos segundos. Por otra parte, es perfectamente conocido el efecto del agua como plastificante en los materiales poliméricos. La absorción/adsorción de agua depende de las condiciones ambientales a las que está expuesto el material y de la composición química de éste. Las PA en general son polímeros que tienden a absorber mayor cantidad de agua que otros termoplásticos como el PP, debido a su capacidad de establecer enlaces de hidrogeno. Además, al ser reforzada con un refuerzo hidrófilo como son las fibras celulósicas, se favorece este fenómeno y es necesario un control de la velocidad y capacidad de absorción [37]. Mediante el estudio publicado en el artículo: "*Fully bio-based composites from PA11-SGW: Notable impact strength and water uptake"* se

examinó el comportamiento al impacto y el proceso de absorción de agua a 23ºC y 40ºC de los compuestos de PA11-SGW.

La resistencia al impacto se estudió mediante el test Charpy con entalla y sin entalla para obtener una caracterización más completa de los materiales. A pesar de que el ensayo se realizó a 23ºC, temperatura inferior a la T_g de la PA11, la PA11 mostró una resistencia con y sin entalla bastante elevada (77,58 y 11,51 $kJ \cdot m^{-2}$ respectivamente). En el caso de los compuestos resultantes, ambas resistencias disminuyeron, tal y como era esperable debido a la mayor rigidez de las fibras, que además limita el movimiento de las cadenas de PA11 y, por tanto, su capacidad para disipar la energía absorbida. No obstante, los valores obtenidos fueron superiores a los obtenidos para el PP reforzado con GF, SGW e incluso algunas PA reforzadas con GF [30,35,38], con un mínimo de 24,8 $kJ \cdot m^{-2}$ en el caso del compuesto de PA11+60%SGW.

En las muestras entalladas, la reducción de la resistencia debido a la presencia de las fibras fue más pronunciada que en las muestras sin entallar. Estos resultados se muestran en concordancia con los esperados ya que las PA en general tienen una gran resistencia al impacto aunque el ensayo se realice por debajo de su temperatura de transición vítrea, pero son muy sensibles a la entalla [39].

Se realizaron unas microfotografías de SEM con el objetivo de observar la rotura de estos materiales (figura 15).

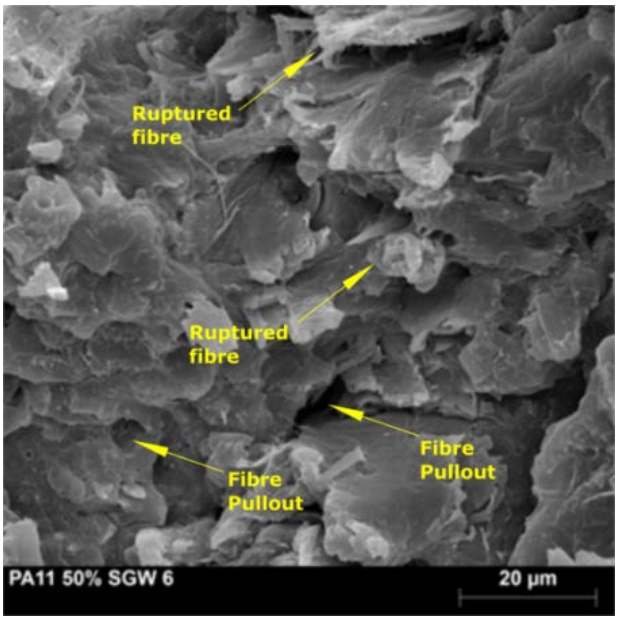

Figura 15. Microfotografía de SEM del compuesto de PA11+50%SGW. En amarillo se señalan fibras rotas y espacios huecos formados por el deslizamiento de una fibra.

En la fotografía de SEM se observaron fibras rotas, causadas por la fractura del material, pero también se observaron agujeros causados probablemente por el deslizamiento de fibras durante el ensayo. La presencia de fibras rotas juntamente con los elevados resultados obtenidos para la energía necesaria para producir una fractura confirmó de nuevo la presencia de una adecuada interfase entre las fibras y los compuestos.

Previamente a los estudios de absorción/adsorción de agua, se analizó el carácter hidrófilo de la PA11 y sus compuestos mediante el ángulo de contacto con agua. En el ensayo, la PA11 obtuvo un ángulo medio de 77º mientras que para sus compuestos con 20 y 50% de SGW el ángulo medio se redujo a 68,8 y 65,9º, respectivamente. El compuesto con un 60% de SGW mostró un ángulo de 69,3º debido a que el compuesto no es del todo homogéneo, dificultando su correcta medida. A través del ángulo medio, se calculó la energía de humectabilidad. Esta energía disminuía al aumentarse el carácter hidrófilo del material, como era esperable.

Los resultados de absorción de agua mostraron mayores M_∞ al aumentar el contenido de fibra en el material compuesto debido al carácter hidrófilo de las fibras SGW (figura 16).

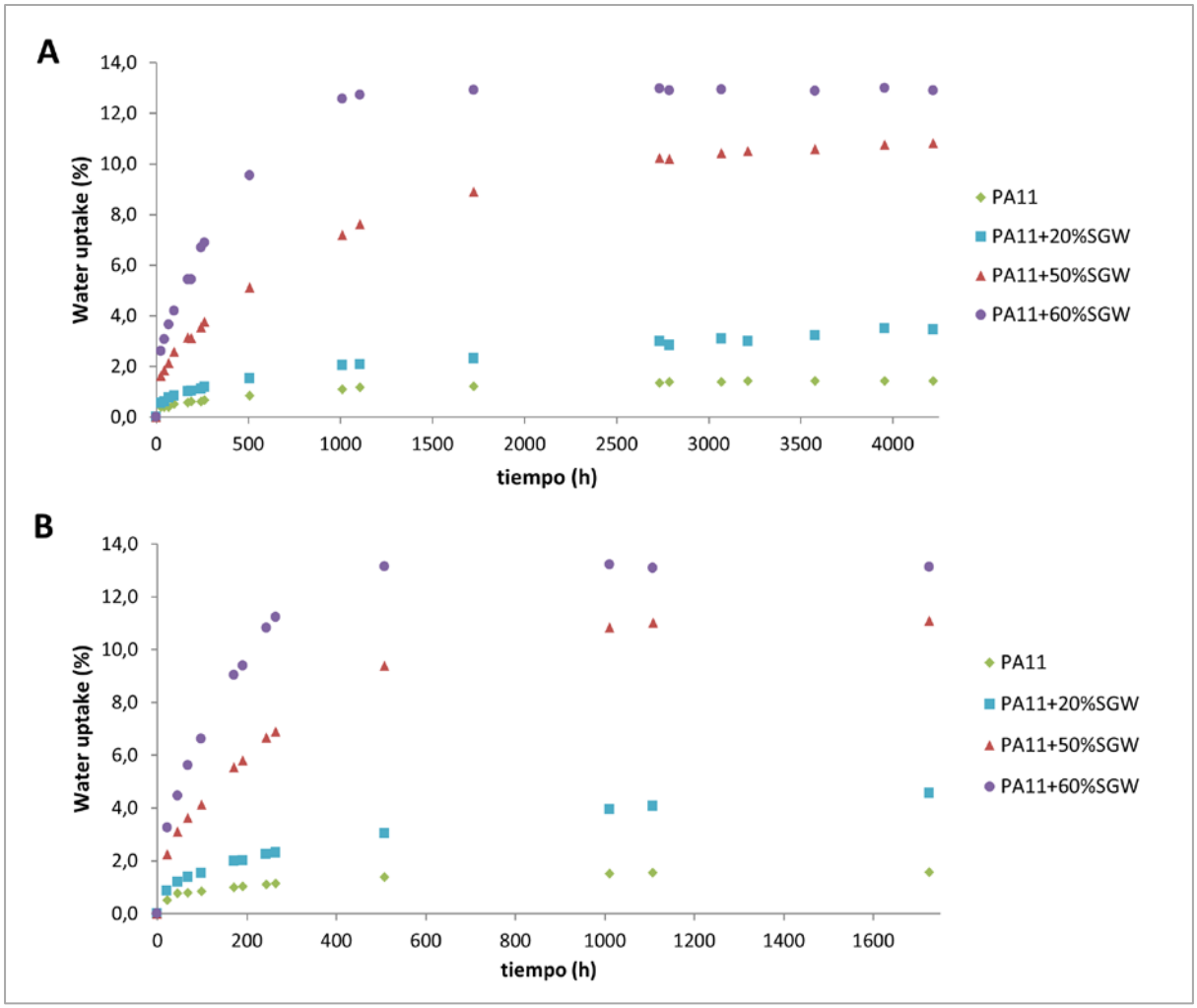

Figura 16. Curvas de absorción de agua de la PA11 y sus compuestas a 23ºC (A) y a 40ºC (B).

Por otra parte, se apreciaron menores tiempos de saturación y un M_∞ ligeramente superiores para el ensayo a 40ºC. A 23ºC el tiempo necesario para la saturación de los materiales era de más de 4000 horas, mientras que a 40ºC unas 1800h.

La modelización de los perfiles de absorción de agua a ambas temperaturas permitió el estudio de las cinéticas de absorción. Las cinéticas de los materiales estudiados mostraron un cambio de comportamiento de la dispersión de Pseudo-Fickian, en el caso de la PA11 y PA11+20%SGW, a Fickian en los compuestos de PA11+50%SGW y PA11+60%SGW. Este cambio se apreció en el valor de la constante n donde para la PA11 y el compuesto de PA11+20%SGW el valor era inferior a 0,4 mientras que para los compuestos de

PA11+50%SGW y PA11+60%SGW era cercano a 0,5. Además, en ambas temperaturas se mostró la misma tendencia. Por otra parte, la constante K relacionada con el sistema experimentó un incremento con la temperatura. Este incremento pero, disminuye con la presencia de fibras que induce a considerar que la rigidez del material tiene un efecto sobre esta constante.

La disminución de la movilidad del solvente, en este caso agua, probablemente es debida a la movilidad reducida de las cadenas de PA11 debido a las fibras de SGW dificultando la penetración. Estos datos estarían a su vez en concordancia con el valor del coeficiente de difusión (D_F), en el que la PA11 tiene valores muy superiores a los de los compuestos con un 20% y un 50% de SGW. En el caso del ensayo a 40ºC, el efecto se ve aumentado hasta casi 3 veces.

Los resultados del compuesto de PA11+60%SGW muestran la mala homogeneidad y humectación de las fibras por la matriz, tal y como ya se observó anteriormente en el análisis de la σ_t^C. Debido a este hecho, el valor de D_F es similar o superior al valor de PA11 para la misma temperatura, ya que las moléculas de agua encuentran una mayor facilidad en su difusión debido a la presencia de aglomeraciones o espacios huecos.

El uso de una ley de Arrenhius permite aproximar la energía necesaria para iniciar el proceso de dispersión (E_d) [40,41], donde se observó una reducción de la energía para los materiales compuestos respecto a la PA11.

Finalmente, los resultados mecánicos y termomecánicos estudiados hasta entonces indicaban la capacidad de los compuestos de PA11-SGW de reemplazar compuestos de PP (no solamente reforzados con GF, también reforzados con fibras celulósicas) de una forma más bien teórica. Pero el objetivo en el desarrollo e innovación de nuevos materiales, es su aplicación en productos del mercado. Muchos de estos compuestos reforzados se emplean en el sector automovilístico [42,43], por lo que se escogió una pieza del interior de un automóvil para modelarse con los compuestos de PA11-SGW y comprobar su competitividad. En la última publicación de esta tesis "*Research on the use of bio-polyamide 11 reinforced with lignocellulosic fibers composites in automotive parts. The case of a car doors handle*", se modelizó una maneta interior de coche con los materiales compuestos de PA11-SGW.

El procedimiento experimental de la modelización de un producto con nuevos materiales se resume en la figura 17.

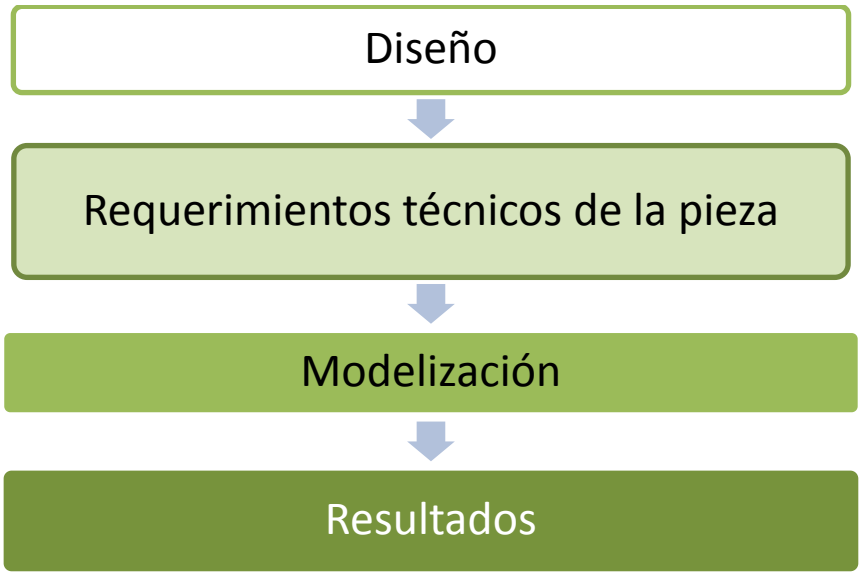

Figura 17. Procedimiento experimental para la modelización de un producto.

En primer lugar, es necesario escoger el producto y realizar el diseño. Tal y como se ha mencionado, para esta publicación se escogió una maneta interior de coche. El diseño se elaboró a partir de una maneta comercial, primero a mano (figura 18) y seguidamente en tres dimensiones con el software SolidWorks® de Dassaults sistemas.

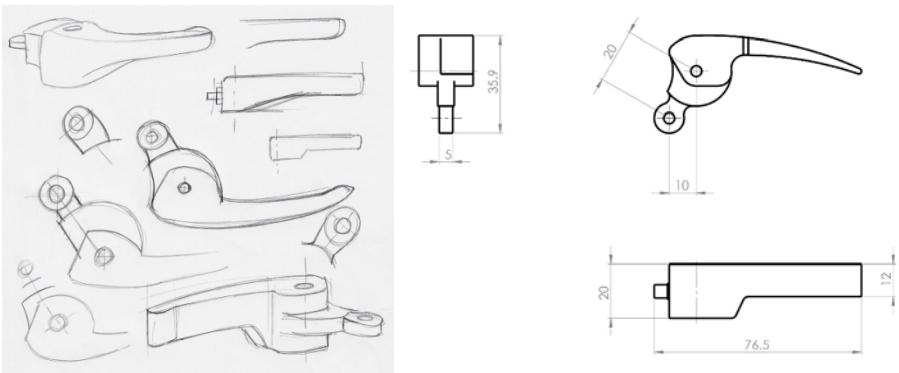

Figura 18. Bocetos y diseño técnico monocromático de la maneta de puerta.

Una vez el diseño de la maneta de la puerta se estableció, se estudiaron los requerimientos técnicos de la pieza. Se asignó el eje de giro, la sujeción y la dirección y valor de la fuerza aplicada. Resultados obtenidos en la literatura muestran que la fuerza máxima que una persona puede realizar en un esfuerzo similar al de abrir una maneta de puerta es de alrededor de 63N [44] por lo que en la modelización se decidió utilizar dos fuerzas: una de 20 N, que corresponde a una fuerza habitual aplicada al abrir una maneta, y una de 70 N, que es superior a la máxima que puede realizar una persona adulta.

El análisis de elementos finitos permite aplicar los parámetros especificados sobre la pieza con las condiciones del material escogido. La maneta se modelizó con los materiales de PA11-SGW y los compuestos de PP-GF, que son el objetivo a substituir. Se extrajeron tres resultados de la modelización: la resistencia de Von Mises, el desplazamiento en porcentaje y en mm, y el factor de seguridad. La resistencia de Von Mises hace referencia a la resistencia máxima capaz de soportar el material, mientras que el factor de seguridad hace referencia a la probabilidad que tiene una pieza de colapsar. Los factores de seguridad y deformaciones obtenidos por el PP+20%GF fueron establecidos como los parámetros mínimos. Además, durante el ensayo se observó que las zonas sometidas a mayor esfuerzo eran aquellas situadas al final de la zona de agarre, en convergencia con el cambio de componente y eje mientras que los mayores desplazamientos se obtenían en la zona de agarre.

La resistencia de Von Mises mostró valores similares para los compuestos de PA11-SGW y PP-GF ya que la pieza, el volumen y su peso es muy similar.

El factor de seguridad de los compuestos de PA11+SGW a 70N mostró que los compuestos de PA11-SGW con un contenido de fibra superior al 20% w/w cumplían los requisitos mínimos para competir con los compuestos comerciales. De forma más estricta, aumentando el factor de seguridad a 2,8 que es el valor del compuesto de PP+20%GF *coupled*, solamente los compuestos superiores al 40% w/w de SGW eran capaces de reemplazarlos. En el caso de las matrices, los valores del factor de seguridad fueron cercanos a 1, por lo que no pueden emplearse sin reforzar en esta pieza. Las deformaciones de PA11-SGW capaces de reemplazar los compuestos de PP-GF fueron inferiores a 4 mm.

Tras el ensayo a la fuerza máxima, se realizó el ensayo de esfuerzos en condiciones habituales (20 N). El factor de seguridad se incrementó para todos los compuestos, como

resultado de la menor fuerza aplicada. En este caso, la competitividad de los compuestos de PA11-SGW se reguló mediante la deformación de los compuestos de PP-GF. En estas condiciones, la deformación fue inferior a 0,6 mm, por lo que estrictamente solo los compuestos con contenidos de SGW superior al 50% w/w pueden remplazarlos. No obstante, la deformación de los compuestos a partir del 30% w/wde SGW fue tan reducida que pudieron cumplir con las especificaciones. La combinación de los resultados obtenidos en ambos test indicaba que los compuestos a partir de un 40% w/w de SGW cumplen con los requisitos.

El peso de las piezas realizadas con compuestos de PA11+SGW a partir de 40% w/w de contenido de fibra se estimó a partir de la densidad de estos compuestos. En todos los casos, el peso es superior (entre un 9 y un 17%) al de los compuestos de PP+GF. Estos resultados no son muy deseables ya que el incremento de peso acaba representando en un coche un incremento del consumo de carburante. No obstante se trata de un cálculo estimado para un volumen fijo, y si las propiedades mecánicas del compuesto permiten la reducción de este volumen, el peso podría ser similar o incluso menor al del compuesto de PP-GF tal y como ya se ha observado con compuestos de PA11 y fibras naturales [45].

Por otro lado, un estudio de ciclo de análisis de vida mediante disponible en el software, permitió una valoración del impacto ambiental y coste energético de la pieza con los diferentes materiales. Para ellos, se supuso que tanto las matrices, PA11 y PP, como las fibras SGW se produjeron en Europa y que tenían un ciclo de vida de 10 años. Los datos de la PA11 no están incluidos en la base de datos por lo que se utilizaron los datos obtenidos del análisis de ciclo de vida de la PA11 realizado por Arkema S.A. [46]. El análisis mostró un coste energético superior para la fabricación de los compuestos de PA11-SGW. Este coste decrecía al reducir el contenido de PA11-SGW. Estos resultados eran esperados ya que el proceso de obtención del aceite de ricino es muy elevado [47] y está menos optimizado que la extracción de poliolefinas del petróleo. El elevado coste energético de la producción de PA11 repercute también en las emisiones de CO_2. No obstante, las emisiones relacionadas con la producción, transporte y fin de vida de los materiales decrecen en comparación con la de los materiales de PP-GF, por lo que, si se consigue optimizar el proceso de obtención del aceite de ricino, estos materiales serian una alternativa sostenible y reciclable a los empleados comercialmente.

3.2 Bibliografía

1. Franco-Marquès, E.; Méndez, J. A.; Pèlach, M. A.; Vilaseca, F.; Bayer, J.; Mutjé, P. Influence of coupling agents in the preparation of polypropylene composites reinforced with recycled fibers. *Chem. Eng. J.* **2011**, *166*, 1170–1178, doi:10.1016/j.cej.2010.12.031.

2. López, J. P.; Méndez, J. A.; El Mansouri, N. E.; Mutjé, P.; Vilaseca, F. Mean intrinsic tensile properties of stone groundwood fibers from softwood. *BioResources* **2011**, *6*, 5037–5049.

3. Zierdt, P.; Theumer, T.; Kulkarni, G.; Däumlich, V.; Klehm, J.; Hirsch, U.; Weber, A. Sustainable wood-plastic composites from bio-based polyamide 11 and chemically modified beech fibers. *Sustain. Mater. Technol.* **2015**, *6*, 6–14, doi:10.1016/j.susmat.2015.10.001.

4. Marrot, L.; Bourmaud, A.; Bono, P.; Baley, C. Multi-scale study of the adhesion between flax fibers and biobased thermoset matrices. *Mater. Des.* **2014**, *62*, 47–56, doi:10.1016/j.matdes.2014.04.087.

5. Dorris, G.; Gray, D. Surface analysis of paper and wood fibres by ESCA [electron spectroscopy for chemical analyses]. II. Surface composition of mechanical pulps. *Cellul. Chem. Technol.* **1978**, *12*, 721–734.

6. Granda, L. A.; Espinach, F. X.; Tarrés, Q.; Méndez, J. A.; Delgado-Aguilar, M.; Mutjé, P. Towards a good interphase between bleached kraft softwood fibers and poly(lactic) acid. *Compos. Part B Eng.* **2016**, *99*, 514–520, doi:10.1016/j.compositesb.2016.05.008.

7. Johansson, L. S.; Campbell, J. M. Reproducible XPS on biopolymers: Cellulose studies. *Surf. Interface Anal.* **2004**, *36*, 1018–1022, doi:10.1002/sia.1827.

8. Kelly, A.; Tyson, W. R. Tensile properties of fibre-reinforced metals-copper/tungsten and copper/molybdenum. *J. Mech. Phys. Solids* **1965**, *13*, 329in1339-338in2350, doi:10.1016/0022-5096(65)90035-9.

9. Bowyer, W. H.; Bader, M. G. On the re-inforcement of thermoplastics by imperfectly

aligned discontinuous fibres. *J. Mater. Sci.* **1972**, *7*, 1315–1321, doi:10.1007/BF00550698.

10. Vilaseca, F.; Valadez-Gonzalez, A.; Herrera-Franco, P. J.; Pelach, M. A.; López, J. P.; Mutjé, P. Biocomposites from abaca strands and polypropylene. Part I: Evaluation of the tensile properties. *Bioresour. Technol.* **2010**, *101*, 387–395, doi:10.1016/j.biortech.2009.07.066.

11. Reixach, R.; Franco-Marquès, E.; El Mansouri, N. E.; Ramirez de Cartagena, F.; Arbat, G.; Espinach, F. X.; Mutjé, P. Micromechanics of mechanical, thermomechanical, and chemi-thermomechanical pulp from orange tree pruning as polypropylene reinforcement: a comparative study. *Bioresources* **2013**, *8*, 3231–3246.

12. Pegoretti, A.; Della Volpe, C.; Detassis, M.; Migliaresi, C.; Wagner, H. D. Thermomechanical behaviour of interfacial region in carbon fibre/epoxy composites. *Compos. Part A Appl. Sci. Manuf.* **1996**, *27*, 1067–1073, doi:10.1016/1359-835X(96)00065-6.

13. Sanadi, A. R.; Young, R. A.; Clemons, C.; Rowell, R. M. Recycled newspaper fibers as reinforcing fillers in thermoplastics: Part I-Analysis of tensile and impact properties in polypropylene. *J. Reinf. Plast. Compos.* **1994**, *13*, 54–67, doi:10.1177/073168449401300104.

14. López, J. P.; Mutjé, P.; Angels Pèlach, M.; El Mansouri, N. E.; Boufi, S.; Vilaseca, F. Analysis of the tensile modulus of polypropylene composites reinforced with stone groundwood fibers. *BioResources* **2012**, *7*, 1310–1323.

15. Hirsch, T. J. Modulus of Elasticity iof Concrete Affected by Elastic Moduli of Cement Paste Matrix and Aggregate. *J. Proc.* **1962**, *59*, 427–452.

16. Halpin, J. C.; Pagano, N. J. The Laminate Approximation for randomly oriented fibrous composites. *J. Compos. Mater.* **1969**, *3*, 720–724.

17. Halpin, J. C. Stiffness and expansion estimates for oriented Short Fiber Composites. *J. Compos. Mater.* **1969**, *3*, 732–734.

18. Cox, H. L. The elasticity and strength of paper and other fibrous materials. *Br. J. Appl. physic* **1952**, *3*, 72.

19. Krenchel, H. Fibre reinforcement. *Alademisk Forl.* **1964**.

20. Stempfle, F.; Ortmann, P.; Mecking, S. Long-chain aliphatic polymers to bridge the gap between semicrystalline polyolefins and traditional polycondensates. *Chem. Rev.* **2016**, acs.chemrev.5b00705, doi:10.1021/acs.chemrev.5b00705.

21. Pepin, J.; Miri, V.; Lefebvre, J.-M. New Insights into the Brill Transition in Polyamide 11 and Polyamide 6. *Macromolecules* **2016**, *49*, 564–573, doi:10.1021/acs.macromol.5b01701.

22. Ardanuy, M.; Antunes, M.; Velasco, J. I. Vegetable fibres from agricultural residues as thermo-mechanical reinforcement in recycled polypropylene-based green foams. *Waste Manag.* **2012**, *32*, 256–263, doi:10.1016/j.wasman.2011.09.022.

23. Panaitescu, D. M.; Frone, A. N.; Nicolae, C. Micro- and nano-mechanical characterization of polyamide 11 and its composites containing cellulose nanofibers. *Eur. Polym. J.* **2013**, *49*, 3857–3866, doi:10.1016/j.eurpolymj.2013.09.031.

24. Joseph, P. V.; Joseph, K.; Thomas, S.; Pillai, C. K. S.; Prasad, V. S.; Groeninckx, G.; Sarkissova, M. The thermal and crystallisation studies of short sisal fibre reinforced polypropylene composites. *Compos. Part A Appl. Sci. Manuf.* **2003**, *34*, 253–266, doi:10.1016/S1359-835X(02)00185-9.

25. Granda, L. A.; Méndez, J. A.; Espinach, F. X.; Puig, J.; Delgado-Aguilar, M.; Mutjé, P. Polypropylene reinforced with semi-chemical fibres of Leucaena collinsii: Thermal properties. *Compos. Part B Eng.* **2016**, *94*, 75–81, doi:10.1016/j.compositesb.2016.03.017.

26. Gironès, J.; Lopez, J. P.; Vilaseca, F.; Bayer, R.; Herrera-Franco, P. J.; Mutjé, P. Biocomposites from Musa textilis and polypropylene: Evaluation of flexural properties and impact strength. *Compos. Sci. Technol.* **2011**, *71*, 122–128, doi:10.1016/j.compscitech.2010.10.012.

27. Espigulé, E.; Vilaseca, F.; Espinach, F. X.; Julian, F.; Mansouri, N.-E. El; Mutjé, P. Biocomposites from Starch-based Biopolymer and Rape Fibers. Part II: Stiffening, Flexural and Impact Strength, and Product Development. *Curr. Org. Chem.* **2013**, *17*, 1641–1646.

28. Singh, V. K.; Bansal, G.; Negi, P.; Bisht, A. Characterization of Flexural and Impact Strength of Jute/Almond Hybrid Biocomposite. *J. Test. Eval.* **2017**, *45*, 20150414, doi:10.1520/JTE20150414.

29. Granda, L. A.; Espinach, F. X.; Méndez, J. A.; Vilaseca, F.; Delgado-Aguilar, M.; Mutjé, P. Semichemical fibres of Leucaena collinsii reinforced polypropylene composites: Flexural characterisation, impact behaviour and water uptake properties. *Compos. Part B Eng.* **2016**, *97*, 176–182, doi:10.1016/j.compositesb.2016.04.063.

30. López, J. P.; Gironès, J.; Mendez, J. A.; Pèlach, M. A.; Vilaseca, F.; Mutjé, P. Impact and flexural properties of stone-ground wood pulp-reinforced polypropylene composites. *Polym. Compos.* **2013**, *34*, 842–848, doi:10.1002/pc.22486.

31. Aydemir, D.; Kiziltas, A.; Erbas Kiziltas, E.; Gardner, D. J.; Gunduz, G. Heat treated wood-nylon 6 composites. *Compos. Part B Eng.* **2015**, *68*, 414–423, doi:10.1016/j.compositesb.2014.08.040.

32. Sears, K. D.; Jacobson, R.; Caulfield, D. F.; Underwood, J. Reinforcement of Engineering Themoplastics with High Purity Wood Cellulose Fibers. In *The Sixth International Conference on Woodfiber- Plastic Composites*; Madison, Wisconsin (USA), 2001; pp. 27–34.

33. Hashemi, S. Hybridisation effect on flexural properties of single- and double- gated injection moulded acrylonitrile butadiene styrene (ABS) filled with short glass fibres and glass beads particles. **2008**, 4811–4819, doi:10.1007/s10853-008-2683-1.

34. Hashemi, S.; Khamsehnezhad, A. Analysis of tensile and flexural strengths of single and double gated injection moulded short glass fibre reinforced PBT/PC composites. *Plast. Rubber Compos.* **2010**, *39*, 343–349, doi:10.1179/174328910X12647080902934.

35. Julian, F.; Méndez, J. A.; Espinach, F. X.; Verdaguer, N.; Mutje, P.; Vilaseca, F. Bio-based composites from stone groundwood applied to new product development. *BioResources* **2012**, *7*, 5829–5842.

36. Armioun, S.; Panthapulakkal, S.; Scheel, J.; Tjong, J.; Sain, M. Sustainable and lightweight biopolyamide hybrid composites for greener auto parts. *Can. J. Chem. Eng.* **2016**, *94*, 2052–2060, doi:10.1002/cjce.22609.

37. Espert, A.; Vilaplana, F.; Karlsson, S. Comparison of water absorption in natural cellulosic fibres from wood and one-year crops in polypropylene composites and its influence on their mechanical properties. *Compos. Part A Appl. Sci. Manuf.* **2004**, *35*, 1267–1276, doi:10.1016/j.compositesa.2004.04.004.

38. Feldmann, M.; Bledzki, A. K. Bio-based polyamides reinforced with cellulosic fibres – Processing and properties. *Compos. Sci. Technol.* **2014**, *100*, 113–120, doi:10.1016/j.compscitech.2014.06.008.

39. Mehrabzadeh, M.; Science, P.; Wales, N. S. Impact Modification of Polyamid 11. 2305–2314.

40. Serpe, G.; Chaupart, N.; Verdu, J. Ageing of polyarnide 11 in acid solutions. *Polymer (Guildf).* **1997**, *38*, 1911–1917, doi:10.1016/S0032-3861(96)00705-7.

41. Yampolskii, Y.; Shishatskii, S.; Alentiev, A.; Loza, K. Correlations with and prediction of activation energies of gas permeation and diffusion in glassy polymers. *J. Memb. Sci.* **1998**, *148*, 59–69, doi:10.1016/S0376-7388(98)00130-6.

42. Koronis, G.; Silva, A.; Fontul, M. Green composites: A review of adequate materials for automotive applications. *Compos. Part B Eng.* **2013**, *44*, 120–127, doi:10.1016/j.compositesb.2012.07.004.

43. Akampumuza, O.; Wambua, P. M.; Ahmed, A.; Li, W.; Qin, X. H. Review of the applications of biocomposites in the automotive industry. *Polym. Compos.* **2017**, *38*, 2553–2569, doi:10.1002/pc.23847.

44. Department of Trade and Industry *Tha Handbook of Measurements and capabilities of*

the Older Adult. Strength Data for Design Safety.; London, 2002;

45. Lacarin, M.; Perwuelz, A.; Pesnel, S.; Rault, F.; Vroman, P. Environmental Study of Biocomposites Intended for Passenger Cars. In *Proceedings 2nd LCA Conference*; Lille, France, 2012.

46. Devaux, J.; Lê, G.; Pees, B. Application of Eco-Profile Methodology To Polyamide 11. 1–11.

47. Silva, O. C. Synthetics Vs . Biomaterials : an Overview Focused on Energy Consumption. In *The Polymer Processing Society 23rd Annual Meeting*; Salvador, Brazil, 2007; pp. 1–8.

CAPÍTULO 4: *CONCLUSIONES*

4.1 Conclusiones

Del trabajo realizado en la presente tesis, se derivan las siguientes conclusiones:

- Se han obtenido materiales compuestos de PA11 y SGW en consonancia con el primer objetivo específico del apartado 1.2 de esta tesis.
- Se estableció el límite de refuerzo de los materiales compuesto en un 50% w/w. No obstante, se pudo fabricar el compuesto con un 60% w/w, pero los resultados de este compuesto indicaron una falta de interacción de las fibra-matriz.
- El estudio de las propiedades macroscópicas de los compuestos indica una buena dispersión del refuerzo en la matriz y también una adecuada interfase entre refuerzo y matriz. La σ_t^C y la σ_f^C mostraban incrementos del 67 y del 132% respecto la matriz de PA11, respectivamente para el material compuesto reforzado al 50% w/w. Los E_t^C y E_f^C con un 50% w/w de fibra SGW alcanzaban valores 3,5 y 3,5 y 3,7 veces superiores a los de la matriz de PA11. La ε_t^C y la ε_f^C de los materiales compuestos decrecían con el contenido de fibra, pero mantenían valores competitivos, superiores al 3%. La resistencia al impacto de los compuestos de PA11-SGW disminuía también con la adición de SGW en el material. A pesar de ello, la resistencia al impacto sin entalla era elevada alcanzando un valor mínimo para el compuesto de PA11+50%SGW de 27,4 $kJ \cdot m^{-2}$.
- Los materiales compuestos de PP-GF *sized* pueden ser remplazados por los compuestos de PA11-SGW en su totalidad excepto el caso de los E_t^C y el E_f^C para el 30% w/w de refuerzo. El E_t^C del material compuesto de PA11-SGW con un 50% w/w era un 21% inferior a los compuestos de PP-GF *sized* reforzados con un 30% w/w. Para el E_f^C la diferencia aumentó hasta un 42%.
- Respecto a los materiales compuestos de PP-GF *coupled*, solamente el compuesto con un 20% w/w puede remplazarse. El compuesto de PP+30%GF *coupled* alcanza una σ_t^C y una σ_f^C un 25% y un 29% superior al compuesto de PA11+50%SGW, respectivamente.
- En la resistencia al impacto, todos los materiales compuestos de PP-GF pueden ser remplazados por los de PA11-SGW. El valor de la resistencia al impacto del material compuesto de PP+30%GF *coupled* es de 21,4 $kJ \cdot m^{-2}$, resultado inferior al alcanzado por el de PA11+50%SGW (27,4 $kJ \cdot m^{-2}$).

- Globalmente, respecto a las propiedades mecánicas se puede concluir que los resultados obtenidos con PA11-SGW aunque no son capaces de substituir en su totalidad los compuestos de PP-GF, sí que se encuentran muy próximos a estos.
- La modelización de la resistencia a tracción permitió obtener la τ, la σ_t^F y el f_c para el material compuesto al 30% w/w. Las correspondientes simulaciones para los materiales compuestos al 20, 40 y 50% mostraron una excelente correlación entre los resultados experimentales y los simulados.
- La modelización del E_t^C se realizó mediante los modelos de Hirsch y Tsai-Pagano, mientras que en el E_f^C solamente se empleó el modelo de Hirsch. En el caso del E_t^C, el E_t^F alcanzó un valor medio de 17,8 y 18,0 GPa, para los modelos de Hirsch y Tsai-Pagano. Estadísticamente esta variación no era representativa en el 99% del intervalo de confianza. Los valores de η_e η_l y η_0 obtenidos mediante ambos modelos apenas difieren. En el caso del E_f^C, el E_f^F mostró un resultado medio de 12,6 GPa, inferior al esperado teniendo en cuenta la anisotropía del ensayo a flexión. En cambio, los valores de η_e η_l y η_0 son similares a los obtenidos a tracción.
- La σ_f^F se determinó de forma teórica y tuvo un valor de 888 MPa, un valor ligeramente inferior al obtenido en la literatura. Este resultado se relacionó también con una adecuada, pero no del todo óptima interfase en los materiales compuestos de PA11-SGW.
- De acuerdo con la RoM modificada aplicada a la σ_t^C y σ_f^C, que los respectivos valores de los f_c de los compuestos de PA11-SGW son del mismo orden atendiendo a las σ_t^F y σ_f^F evaluadas.
- La τ obtenida a partir de los modelos micromecánicos indicaba una correcta pero no óptima interfase. Así el valor obtenido es prácticamente idéntico al criterio de Tresca pero inferior al predicho por Von Mises.
- En consecuencia, parece claro que las interacciones fisicoquímicas en la interfase son mediante enlaces de hidrogeno y otras interacciones intermoleculares. En cualquier caso, con energías de enlace inferiores a los enlaces covalentes que generan algunos agentes de acoplamiento. El análisis de la composición superficial de las fibras corroboró la capacidad de las SGW de establecer este tipo de interacciones.

- Este tipo de interacciones justificaría el valor de la σ_t^F obtenida dado que ella depende de la propia resistencia intrínseca de la fibra, del tipo de interacción con la matriz y del número de enlaces por unidad de volumen que se establecen.
- La estabilidad térmica de los materiales compuestos de PA11-SGW fue inferior a la de la matriz debido a la inferior temperatura de degradación de las fibras. A pesar de ello, se incrementó la estabilidad de la matriz por la presencia de las fibras.
- No se observó ningún efecto significativo de las fibras SGW sobre las principales temperaturas de transición de la PA11 (T_m, T_c y T_g).
- La presencia de las fibras no mostró una variación de la T_g de los materiales compuestos, pero la pérdida de rigidez del material compuesto asociada al traspaso de la T_g fue disminuida por la rigidez de las fibras.
- La cristalinidad de los compuestos de PA11-SGW no aumentó en presencia de las fibras SGW, pero favorecían la forma α' respecto a la γ durante la cristalización controlada del DSC.
- La microestructura de los materiales tras el proceso de inyección mostró la forma δ de forma mayoritaria para todos los compuestos de PA11. No obstante, se observó la coexistencia de la forma γ en la PA11. En los materiales compuestos esta fase se reducía o desparecía.
- Tras la aplicación del tratamiento *annealing*, el porcentaje de fases cristalinas aumentó en el material y se observó en el DSC el crecimiento de fase cristalina. Estos cristales migraban hacia mayor temperatura al aumentar el contenido de fibra. La T_m sufrió un ligero incremento por la aparición de esta fase. En el caso de la T_g, la aparición de estos cristales producidos por el *annealing* produjo mayores diferencias cuando menor era el contenido de SGW. El análisis de XRD de las muestras tratadas mostró la fase α' tras el tratamiento y la desaparición de la fase γ en la matriz.
- Los perfiles de absorción de agua de los compuestos de PA11-SGW mostraron mayores M_∞ al incrementar el contenido de SGW debido al carácter hidrófilo de las fibras. Al aumentar la temperatura a una temperatura cercana a la T_g, se incrementaba ligeramente el M_∞ a la vez que disminuía el tiempo de absorbancia.
- La modelización de las curvas de absorción de agua estableció que los materiales compuestos con bajos contenidos de SGW seguían una tendencia Pseudo-Fickian

mientras que a elevados contenidos era Fickian. Esta tendencia se mantenía en las dos temperaturas estudiadas.

- El cálculo de la energía necesaria para iniciar el proceso de difusión mostró una menor energía para los materiales compuestos. Esta energía a su vez disminuía en aumentar el contenido de refuerzo.
- La competitividad de los materiales de PA11-SGW para reemplazar compuestos de PP-GF fue comprobada a través de la modelización de una maneta interior de la puerta de un coche. Se observó que únicamente los compuestos con un contenido superior al 40% de SGW alcanzaban valores similares de deformación y factor de seguridad a los obtenidos con compuestos de PP-GF. Además, el peso de las piezas era ligeramente superior en el caso de los compuestos de PA11-SGW. El análisis de LCA mostró un menor impacto en el caso de los compuestos de PP-GF. No obstante, el mayor impacto ambiental del uso de los compuestos de PA11-SGW se deriva del elevado coste energético y por ende de CO_2 de la obtención del monómero a partir del aceite de ricino. Si se optimiza el proceso, se reducirá drásticamente su impacto.
- Finalmente, cabe mencionar, que la fabricación de estos materiales compuestos de PA11-SGW ha demostrado que son una alternativa sostenible a los compuestos de PP-GF. Estos resultados suponen un avance en el cumplimiento de muchos de los principios para la producción de materiales compuestos sostenibles.

4.2 Perspectivas de futuro

Los resultados obtenidos en esta tesis son muy positivos y suponen un gran avance en el desarrollo de materiales sostenibles, pero aun no pueden substituir en su totalidad los compuestos de PP-GF. En esta línea, se proponen algunas investigaciones para el futuro.

La reducción de los extractivos superficiales de las fibras podría incrementar la interacción entre las SGW y la PA11, incrementando las propiedades mecánicas del material. Esta mejora se ha observado anteriormente en materiales compuestos de PP reforzado con fibras naturales.

Debido a la problemática observada en los resultados de los módulos elásticos de los compuestos de PA11-SGW, el uso de fibras con un menor contenido en lignina podría suponer una alternativa, pues se ha observado que una disminución de la lignina en el material produce un incremento del módulo de la fibra. Por otro lado, los resultados

experimentales previos a esta tesis demostraron la pobre dispersión de las fibras blanqueadas en la matriz de PA11. En esta línea, determinar el contenido adecuado de lignina podría solventar la diferencia en el módulo.

Por otra parte, en el caso de los materiales compuestos con un elevado contenida de fibras, se plantea el uso de una segunda extrusión en una extrusora monofuso. Esta etapa podría favorecer la dispersión de las fibras en el material, evitando de esta manera los problemas observados en el material compuesto de PA11+60%SGW.